

AMYOTROPHIC LATERAL SCLEROSIS IN TURKEY:
STUDIES ON FAMILIAL AND SPORADIC ALS
USING HIGH-THROUGHPUT GENOMIC TECHNOLOGIES

by

Aslıhan Özoğuz

B.S., Cerrahpaşa Medical School Medical Biological Sciences, 2001

M.S., Molecular Biology and Genetics Boğaziçi University, 2004

Submitted to the Institute for Graduate Studies in
Science and Engineering in partial fulfillment of
the requirements for the degree of
Doctor of Philosophy

Graduate Program in Molecular Biology and Genetics
Boğaziçi University

2010

AMYOTROPHIC LATERAL SCLEROSIS IN TURKEY:
STUDIES ON FAMILIAL AND SPORADIC ALS
USING HIGH-THROUGHPUT GENOMIC TECHNOLOGIES

APPROVED BY:

Prof. A. Nazlı Başak
(Thesis Supervisor)

Prof. S. Hande Çağlayan

Assoc. Prof. Esra Battaloğlu

Prof. Yeşim Parman

Prof. Uğur Özbek

DATE OF APPROVAL: 22.01.2010

*To my dearest mother
and
to my beloved father*

ACKNOWLEDGEMENTS

This study represents work performed at Boğaziçi University, Molecular Biology and Genetics Department between 2004-2009. Parts of it were carried out at the Cecil Day Laboratory at Harvard Medical School, MGH (August 2007-October 2007) and Yale Medical School, Neurogenetics Department (October 2009-December 2009).

I would like to express my sincere gratitude and regards to my thesis supervisor Prof. A. Nazlı Başak for her continuous guidance, valuable criticism and strong encouragement since 2001. I am very grateful for her support and great trust in me.

I would like to extend my thanks to Prof. Hande Çağlayan, Assoc. Prof. Esra Battaloğlu, Prof. Yeşim Parman and Prof. Uğur Özbek for devoting their time to evaluate this thesis. I am also thankful to Hilmi Özçelik for his valuable contributions and criticism.

I would like to express my graditudes to Prof. Robert H. Brown, Jr. and Dr. John E. Landers for their hospitality and guidance during my study at Harvard University Cecil Day Laboratory. I am also grateful to Prof. Murat Günel from Yale University Medical School Department of Neurosurgery for giving me the opportunity to establish high technology methodology in my research and Dr. Kaya Bilguvar, Dr. Ali Kemal Öztürk, Winson Ho, Mehmet Bakırcıoğlu, Tanyeri Barak and Dr. Hande Kaymakçalan at Yale University Medical School Department of Neurogenetics for their help and friendship during my stay. I also would like to thank to Prof. Piraye Oflazer, Prof. Feza Deymeer, Dr. Filiz Koç and all other valuable clinicians who provided the ALS blood samples. Last not least, I thank patients and their families for their cooperation.

I would like to express my thanks to Suna Lahut, A. Kadir Özkan, Didem Eruslu, long-time colleagues Dr. Mehmet Ozansoy, Dr. Caroline Pirkevi, Dr. Özlem Yalçın Çapan, İnanç Fidancı, Dr. Sibel Uğur as well as Dr. İzzet Ünlüer, Altar Sorkaç, Gülçin Vardar, Arman Aksoy, Aslı Şahin, Aslı Gündoğdu, Ece Terzioğlu Kara, Arzu Öztürk, Murat Çetinkaya, Selda Dağdeviren, Ilknur Aydın and Onur Birol. Being a part of NDAL team

has been a life-changing experience for me. At this point, I would also like to acknowledge the continuous support of Boğaziçi University Research Funds and Suna-İnan Kıraç Foundation to our studies.

I am also very grateful to my friends for their sincere support and friendship.

Last but not least, I would like to thank my mother and my family for their endless emotional and financial support throughout my graduate education. Nothing would have been possible without them, thank you.

ABSTRACT

AMYOTROPHIC LATERAL SCLEROSIS IN TURKEY: STUDIES ON FAMILIAL AND SPORADIC ALS USING HIGH-THROUGHPUT GENOMIC TECHNOLOGIES

Amyotrophic Lateral Sclerosis (ALS) is a late-onset neurodegenerative disease, characterized by death of motor neurons in cortex, brainstem and spinal cord. It is a multifactorial disease with interacting pathogenic mechanisms. Most incidences are sporadic (SALS), while 10 per cent of cases have a family history (FALS). The genetics of ALS is complex; eight genes and six loci with autosomal dominant (AD), autosomal recessive and X-linked patterns of inheritance have been identified thus far.

In the framework of this study, 198 Turkish ALS cases were investigated for possible mutations in the SOD1 gene. Five FALS cases were shown to carry disease-causing SOD1 mutations, while six were carriers of a rare polymorphism. In the next step, AD, nonconsanguineous FALS and juvenile cases were analyzed for the TDP-43, FUS and ANG genes via DNA sequencing. One homozygous D90A case, represented as recessive, was investigated by haplotype analysis and was compared to 21 Scandinavian ALS cases in search of a common ancestry. Additionally, 15 FALS and 13 juvenile cases, who were negative for the tested genes, were analyzed by whole genome genotyping for identification of new ALS genes. While no significant regions were obtained, a recessive family was preselected for the identification of homozygosity regions. Five candidate genes located within homozygosity regions were examined in one of the family member; no mutations were identified. The same individual was also assessed by whole exome resequencing. Furthermore, this study also contributed to a collaborative genome-wide association study in SALS, where 14 month-survival advantage was shown for homozygous CC allele at rs1541160 SNP in the gene coding KIFAP3. This is the most comprehensive study performed in Turkey on the molecular genetics of ALS. The high-throughput methodologies used and the findings presented in this thesis are expected to shed light to the complex pathogenesis of amyotrophic lateral sclerosis.

ÖZET

TÜRKİYE’DE AMİYOTROFİK LATERAL SKLEROZ: AİLESEL VE SPORADİK ALS’DE YÜKSEK-ÖLÇEKLİ GENOMİK YÖNTEMLERİN UYGULANMASI

Amiyotrofik Lateral Skleroz (ALS), korteks, beyin sapı ve omurilikteki motor nöronların ölümü ile karakterize olan, geç başlangıçlı nörodejeneratif bir hastalıktır. Birbiri ile ilişkili patojenik mekanizmaları içeren çok faktörlü bir hastalıktır. ALS’deki olguların yüzde 90’ı sporadik iken (SALS), yüzde 10’unda aile öyküsü gözlenir (FALS). ALS’nin genetiği karmaşıktır; bugüne kadar otozomal dominant (OD), otozomal resesif ve X’e bağlı geçiş özellikli sekiz gen ve altı değişik lokus tanımlanmıştır.

Bu çalışma çerçevesinde, 198 Türk ALS hastası SOD1 genindeki olası mutasyonlar için araştırıldı. Beş FALS olgusunun, hastalığa neden olan SOD1 mutasyonu taşıdığı gösterilirken, yedi tanesi seyrek gözlenen bir polimorfizmin taşıyıcısıydı. Bir sonraki aşamada, OD ve akraba ilişkisi olmayan FALS ve juvenil olgular, DNA sekanslama yöntemi ile, TDP-43, FUS and ANG genleri açısından incelendi. Ayrıca, resesif olarak kalıtılan bir homozigot D90A FALS olgusu, ortak kalıtımın tanımlanması amacıyla, 21 İskandinav ALS olgusu ile haplotip analizi ile incelendi. En son aşamada, çalışılan genlerde mutasyon bulunmayan 15 FALS ve 13 juvenil olgu, yeni ALS genlerinin tanımlanması için tüm genom genotipleme analizi ile değerlendirildi, ama henüz anlamlı bir bölge bulunamadı. Resesif bir aile, homozigotluk haritalaması için seçildi ve bu ailenin bir bireyinde, homozigot bölgeler içerisinde yer alan beş aday gen incelendi. Aynı birey, ‘*whole exome resequencing*’ ile de değerlendirildi. Tez çerçevesinde, ayrıca SALS olgularında yapılan kolaboratif bir genom-çapı SNP analizi, KIFAP3 genindeki rs1541160 SNP’inin homozigot CC alelinin ALS’de yaşamı 14 ay uzatma avantajı sağladığını gösterdi. Bu çalışma ALS’nin moleküler patogenezi üzerine Türkiye’de bugüne kadar yapılmış en kapsamlı çalışmadır. Kullanılan yüksek-ölçekli genomik yöntemlerin ve sunulan bulguların ALS’nin kompleks patogenezinin anlaşılmasına ışık tutacağı umulmaktadır.

TABLE OF CONTENTS

ACKNOWLEDGEMENTS	iv
ABSTRACT.....	vi
ÖZET	vii
LIST OF FIGURES	xiv
LIST OF TABLES	xxvi
LIST OF ABBREVIATIONS.....	xxxix
1. INTRODUCTION	1
1.1. Histopathological Features of ALS	3
1.2. Molecular Genetics of ALS.....	4
1.3. Superoxide Dismutase 1 (SOD1)	5
1.4. Mutations in SOD1 Gene	7
1.5. Possible Mechanisms Involved in ALS Pathogenesis.....	8
1.5.1. Oxidative Damage	9
1.5.1.1. Peroxidase Hypothesis	9
1.5.1.2. Peroxynitrate Hypothesis	10
1.5.2. Glutamate-induced Excitotoxicity.....	11
1.5.3. Protein Aggregation.....	13
1.5.4. Cytoskeletal Abnormalities and Defects in Axonal Transport.....	14
1.5.5. Mitochondrial Involvement in ALS	16
1.5.6. Non-cell Autonomous Nature of Motor Neuron Death.....	17
1.6. A Special Focus on Three Autosomal Dominant ALS Genes	20
1.6.1. DNA Binding Protein	20
1.6.2. Fused in Sarcoma	22
1.6.3. Angiogenin	23
1.7. D90A-SOD1 Mutation: a Possible Protective Factor in Homozygotes	23
1.8. Genome-wide Association Studies in ALS	27
1.9. Copy Number Variation	29
2. PURPOSE.....	31

3. MATERIALS	32
3.1. DNA Samples.....	32
3.1.1. DNA Samples of Turkish ALS Patients.....	32
3.1.2. Family Members of ALS147.....	33
3.1.3. DNA Samples of Scandinavian Origin.....	34
3.1.4. Mutational Analysis of Autosomal Dominant and Nonconsanguineous Familial and Juvenile ALS Cases in the Turkish Cohort.....	35
3.2. Fine Chemicals	36
3.2.1. Primers for PCR Amplification and DNA Sequencing of SOD1.....	36
3.2.2. Primers for PCR Amplification of Microsatellite Markers	37
3.2.3. Primers for PCR Amplification of TDP-43.....	38
3.2.4. Primers for PCR Amplification of ANG	38
3.2.5. Primers for PCR Amplification of FUS	38
3.2.6. Primers for PCR Amplification of CPEB3.....	40
3.2.7. Primers for PCR Amplification of USP53	41
3.2.8. Primers for PCR Amplification of UCHL3.....	42
3.2.9. Primers for PCR Amplification of RAB27A.....	43
3.2.10. Primers for PCR Amplification of IL21	43
3.2.11. Probes for Expression Analysis.....	44
3.2.12. Antibodies for Western Blot Analysis.....	45
3.2.13. Brain Tissue Lysates for Western Blot Analysis.....	45
3.3. Enzymes	46
3.3.1. PCR Amplification	46
3.3.2. Total RNA preparation	46
3.3.3. cDNA Synthesis from Total RNA.....	46
3.3.4. Real-time Quantitative Polymerase Chain Reaction (qRT-PCR).....	46
3.3.5. Restriction Enzyme Analysis	47
3.4. Buffers and Solutions	47
3.4.1. DNA Extraction.....	47
3.4.2. Polymerase Chain Reaction (PCR)	48
3.4.2.1. PCR of Exon 1 of SOD1 and Microsatellite Markers	48
3.4.2.2. PCR of Exons 2, 3, 4 and 5 of SOD1	48

3.4.2.3. Restriction Enzyme Analysis	49
3.4.2.4. PCR of TDP-43, FUS and ANG	49
3.4.2.5. Total RNA Preparation and Real-time Quantative PCR	49
3.4.3. Gel Eletrophoresis	49
3.4.3.1. Agarose Gel Eletrophoresis for PCR of SOD1 and Microsatellite Markers.....	49
3.4.3.2. Agarose Gel Eletrophoresis for Detection of RNA Concentration	50
3.4.3.3. Gel Eletrophoresis of Proteins	50
3.4.4. Whole Genome Genotyping of Turkish Familial and Juvenile ALS Cases	51
3.4.5. Western Blot Analysis.....	52
3.5. Chemicals	53
3.6. Kits	53
3.7. Equipments.....	53
4. METHODS	57
4.1. DNA Extraction from White Blood Cells	57
4.1.1. Sodium Chloride Extraction.....	57
4.1.2. Extraction by MagNA Pure Compact Instrument	58
4.2. Quality Control of Genomic DNA	58
4.2.1. Qualitative Analysis by Agarose Gel Eletrophoresis	58
4.2.2. Quantitative Analysis by Spectrophotometric Measurement of DNA	58
4.3. Investigation of Mutations in the SOD1 Gene	59
4.3.1. PCR Amplifications of Exons	59
4.3.1.1. PCR Amplification of Exon 1	59
4.3.1.2. PCR Amplification of Exons 2, 3, 4 and 5	60
4.3.2. DNA Sequencing of SOD1	60
4.3.3. Restriction Enzyme Analysis the D90A-SOD1 Mutation.....	61
4.4. Haplotype Analysis of D90A Mutation	61
4.4.1. PCR Amplification of the Microsatellite Markers	61
4.4.2. Determination of Fragment Sizes by GeneScan Analysis.....	63

4.5. Mutational Analysis of Autosomal Dominant and Nonconsanguineous Familial and Juvenile ALS Cases in the Turkish Cohort	64
4.5.1. Amplification of Genomic DNA Using the REPLI-g Mini Kit	64
4.5.2. PCR Amplifications of TDP-43, ANG and FUS.....	65
4.5.3. DNA Sequencing of TDP-43, FUS and ANG.....	65
4.6. Whole Genome Genotyping of Turkish Familial and Juvenile ALS Cases	66
4.6.1. Amplification of DNA Samples	67
4.6.2. Fragmentation of Amplified DNA	68
4.6.3. Precipitation.....	68
4.6.4. Resuspension of DNA	69
4.6.5. Hybridization of DNA onto BeadChips	69
4.6.6. Staining and Finalization of Genotyping.....	71
4.6.7. Evaluation of Genotyping Data	71
4.6.7.1. Loss-of-heterozygosity (LOH)	72
4.6.7.2. Copy Number Variation (CNV)	73
4.6.7.3. Further Evaluation by PLINK	73
4.7. Special Focus on a Turkish Autosomal Recessive ALS Family: ALS252, ALS256 and ALS257	74
4.7.1. PCR Amplifications of CPEB3, IL21, RAB27, UCHL3 and USP53.....	74
4.7.2. DNA Sequencing of CPEB3, IL21, RAB27, UCHL3 and USP53.....	74
4.7.3. Whole Human Exome Analysis	75
4.8. Genome-wide Association (GWA) Study in SALS	76
4.8.1. Genotyping of Samples	76
4.8.2. Detection of the Expression Levels of SNPs.....	76
4.8.2.1. Total RNA Preparation.....	76
4.8.2.2. cDNA Synthesis From Total RNA.....	77
4.8.2.3. Relative Quantification of Gene Expression by qPCR.....	77
4.8.2.4. Running Samples in TaqMan® 7900HT Sequence Detection System.....	78
4.8.2.5. Evaluation of qPCR Results	79

4.8.3. Western Blot Analysis	80
4.8.3.1. Preparation of Cell Lysates	80
4.8.3.2. Quantitative Analysis of Protein	81
4.8.3.3. Running Lysates on Polyacrylamide Gel	82
4.8.3.4. Blotting	83
4.8.3.5. Blocking of the Blots	83
4.8.3.6. First Antibody Hybridization	84
4.8.3.7. Second Antibody Hybridization	84
4.8.3.8. Exposure of the Blot	84
5. RESULTS	85
5.1. Mutation Analysis on Turkish SALS and FALS Patients: Investigation of SOD1 in the Turkish ALS Cohort	85
5.1.1. PCR Amplification of SOD1	85
5.1.2. DNA Sequencing Analysis of FALS Cases	85
5.1.2.1. N86S	85
5.1.2.2. H71Y	86
5.1.2.3. L144F	88
5.1.2.4. D90A	89
5.1.2.5. A4S and IVS-III-34 A→C transversion	90
5.1.2.6. IVS-III-34 A→C transversion	91
5.1.3. DNA Sequencing Analysis of SALS Cases	92
5.1.4. Overall Results of SOD1 Analysis in the Turkish Cohort	95
5.2. Further Analysis of the D90A Mutation	95
5.2.1. DNA Sequencing of the Family members of ALS147	95
5.2.2. Restriction Enzyme Analysis of D90A	97
5.2.3. Haplotype Analysis of the D90A Family	98
5.2.3.1. PCR Amplification of Microsatellite Markers	98
5.2.3.2. Genescan Analysis of the Microsatellite Markers	99
5.3. Further Mutational Analysis of ALS Cases in the Turkish Cohort	103
5.3.1. PCR Amplification and DNA Sequencing Analysis of TDP-43	103
5.3.2. PCR Amplification and DNA Sequencing Analysis of ANG	103
5.3.3. PCR Amplification and DNA Sequencing Analysis of FUS	105
5.4. Whole Genome Analysis of Turkish Familial and Juvenile	

ALS Cases	111
5.4.1. Chromosomal Regions with Duplications, Homozygous and Heterozygous Deletions.....	111
5.4.2 Detection of Homozygosity Regions.....	114
5.5. Special Focus on a Turkish Recessive ALS Family: ALS252, ALS256 and ALS257.....	115
5.6. Mutation Analysis of CPEB3, IL21, RAB27, UCHL3 and USP53 in a Recessive Turkish ALS Family.....	122
5.6.1. PCR Amplification and DNA Sequencing of CPEB3.....	123
5.6.2. PCR Amplification and DNA Sequencing of USP53	123
5.6.3. PCR Amplification and DNA Sequencing of UCHL3.....	124
5.6.4. PCR Amplification and DNA Sequencing of RAB27	125
5.6.5. PCR Amplification and DNA Sequencing of IL21	125
5.7. Whole Human Exome Analysis of ALS256	126
5.8. Genome-wide Association Study in Caucasian SALS Cases	128
5.8.1. The Expression Profile of B4GALT6.....	131
5.8.2. The Expression Profile of ADAM17TS	132
5.8.3. The Expression Profile of KIFAP3	133
5.8.3.1. Real-time PCR Analysis.....	133
5.8.3.2. Western blot Analysis of KIFAP3.....	135
6. DISCUSSION.....	137
6.1. Mutational Analysis of SOD1 in the Turkish ALS Cohort.....	139
6.1.1. The N86S Patient	140
6.1.2. The H71Y Patient.....	142
6.1.3. The D90A Patient.....	143
6.2. Haplotype Analysis of the Turkish ALS Patient with the Homozygous D90A Mutation	144
6.3. Investigation of Mutations in Other ALS Genes.....	145
6.4. The Discrimination of SALS and FALS Is Not Always Straightforward but Important For The Geneticist.....	146
6.5. Whole Genome Genotyping of Familial and Juvenile ALS Cases in the Turkish Cohort	147
6.6. Whole Exome Resequencing	149

6.7. Genome-wide Association Study in Caucasian SALS Cases	151
6.7.1. Linkage Analysis.....	151
6.7.2. Genome-wide Association Studies.....	152
6.7.3. Gene Expression Analysis.....	154
6.7.4. The Effect of Reduced Expression of KIFAP3 on Survival in SALS Patients.....	155
6.7.4.1. The Parameters that Provided Success in This GWA Study.	156
6.7.4.2. KIFAP3 in Axonal Transport	157
6.8. Concluding Remarks	159
APPENDIX A: PRODUCTS OF THIS THESIS.....	161
APPENDIX B: PATIENT REGISTRY FORM FOR ALS	163
APPENDIX C: REVISED EL ESCORIAL CRITERIA FOR ALS DIAGNOSIS	164
APPENDIX D: IMBREEDING COEFFICIENCIES OF TURKISH FALS AND JUVENILE CASES.....	165
APPENDIX E: REGIONS OF HOMOZYGOSITY IN FALS, JUVENILE ALS CASES AND CONTROLS	166
APPENDIX F: P VALUES FOR PREVIOUSLY REPORTED SNPS	188
APPENDIX G: LINKAGE DISEQUILIBRIUM PLOT FOR RS1541160.....	189
APPENDIX H: SNPS WITH BEST P VALUES IN THE FOUR TESTED CATEGORIES	190
APPENDIX I: SENSITIVITY ANALYSIS OF RS1541160	191
APPENDIX J: HOMOZYGOUSITY REGIONS IN ALS157 AND ALS158.....	192
REFERENCES	194

LIST OF FIGURES

Figure 1.1. Affected regions in ALS.....	2
Figure 1.2. Demographics in ALS	3
Figure 1.3. a. Number of degenerating axons at different disease stages; b. number of motor neurons at different disease stages.....	4
Figure 1.4. Secondary structure of SOD1.....	6
Figure 1.5. SOD1-mediated dismutation of superoxide	7
Figure 1.6. Glutamate release mechanism in normal and ALS cases	12
Figure 1.7. Possible effects of mutant SOD1 aggregation.....	13
Figure 1.8. Axonal transport in motor neurons.....	14
Figure 1.9. Mitochondrial dysfunction in ALS.....	17
Figure 1.10. Crosstalk between glial cells and motor neurons	19
Figure 1.11. The structure and functions of TDP-43	20
Figure 1.12. Schematic representation of FUS	22
Figure 1.13. The results of the first (a) and second (b) linkage studies around the SOD1 gene in D90A homozygous patients.....	26
Figure 1.14. Common variants in disease	27

Figure 3.1.	The family tree of ALS147.....	33
Figure 3.2.	The positions of the microsatellite markers on chromosome 21	37
Figure 3.3.	Schematic representation of chromosomal location of the probes	44
Figure 4.1.	Steps of genotyping array	66
Figure 4.2.	An example showing B allele frequency in chromosome 2	71
Figure 4.3.	An example showing log R graph for chromosome 2.....	72
Figure 4.4.	Schematic representation of whole exome resequencing	75
Figure 5.1.	Chromatogram, showing the sequencing profile of ALS191, carrying AAT→AGT transition in exon 4 position 86 (N86S)	85
Figure 5.2.	Pedigree of ALS191	86
Figure 5.3.	Chromatogram, showing the sequencing profile of ALS226, carrying CAC→TAC transition in exon 3 position 71 (H71Y).....	86
Figure 5.4.	Chromatograms, showing the sequencing profiles of family members of ALS226	87
Figure 5.5.	Family tree of ALS226	87
Figure 5.6.	Chromatogram, showing the sequencing profile of ALS61, carrying TTG→TTC transversion in exon 4 position 144 (L144F).	88
Figure 5.7.	Family tree of ALS61	88

Figure 5.8. Chromatogram, showing the sequencing profile of ALS147, carrying GAC→GCC transversion in exon 4 position 90 (D90A).....	89
Figure 5.9. Family tree of ALS147	89
Figure 5.10. Chromatograms showing the sequencing profile of ALS221, carrying both (a) the GCC→TCC transversion in exon 1 position 4 (A4S) and (b) IVS-III-34 A→C transversion.....	90
Figure 5.11. Multiple sequence alignment of a part of intron 3.....	91
Figure 5.12. Chromatogram, showing the sequencing profile of ALS215, carrying the IVS-III-34 A→C transversion	91
Figure 5.13. The family tree of ALS215.....	91
Figure 5.14. Chromatograms, showing the sequencing profiles of SALS patients with IVS-III-34 A→C transversion.....	92
Figure 5.15. The family tree of ALS1.....	92
Figure 5.16. The family tree of ALS40.....	93
Figure 5.17. The family tree of ALS120.....	93
Figure 5.18. The family tree of ALS122.....	94
Figure 5.19. Family tree of ALS242	94
Figure 5.20. Chromatograms, showing the sequencing profiles of family members of ALS147	96
Figure 5.21. Revised pedigree of ALS147, according to the genotype at position 90 ..	96

Figure 5.22. RE analysis of D90A mutation by ItaN of ALS147 and his family members	96
Figure 5.23. Genescan analysis for D21S213 (a) homozygous, (b) heterozygous individual	99
Figure 5.24. Genescan analysis for D21S219 (a) homozygous, (b) heterozygous individual	99
Figure 5.25. Genescan analysis for D21S224 (a) homozygous, (b) heterozygous individual	100
Figure 5.26. Genescan analysis for D21S263 (a) homozygous, (b) heterozygous individual	100
Figure 5.27. Genescan analysis for D21S272 (a) homozygous, (b) heterozygous individual	100
Figure 5.28. Genescan analysis for D21S21270 (a) homozygous, (b) heterozygous individual	101
Figure 5.29. Pedigree and haplotypes of patient ALS147 and family members	102
Figure 5.30. Chromotograms, showing sequence profiles of patients, carrying rs11701 in ANG	103
Figure 5.31. Chromotograms, showing sequence profiles of patients, carrying rs11701 in ANG	104
Figure 5.32. Chromotogram, showing rs929867 in the FUS gene of ALS97	105
Figure 5.33. Chromotograms, showing sequence profiles of patients carrying a novel GTA→GTG transversion at codon 10 of FUS	105

Figure 5.34. Chromotograms, showing sequence profiles of patients carrying the rs1052352 in FUS	106
Figure 5.35. Chromotograms, showing sequence profiles of patients carrying the rs741810 in FUS	107
Figure 5.36. Chromotograms, showing sequence profile of ALS178, carrying a novel C→T change in intron 5 of FUS.....	107
Figure 5.37. Chromotograms, showing sequence profiles of patients, carrying the rs1052352 in FUS.....	108
Figure 5.38. Chromotograms, showing sequence profiles of patients, carrying the rs741810 in FUS	108
Figure 5.39. Chromotograms, showing sequence profile of ALS57, carrying the rs73530283 in FUS	109
Figure 5.40. The B allele frequency analysis of chromosome 2 in ALS132	111
Figure 5.41. Changes in patterns of log R and B allele frequency in duplication	111
Figure 5.42. Changes in patterns of log R and B allele frequency homozygous deletion.....	112
Figure 5.43. Changes in patterns of log R and B allele frequency heterozygous deletion	112
Figure 5.44. An example to ‘Homozygosity Mapping Graph’, .showing homozygous regions of chromosome 1 in ALS and controls	115
Figure 5.45. Family tree of ALS252, ALS256 and ALS257	116

Figure 5.46. Homozygous regions in chromosome 4 for ALS252, ALS254, ALS257 and controls.	117
Figure 5.47. Homozygous regions in chromosome 5 for ALS252, ALS254, ALS257 and controls	118
Figure 5.48. Homozygous regions in chromosome 7 for ALS252, ALS254, ALS257 and controls	118
Figure 5.49. Homozygous regions in chromosome 9 for ALS252, ALS254, ALS257 and controls	119
Figure 5.50. Homozygous regions in chromosome 10 for ALS252, ALS254, ALS257 and controls	119
Figure 5.51. Homozygous regions in chromosome 12 for ALS252, ALS254, ALS257 and controls	120
Figure 5.52. Homozygous regions in chromosome 13 for ALS252, ALS254, ALS257 and controls	120
Figure 5.53. Homozygous regions in chromosome 18 for ALS252, ALS254, ALS257 and controls	121
Figure 5.54. Homozygous regions in chromosome 22 for ALS252, ALS254, ALS257 and controls	121
Figure 5.55. GWAS results according to site of onset, age of onset and survival.....	128
Figure 5.56. a.GWAS result on survival, b. a closer view of rs1541160 region where dark points are SNPs within this study and light points are imputed SNPs	129

Figure 5.57. The effect of different alleles of rs1541160 on survival in SALS patients	130
Figure 5.58. Hs00191135 expression in cortex, according to alleles	131
Figure 5.59. Hs00191135 expression in cerebellum, according to alleles.....	132
Figure 5.60. Hs00330236 expression in brain, according to alleles	132
Figure 5.61. Hs00330236 expression in cortex, according to alleles	133
Figure 5.62. Hs00183973 expression in cortex, according to alleles	133
Figure 5.63. Hs00183973 expression in cerebellum, according to alleles.....	134
Figure 5.64. Hs00946074 expression in cortex, according to alleles	134
Figure 5.65. Hs00946074 expression in cerebellum, according to alleles.....	135
Figure 5.66. Western blot analysis of KIFAP3 expression in association with rs1541160 genotype.....	135
Figure 5.67. The relative expression of TT and CC genotype for rs1541160 in occipital cortex	136
Figure 6.1. An overall representation of the proposed mechanisms in ALS	138
Figure 6.2. Distribution of Turkish ALS cases according to different subgroups.....	139
Figure 6.3. SOD1 gene analysis results of Turkish FALS cases	140
Figure 6.4. Suggested migration routes of Vikings	145

Figure 6.5. A stepwise approach from whole exome resequencing to determine possible candidate genes.....	150
Figure 6.6. Schematic representation of different approaches used in the identification of new disease genes	152
Figure 6.7. Kinesin and representation of anterograde transport.....	157
Figure 6.8. Schematic representation of protein.interactions of KIFAP3 and ALS genes	158
Figure A.1. Review article on the genetics of ALS	161
Figure A.2. Research article on GWA study of Caucasian SALS cases by Landers et al.....	162
Figure E.1. Homozygous regions in chromosome 1 for FALS, juvenile cases and controls	166
Figure E.2. Homozygous regions in chromosome 2 for FALS, juvenile cases and controls	167
Figure E.3. Homozygous regions in chromosome 3 for FALS, juvenile cases and controls	168
Figure E.4. Homozygous regions in chromosome 4 for FALS, juvenile cases and controls	169
Figure E.5. Homozygous regions in chromosome 5 for FALS, juvenile cases and controls	170
Figure E.6. Homozygous regions in chromosome 6 for FALS, juvenile cases and controls	171

Figure E.7. Homozygous regions in chromosome 7 for FALS, juvenile cases and controls	172
Figure E.8. Homozygous regions in chromosome 8 for FALS, juvenile cases and controls	173
Figure E.9. Homozygous regions in chromosome 9 for FALS, juvenile cases and controls	174
Figure E.10. Homozygous regions in chromosome 10 for FALS, juvenile cases and controls	175
Figure E.11. Homozygous regions in chromosome 11 for FALS, juvenile cases and controls	176
Figure E.12. Homozygous regions in chromosome 12 for FALS, juvenile cases and controls	177
Figure E.13. Homozygous regions in chromosome 13 for FALS, juvenile cases and controls	178
Figure E.14. Homozygous regions in chromosome 14 for FALS, juvenile cases and controls	179
Figure E.15. Homozygous regions in chromosome 15 for FALS, juvenile cases and controls	180
Figure E.16. Homozygous regions in chromosome 16 for FALS, juvenile cases and controls	181
Figure E.17. Homozygous regions in chromosome 17 for FALS, juvenile cases and controls	182

Figure E.18. Homozygous regions in chromosome 18 for FALS, juvenile cases and controls	183
Figure E.19. Homozygous regions in chromosome 19 for FALS, juvenile cases and controls	184
Figure E.20. Homozygous regions in chromosome 20 for FALS, juvenile cases and controls	185
Figure E.21. Homozygous regions in chromosome 21 for FALS, juvenile cases and controls	186
Figure E.22. Homozygous regions in chromosome 22 for FALS, juvenile cases and controls	187
Figure F. P values for three hits which were previously reported as significant in susceptibility.....	188
Figure G. Linkage disequilibrium plot of rs151160	189
Figure H. SNPs with best P values in the four tested categories	190
Figure I. Sensitivity analysis of rs151160 within the populations under study	191

LIST OF TABLES

Table 1.1.	Genes responsible for FALS	5
Table 1.2.	Genetic variants (SNPs) in SALS that have been identified by GWA.....	29
Table 3.1.	Centers that have sent ALS samples to NDAL	32
Table 3.2.	Origins and genotypes of Scandinavian samples	34
Table 3.3.	Autosomal dominant FALS cases	35
Table 3.4.	Familial ALS cases	35
Table 3.5.	Juvenile ALS cases	36
Table 3.6.	Primer pairs used in PCR amplification of the SOD1 gene	36
Table 3.7.	Primer pairs used in the PCR amplification of microsatellite markers	37
Table 3.8.	Primer pairs used in the PCR amplification of TDP-43	38
Table 3.9.	Primer pair used in the PCR amplification of ANG	38
Table 3.10.	Primer pairs used in the PCR amplification of FUS.....	39
Table 3.11.	Primer pairs used in the PCR amplification of CPEB3	40
Table 3.12.	Primer pairs used in the PCR amplification of USP53.....	41
Table 3.13.	Primer pairs used in the PCR amplification of UCHL3	42

Table 3.14. Primer pairs used in the PCR amplification of RAB27A.....	43
Table 3.15. Primer pairs used in the PCR amplification of IL21	43
Table 3.16. Probes used in gene expression analysis	44
Table 3.17. Antibodies used in western blot analysis.....	45
Table 3.18. Brain lysates used in western blot analysis	46
Table 4.1. PCR reagents used for the amplification of exon 1	59
Table 4.2. Annealing temperatures for the amplification of exons 2, 3, 4 and 5.....	60
Table 4.3. PCR reagents used for the amplifications of exons 2, 3, 4 and 5	60
Table 4.4. ItaI Restriction enzyme and its recognition site	61
Table 4.5. Annealing temperatures for the amplification of microsatellite markers..	62
Table 4.6. PCR reagents used for the amplifications of D21S213, D21S219, D21S224, D21S263 and D21S272	62
Table 4.7. PCR reagents used for the amplifications of D21S1270	63
Table 4.8. PCR reagents used for the amplifications of TDP-43, FUS and ANG	65
Table 4.9. Reagents used in cDNA synthesis	77
Table 4.10. Reagents of qPCR master mix.....	78
Table 4.11. Formulas for the dilutions of six standards	81

Table 5.1.	Brief clinical information of SALS patients with IVS-III-34 A→C transversion.....	94
Table 5.2.	Overall representation of changes detected in SOD1 analysis.....	95
Table 5.3.	Fragment sizes from ItAI digestion of exon 4.....	97
Table 5.4.	The family members of ALS147 and their genotypes at position 90.....	98
Table 5.5.	The sizes of PCR products and corresponding repeat numbers for..... each markers	98
Table 5.6.	Presentation of all SNPs identified in ANG in familial, juvenile and autosomal dominant ALS cases under study.....	104
Table 5.7.	Summary of SNPs identified in FUS in familial and juvenile ALS cases	109
Table 5.8.	Summary of SNPs identified in FUS in autosomal dominant ALS cases	110
Table 5.9.	Unreported homozygous and heterozygous regions that have been detected in the familial and juvenile Turkish patient samples	112
Table 5.10.	Revised consanguinity pattern of some ALS cases.....	114
Table 5.11.	Homozygosity regions common for ALS252, ALS256 and ALS257.....	117
Table 5.12.	Candidate gene selected after the selective evaluation of homozygosity mapping	122
Table 5.13.	Variations observed in CPEB3 gene of ALS256.....	123

Table 5.14. Variations observed in USP53 gene of ALS256	124
Table 5.15. Variations observed in the UCHL3 gene of ALS256.....	125
Table 5.16. Variations observed in RAB27 gene of ALS256	125
Table 5.17. Variations observed in IL21 gene of ALS256.....	125
Table 5.18. Sequence changes detected in whole exome analysis	126
Table 5.19. Overall representation of ALS genes analyzed	127
Table 5.20. Variations identified in SOD1, TDP-43, FUS and ANG.....	127
Table 5.21. Summary of unreported homozygous and heterozygous deletion regions detected via whole genome analysis of familial and juvenile cases.....	127
Table 5.22. Three significant SNPs for susceptibility, survival and age of onset	130
Table 6.1. Susceptibility and Modifier Genes in SALS	154
Table C. El Escorial criteria used for the diagnosis of ALS.....	164
Table D. Inbreeding coefficient results of FALS and juvenile cases.....	165
Table J. Homozygosity regions of ALS157 and ALS158	192

LIST OF ABBREVIATIONS

AD	Autosomal Dominant
ALS	Amyotrophic Lateral Sclerosis
ALS-FTD	Amyotrophic Lateral Sclerosis-Frontotemporal Dementia
ALS-FTD-PD	Amyotrophic Lateral Sclerosis-Frontotemporal Dementia-Parkinsonism
AMPA	α -amino-3-hydroxy-5-methyl-4-isoxazole propionic acid
ANG	Angiogenin
AR	Autosomal Recessive
ATP	Adenosine Triphosphate
B2M	Beta-2-microglobulin
BDNF	Brain-derived Neurotrophic Factor
bp	Basepair
BPB	Bromophenol Blue
Ca ⁺²	Calcium Ion
CCS	Copper Chaperones
CGMP	Cyclic Guanosine Monophosphate
CNS	Central Nervous System
CNTF	Ciliary neurotrophic factor
CN	Copy Number
CNV	Copy Number Variation
COX2	Cyclooxygenase 2
Cu ⁺²	Copper Ion
DCTN1	Dynactin 1
DMSO	Dimethyl Sulfoxide
dNTP	Deoxyribonucleotides
DPP6	Dipeptidyl Peptidase VI
e-	Electron
EAAT	Excitatory Amino Acid Neurotransmitter
ER	Endoplasmic Reticulum
EtBr	Ethidium Bromide

FALS	Familial Amyotrophic Lateral Sclerosis
FUS	Fused in Sarcoma
GA	Golgi Apparatus
GDNF	Glial Cell Line-derived Neurotrophic Factor.
GluR2	Glutamate Receptor Type 2
GWA	Genome-wide Association
H ₂ O ₂	Hydrogen Peroxide
His	Histidine
HSP	Heat Shock Protein
IF	Intermediate Filament
IGV	Illumina Genome Viewer
IPC	Insoluble Protein Complexes
ITPR2	Inositol-1,4,5-Triphosphate Receptor, Type 2
kb	Kilobase
kDa	Kilodalton
KIFAP3	Kinesin-associated Protein 3
KSP	Lys-Ser-Pro phosphorylation sites
LMN	Lower Motor Neuron
log	Logarithm
LOH	Loss-of-heterozygosity
MAPT	Microtubule-associated Protein Tau
Mg ⁺²	Magnesium Ion
ml	Milliliter
mRNA	Messenger RNA
MgCl ²	Magnesium Chloride
MtDNA	Mitochondrial DNA
mV	Milivolt
NF	Neurofilament
NF-H	Heavy Chain Neurofilament
NF-L	Light Chain Neurofilament
NF-M	Medium Chain Neurofilament
ng	Nanogram
NMDA	N-methyl-D-aspartic acid

nM	Nanomole
NO	Nitric Oxide
NOS	Nitrite Oxide Synthases
O ₂	Oxygen
O ₂ ⁻	Superoxide
OD	Optic Density
qPCR	Real-time Polymerase Chain Reaction
Para	paralysis
PCR	Polymerase Chain Reaction
PMW	Pre-muscle Weakness Stage
RD	Rapid Decline Stage
RE	Restriction Enzyme
ROS	Reactive Oxygen Species
RRM1	RNA recognition motif 1
RRM2	RNA recognition motif 2
SALS	Sporadic Amyotrophic Lateral Sclerosis
SD	Slow Decline Stage
SDS	Sodiumdodecylsulphate
SETX	Senataxin
SNP	Single Nucleotide Polymorphism
SOD1	Superoxide Dismutase1
TAE	Tris-Asetic Acid-EDTA
TBE	Tris-Boric Acid-EDTA
TARDBP	TAR DNA binding protein
TDP-43	TAR DNA binding protein
U	Unit
Ub	Ubiquitin
UMN	Upper Motor Neuron
UPS	Ubiquitin Proteosome System
UV	Ultraviolet
VABP	Vesicle-associated Membrane Prtein-associated Protein B
VEGF	Vascular Endothelial Growth Factor
Zn ⁺²	Zinc Ion

1. INTRODUCTION

Amyotrophic Lateral Sclerosis (ALS) is one of the most common late-onset neurodegenerative diseases. It was first described by Jean-Martin Charcot in 1869 (Charcot *et al.*, 1869). Today, it is also known as Motor Neuron Disease or Lou Gehrig's Disease, after the death of the famous baseball player from ALS in 1941 (Oliveira *et al.*, 2009).

In general terminology, 'Motor Neuron Disease' is used to define a diverse group of inherited disorders with their own recognizable clinical features and a definite final destination of loss of upper and/or lower motor neurons. ALS is the most common subtype, thus is also named as ALS/MND. The diagnosis is mainly of exclusion of other subtypes. Today, the most reliable and uniform diagnosis is based on El Escorial criteria which determines the classification and diagnosis of suspected, possible, probable and definite ALS cases, depending on clinical, electrophysiological and neuropathological examinations (Appendix C) (Hand *et al.*, 2002).

ALS is characterized by the selective death of motor neurons in the motor cortex, brainstem and spinal cord (Figure 1.1). The clinical picture is determined by the 'center of gravity' of the progression of the disease (Shaw, 2001). While spasticity, slow speech, and clonic jaw reflexes are the representatives of upper motor neuron (UMN) degeneration, atrophy, fasciculations and weakness are of lower motor neuron (LMN) degeneration (Lomen-Hoerth, 2008; Aguilar *et al.*, 2007).

'Amyotrophic', a combination of Greek terms where 'a' stands for negative, 'myo' for muscle and 'trophic' for nourishment, describes the progressive skeletal muscle atrophy due to the progressive loss of motor neurons. The atrophy of the large motor neurons in the spinal cord replaces them with fibrous astrocytes which results in the hardening of the anterior and lateral columns, hence the term 'lateral sclerosis' (Hirano, 1991; Aebischer *et al.*, 2007).

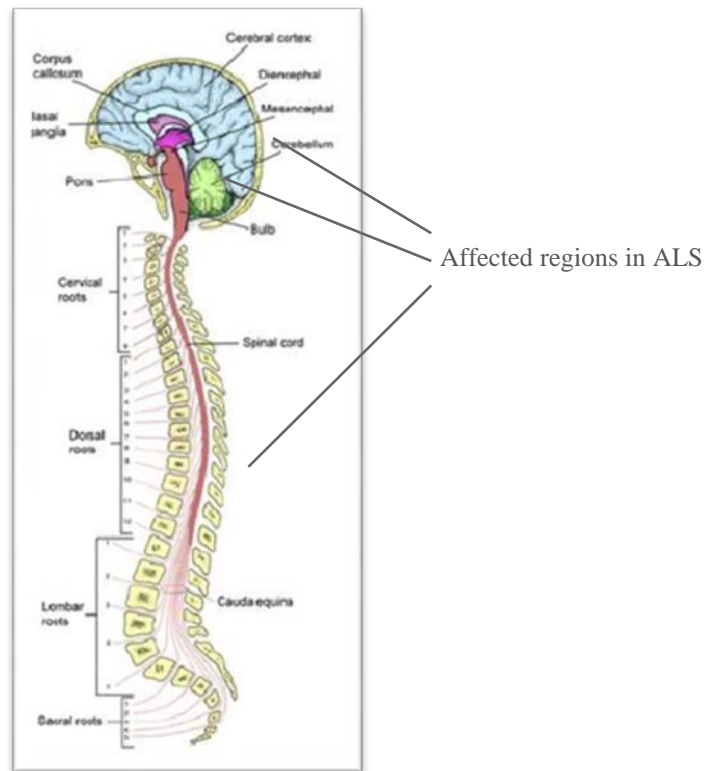


Figure 1.1. Affected regions in ALS

ALS is a progressive disease in which weakness in extremities results in total paralysis, except for extraocular muscles and pelvis sphincter which are controlled by motor neurons in the oculomotor nuclei in the brainstem and Onuf's nuclei in the spinal cord, respectively (Shaw *et al.*, 2005; Cluskey *et al.*, 2001). Generally, sensory and cognitive functions are mostly spared. Even though several studies have shown executive dysfunction and mild memory decline, implying cognitive impairment, more research is needed for a definite understanding (Abrahams *et al.*, 2005).

ALS has an incidence of two to three per 100,000, fairly uniform throughout the world, with several exceptional high incidence foci, like the island of Guam and the Kii peninsula (Shaw *et al.*, 2005). The prevalence is six to ten per 100,000 (Roman *et al.*, 1996). Although ALS is mostly described as late-onset, juvenile forms are also observed (Figure 1.2a). Death occurs within two to five years as a result of respiratory failure (Cleveland, 1999) (Figure 1.2b). However, long-term survival is also observed which is associated with the site of symptom onset (Figure 1.2c).

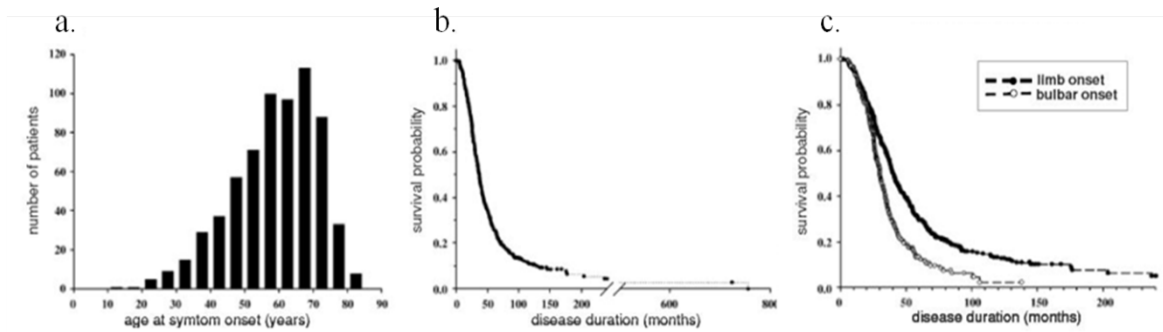


Figure 1.2. Demographics in ALS (adapted from Strong, 2003)

Approximately, 10 per cent of ALS cases are familial (FALS), whereas sporadic ALS (SALS) comprises 90 per cent (Julien, 2001). Interestingly, FALS and SALS are almost indistinguishable in terms of clinical features. However, minor differences are present. First of all, the age of onset is around 46 years in FALS, compared to 56 years for SALS. Secondly, the male:female ratio is 1:1 in FALS, whereas it is 1.7:1 in SALS (Veldink *et al.*, 2003). However, the ratio in SALS decreases with increasing age and reaches a 1:1 ratio after 70 years of age. Thirdly, the prognosis of FALS patients is usually longer than SALS patients (Hand *et al.*, 2002).

1.1. Histopathological Features of ALS

The pathological findings specific to ALS have been grouped into four different stages, depending on the time course of muscle strength changes in an ALS mouse model. These are pre-muscle weakness stage (PMW), during which muscle strength is maintained at the normal level, rapid decline stage (RD), during which there is a sharp decline in muscle strength up to 50 per cent, slow decline stage (SD), during which a slow decline in ability is observed and paralysis (Para), during which paralysis of limb muscles has begun and the mouse can no longer hold onto the wire (Kong *et al.*, 1998). The time and amount of degeneration of axons in spinal cord is in concordance with the motor neuron loss which is indicative of reciprocal interaction of these cells (Figure 1.3).

The most prominent feature of the PMW stage is the presence of abnormal mitochondria, including dilated and disorganized cristae, leakage of the outer membrane, broken outer membrane and early vacuoles that still carry remnants of mitochondria

(Jaarma *et al.*, 2001). The fragmentation of the neuronal Golgi apparatus begins before the onset of RD stage (Stieber *et al.*, 2000). Neurofilament accumulations can be observed adjacent to vacuoles in axons which suggest that failure in slow axonal transport begins before the onset of the RD stage. However, the vacuolation is a transient process: its occurrence is in concordance with the onset of muscle weakness, but the vacuolation decreases in size and number toward the end stage (Kong *et al.*, 1998).

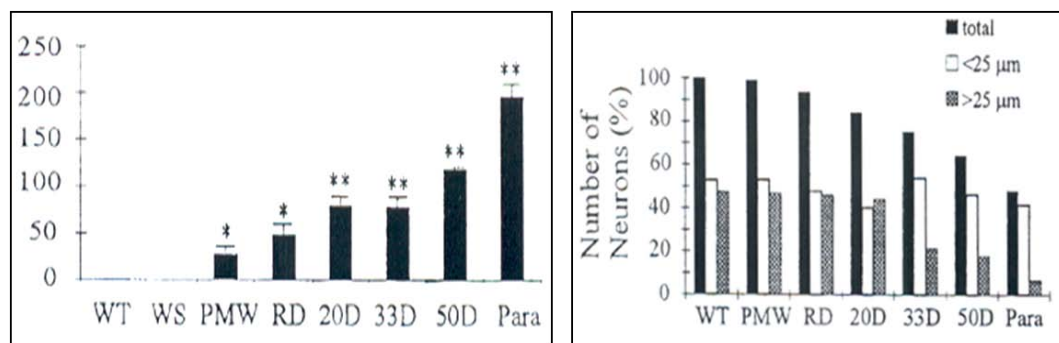


Figure 1.3. a. number of degenerating axons at different disease stages; b. number of motor neurons at different disease stages (Kong *et al.*, 1998).

Other histopathological findings include: i. reactive gliosis, ii. reduced caliber of distal axons, iii. neurofilament (NF) and periferin accumulation in axons and neuronal cell bodies, iv. perikaryal inclusions, consisting of phosphorylated NFs, and sometimes SOD1 and ubiquitin, v. conglomerate hyaline inclusions, consisting of phosphorylated and nonphosphorylated NFs (Rowland *et al.*, 2001, Aguilar *et al.*, 2007), vi. Lewy-body like inclusions and vii. attenuation of dendrites.

1.2. Molecular Genetics of ALS

An important breakthrough in unraveling the molecular mechanisms of ALS was achieved when Deng *et al.* discovered the gene responsible for a group of FALS cases in 1993. This major locus has been localized to chromosome 21q22.1; it encodes the Superoxide Dismutase 1 (SOD1) enzyme (Deng *et al.*, 1993). SOD1 has been related to dominant pattern of inheritance in FALS cases. It is responsible for 20 per cent of all FALS cases which corresponds to 2 per cent of all ALS cases. Mutations in the SOD1 gene

have also been reported for SALS cases, however, the number is fairly small. Since then, many studies have identified different loci/genes responsible for FALS (Table 1.1).

Table 1.1. Genes responsible for FALS

ALS Type	Inheritance Pattern	Onset	Chromosomal Location	Gene	Function
ALS1	AD	Adult	21q22.1	SOD1	Superoxide dismutase, Antioxidant defence
ALS2	AR	Juvenile	2q33	Alsin	Guanine nucleotide exchange factor for RAB5A
ALS3	AD	Adult	18q21	Unknown	Unknown
ALS4	AD	Juvenile	9q34	SETX	DNA/RNA helicase, DNA repair
ALS5	AR	Juvenile	15q15.1-q21.1	Unknown	Unknown
ALS6	AD	Adult	16q12	FUS	DNA-RNA binding, RNA processing
ALS7	AD	Adult	20p13	Unknown	Unknown
ALS8	AD	Adult	20q13.3	VAPB	Vesicle-associated membrane protein
ALS9	AD and sporadic	Adult	14q11.2	ANG	potent inducer of neovascularization and angiogenesis
ALS10	AD	Adult	1q36	TDP-43	DNA-RNA binding
ALS-FTD	AD and sporadic		2q13	DCTN1	Promotion of synapse stability
ALS-FTD-2	AD	Juvenile	9q13.2-21.3	Unknown	Unknown
ALS-FTD-PD	AD		17q	Unknown	Unknown
ALS-FTD-PD	AD		17q21	MAPT	Assembly of microtubules

In search of understanding ALS, since both FALS and SALS show similar clinical and pathological characteristics, SOD1, which seems to be the predominant protein responsible for the disease, has been investigated thoroughly.

1.3. Superoxide Dismutase 1 (SOD1)

Superoxide Dismutase 1 (SOD1) is a small cytosolic protein which is ubiquitously expressed in most cells, including red blood cells (Siddique *et al.*, 1996). It is highly abundant in neurons, comprising approximately 1 per cent of total cytosolic protein (Cleveland, 1999). In humans, it is located on chromosome 21q22.1 and spans 12 kb of DNA. It has five exons and four introns.

The genomic organization of SOD1 is very similar among species. The promoter region comprises TATA and CCAAT boxes, as well as several highly conserved GC-rich regions. Such a high incidence of homology in the 5' flanking region implies that intense

evolutionary factors have preserved key regulatory regions for this gene. The 3' end has poly A sequences that determine the establishment of two mature mRNA transcripts of 0.7 and 0.9 kb (Zelko *et al.*, 2002).

The five exons encode a 21 kDa protein of 153 highly conserved amino acids which functions as a homodimer. The polypeptide chain is folded into a flattened cylinder of eight strands of antiparallel β -structure, which are arranged in two interlocking Greek key motifs to form the β -barrel (Siddique *et al.*, 1996). Inside this β -barrel extends two large nonhelical loops (Figure 1.4). One of these loops contains the essential residues for the establishment of the electrostatic guidance of O_2^- , while the second one contributes to the dimer interface. Stable dimers are formed by strong hydrophobic interactions between individual monomers at the interface. At the end of the β -barrel, each monomer contains a cave-like active site, embedding one atom of copper and zinc. Copper (Cu^{+2}) binding is coordinated by four histidine residues (His46, His48, His63 and His120), while zinc ion (Zn^{+2}) is coordinated by three histidines (His63, His71, His80) and one aspartic acid (Asp83). Thus, His63 is in interaction with both atoms, forming a histidine bridge (Valentine *et al.*, 1999). Cu^{+2} is essential for the dismutase activity, whereas Zn^{+2} is involved in structural stability of the enzyme, maintaining pH stability of the dismutation reaction and the rapid dissociation of the H_2O_2 produced (Cozzolino *et al.*, 2008).

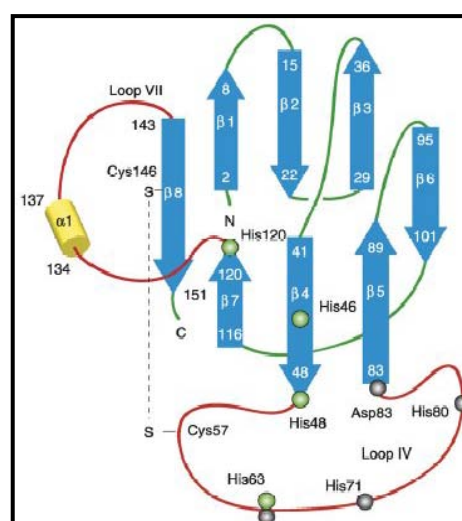


Figure 1.4. Secondary structure of SOD1. Beta strands are shown as blue arrows.

Gray spheres: Zn-binding residues; green spheres: Cu-binding residues

(Shaw *et al.*, 2007).

SOD1 is one of the most important antioxidant enzymes in the cell. The major function of the enzyme is to detoxify O_2^- via forming O_2 and H_2O_2 . H_2O_2 is then further detoxified to H_2O by either glutathione peroxidase or catalase (Figure 1.5). In this respect, O_2^- is guided to the Cu-containing active site through a positively-charged electrostatic guidance channel. This channel is established by twenty-one highly conserved amino acids, and the positive charge is produced by the amino acids Lys122, Lys134 and Arg143. Arg143 stabilizes the position of O_2^- in relation to the Cu atom. The electrostatic guidance channel narrows down in a stepwise fashion from a 24\AA to a 10\AA width and ends up in an opening of less than 4\AA just above the Cu atom. Such a structure enables selective access of small negatively charged O_2^- to the active site. The dismutase activity occurs at a rate of $2 \times 10^9 \text{ M}^{-1} \text{ sec}^{-1}$ (Siddique *et al.*, 1996).

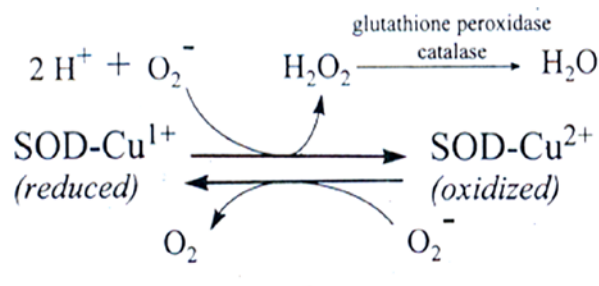


Figure 1.5. SOD1-mediated dismutation of superoxide (Cleveland, 1999).

1.4. Mutations in SOD1 Gene

Until today, 148 distinct mutations have been identified in the SOD1 gene (Jonsson *et al.*, 2009). Most of them are missense mutations, while the rest represent insertions, deletions and splice junction mutations. Polymorphisms have also been detected in SOD1 (Shaw, 2005).

Physical properties of SOD1 (half-life, stability, protein solubility, etc.) differ greatly between various SOD1 mutations, but they do not appear to correlate with severity of the disease (Elliott, 2001). The enzymatic activity of mutant SOD1 enzyme differs, such that some are almost inactive (H46R), while others retain dismutase activity (G93A) (Simpson *et al.*, 2006). More interestingly, there seems to be no correlation between the age of onset or duration of the disease with the dismutase activity. Different mutations do

not exhibit different clinical phenotypes. Similarly, FALS patients with SOD1 mutations are clinically almost indistinguishable from SALS patients (Cole *et al.*, 1999). Different mutations do not seem to affect the onset of the disease. However, they do have an effect on the progression and survival. In North America, the most common mutation among FALS cases is A4V, which exhibits an aggressive rapid progression; death occurs usually within 1.2 years from the age of onset (Rosen *et al.*, 1993). Survival for most SOD1 mutation carriers ranges from three to five years, while H46R, G41D, G93C and G37R have the longest duration of about 18-20 years. Still, even patients of the same family with the same SOD1 mutation can exhibit significant phenotypic differences (Siddique *et al.*, 1996). This suggests that phenotype is finalized with the combinatorial effects of genetic and environmental factors (Shaw, 2005).

SOD1-linked FALS cases were associated with autosomal dominant inheritance pattern. However, today, five different modes of inheritance have been linked to SOD1-FALS: dominant inheritance with high penetrance, dominant inheritance with reduced penetrance, recessive inheritance, compound heterozygosity and a de novo mutation.

1.5. Possible Mechanisms Involved in ALS Pathogenesis

The cytoplasmic dismutase activity of mice carrying a mutation in the SOD1 gene is usually 30-70 per cent of the normal activity (Siddique *et al.*, 1996). Such a decrease may result from the random dimerization of mutant and wild-type heterodimers, which are highly unstable. Formation of an unstable structure also decreases the half-life of the protein: the half-life of the normal SOD1 protein is about 30 hours, whereas half-life of A4V is about seven hours (Siddique *et al.*, 1996). Thus, the initial idea favored the concept that motor neuron degeneration was related to the loss of cell's ability to overcome free radical toxicity.

However, studies with transgenic and knockout mice revealed that the basic mechanism, leading to FALS or SALS phenotype, is not the reduction in dismutase activity (Brown, 1998). Although several mutations, such as A4V or G85R, have reduced dismutase activity, others, such as G37R, G93A or D90A establish normal levels. There is no correlation between the phenotype and the extent of residual SOD1 dismutase activity.

While the deletion of both alleles, thus the absence of normal SOD1 protein, causes no change in phenotype, transgenic mice expressing a mutant protein show progressive motor neuron loss. These results indicate that the scavenging capacity of SOD1 is not related to toxicity. Similarly, the overexpression of the wild-type protein exhibits no phenotypic difference, whereas the overexpression of mutant SOD1 produces a lethal, paralytic state (Elliott, 2001). Overall results imply that mutant SOD1-induced disease is not a consequence of a reduction in dismutase activity, but rather a 'gain-of-function'. Today, eight different mechanisms have been shown to contribute to this gain-of-toxic function.

1.5.1. Oxidative Damage

Reactive oxygen species (ROS) are by-products of aerobic metabolism (Coyle *et al.*, 1993; Lenaz, 1998). The accumulation of ROS may be very toxic to cells, thus ROS are removed/converted by antioxidant defence mechanisms, including: i. removal by superoxide dismutase, catalase and peroxidase, ii. scavenging by low molecular weight agents (coenzyme Q), iii. limiting the availability of prooxidants, iv. removal or repairment of damaged proteins by heat shock proteins. However, in case of SOD1-linked ALS, the system 'leaks', such that mutations in SOD1 alter the conformation of the protein, leading to a more open conformation where aberrant substances can reach the active site. This toxic property has been associated with two hypotheses (Bendotti *et al.*, 2004).

1.5.1.1. Peroxidase hypothesis. In addition to dismutase activity, SOD1 also has peroxidase activity where it uses the H_2O_2 , produced through dismutase reaction, as a substrate to generate hydroxyl radicals in a Fenton-type reaction (Bär, 2000). However, this reaction is self-limiting.

On the other hand, most ALS mutations exhibit enhanced peroxidase activity. These mutations alter the highly conserved interactions within the homodimer structure. Change in Zn^{+2} -binding capacity leads to destabilization of the protein backbone which causes the opening of the active channel (Yim *et al.*, 1996). As a result, Cu^{+2} located at the active site becomes more accessible to H_2O_2 . Such an interaction causes an increase in the generation of hydroxyl radicals. Higher concentrations of hydroxyl radicals, generated by enhanced peroxidase activity of the mutant SOD1 enzymes, cause damage to cellular

macromolecules, including SOD1 itself. As a result, SOD1 is inactivated and Cu^{+2} is released (Kang *et al.*, 2000).

However, similar evidence for hydroxyl radicals is not found in many other transgenic mouse models at any stage of the disease. Also, vitamin E does not appear to alter the outcome of the disease (Ahmed *et al.*, 2000). These results indicate that either different mutations produce disease via different mechanisms or the enhanced peroxidase activity is not necessary for neuronal death.

1.5.1.2. Peroxynitrate hypothesis. Some mutations in FALS cause the clumsy binding of Cu^{+2} to the active site which decreases the normal SOD1 activity, resulting in higher O_2^- concentration. O_2^- can interact with nitric oxide more easily than with native SOD1. NO is a free radical synthesized by nitrite oxide synthases (NOS) in a Ca^{+2} -dependent manner (Estéves *et al.*, 2002). Thus, its activity can be upregulated in conditions, where intracellular Ca^{+2} is raised, such as during glutamate excitotoxicity, which is significantly observed in ALS. The interaction results in increased nitrotyrosine levels.

Also, in the case of Zn^{+2} -deficiency, mutant subunits of SOD1 fail to bind or retain Zn^{+2} efficiently (Liohev *et al.*, 2003). In this case, rather than acting as a scavenger of O_2^- , Zn^{+2} -deficient SOD1 steals e- from cellular antioxidants and transfer these e- to O_2 to produce O_2^- (Williamson *et al.*, 2000). Then, this superoxide combines with NO to form peroxynitrite.

Neurofilaments are exceptionally vulnerable to nitration. The interaction between NFs and Zn^{+2} -deficient SOD1 is a vicious cycle: As more Zn^{+2} is bound to NFs, more Zn^{+2} -deficient SOD1 accumulates and more peroxynitrite is generated, which nitrates NFs, causing more NFs to accumulate until enough peroxynitrite is produced to trigger apoptosis of the cell (Morrison *et al.*, 2000).

On the other hand, both mechanisms regarding oxidative damage by the peroxynitrite reaction have contradictory experimental results. While Cu^{+2} seems like important for proper dismutase activity, when copper chaperones (CCS) were removed, Cu^{+2} loading to SOD1 was reduced at least 90 per cent, but no change in disease onset,

progression or pathology was observed (Subramania *et al.*, 2002). Similarly, in a cell culture model, limiting NO synthesis by inhibition of NOS by 14-folds was expected to ameliorate disease. However, neither the onset nor the progression of the disease were altered (Cleveland *et al.*, 2001). Thus, the predominant role of oxidative damage in ALS pathogenesis should still be considered with caution.

1.5.2. Glutamate-induced Excitotoxicity

Glutamate is the major excitatory amino acid (EAA) neurotransmitter in the central nervous system (Brown *et al.*, 2000). It is released from the presynaptic neuron to the synaptic cleft via a Ca^{+2} -dependent mechanism and binds to two types of receptors on the postsynaptic membrane: ionotropic (NMDA, AMPA and kainite receptors) and metabotropic receptors (Figure 1.6) (Hand *et al.*, 2002). NMDA channels are blocked with Mg^{+2} at resting state and Mg^{+2} blockage is removed upon membrane depolarization (Brown *et al.*, 2000). AMPA and kainite receptors are the primary regulators of fast excitatory neurotransmission (Kwak *et al.*, 2005). Binding of glutamate to AMPA opens up the associated ion channels, resulting in the entry of Na^{+} and H_2O . This depolarization, leading to the opening of NMDA receptor-linked Na^{+} - Ca^{+2} channels, facilitates Ca^{+2} influx, resulting in the excitation of neurons.

Glutamate-induced excitotoxicity is a pathological process which causes degeneration of motor neurons due to the disruption of intracellular Ca^{+2} homeostasis and production of free radicals (Heath *et al.*, 2002). The involvement of glutamate in ALS pathogenesis was first thought upon when increased levels of glutamate and aspartate were detected in cerebrospinal fluid of ALS mice (Hand *et al.*, 2002).

Excess activation by glutamate can cause cell death via increase in Ca^{+2} level (Julien, 2001). Thus, it should be removed from the synaptic cleft. The activity of glutamate at the synaptic cleft is regulated by receptor inactivation and high-affinity glutamate up-take by transporter proteins, named excitatory amino acid transporters, EAAT (Figure 1.6). So far, five EAAT (EAAT1-5) have been identified. Among these, EAAT2 is expressed specifically in astrocytes (Maragakis *et al.*, 2001). 60-70 per cent of SALS patients were shown to have a loss of 35-95 per cent of EAAT2 protein in the motor

cortex and spinal cord (Cluskey *et al.*, 2001), while no change in number of astrocytes occurred (Lin *et al.*, 1998; Maragakis *et al.*, 2004). Several studies have shown that the decline in EAAT2 protein levels is a consequence of aberrant translation or post-translational processing, such as exon skipping and intron retention (Deitch *et al.*, 2002).

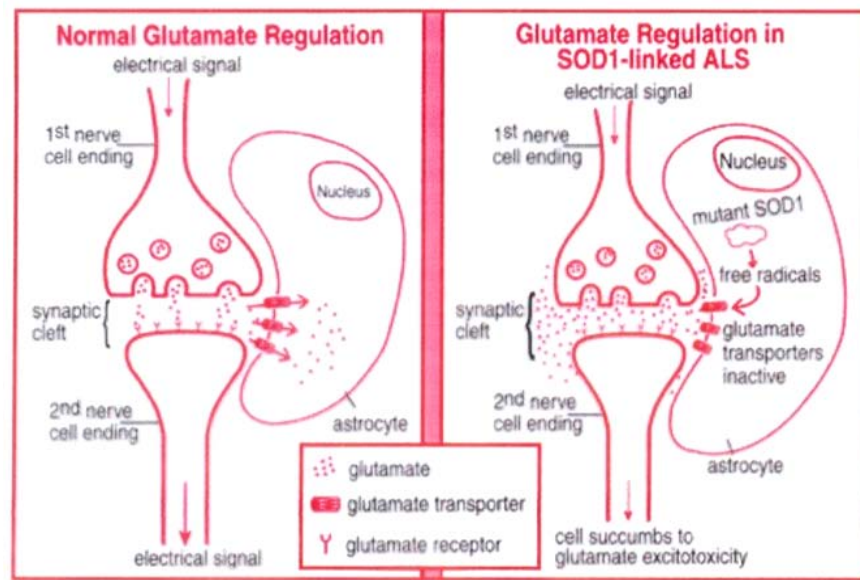


Figure 1.6. Glutamate release mechanism in normal and ALS cases
(<http://www.als-mda.org>)

The inadequate removal of glutamate due to EAAT2 deficiency results in increase of glutamate concentration in the synaptic cleft (Boillée *et al.*, 2006). Continuous binding to the postsynaptic membrane causes continuous stimulation of Ca^{+2} -permeable AMPA channels, resulting in further depolarization and Ca^{+2} release to cytoplasm. Motor neurons are highly vulnerable to such a condition because of two main properties: i. low Ca^{+2} -buffering capacity due to low expression of Ca^{+2} -binding proteins (Van Damme *et al.*, 2002) and ii. relatively high expression of Ca^{+2} -permeable AMPA receptors, lacking GluR2 subunit (high Ca^{+2} permeability) (Van Den Bosch *et al.*, 2006). At the final curtain, mitochondria get into action; however, in ALS, mitochondria also lose their Ca^{+2} -buffering ability after a certain time (Menzies *et al.*, 2002). Thus, motor neurons are taken to apoptosis.

Today, although glutamate-induced excitotoxicity being a cause or consequence in ALS pathogenesis is still discussed, so far, the only 'effective treatment' in ALS has been

an anti-glutamate drug, riluzole (Labomblez *et al.*, 1996), which impedes disease progression via inhibition of glutamergic transmission, an implication of a crucial role of excitotoxicity in ALS pathology (Meininger *et al.*, 2000).

1.5.3. Protein Aggregation

When a protein is misfolded in cytoplasm, firstly, chaperon proteins act upon and refold the abnormal protein. If not succeeded, ubiquitin-proteasome pathway (UPS) is activated where the misfolded protein is first ‘tagged’ by ubiquitins (Ub) and then degraded to small fragments by proteasome (Ross *et al.*, 2005). However, this mechanism is compromised in most neurodegenerative diseases.

Conformational instability of mutant SOD1 results in the formation of intracellular aggregates, a very common hallmark of neurodegenerative diseases (Pasinelli and Brown, 2006). These aggregates occur before the onset of disease in motor neurons and astrocytes and increase in abundance during progression (Mendonca *et al.*, 2006). They are ‘non-native, sub-microscopic and detergent-insoluble structures which include mutant SOD1, as well as CCS, heat shock proteins (HSP), NFs, Bunina bodies, Ub and hyaline inclusions (Cozzolino *et al.*, 2008). Aggregation of mutant SOD1 is selective for motor neurons. The sequence of events is misfolding, followed by polyUb, accumulation, aggregation and inhibition of UPS (Figure 1.7) (Urushitani *et al.*, 2002).

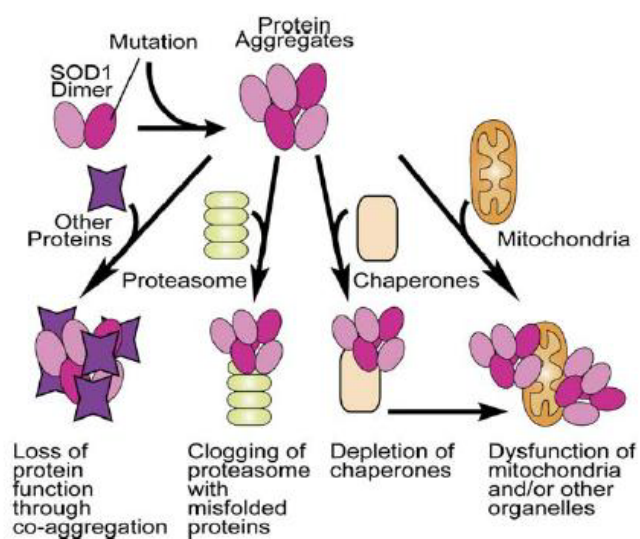


Figure 1.7. Possible cellular effects of mutant SOD1 aggregation (Boillée *et al.*, 2006)

However, there is still uncertainty as to whether: i. protein aggregates are toxic for the cell because they sequester other proteins necessary for normal cellular functions and disrupt retrograde transport (Bruijn *et al.*, 2004), ii. these structures are beneficial such that they help the removal of toxic material from the cytoplasm or iii. they are harmless by products of degenerating process (Shaw, 2005).

1.5.4. Cytoskeletal Abnormalities and Defects in Axonal Transport

Motor neurons are composed of a cell body, extensive dendrites and axonal processes and this special morphology is established by cytoskeletal elements and continuous transport of organelles from the cell body to the axonic end (anterograde transport by kinesins) and vice versa (retrograde transport by dyneins). The neuronal cytoskeleton is composed of microtubules, actin and neurofilaments (Ström *et al.*, 2008).

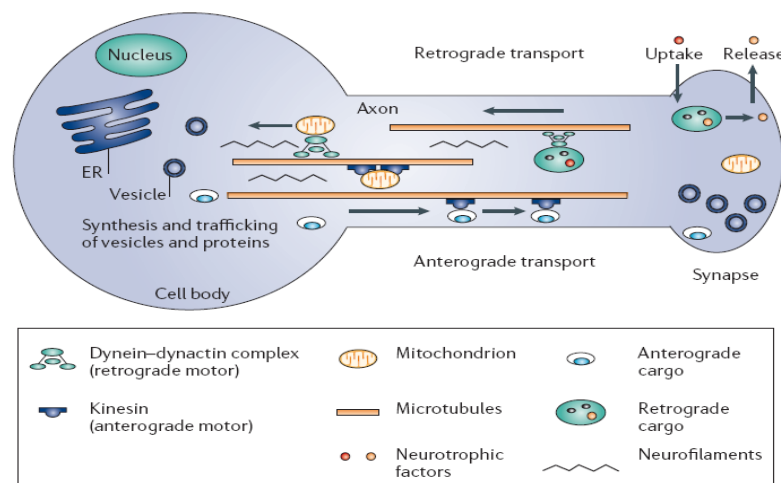


Figure 1.8. Axonal transport in motor neurons (Pasinelli and Brown, 2006)

Neurofilaments, the major type of IF in motor neurons, are cytoskeletal proteins that are subcategorized as light (NF-L), medium (NF-M) and heavy (NF-H) (Julien *et al.*, 2000). While NF-L forms the core of the NF neurofibril, the tail domains of NF-M and NF-H spread radically from the neurofibril to establish the spacing between adjacent neurofibrils and interactions with other proteins. NF-L is responsible for forming heterodimers with NF-M and NF-H to establish the proper 10 nm filaments, while NF-H and NF-M control axonal caliber (Lee *et al.*, 1996).

NFs are detected in the form of spheroids in motor neurons of 1 per cent of SALS patients. Accumulations in cell body and proximal axons of motor neurons can occur in mice overexpressing NF-L or NF-H subunits or in mice expressing mutations in NF-L (Xu *et al.*, 1993; Cote *et al.*, 1993; Lee *et al.*, 1994). Also, one per cent of SALS patients were shown to carry mutations in the KSP repeat region of NF-H (Figlewicz, 1994). Interestingly, the overexpression of NF-H, despite of forming accumulations, improves survival as of six months in mutant SOD1 mice. Two hypotheses are suggested. The first one claims that NFs act as Ca^{+2} chelators . They have multiple Ca^{+2} -binding sites. Thus, by scavenging the toxic amount of Ca^{+2} that accumulated due to glutamate excitotoxicity, the motor neurons are rescued (Cluskey *et al.*, 2001). Alternatively, the second hypothesis suggests the role of acting as a sink for ROS. This way, the destructive effects of these toxic molecules are reduced (Couillard-Despres *et al.*, 1998). However, no definite change in pattern or amount of protein-bound neurotoxicity has been detected so far.

Both anterograde and retrograde transports are disturbed in ALS (Sasaki *et al.*, 1996). Fast and slow axonal transports are responsible for transport of cargo necessary for synaptic activity and axonal cytoskeletal of cytosolic proteins, respectively (Barry *et al.*, 2007). Dynein protein works in complex with dynactin and mutations have been detected in the p150 subunit of dynactin (Laird *et al.*, 2005). The expression of this mutant in transgenic mice results in 60 per cent decrease in motor neuron number (Puls *et al.*, 2003).

Mutant SOD1 interaction with dynein-dynactin complex may be through several pathways: i. sequestration of dynein, ii. disassembly of microtubule formation and disruption of stability, iii. interruption of motor activity of dynein, iv. disruption of dynein-dynactin complex, v. interruption of interaction of dynein-dynactin complex with microtubule or vi. 'masking' of cargo-binding proteins (Ström *et al.*, 2008).

In total, the aberrant increase in dynein-mutant SOD1 interaction and decline in dynein-dynactin function have several consequences: i. reduced transport of neurotrophic factors, responsible for long-term survival of motor neurons, ii. disruption of distribution and dynamics of mitochondria and iii. impairment of structure and function of ER-Golgi network (Burkhardt *et al.*, 1997). When a certain threshold is reached, deficits in reduced retrograde transport can no longer be tolerated by motor neurons; thus, motor neuron

degeneration occurs (Ström *et al.*, 2008). On the other hand, dynein displays an autophagic function where it binds misfolded proteins at the distal end and transports them retrogradely to the cytoplasm. In the cytoplasm, aggresomes are formed and attached to the membrane with the guidance of lysosomes (Johnston *et al.*, 2002; Taylor *et al.*, 2003). Considering the tendency of mutant SOD1 to interact with dynein-dynactin complex, such an interaction between the mutant protein and the transport protein complex may be beneficial for the sequestration of mutant SOD1 into aggresomes and inhibition of its toxic effects via autophagy (Gal *et al.*, 2007).

1.5.5. Mitochondrial Involvement in ALS

Mitochondria are the ‘powerhouses of cells’ due to their ATP-producing ability (Menzies *et al.*, 2002). They have three main functions in cells: i. supplying energy (ATP) for various cellular functions through respiratory chain reaction, ii. establishing Ca^{+2} homeostasis in neurons via sequestering excess cytoplasmic Ca^{+2} and iii. leading cells to enter apoptosis when cellular toxicity cannot be controlled. In general, they build up a balance between life and death in cells (Hervias *et al.*, 2006).

In ALS, mitochondria display both morphological and functional changes (Manfredi *et al.*, 2005). Morphological changes include the formation of vacuoles through the expansion of the outer membrane, together with the shrinkage of the inner membrane and dilated structure with disorganized cristea (Xu *et al.*, 2004). These morphological changes bring about several functional defects:

- mitochondria membrane becomes depolarized which reduces the efficiency of the respiratory chain reaction,
- decline in bioenergetic occurs as a result of decrease in the capacity to consume O_2 and to synthesis ATP,
- Ca^{+2} -buffering capacity is impaired. This has two main consequences. Firstly, mitochondria are in charge of short-term buffering of Ca^{+2} . When there is repetitive stimulation by glutamate (like in ALS), decline in such a property results in accumulation of Ca^{+2} in cytoplasm, leading to glutamate-induced excitotoxicity (Tateno *et al.*, 2004). Meanwhile, elevated Ca^{+2} level destructs mitochondrias’

integrity and encourage free radical production from mitochondria, leading to cumulative oxidative stress (Reynolds 1999). Such an increase in ROS inactivates Ca^{+2} -binding proteins, resulting in further excitotoxicity (Figure 1.9) (Hervias *et al.*, 2006).

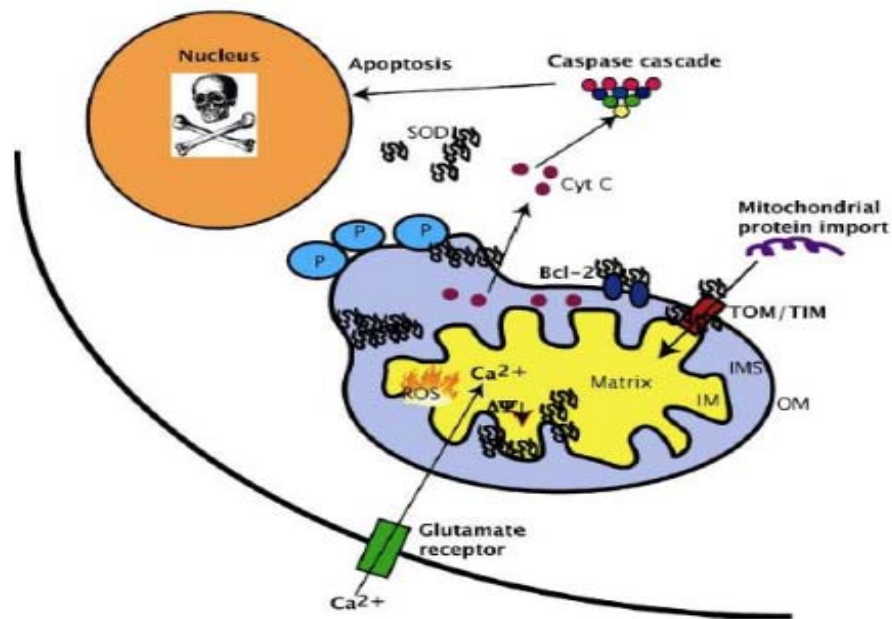


Figure 1.9. Mitochondrial dysfunction in ALS (Manfredi *et al.*, 2005)

Meanwhile, mutant SOD1 penetrates into mitochondria and localizes to inner membrane, matrix and outer membrane (Kwong *et al.*, 2006). Defects in morphology and decline in function trigger apoptotic pathway with the release of cytochrome c. Factors that initiate cytochrome c release are: i. translocation of proapoptotic Bax to mitochondria, ii. the porous structure of outer membrane, iii. entry of mutant SOD1 to mitochondrial interspace and iv. interaction of mutant SOD1 with Bcl-2 in mitochondria (Ly *et al.*, 2006). The outcome of these events is apoptosis (Pasinelli and Brown, 2006).

1.5.6. Non-cell autonomous Nature of Motor Neuron Death

The first evidence of the contribution of nonneuronal cells in ALS pathogenesis was that expression of mutant SOD1 in neither motor neurons nor glia cells on its own resulted in motor neuron degeneration (Pramatarova *et al.*, 2001; Gong *et al.*, 2000). Then, chimeric animal models were constructed. When mutant SOD1-expressing motor neurons

were neighbored with nontransgenic glial cells, delayed onset and extended survival were observed. In a reciprocal cross, motor neurons with wild-type SOD1 were again affected, probably due to mutant SOD1-expressing glial cells (Lobsiger *et al.*, 2007). Thus, it is concluded that mutant SOD1 expression in motor neurons determine disease onset, while mutant SOD1 expression in glial cells mediates disease progression (Clement *et al.*, 2003). Today, it is strongly accepted that neurodegeneration of motor neurons in ALS is a consequence of toxicity by combinatorial contributions of vulnerable motor neurons and their neighboring non-neuronal cells (Lobsiger *et al.*, 2007).

Glial cells are microglia, astrocytes and oligodendrocytes. The possible involvement can be generalized as either direct toxicity or reduction in the supporting function to neurons (Figure 1.10). Astrocytes play a vital role in the regulation of motor neurons' function and viability via the 'shaping' of synaptic integrity, strength and plasticity through the release of neurotrophic factors (BDNF, CNTF, GDNF and VEGF) and regulation of synaptic glutamate level (EAAT2 transporter) (Jullien, 2007; Staats *et al.*, 2009). Astroglial cells have multiple effects:

- EAAT2 level is highly decreased, leading to excitotoxicity.
- Activated astroglia lose their ability of providing neurotrophic factors to motor neurons.
- The integrity of synaptic cleft is disturbed.
- Inflammatory response elements are released.
- NF- κ B stimulates the release of cyclooxygenase 2 (COX2). This increases the synthesis rate of prostaglandins, resulting in the free radical generation and triggering of glutamate release from astrocytes. Such events will exacerbate the situation via both oxidative stress and excitotoxicity.
- NO synthesis is highly initiated. NO can diffuse through cell membrane, infuse to motor neuron cytoplasm, interact with mutant SOD1 and produce peroxynitrate. Reciprocally, ROS in motor neurons can interact with glutamate transporters on the surface of astrocytes and disrupt their transport ability.

- Neuronal differentiation is induced. Meanwhile, motor neurons are encouraged to become sensitive to AMPA-mediated glutamate stimulation, meaning high permeability to Ca^{+2} , and thus vulnerability.
- Chromagrains, chaperon-like proteins, induce release of mutant SOD1 to the extracellular space. This alerts microglia and inflammatory elements are released (Van Den Bosch *et al.*, 2008).

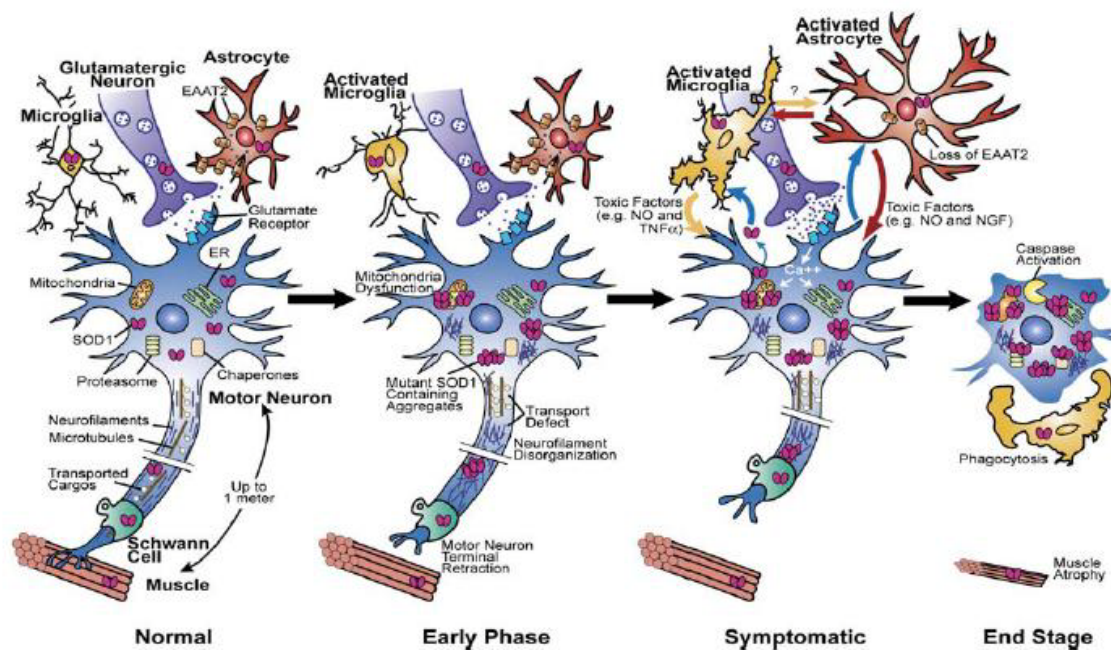


Figure 1.10. Crosstalk between glial cells and motor neurons (Boillée *et al.*, 2006).

Proliferation of activated microglia is a prominent hallmark in ALS, occurring before disease onset (Alexianu *et al.*, 2001). Microglia, macrophages of the CNS, are activated upon inflammation. Microgliosis is a consequence of ‘prolonged/aberrant inflammatory response or a sustained secretion of proinflammatory cytokines’ (Neusch *et al.*, 2007). During microgliosis, NADPH oxidases-dependent oxygen species are produced.

No definite involvement of oligonucleotides in ALS pathogenesis has been proved. However, the presence of these cells in mutant SOD1-induced aggregations aroused interest (Neusch *et al.*, 2007).

In conclusion, the general picture shows that there is a vicious cycle where the inflammatory response generated by glial cells induces proinflammatory elements from

neurons that induce glial cells back and in the final stage, cells are driven to apoptosis (Boillée *et al.*, 2006).

1.6. A Special Focus on Three Autosomal Dominant ALS Genes

1.6.1. TAR DNA binding protein

TAR DNA binding protein (TDP-43) is a 414 aminoacid protein which is coded by the TARDBP gene on chromosome 1. It is ubiquitously expressed in all tissues, including heart, lung, muscle and brain (Kwong *et al.*, 2007). It has six exons and is alternatively spliced to form at least four isoforms (Figure 1.11). The expressed protein consists of two highly-conserved RNA recognition motifs, named RRM1, responsible for binding to single-stranded UG or TG repeats with high affinity, and RRM2, responsible for RNA binding and nuclear export of the protein, and a glycine-rich region at the C-terminal, which may be responsible for protein-protein interactions, its exon skipping and splicing inhibitory activity (Buratti *et al.*, 2001; Wang *et al.*, 2004).

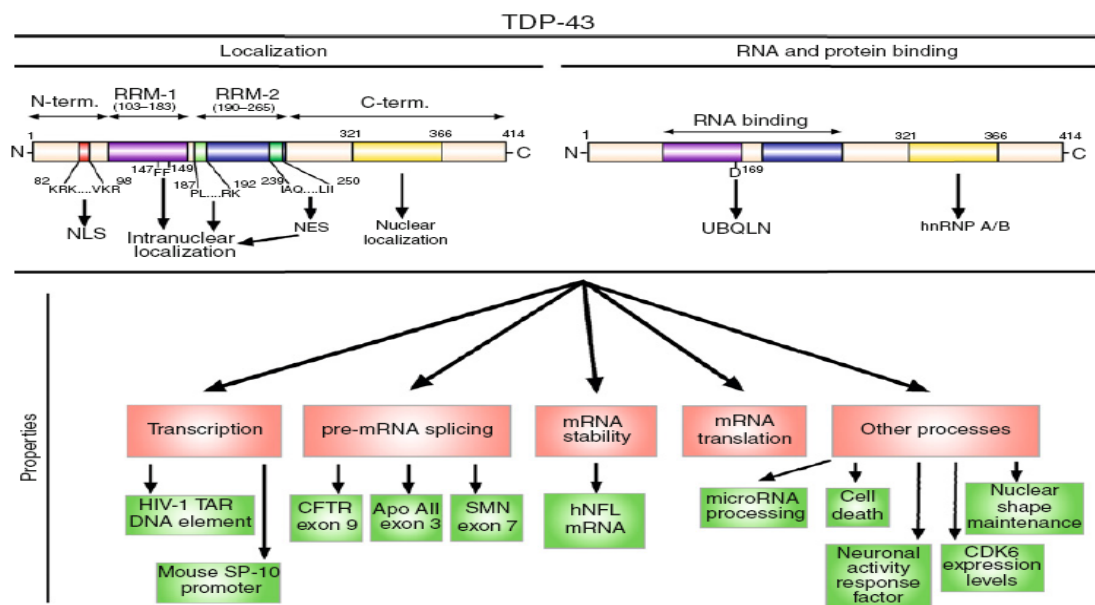


Figure 1.11. The structure and functions of TDP-43 (Buratti *et al.*, 2009)

TDP-43 is very important since it binds both DNA and RNA, thereby exhibits diverse functions, including regulation of transcription, pre-mRNA splicing, mRNA

stability, mRNA translocation, cell death, neuronal activity response, CDK6 expression and the maintenance of nuclear shape.

In normal conditions, TDP-43 is predominantly located in the nucleus, only a small portion is present in the cytoplasm. However, in ALS, biochemical modifications (ubiquitination, hyperphosphorylation and degradation) occur which causes changes in the localization and the function of the protein (Figure 1.11). Firstly, there is an obvious increase in the cytoplasmic level where it tends to aggregate and form insoluble ubiquitin-positive inclusions with C-terminal fragmented, hyperphosphorylated TDP-43 (Pesiridis *et al.*, 2009). These inclusions are present in both SALS and non-SOD1 linked FALS cases. However, the absence of these aggregates in SOD1-FALS cases evokes the idea that the motor neuron degeneration may be different for SOD1-positive and non-SOD1 cases (Cook *et al.*, 2008). Secondly, under normal conditions, TDP-43 is responsible for the regulation of phosphorylation processes. However, in disease state, it itself is hyperphosphorylated. Thirdly, the degradation of the protein is established by UPS. Unlike wild-type TDP-43, the mutant protein cannot interact with UPS, thus it accumulates in the cytoplasm.

Thus far, 70 different mutations have been identified. These are all missense mutations, except for one truncating mutation (Van Damme *et al.*, 2009). They are majorly in highly-conserved amino acids in exon 6. These mutations at different sites may exhibit their deleterious effects through hyperphosphorylation or increasing the tendency to aggregate via the formation of disulfide bonds. All mutations have been linked to autosomal dominant inheritance with mostly extremity involvement. They are responsible for 4.8 per cent of FALS cases (Corrado *et al.*, 2009).

Today, it is still doubtful whether mutant TDP-43 exhibits a loss of function or a gain of function effect. Loss of function theory declares that since it is involved in the regulation of major cellular events, many cellular processes will be misregulated. Meanwhile, gain of function theory states that the deleterious effect of the mutant protein is more destructive to the cell than the absence of nuclear TDP-43. Yet, there is still a lot to be discovered.

1.6.2. Fused in Sarcoma

In the light of the finding of TDP-43 DNA-RNA binding protein in ALS, Vance *et al.* sequenced other DNA-RNA binding genes in a large British family with FALS and identified a mutation in the Fused in Sarcoma (FUS) gene (Lagier-Tourenne *et al.*, 2009).

FUS gene, located on chromosome 16, is a 526 amino acid protein which consists of 15 exons. It has a SYQC-rich region at the N-terminal which functions as a transcriptional activation domain, two G-rich regions, an RNA binding domain, a Cys₂/Cys₂-zinc finger domain and RGG-rich region at the C-terminal which contains a nuclear localization signal domain (Figure 1.12). It is ubiquitously expressed in all cells. Under normal physiological conditions, it is predominantly located in the nucleus (Morohoshi *et al.*, 1998).

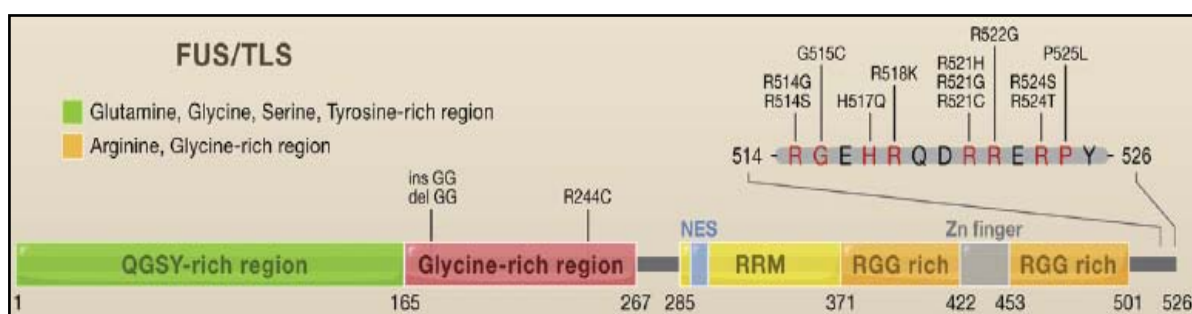


Figure 1.12. Schematic representation of FUS

FUS is also involved in the regulation of transcription, mRNA splicing, translation and mRNA transport to cytoplasm (Vance *et al.*, 2009).

FUS have been shown to be the third most significant gene responsible for autosomal dominantly inherited FALS (4 per cent) (Slegers *et al.*, 2009). These cases are represented with symmetrical, proximal and axial weakness at onset which is fairly different from classical ALS where a single limb at the distal is affected (Ravits *et al.*, 2007). The age of onset and duration vary between and within mutations. Most mutations are the substitution of arginine at the carboxyl terminus. Analysis of brain and spinal cord specimen from ALS patients carrying a FUS mutation showed the normal presence of FUS in nuclei but abnormal aggregates in cytoplasm. It is still not clear whether it is the loss of

function or the gain of function of FUS that creates a disease pathology, but the discovery of TDP-43 and FUS, two RNA binding proteins, arises the attention on genes involved in RNA processing (Traynor *et al.*, 2009).

1.6.3. Angiogenin

Angiogenin (ANG) is a member of the pancreatic RNase superfamily which is responsible for new blood vessel formation. It has been conserved in all vertebrates. ANG gene is located on chromosome 14 and encodes a 14kDa product (Greenway *et al.*, 2006).

ANG is stimulated upon hypoxia and triggers angiogenesis. It is also expressed in the nervous system where it acts as a hypoxia inducible factor; thus, it exhibits a neuroprotective role for motor neurons under hypoxia or excitotoxicity (Kieran *et al.*, 2005). It also acts on endothelial cells in the nervous system and helps maintenance of normal vasculature.

Thus far, 14 missense mutations have been identified. ANG has been described as the second most frequent gene shown to be responsible for ALS, following SOD1, at least in some populations (Kishikawa *et al.*, 2008). These mutations are different from other gene mutations in that they exhibit a definite loss of function effect. The mutated protein lacks the ability to stimulate neurite outgrowth and to protect neurons from hypoxia (Wu *et al.*, 2007).

1.7. D90A-SOD1 Mutation: a Possible Protective Factor in Homozygotes

Following the identification of SOD1 as an ALS-causing gene, many mutations were identified, all of which were linked to autosomal dominant pattern of inheritance, including D90A (Robberect, 2000). However, in 1995, in a study by Andersen *et al.*, D90A heterozygotes (2.5 per cent of the Scandinavian population) were shown to be phenotypically normal, while only D90A homozygotes displayed ALS phenotype (Andersen *et al.*, 1995; Sjalander *et al.*, 1998). In North American and most European populations, D90A heterozygotes exhibit a rather aggressive phenotype where the symptoms can initiate from any territory and the disease progression is rapid (Robberect *et al.*, 1996; Parton *et al.*, 2002). Meanwhile, D90A homozygotes in Scandinavian

populations share a highly distinctive phenotype of a limb-onset slow-progression with a median survival of 11.7 years (Andersen *et al.*, 1996). Also, mutations that cause gain-of-function are inherited in a dominant manner. Indeed, the same mutation exhibiting both dominant and recessive pattern of inheritance for the same disease is very unique (Jonsson *et al.*, 2002).

Such a diversity in the clinical picture and transmission between populations arose the idea of a possible protective factor linked to D90A-SOD1 in Scandinavian populations (Andersen *et al.*, 1997). This factor not only reduces the susceptibility to the harmful effects of the mutant SOD1, but also modifies the clinical phenotype of Scandinavian D90A homozygotes. This hypothesis initiated linkage studies (Al-Chalabi *et al.*, 1998). The existence of a protective factor were supported by six notions:

- D90A mutation is inherited in an autosomal dominant manner by default since recessive families share a single common founder whereas dominant families share several.
- D90A is located nearby a β -barrel on the periphery of SOD1; it has little influence on dimer-dimer interaction or the catalytic activity; it is a highly conserved position. However, another mutation at the same position (D90V) is dominantly-inherited which disproves the emphasis on unimportant position.
- When toxic gain-of-function is considered, having two copies of the mutant allele should exabarate the disease phenotype. N86S is located at a similar position to D90A. N86S homozygotes exhibit a very severe phenotype with an onset of 13 years and survival of 14 weeks whereas D90A homozygotes, by contrast, exhibit a milder slowly-progressive phenotype (Hayward, 1997).
- While dominant D90A cases show a great diversity in phenotype, recessive cases show a uniform clinical picture.
- The allele frequency in Northern Scandinavia is 2.8 per cent (Beckman *et al.*, 1973), while it is 0.03 per cent in UK (Harris *et al.*, 1974). However, the presence of both recessive and dominant D90A families in Scandinavia cannot be a consequence of high incidence, since none of the heterozygotes in the recessive

families develop ALS (even some who are ≥ 90 years old) and >50 per cent of heterozygotes in other European populations do.

- The risk of D90A heterozygotes in Scandinavian populations is not any higher than of the rest of the population, while in Non-Scandinavian populations, the presence of a single mutant allele increases the risk of developing ALS (Broom *et al.*, 2009).

These studies argued that D90A common founder arose 895 generations ago where the recessive haplotype was of Scandinavian origin, going back to 63 generations and was distributed throughout the world by Viking migration (Broom *et al.*, 2006).

Linkage is 'the tendency of genes or loci to be inherited together as a result of their close proximity on a single chromosome' (Strachan and Read, 1999). Since this modifier factor is believed to be population-specific, it should be segregating along with D90A mutation, probably closely located to the SOD1 gene. Thus, the strategy in search of a modifying protective factor is linkage analysis which aims to statistically associate a genetic variant with a disease, based on the cosegregation of variants and disease in families. Different groups have studied recessive and dominant D90A pedigree in only Scandinavian, only European and both Scandinavian and European population (Figure 1.13) (Al-Chalabi *et al.*, 1998; Parton *et al.*, 2002).

In 2006, Broom *et al.* analyzed promoters and coding sequences of the four genes that reside between Shylock and Goneril (LOC150051, FBXW1BP1, KIAA1172 and LOC140282) (Broom *et al.*, 2006). None of the identified 15 variations was associated positively with D90A homozygosity.

Since sequence alterations that reside in the noncoding regions may also affect the expression of the splicing of a gene, the next aim was the sequencing of the entire 265 kb region between Shylock and Goneril. Scandinavian D90A homozygote and heterozygote samples were further analyzed using microsatellite markers. No polymorphic repeat sequences were detected downstream of SOD1. However, recombination was observed in five novel polymorphic markers upstream of SOD1 which enabled the narrowing of the candidate region to 107 kb between M20 and Goneril. Single nucleotide polymorphisms

(SNP) analysis within this region did not reveal any recombination event, thus the whole conserved 107 kb region was fully sequenced. The candidate protective factor should be: i. present homozygously in D90A homozygote recessive families, ii. absent in affected D90A heterozygote dominant families, iii. present in D90A heterozygote Scandinavian populations and iv. absent in affected D90A heterozygote non-Scandinavian populations. In total, 1130 potential insertion-deletions and 291 SNPs were identified; however none of these variations revealed a positive association (Broom *et al.*, 2009).

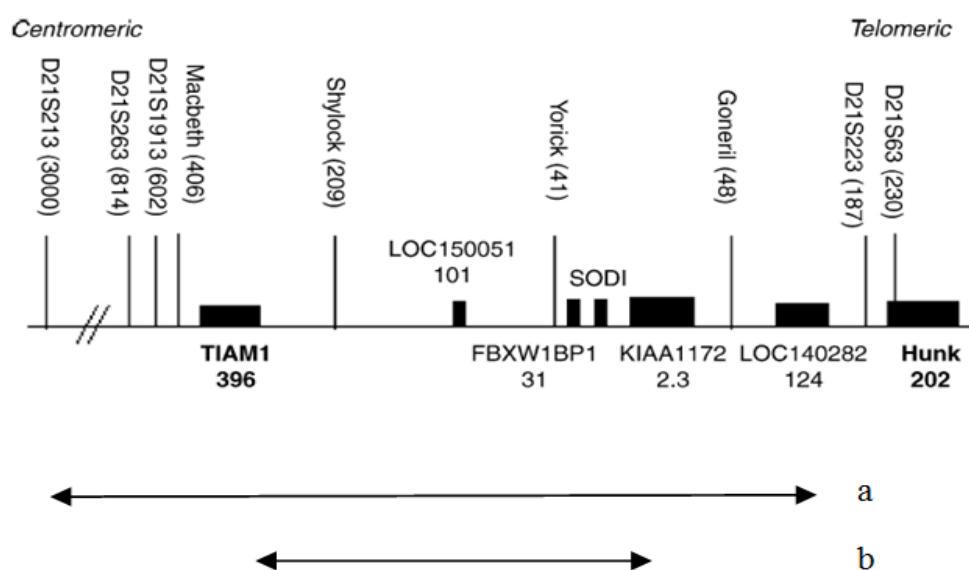


Figure 1.13. The results of the first (a) and second (b) linkage studies around the SOD1 gene in D90A homozygous patients (revised from Broom *et al.*, 2006)

In conclusion, the current data indicate that Scandinavian D90A haplotype is not linked to a protective factor. The difference in mode of inheritance and phenotype was addressed by two hypothesis: i. D90A is a only a benign mutation that can exhibit a disease phenotype when present in two copies. In non-Scandinavian dominant pedigrees, D90A acts as a risk factor that contributes to the disease-causing effect of another yet unidentified cause of ALS. In line of this idea, transgenic mice develop the disease only if they have high level of D90A expression (Brannstrom *et al.*, 1998; Zetterstrom *et al.*, 2007; Jonsson *et al.*, 2009) or ii. there is more than one protective factor in Scandinavian population. Thus, D90A heterozygotes in recessive families do not necessarily lose the protective factor through recombination.

1.8. Genome-wide Association Studies in ALS

Genome-wide association (GWA) approach is defined as a study investigating genetic variations across the entire genome for the identification of genetic associations between observable traits or presence/absence of a disease. In this respect, together with clinical and phenotype data, it increases the chance of unraveling biological processes affecting health state. It relies on the ‘common disease, common variant’ notion which defends the genetic risk for a common disease being mostly related to small number of common genetic variants (Chanock *et al.*, 2007; Hunter *et al.*, 2008; Pearson *et al.*, 2008).

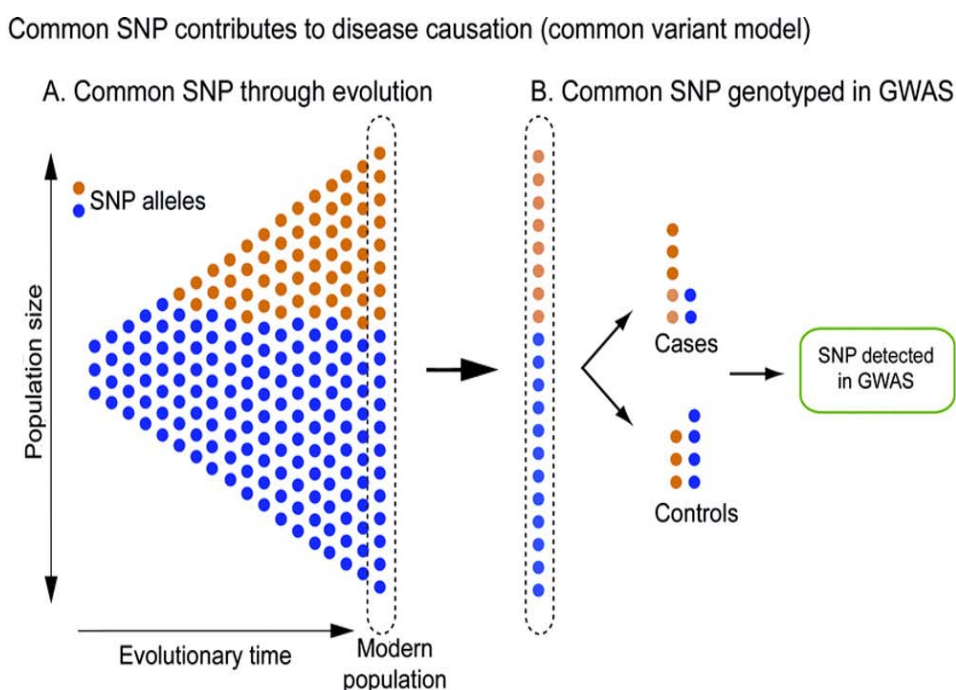


Figure 1.14. Common variants in disease (adapted from Mullen *et al.*, 2009)

The initial GWA analysis is based on the search for single base variations, called as SNPs, which occur more frequently in patients with a particular disease with respect to normal individuals. It is proposed that through generations, a single DNA base is transmitted (blue) until a variant occurs (yellow) which becomes a SNP (Figure 1.14). Initially, the new variant is rare. It exhibits such a small effect so that it is not removed by selection; thus, by random chance through generations, it becomes more frequent.

Several SNPs cluster together on a chromosomal region where they are inherited as blocks, named as haplotype blocks. The human genome is composed of 3 billion bases. Thus far, more than 12 million SNPs have been identified. Since it would be time-consuming and expensive to detect changes in all SNPs individually, a more practical approach has been preferred where SNPs in linkage disequilibrium within a haplotype block is used as a proxy. These are named as 'tagged-SNPs' (Beckmann *et al.*, 2007). Tagged-SNPs point out chromosomal regions with different haplotype distributions in healthy and diseased individuals. In a further attempt, each region would be studied in detail for the identification of location of the definite variant and the corresponding gene. Clearly, this approach increases the sensibility and speed of research.

GWA approach has been more practical, informative and applicable after the establishment of three major practices: the discovery of >10.000.000 SNPs, the construction of the HapMap Project which supplies information on the association between the alleles of the neighbouring SNPs and the development of high-throughput genotyping technologies (Traynor *et al.*, 2007; Wang *et al.*, 2009). The successful applications of this approach have identified novel genetic loci for common diseases, such as age-related macular degeneration (Klein, 2005), type 2 diabetes (Frayling, 2007), heart disease (McPherson, 2007) and cancer (Easton, 2007).

However, when ALS is concerned, the picture becomes more complicated. Various genes have been identified for FALS. The genetics of SALS, on the other hand, is not well-defined; it has still not been completely classified as monogenic, multigenic or multifactorial (interaction of genetic and environmental factors) (Schymick *et al.*, 2007). It is proposed that sporadic forms of ALS are caused by multiple genetic variants which are relatively weak contributors to risk by themselves. Different GWA studies have identified several ALS-associated loci (Table 1.2). However, attempts have not been as successful as expected until now and contradictory results exist. In complex disorders, only a small percentage of the results (1 per cent) could be replicated. For example, the study by Landers *et al.* could not replicate three previously reporter variants in ITPR2, DPP6 and FLJ10986, which were claimed to be involved in susceptibility (Appendix F).

Table 1.2. Genetic variants (SNPs) in SALS that have been identified by GWA

Gene	Localization	Putative Function	Study Population	Replicated
DPP6	7q36.2	alter expression of neuronal A-type K channels	US Caucasin Irish	Yes; US Caucasin, Dutch, Polish
FGGY	1p32.1	possible role in energy metabolism	US Caucasin	No
ITPR2	12p11	mediated intracellular Ca ⁺² release	Dutch, Belgian, Swedish	No
UNC13A	19p13.3	regulates release of neurotransmitters, like Glu, at neuromuscular synapses	Dutch, Belgian, Swedish, Irish,	No
rs2814707 rs3849942	9p21.2	--	Dutch, Belgian, Swedish, German, Polish	No

1.9. Copy Number Variation

Although much has been expected of SNPs in explaining most common disease, they have been shown to be responsible only for 2-15 per cent (McCarroll, 2008). Recently, importance of structural genetic variation in the modification of gene expression and disease phenotype has raised recognition (Ionita-Laza *et al.*, 2009). Among these, copy number variation (CNV) is defined as a structural variation in genome which results in copy number changes in a specific region that spans more than 1000 bases (Freeman *et al.*, 2006). It is considered as a rare variant when observed with a frequency of < 1 per cent. Currently, there are >3600 CNV loci, corresponding to 18 per cent of the whole genome (Blauw *et al.*, 2008).

Several distinguishing features of CNVs compete with SNP analysis. Firstly, although spread widely in the entire genome, SNPs are only one base changes; thus, only minority which affect functional elements may cause a phenotypic variation. On the other

hand, CNVs are large regions, from kilobases to megabases. In this respect, although they are less abundant, any variation in copy number will surely affect a wide range of genes (Sebat *et al.*, 2004). Secondly, when the causative variation is distributed throughout the genome, tagged-SNPs are deficient in discrimination of controls and affected individuals. CNV analysis is more advantageous since it does not require a specific haplotype pattern, but rather relate the overall gene dosage to phenotype (Beckmann *et al.*, 2007). Since the discovery of importance of CNVs in disease, new generation SNP arrays have been developed which also include SNPs within definite and potential CNV regions (McCarroll, 2008).

In a recent paper by Blauw *et al.*, 406 SALS cases with Dutch origin and 450 healthy controls were subjected to whole genome CNV analysis (Blauw *et al.*, 2008). This study revealed CNVs mapped to 935 non-overlapping loci which were insignificant after Bonferroni correction. Further analysis revealed 2238 CNVs with deletions and duplications which affected 2021 genes. However, among these, only gene, named as ENSG00000186259, was homozygously deleted in a majority of patients. Other genes that were mentioned as plausible candidates were ANXA5, GEMIN6 and MTMR7. However, the results of this study have not been replicated yet.

PURPOSE

The aetiology of ALS was a total mystery until the identification of SOD1 as the major gene in FALS which opened up a new era in the investigation of disease-causing mechanisms. Several SOD1-related/induced pathways have been defined in different SOD1 mouse models and cell lines. Recently, two genes have also been implicated in familial cases. In this respect, this study aims

- to search for possible mutations in the previously defined ALS genes in 198 Turkish ALS cases.

Thus far, animal models and cell lines of previously defined ALS genes have not been as informative as expected since they are responsible in total for only ~2 per cent of all cases. Thus, it is important to identify other genes involved in the disease for understanding the pathogenesis. In this respect, this study aims to identify new ALS genes in FALS via

- the utilization of whole genome genotyping strategy in familial and juvenile cases,
- the establishment of a new approach, named whole exome sequencing, which amplifies ~180,000 coding exons of 18,673 protein-coding genes and 551 miRNA exons at once.

ALS is a complex genetic disease with phenotypic heterogeneity. This brings about the importance of relative contributions of genetic and environmental factors. Along this line, this study will contribute to a large-scale genome-wide association study which aims to identify genetic variants that are associated with differing phenotypes in SALS, including site of onset, age of onset, risk and duration of the disease.

Overall, the investigation of the molecular genetics of FALS and SALS from both overlapping and differing perspectives by the utilization of different approaches is expected to identify new ALS-causing genes and modifiers of the phenotype.

3. MATERIALS

3.1. DNA Samples

3.1.1. DNA Samples of Turkish ALS Patients

In the framework of this thesis, a total of 198 ALS patients were analyzed. Among these, 29 were of familial type, while 156 were sporadic and 13 were juvenile patients. Samples referred by each center are shown in Table 3.1.

Table 3.1. Centers that have sent ALS samples to NDAL

Medical Center	Sample Number
İstanbul University, Çapa Medical School, Dept. of Neurology	68
Çukurova University, Medical School, Dept. of Neurology	63
Personal Contacts	20
ALS Association	15
İzmir SSK Education Hospital, Dept. of Neurology	8
Süreyya Paşa Clinic, Dept. of Neurology	6
İstanbul University, Cerrahpaşa Medical School, Dept. of Neurology	4
Kahramanmaraş Yenişehir Hospital, Dept. of Neurology	3
Şişli Etfal Hospital, Dept. of Neurology	2
Ege University, Medical School, Dept. of Neurology	2
Amerikan Hospital, Dept. of Neurology	1
Yeditepe University, Medical School, Dept. of Neurology	1
Adnan Menderes University, Medical School, Dept. of Neurology	1
Celal Bayar University, Medical School, Dept. of Neurology	1

3.1.2. Patient ALS147 and Family Members

Blood samples from the family members of patient ALS147 were collected for haplotype analysis.

Patient ALS147 originates from Milas, Muğla. The parents of the index case were first cousins (Figure 3.1). His mother is at her 80s; she is phenotypically normal. His father passed away at ~70 years of age, he was also phenotypically normal. His older sister was diagnosed with ALS at the age of 48. She passed away relatively soon due to bad caregiving.

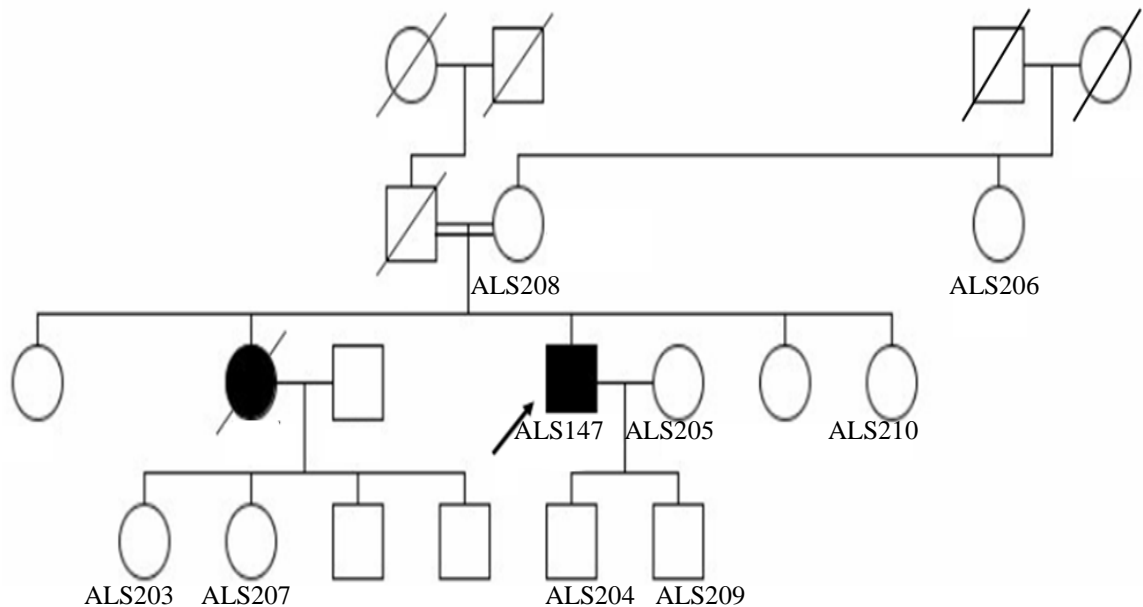


Figure 3.1. Family tree of ALS147

The first symptoms of the index case were weakness in legs, dizziness, sore throat and depression at the age of 48. Within six months, weakness started spreading to other extremities; now, he walks with canes. Meanwhile, difficulties in swallowing and breathing have also developed. However, he can still feed normally. Having the disease for five years, when compared to classical ALS progression, his clinical picture can be described as ‘slowly progressive’.

3.1.3. DNA Samples of Scandinavian Origin

For haplotype analysis of patient ALS147, comparative linkage study was established with samples shared generously by Peter Andersen from Umeå University. The origins and genotypes of these samples are shown in Table 3.2.

Table 3.2. Origins and genotypes of Scandinavian samples

Scandinavian ID	SOD1 Mutation	Ethnicity	Comments
6	D90A homozygous	Swedish	--
208	D90A homozygous	Finnish	--
292	D90A homozygous	Finnish	--
327	D90A homozygous	Finnish	--
339	D90A homozygous	Finnish	--
340	D90A heterozygous	Finnish	PD; mother of SOD339
356	D90A homozygous	Finnish	--
463	D90A homozygous	Finnish	--
466	D90A homozygous	Swedish	--
578	D90A homozygous	Finnish	--
586	D90A homozygous	Swedish	--
727	D90A homozygous	Swedish	--
789	D90A homozygous	Swedish	--
822	D90A homozygous	Finnish	--
1235	D90A homozygous	Norwegian	--
1339	D90A homozygous	Swedish	--
1546	D90A homozygous	Russia	--
1609	D90A homozygous	Swedish	--
1846	D90A heterozygous	Swedish	--
1950	D90A heterozygous	Norwegia	--
3867	D90A heterozygous	Germany	--

3.1.4. Mutational Analysis of Autosomal Dominant and Nonconsanguinous Familial and Juvenile ALS Cases in the Turkish Cohort

Autosomal dominant cases are described in Table 3.3, detailed information on familial and juvenile cases are shown in Tables 3.4 and 3.5, respectively. These cases are characterized with late age of onset and more than one affected individual within the pedigree.

Table 3.3. Autosomal dominant FALS cases

ALS ID	Age of Onset	Consanguinity	Other affected family members
ALS56	46	no	Mother and older sister
ALS57	51	no	Mother (ALS59): ALS-like symptoms.
ALS59	~60	no	Son (ALS57)
ALS170	48	no	Younger brother (ALS171) and younger sister (ALS172)
ALS171	47	no	Older (ALS170) and younger sisters (ALS172)
ALS172	45	no	Older brother (ALS171) and older sister (ALS170)
ALS184	45	no	Grandfather, uncle, father and older brother; all ex.
ALS215	60	no	Father and younger sister
ALS220	45	no	Father, uncle and her father's cousin; all ex Her cousin; alive

Table 3.4. Familial ALS cases

ALS ID	Inheritance Pattern	Age of Onset	Consanguinity	Other affected family members
ALS41	AR FALS	18	no	Grandmother similar to ALS
ALS46	AD FALS	23	yes	Father died of ALS
ALS68	AR FALS	44	yes	Older sister died of ALS. Another older sister suspected of ALS; died of another reason
ALS97	AR FALS	46	not reported	Younger stepsister died of ALS.
ALS173	AR FALS	58	no	Two younger sisters (ALS174 and ALS189)
ALS174	AR FALS	--	no	Older (ALS173), younger sisters (ALS189)
ALS189	AR FALS	--	no	Two older sisters (ALS173 and ALS174)
ALS175	FALS	22	no	Two younger brothers similar to ALS
ALS202	FALS	56	no	Younger brother died of ALS.
ALS223	FALS	44	no	His cousin had ALS; died of another reason.

Table 3.5. Juvenile ALS cases

ALS ID	Inheritance Pattern	Age of Onset	Consanguinity	Other affected family members
ALS49	Juvenile	9	yes	--
ALS85	Juvenile	17	no	Older brother (ALS86)
ALS86	Juvenile	19	no	Younger brother (ALS85)
ALS96	Juvenile	9	yes	--
ALS132	Juvenile	14	yes	Younger sister (ALS133)
ALS133	Juvenile	16	yes	Older brother (ALS132)
ALS135	Juvenile	12	not reported	--
ALS150	Juvenile	16	yes	--
ALS155	Juvenile	--	not reported	--
ALS157	Juvenile	--	not reported	Younger brother (ALS158)
ALS158	Juvenile	--	not reported	Older brother (ALS157)
ALS167	Juvenile	13	yes	--
ALS178	Juvenile	17	no	--

3.2. Fine Chemicals

3.2.1. Primers for PCR Amplification and DNA Sequencing of SOD1

The primers for the amplification of all five exons of the SOD1 gene were as described in Deng *et al.*, 1993. They were purchased from Roche, Germany. The sequences are shown in Table 3.6. The primers in bold were also used for DNA sequencing.

Table 3.6. Primer pairs used in PCR amplification of the SOD1 gene

Primer Name	Primer Sequence	Product Size (bp)
Exon 1 Forward Exon 1 Reverse	F-5' TTCCGTTGCAGTCCTCGGAAC R-5' CGGCCTCGCAAACAAGCCT	156
Exon 2 Forward Exon 2 Reverse	F-5' TTCAGAACTCTCTCCAATT R-5' ACGTTAGGGGCTACTCTAGT	207
Exon 3 Forward Exon 3 Reverse	F-5' TGGGAACTTTAATTCATAATT R-5' AGTATACCATATGAACTCCA	182
Exon 4 Forward Exon 4 Reverse	F-5' CATCAGCCCTAATCCATCTGA R-5' CCGACTAACAATCAAAGTGA	236
Exon 5 Forward Exon 5 Reverse	F-5' AGTGATTTACTTGACAGCCCA R-5' TTCTACAGCTAGCAGGATAACA	216

3.2.2. Primers for PCR Amplification of Microsatellite Markers

Microsatellite markers used in the haplotype analysis of the D90A homozygote Turkish patient were suggested by Peter Andersen (University of Umeå) and the primers for PCR amplification were designed using Primer3 program. The sequences were confirmed with Entrez Mapviewer and BLAST programs (Figure 3.2). These primers were ordered from Roche, Germany.

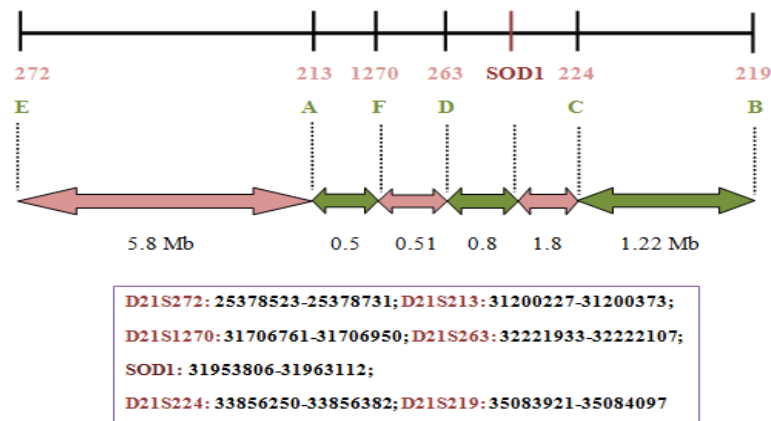


Figure 3.2. The positions of the microsatellite markers on chromosome 21. The numbers below arrows are the distances between each marker, represented in Mb

The exact size of each PCR product was determined by GeneScan Analysis. For this purpose, forward primers, labeled with FAM at the 5' end, were used. They were purchased from Roche, Germany. The sequences of the primers are listed in Table 3.7.

Table 3.7. Primer pairs used in the PCR amplification of microsatellite markers

Microsatellite Marker	Primer Sequence
D21S213 Forward	(5' FAM-) TAGAGGCTTGAATTGGCTGG
D21S213 Reverse	GTGTTTCATTAGACACACCC
D21S219 Forward	(5' FAM-) GCCTCTTGACTTTTTGGC
D21S219 Reverse	GCTGCAAGCCTTCTACATT
D21S224 Forward	(5' FAM-) GATCTATGGCTAACCACTAA
D21S224 Reverse	ATGATAATGTTCTCACTGTTT
D21S263 Forward	(5' FAM-) GTTAAGGGTGAAATTGGCTT
D21S263 Reverse	TGGAGATAGCATCACTAACA
D21S272 Forward	(5' FAM-) TTGGCTTTGGAACCAG
D21S272 Reverse	CATCAGCAAGGGTCCTC
D21S1270 Forward	(5' FAM-) AGAGCAATATAGAGCAGACAAGT
D21S1270 Reverse	AATGGAACAATTTATCCTTAGTTT

3.2.3 Primers for PCR Amplification of TDP-43

The primers were designed using Primer3 program (Table 3.8). The sequences were confirmed by Geneviewer, Entrez Mapviewer and BLAST programs. They were purchased from Invitrogen, USA. The primers in bold were also used for DNA sequencing.

Table 3.8. Primer pairs used in the PCR amplification of TDP-43

Primer Name	Primer Sequence	Product Size (bp)
Exon 1 Forward	ATCACTACCCTTACCTTCACC	573
Exon 1 Reverse	TCGTGGTCTTCCAAACTTGTC	
Exon 2 Forward	AGAGGGAGAGATTGTAATCCG	615
Exon 2 Reverse	AAGGTAACAAGATTGTGGCTGG	
Exon 3 Forward	TTAAGCCACTGCATCCAGTTG	412
Exon 3 Reverse	TATTCAGCATGCACTAAGGGC	
Exon 4 Forward	ACGTTACTCTTCACTGAAGCC	740
Exon 4 Reverse	GAATAGCAATTAGCTGCATGGG	
Exon 5 Forward	GACTGAAATATCACTGCTGCTG	765
Exon 5 Reverse	TTGAATCCCACCATTCTATACC	

3.2.4. Primers for PCR Amplification of ANG

The primers for the amplification and direct DNA sequencing of the coding sequence of the ANG gene and its 40 bp flanking region, were as described by Greenway *et al.* (Table 3.9) (Greenway *et al.*, 2004). They were purchased from Invitrogen, USA. The primers in bold were also used for DNA sequencing.

Table 3.9. Primer pair used in the PCR amplification of ANG

Primer Name	Primer Sequence	Product Size (bp)
Exon 1 Forward	TGTTCTTGGGTCTACCACACC	550
Exon 1 Reverse	AATGGAAGGCAAGGACAGC	

3.2.5. Primers for PCR Amplification of FUS

For the amplification of 15 exons of FUS, the primer sequences in Vance *et al.*, 2009 were used (Table 3.10). They were confirmed by Geneviewer, Entrez Mapviewer and

BLAST programs. They were purchased from Invitrogen, USA. The primers in bold were also used for DNA sequencing.

Table 3.10. Primer pairs used in the PCR amplification of FUS

Primer Name	Primer Sequence	Product Size (bp)
Exon 1 Forward Exon 1 Reverse	ACCCTCTACCTGCCCTACG GTCCCACTGAAAACGAAAAG	296
Exon 2-3 Forward Exon 2-3 Reverse	TTCATCAGTGCTTGAGTTAAGG AACAGGACCAGACTCCGTC	449
Exon 4 Forward Exon 4 Reverse	TGAGAGGCTGGCTTTATGAG TGCTGGTCCCTTTATCATTC	324
Exon 5 Forward Exon 5 Reverse	TGTTGGGTACAGAGAATGGAC AGCCTCAGCAACAGAGACAG	375
Exon 6 Forward Exon 6 Reverse	TTCTTTTGTCTTCATTGCC ATGCACTAGGGACTGGCTTC	434
Exon 7 Forward Exon 7 Reverse	GGTCAGGAAGGGATGTATTTTAG AACAGGTGGCATTCTACCCTAC	235
Exon 8 Forward Exon 8 Reverse	CCTGTTGACTAACGGCTCATC TCTCAGACCTAAATCACTGGGG	178
Exon 9 Forward Exon 9 Reverse	TGATACCAGTTGCTTGATGG TGCTGGCAACCATTAAAGAC	295
Exon 10 Forward Exon 10 Reverse	AGTAACTGGGAAGAGGGGAG TATGGCTTGTTTCCTAAGGC	321
Exon 11 Forward Exon 11 Reverse	CGCTTCTCTTGTATTTTCGG CATTCCATGCAAGCCTTTAC	247
Exon 12 Forward Exon 12 Reverse	GTGCAGAAGATGGTAAAGGC CTTCTTTGGAAAACACGCAC	304
Exon 13 Forward Exon 13 Reverse	TCCTCACTGTATCTCTAAAGTCACC CATATTCCCATTCCCCTATG	293
Exon 14 Forward Exon 14 Reverse	CACATGGGTAAGAAAGGCAG TCTCAACAAAACCCTGTTATCC	348
Exon 15 Forward Exon 15 Reverse	TACTCGCTGGGTTAGGTAGG TTCCAGGAAAGTGAAAAGGG	344

3.2.6. Primers for PCR Amplification of CPEB3

The primers used in the amplifications of CPEB3 are shown in Table 3.11. Exon 1 of CPEB3 was divided into three different fragments for a more convenient amplification. All primers were designed by Geneviewer, Entrez Mapviewer and BLAST programs.

They were purchased from Invitrogen, USA. The primers in bold were also used for DNA sequencing.

Table 3.11. Primer pairs used in the PCR amplification of CPEB3

Primer Name	Primer Sequence	Product Size (bp)
Exon 1 Forward-a Exon 1 Reverse-a	GGTGGCGATGGATTTTCGC AAGTGCCTCCGAAGACTGG	562
Exon 1 Forward-b Exon 1 Reverse-b	AGGACAGCTTCTTCCAGGG AGGCTGCATTCACGCTTTGG	396
Exon 1 Forward-c Exon 1 Reverse-c	ACCAGCAAGCCGTCCTCG AGCTGGACATTGCTGCCCT	470
Exon 2 Forward Exon 2 Reverse	TTCATGTCATCAATCCACAGC TGA CTGATAACAATCCACCTTG	456
Exon 3 Forward Exon 3 Reverse	ACTGCTTTGGCCTTTGATAGC CTTTCAGCGGAAGGTTAAAATG	290
Exon 4 Forward Exon 4 Reverse	TCCTGTTAATCTTGGAAAAGCC ACCAAATAGTCTCACCTCCTATGC	434
Exon 5 Forward Exon 5 Reverse	AAAAGACATGTTTTGTGCTCTTC GAAACAATCAGTGTGCTTCAGG	368
Exon 6 Forward Exon 6 Reverse	ATTTGCCAAAATGAAACAACAG CTACTGCATAGCAAGGCCAAG	346
Exon 7 Forward Exon 7 Reverse	TTTGTTTGGGTCATGTTTCATTG TTGGGAGAAAACCTTTAATCCTG	401
Exon 8 Forward Exon 8 Reverse	CAGTGAGGACCTTCCCTACTTG GATCATAAGGTGCCTTTCTTCC	445
Exon 9 Forward Exon 9 Reverse	CAGTATCAGCAGAGTTGAAAGC GAGAACGAATGCACAGATTTCC	466

3.2.7. Primers for PCR Amplification of USP53

The primers used in the amplifications of USP53 are shown in Table 3.12. Exon 4 and 5 were combined for a more convenient amplification. All primers were designed by Geneviewer, Entrez Mapviewer and BLAST programs. They were purchased from Invitrogen, USA. The primers in bold were also used for DNA sequencing.

Table 3.12. Primer pairs used in the PCR amplification of USP53

Primer Name	Primer Sequence	Product Size (bp)
Exon 1 Forward Exon 1 Reverse	CATCAGGAAAGATATGGACTTGG CAGCCAAAACACTTTTGCTCC	447
Exon 2 Forward Exon 2 Reverse	AAGTTACTTGTTTCGCCTTTTGC ACTGTTAATCACCTGACAGTGAAC	314
Exon 3 Forward Exon 3 Reverse	CTGAAATGTCGTTAAAGCTGGC AAGTTGAGGCTTGAAGGATGG	348
Exon 4-5 Forward Exon 4-5 Reverse	GATTAGAGAGGAAAGCTGAAAAGC GAGAGGGGAAATTCATGTATGC	524
Exon 6 Forward Exon 6 Reverse	TCACTTTATGGAAATGTA CTTTATGG ATCAATATATGCTTCACAACTTAGG	471
Exon 7 Forward Exon 7 Reverse	TGACTTCAAGAGTTTTATTCTGC GTTTGTAATTGAAAGCCATTCC	562
Exon 8 Forward Exon 8 Reverse	AACAATGTGATGTCAGTGGTGC AATGGACTGGTTTAAAAGCTGG	524
Exon 9 Forward Exon 9 Reverse	AACTCAGAGTCTGTCTTTTCATGT AGCCTCTTCTGTGATTGTGTGA	479
Exon 10 Forward Exon 10 Reverse	ATTCAAACATCTCTTCTCATGGG CATGGAATCAAACCTGGTCAGG	401
Exon 11 Forward Exon 11 Reverse	AAAATACAACATGCATCTCCAGTG GAGTGAACCTCACCTCTTC	638
Exon 12 Forward-a Exon 12 Reverse-a	TCATTAAGCATA CACAAGGACTGG GCTGCTATCACAGCTGTTTCC	475
Exon 12 Forward-b Exon 12 Reverse-b	TCAAGTAAATCCCAGATTCTTGC GTACCATTTCATCGATAACAGG	533
Exon 12 Forward-c Exon 12 Reverse-c	TTGTAGAGGGTAAAGTGCATGG GATGATACCAATTGAAGTCTGTGC	521
Exon 13 Forward Exon 13 Reverse	GCAGTCCATAATACCTGATGTG TCAATGTGGAAAGTATAGCATGC	377

Table 3.12. Primer pairs used in the PCR amplification of USP53 (continued)

Primer Name	Primer Sequence	Product Size (bp)
Exon 14 Forward Exon 14 Reverse	GAAATTTTGCATAAAGCATTCC ATTCCAATAAGAAAGGCATC	424
Exon 15 Forward-a Exon 15 Reverse-a	TGACATAAAGAGTTTGGATTTGG TATTTTGTGCTGGATGAGAGG	502
Exon 15 Forward-b Exon 15 Reverse-b	TGAATGCAAATTTTCTGAGTGG GTTAGTTGAGGAGCTGGATGG	547
Exon 15 Forward-c Exon 15 Reverse-c	TCAGAGAAAAGCGAATCTACACC GGCCTCTGAGAAGTAAAAGTTGG	545

3.2.8. Primers for PCR Amplification of UCHL3

The primers used in the amplifications of UCHL3 are shown in Table 3.13. Exon 1 and 2 were combined for a more convenient amplification. All primers were designed by Geneviewer, Entrez Mapviewer and BLAST programs. They were purchased from Invitrogen, USA. The primers in bold were also used for DNA sequencing.

Table 3.13. Primer pairs used in the PCR amplification of UCHL3

Primer Name	Primer Sequence	Product Size (bp)
Exon 1-2 Forward Exon 1-2 Reverse	GAGCGGTTAAGAGGGTGAGAG CCCTCAAGAAATTAATCCCAG	447
Exon 3 Forward Exon 3 Reverse	CCTTTATAGGTATTAGATACAGAG TGCCTAATTTTATGCAAGAAGGG	701
Exon 4 Forward Exon 4 Reverse	GCATTTTTTCTTTTACAGACTGAG GAAGAAAGAATTAGAGCACCACC	323
Exon 5 Forward Exon 5 Reverse	AAAATAAAGCATTCCCTGCTTCC GGCAACTTATCAGCATTGTGG	549
Exon 6 Forward Exon 6 Reverse	TACAGCAATTCATTTGATTACCC TTGTCAAACATGTCCTTTTGC	422
Exon 7 Forward Exon 7 Reverse	TCCATTATACCAAACATTAAGCC AAAAGGAAAAGTGTGCTATGTC	372
Exon 8 Forward Exon 8 Reverse	GGAAAATGGAAGTTGAAAGCAC TTGGATTTTCTAGAGAGAACAAGG	263
Exon 9 Forward Exon 9 Reverse	TCATTTGAAAAGGAAGTTTGC CATTGCACCTTTAACCTGGAG	381

3.2.9. Primers for PCR Amplification of RAB27A

The primers used in the amplifications of RAB27A are shown in Table 3.14. All primers were designed by Geneviewer, Entrez Mapviewer and BLAST programs. They were purchased from Invitrogen, USA. The primers in bold were also used for DNA sequencing.

Table 3.14. Primer pairs used in the PCR amplification of RAB27A

Primer Name	Primer Sequence	Product Size (bp)
Exon 1 Forward	TTAGGTCTTCAAGGATGGTGAAC	495
Exon 1 Reverse	TGTTGCCTGGATTGAACATAAC	
Exon 2 Forward	ACATGGTTGTATTCCAGATGGC	416
Exon 2 Reverse	CATAACCTCTCCCTTGACCTTG	
Exon 3 Forward	TCACAAGCTGGTTCTTGTCATC	435
Exon 3 Reverse	CTCCTCCAAAACGATTTGTCAC	
Exon 4 Forward	TATTTCTGCCCAACTATTTCAG	524
Exon 4 Reverse	GTTTGAGAAAATGGGACCAAAG	
Exon 5 Forward	CTGGGGTGGTAAAATGTTTGTC	477
Exon 5 Reverse	GAACCGGATGCTTTATTCGTAG	

3.2.10. Primers for PCR Amplification of IL21

The primers used in the amplifications of IL21 are shown in Table 3.15. Exon 1 was a noncoding region. All primers were designed by Geneviewer, Entrez Mapviewer and BLAST programs. They were purchased from Invitrogen, USA. The primers in bold were also used for DNA sequencing.

Table 3.15. Primer pairs used in the PCR amplification of IL21

Primer Name	Primer Sequence	Product Size (bp)
Exon 2 Forward	TCCCTGAAGGATGAATAAATAGG	487
Exon 2 Reverse	TCATGCTAATGTCTTTCTTATTGG	
Exon 3 Forward	GCTCCTTTCTCTCTTATCTGCG	451
Exon 3 Reverse	TGGCTACAGGTGTGTGTGTATG	
Exon 4 Forward	TTTCATTGATTTCTAGACATGCC	328
Exon 4 Reverse	CCCATCGCTAATATATTGTACTCC	

3.2.11. Probes for Expression Analysis

The probes used for quantitation of B4GALT6, KIFAP3 and ADAMTS17 are shown in Table 3.16. Following is the schematic representation of chromosomal location of the probes used in this study (Figure 3.3).

Table 3.16. Probes used in gene expression analysis

SNP/Probe ID	Corresponding gene	Alleles
Hs00191135	B4GALT6	A→G
Hs00183973	KIFAP3	T→C
Hs00946074	KIFAP3	T→C
Hs00330236	ADAMTS17	A→G

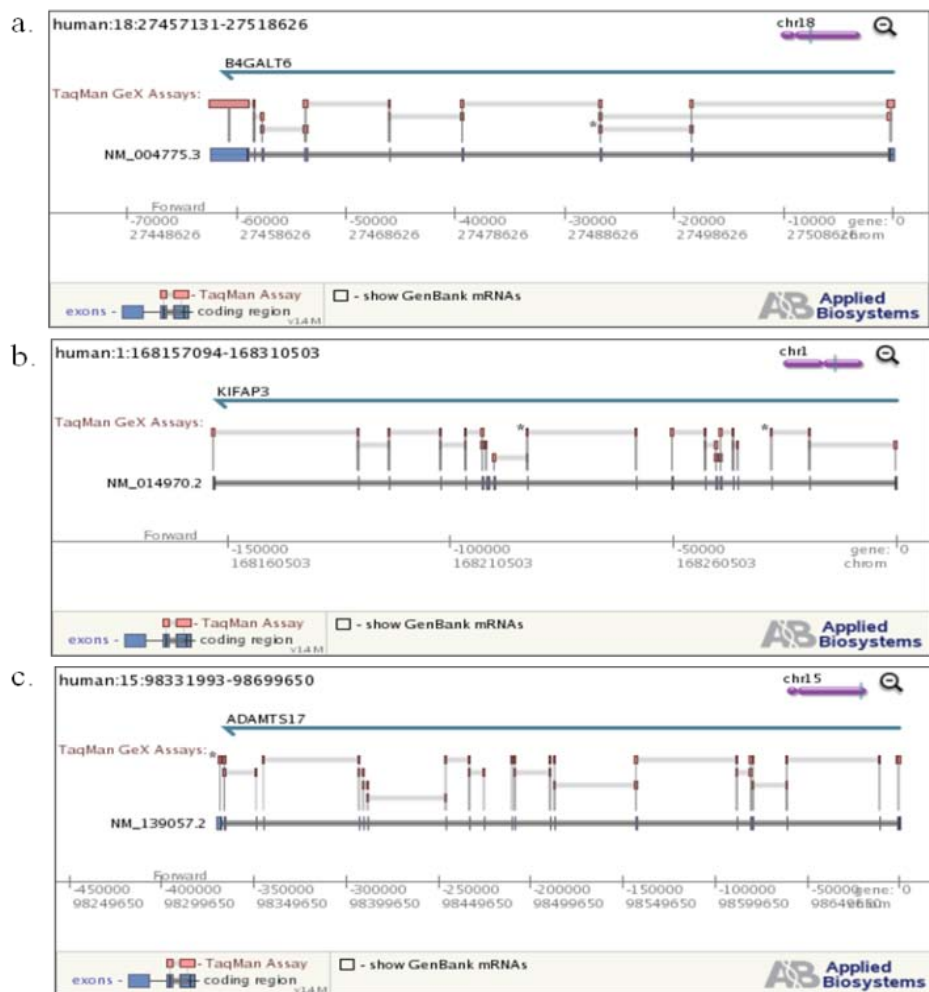


Figure 3.3. Schematic representation of chromosomal location of the probes

As internal control, human β -2-microglobulin was used. All probes were purchased from Applied Biosystems, USA

3.2.12. Antibodies for Western Blot Analysis

KIFAP3 and secondary antibodies were purchased from Santa Cruz Biotechnology, USA; actin antibody was from Sigma Aldrich, USA. The properties are as listed in Table 3.17.

Table 3.17. Antibodies used in Western blot analysis

Antibody	Commercial Code	Status	Source	Concentration	Property
KIFAP3	sc-55598	primary Ab	mouse monoclonal	200 μ g/ml	aa 494-793 at C-terminal
Actin	A2066	primary Ab	rabbit polyclonal	200 μ g/ml	aa 1-11 at C-terminal
goat anti-ouse	sc-2005	secondary Ab	Goat	200 μ g/ml	horseradish peroxidase conjugated
donkey anti-goat	sc-2020	secondary Ab	Donkey	200 μ g/ml	horseradish peroxidase conjugated
rabbit anti- goat	ab7132	secondary Ab	rabbit polyclonal	1.000 mg/ml	horseradish peroxidase conjugated

3.2.13. Brain Tissue Lysates for Western Blot Analysis

Brain tissue lysates were purchased from Abcam, USA. The properties are represented in Table 3.18

Table 3.18. Brain lysates used in Western blot analysis

Commercial Code	Source	Property	Concentration
ab29466	whole brain	adult normal	3.750 mg/ml
ab30078	cerebellum	adult normal	3.750 mg/ml

3.3. Enzymes

3.3.1. PCR Amplification

GoTaq DNA Polymerase : 5 U/ μ l, Promega, USA

ExTaq DNA Polymerase : 5 U/ μ l, Takara, Japan

Taq DNA Polymerase : Invitrogen, USA

3.3.2. Total RNA preparation

AmpliTaq Gold[®] : Applied Biosystems, USA

3.3.3. cDNA Synthesis from Total RNA

RT Enzyme Mix : Invitrogen, USA

RNaseOUT : Invitrogen, USA

E.coli RNase H : Invitrogen, USA

3.3.4. Real-time Quantative Polymerase Chain Reaction (qRT-PCR)

Platinum[®]Taq DNA Polymerase : 60U/ml
Invitrogen, USA)

3.3.5. Restriction Enzyme Analysis

ItaI : 10 U/ μ l,
Roche, Germany

3.4. Buffers and Solutions

3.4.1. DNA Extraction

Lysis Buffer : 155 mM NH₄Cl
10 mM KHCO₃
1 mM Na₂EDTA (pH 7.4)

Nuclease Buffer : 10 mM Tris-HCl (pH 8.0)
400 mM NaCl
2 mM Na₂EDTA (pH 7.4)

Sodium Chloride (NaCl) : 5 M saturated stock solution

Sodiumdodecylsulphate (SDS) : 10 per cent SDS (w/v) (pH 7.2)
Sigma, Germany

Proteinase K : 20 mg/ml in H₂O
Promega, USA

Ethanol : Absolute Ethanol
Riedel de-Häen, Germany

TE Buffer : 20 mM Tris-HCl (pH 8.0)
1 mM Na₂EDTA (pH 8.0)

3.4.2. Polymerase Chain Reaction (PCR)

3.4.2.1. PCR of Exon 1 of SOD1 and microsatellite markers.

MgCl ₂	:	25 mM in dH ₂ O Takara, Japan
10X MgCl ₂ Free Buffer	:	20 mM Tris-HCl (pH 8.0) 100 mM KCl 0.1 mM EDTA 1 Mm DTT 0.5 per cent Tween [®] 20 0.5 per cent Nonidet P-40 50 per cent Glycerol Takara, Japan
Deoxyribonucleotides (dNTP)	:	25 mM, Takara, Japan
Betaine	:	5M, Sigma, Germany
DMSO	:	Proprietary formulation Qiagen, Germany

3.4.2.2. PCR of exons 2, 3, 4 and 5 of SOD1.

5X MgCl ₂ Free Buffer	:	Proprietary formulation Promega, USA
Magnesium Chloride (MgCl ₂)	:	25 mM in dH ₂ O Promega, USA
Deoxyribonucleotides (dNTP)	:	100 mM of each dNTP Promega, USA

3.4.2.3. Restriction enzyme analysis.

SuRE/Cut Buffer H : 10X Enzyme Buffer for Ital
Roche, Germany

3.4.2.4. PCR of TDP-43, FUS and ANG

2X PCR PreMix® : Epicentre Biotechnologies, USA

3.4.2.5. Total RNA preparation and real-time quantitative PCR.

2X Platinum® PCR Supermix : 40 mM Tris-HCL (Ph 8.4)
100 mM KCL
6 mM MgCl₂
400 μM dGTP, dATP, dCTP
800 μM dUtp
40 U/ml UDG
Stabilizers
Invitrogen, USA

AccuGene Mol BioGrade water : Cambrex, USA

DEPC-treated H₂O : MP Biochemicals Inc, USA

3.4.3. Gel Electrophoresis

3.4.3.1. Agarose gel eletrophoresis for PCR of SOD1 and microsatellite markers.

Agarose : Agarose Basica Le, Prone, EU

1 or 2 per cent Agarose Gel : 1 or 2 per cent Agarose in 0.5X TBE Buffer,
containing 0.5 μg/ml Ethidium Bromide

DNA Ladder	:	1000 bp (Invitrogen, USA) 50 bp (MBI Fermentas, Lithuania) 100 bp (Promega, USA)
Ethidium Bromide (EtBr)	:	10 mg/ml
6X Loading Dye	:	10 mM Tris-HCl (pH 7.6) 0.03 per cent Bromophenol Blue 0.03 per cent Xylene Cyanol FF 60 per cent glycerol 60 mM EDTA Fermentas, Lithuania
10X TBE Buffer	:	0.89 M Tris-Base 0.89 M Boric acid 20 mM Na ₂ EDTA (pH 8.3)

3.4.3.2. Agarose gel electrophoresis for detection of RNA concentration

AccuGENE 10X MOPS Buffer	:	Cambrex, USA
1.25 per cent SeaKem Gold Agarose	:	Cambrex, USA
Formaldehyde RNA Loading Buffer	:	Cambrex, USA

3.4.3.3. Gel electrophoresis of proteins

Novex 10 per cent Tris-Glycine 1.0mm Gel	:	Invitrogen, USA
SimplyBlue™ SafeStain	:	Invitrogen, USA

3.4.4. Whole Genome Genotyping of Turkish Familial and Juvenile ALS Cases

Sterile water	:	American Bioanalytical, USA
MA1	:	Illumina, USA
MA2	:	"
FMS	:	"
PM1	:	"
100 per cent 2-propanol	:	"
RA1	:	"
PB1	:	"
XC1	:	"
XC2	:	"
XC3	:	"
XC4	:	"
TEM	:	"
STM	:	"
ATM	:	"
95 per cent formamide	:	EMD Chemicals, USA

3.4.5. Western Blot Analysis

Precision Plus Protein Kaleidoscope Standards	:	BIO-RAD, USA
Blotting-Grade Blocker	:	BIO-RAD, USA
RIPA Buffer	:	Fisher Scientific, USA
BupH Phosphate Buffered Saline (PBS)	:	Pierce Biotechnology, USA
SuperSignal West Femto Maximum Sensitivity Substrate	:	Pierce Biotechnology, USA
Novex Tris-Glycine SDS 10X Running Buffer	:	Invitrogen, USA
Novex Tris-Glycine SDS 2X Sample Buffer	:	Invitrogen, USA
Novex Tris-Glycine 25X Transfer Buffer	:	Invitrogen, USA
Methanol	:	Sigma Aldrich, USA
B-Mecaptoethanol	:	Sigma Aldrich, USA
Protease Inhibitor Mixture Tablets	:	Roche, Germany
SDS	:	Sigma Aldrich, USA

3.5. Chemicals

Specific chemical solutions, including RNase Away, were all purchased from Molecular BIOproducts, USA. Alconox powder detergent was supplied from Illumina, USA.

3.6. Kits

BCA Protein Assay Kit	:	Fisher Scientific, USA
REPLI-g Mini Kit	:	Qiagen, USA
XCell II™ Blot Module Kit CE	:	Invitrogen, USA

3.7. Equipment

96-well Plate	:	Applied Biosystems, USA
96-well plate sealer	:	EdgeBio, USA
96-well semi/skirted PCR Plate	:	Eppendorf, Germany
Adhesive PCR Films	:	Applied Biosystems, USA
Aluminum Sealing	:	Fisher Scientific, USA
Autoclave	:	Model MAC-601, EYELA, Japan Model ASB260T, Astell, UK
Balances	:	Electronic Balance Model VA124 Gec Avery, UK Electronic Balance Model CC081 Gec Avery, UK

Benchtop 96 Tube Working Rack	:	Stratagene, USA
Benchtop Cooler	:	StrataCooler® 96 Stratagene, USA
Centrifuges	:	Centrifuge 5415C, Eppendorf, Germany Centrifuge 5804, Eppendorf, Germany Universal 16R, Hettich, Germany Allegra X22-R, Beckman Coulter, USA Eppendorf Centrifuge 5810 Eppendorf, USA
Deep Freezers	:	2021D (-20 ⁰ C), Arçelik, Turkey Sanyo (-70 ⁰ C), Sanyo, Japan
Documentation System	:	GelDoc Documentation System BIO-RAD, USA
Electrophoretic Equipments	:	i-MyRun-N, CosmoBio., Ltd. Japan Minicell Primo E320, Thermo, USA Mini Sub Cell GT, BIO-RAD, USA XCell SureLock™ Mini-Cell, Invitrogen, USA Wide Sub Cell GT BIO-RAD, USA Sequi-Gen Cell, BIO-RAD, USA
Gel loading tips	:	Invitrogen, USA
Heat Blocks	:	Thermostat Heater 5320 Eppendorf, Germany Illumina, USA
Hyb Chamber Gasket	:	Illumina, USA

Hybridization Bags	:	VWR, USA
Hybridization Oven	:	Illumina, USA
Hyperfilm ECI-high performance chemiluminescence film 8x10 inch	:	Amersham Biosciences, USA
Incubator	:	Hybex Microsample Incubator SciGene, USA
Invitrolon™ PVDF membrane	:	Invitrogen, USA
Laboratory Air Gun	:	Illumina, USA
Magnetic Stirrer	:	Chiltern Hotplate Magnetic Stirrer, HS31, UK
Nutator Mixer	:	VWR, USA
Ovens	:	MD 554, Microwave Oven Arçelik, Turkey EN 400 (37°C), Nüve, Turkey BD53 (56°C), Binder, Germany
Power Supplies	:	ECPS 3000/150 Constant Power Supply Pharmacia, Sweden Model 200, BRL, USA Powerpac 1000, BIO-RAD, USA
Refrigerator	:	4250T, Arçelik, Turkey
Reservoir	:	Corning Incorporated Costar, USA

Spectrophotometer	:	NanoDrop ND-1000, Thermo, USA
TaqMan 7900HT Sequence Detection System	:	Applied Biosystems, USA
Tecan Freedom Evo	:	Tecan, Switzerland
Thermocyclers	:	C312, Techne, UK Techgene, Progene, UK Touchgene Gradient, Progene, UK iCycler, BIO-RAD, USA
Vacuum Desiccator	:	Barnstead Reservoir, Thermo Scientific, USA
Vortex	:	Fisons WhirliMixer, UK Reax Top, Heidolph, Germany Illumina, USA
Water Purification	:	Millipore, USA

4. METHODS

4.1. DNA Extraction from White Blood Cells

DNA from each sample was obtained via two alternative extraction methods.

4.1.1. Sodium Chloride Extraction

To extract genomic DNA from white blood cells (leukocytes), 10 ml of peripheral blood samples were collected in anticoagulant (K₂EDTA) containing tubes. First, 30 ml cold lysis buffer was added on the blood samples to lyse the membrane of leukocytes. Following the incubation at 4°C for 15 minutes, they were centrifuged at 5K for 10 minutes at 4°C. This results in the precipitation of the cellular nuclei. After discarding the supernatant, the pellet was resuspended in 10 ml cold lysis buffer and centrifuged again at 5K for 10 minutes at 4°C. The nuclear pellet was resuspended in lysis buffer and centrifuged at the same conditions until a clean pellet was obtained. In order to lyse the nuclear envelope, the nuclear pellet was resuspended in nuclease buffer. The nuclear proteins were degraded by treating the suspension with proteinase K (150 µg/ml) and SDS (0.14 per cent). Then, the suspension was incubated at either 37°C for overnight or at 56°C for three hours.

Following the incubation, the degraded proteins were precipitated by treating the suspension with 5 ml of cold distilled water and 5 ml of 5M NaCl solution. The tubes were shaken vigorously and centrifuged at 5K for 20 minutes at room temperature which resulted in the precipitation of proteins in the pellet. The supernatant, containing the genomic DNA, was transferred into a new Falcon tube. In order to precipitate the DNA, two volumes of cold absolute ethanol were added to the supernatant. The tubes were gently inverted until DNA threads were visible. By fishing out with a pipette, the DNA was quickly taken into an Eppendorf tube and left to dry. When all ethanol was evaporated, the DNA was dissolved in TE buffer and stored at 4°C.

4.1.2. Extraction by MagNa Pure Compact Instrument

MagNA Pure Compact Instrument is a specifically designed robotic system which extracts nucleic acids (DNA and RNA) from blood or tissue samples. The extraction principle relies on the specific binding affinity of magnetic beads to DNA. Following lysing of cell membrane and nuclear envelope, DNA binds to magnetic beads; thus, it is isolated from remnants of the cell. DNA is 'freed' of beads during elution step. There are two different MagNA Pure Compact Nucleic Acid Isolation Kits: i. small volume kit requires 500 μ l of blood and ii. large volume kit requires 1 ml of blood. Final elution volumes are 100 and 200 μ l of DNA, respectively.

4.2. Quality Control of Genomic DNA

4.2.1. Qualitative Analysis by Agarose Gel Electrophoresis

Genomic DNA was analyzed on a 1 per cent agarose gel, which was prepared by dissolving 1 g of agarose in 100 ml 0.5X TBE buffer. Agarose was dissolved in TBE buffer by boiling it in a microwave. EtBr, which intercalates into DNA and thus enables its visualization under UV light, was added into the agarose solution with a final concentration of 0.5 μ g/ml. Then, the homogenous mixture was poured onto an electrophoresis plate and left to polymerize at room temperature. For loading, DNA samples were mixed with 10X loading dye to a final concentration of 1X. The gel was placed into an electrophoresis tank, containing 0.5X TBE and run at 150 volt for 15-20 minutes, depending on the size of the expected fragment. When migration was completed, the gels were visualized under UV light and documented.

4.2.2. Quantitative Analysis by Spectrophotometric Measurement of DNA

DNA concentrations were also measured by a spectrophotometer. 50 μ g of double stranded DNA has an absorbance of 1.0 at 260 nm (OD_{260}). Each sample was diluted to a factor and the absorbance was read at 260 nm in a spectrophotometer. The concentration was calculated by the following equation:

$$50 \mu\text{g/ml} \times \text{OD}_{260} \times \text{dilution factor} = \text{concentration of genomic DNA } (\mu\text{g/ml})$$

4.3. SOD1 Analysis

4.3.1. PCR Amplifications of Exons

Polymerase Chain Reaction (PCR) is used to amplify the region of interest. The amplification of each exon was established by the addition of 10 ng (exon 2, 3, 4 and 5) or 100 ng (exon 1) of DNA template to PCR reagents.

Following amplification, PCR products were run on two per cent agarose gels. A 5 μl aliquot of each product was mixed with 5 μl 1X loading dye and run at 150 volt with 100 bp DNA ladder for 10-15 minutes. The gels were visualized under UV light and documented.

4.3.1.1. PCR amplification of exon 1. Exon 1 of the SOD1 gene was amplified by specific primers (Table 3.5). The reagents used are shown in Table 4.1 and Hot Start PCR amplification protocol is as follows:

Table 4.1. PCR reagents used for the amplification of SOD1 exon 1

Reagent	Volume (μl)	[Stock]	[Final]
Buffer (25 mM MgCl_2 included)	2.5	10X	1X (2.5 mM MgCl_2)
dNTP	2	2.5 mM	0.2 mM
Betaine	6.5	5M	1.3M
DMSO	0.32	100 per cent	1.28 per cent
Forward Primer	0.4	10 μM	0.16 μM
Reverse Primer	0.4	10 μM	0.16 μM
ExTaq Polymerase	0.2	5U/ μl	1U/ μl

Initial denaturation:	94°C	5 minutes	
Hot start:	80°C	hold	
Denaturation:	94°C	45 seconds	} 40 cycles
Annealing:	59.5/61.9°C	45 seconds	
Extension:	72°C	45 seconds	
Final Extension:	72°C	5 minutes	

4.3.1.2. PCR amplification of exons 2, 3, 4 and 5. The amplifications of exons 2 through 5 were established by specific primers (Table 3.5). The annealing temperatures for the amplification of each exon are shown in Table 4.2. The reagents are listed in Table 4.3 and the amplification protocol is as below:

Initial denaturation:	94°C	4 minutes	} 32 cycles
Denaturation:	94°C	30 seconds	
Annealing:	$\Delta A^{\circ}C$	30 seconds	
Extension:	72°C	30 seconds	
Final Extension:	72°C	8 minutes	

Table 4.2. Annealing temperatures for the amplification of SOD1 exons 2, 3, 4 and 5

Exon Number	Annealing Temperature (°C)	MgCl ₂ Volume (μl)	[MgCl ₂]
2	52.2	2.0	2 mM
3	54.5	2.5	2.5 mM
4	59.4	2.0	2 mM
5	57.3	2.0	2 mM

Table 4.3. PCR reagents used for the amplifications of SOD1 exons 2, 3, 4 and 5

Reagent	Volume (μl)	[Stock]	[Final]
Buffer	2.5	5X	1X
MgCl ₂	as in Table 4.2	25 mM	as in Table 4.2
dNTP	2	25 mM	0.2 mM
Forward Primer	0.5	20 μM	0.4 μM
Reverse Primer	0.5	20 μM	0.4 μM
GoTaq Polymerase	0.2	5U/μl	1U/μl

4.3.2 DNA Sequencing of SOD1

All PCR products were subjected to DNA sequencing (Iontek, Istanbul or Refgen Biyoteknoloji, Ankara). The results, in form of chromatograms, were obtained online as pdf files.

4.3.3. Restriction Enzyme Analysis of the D90A-SOD1 Mutation

D90A mutation which was detected via DNA sequencing of SOD1 exon 4 was further confirmed by restriction enzyme analysis. DNA samples of the index case and his family members (Figure 3.1) were once more amplified by PCR, with conditions indicated in Section 4.3.1.2. The amplified products were applied to a two per cent agarose gel with 100 bp DNA ladder. The gel was allowed to run at 150 volt for 10-15 minutes and visualized under UV light.

Restriction enzyme digestion was carried out in 10 µl volume containing 1 µl 10X buffer, 1 unit of *ItaI* restriction enzyme (Table 4.4) and 8 µl of each PCR product. The tubes were placed in 37°C incubator for overnight. The samples were loaded to a two per cent agarose gel with 50 bp ladder. The gel was run at 150 volt for 15 minutes and visualized under UV light.

Table 4.4. *ItaI* restriction enzyme and its recognition site

SOD1 Mutation	Localization	Restriction Enzyme	Wild-type Sequence	Mutant Sequence and Digestion Site
D90A	exon 4	<i>ItaI</i>	ACT GAC AAA	ACT GC [↓] C AAA

4.4. Haplotype Analysis of D90A Mutation

4.4.1. PCR Amplification of the Microsatellite Markers

A total of six microsatellite markers located upstream (D21S213, D21S263, D21S272 and D21S1270) and downstream of SOD1 (D21S219 and D21S224) were used to construct and compare the haplotype of a Turkish D90A homozygote ALS family to 22 Scandinavia samples (Figure 3.11).

The following Hot Start PCR protocol was applied for the amplification of five microsatellite markers (D21S213, D21S224, D21S263, D21S272 and D21S219), using the specific primers and reagents, as in Table 3.7 and Table 4.6, respectively. The annealing temperatures are shown in Table 4.5.

Initial denaturation:	94°C	5 minutes	
Hot start:	80°C	hold	
Denaturation:	94°C	45 seconds	} 24 cycles
Annealing:	$\Delta A^{\circ}C$	45 seconds	
Extension:	72°C	45 seconds	
Final Extension:	72°C	5 minutes	

Table 4.5. Annealing temperatures for the amplification of microsatellite markers

Microsatellite marker	Annealing (°C)
D21S213	52.2/53.9
D21S219	52.2/53.9
D21S224	52.2/53.9
D21S263	56.8/57.6
D21S272	52.2/53.9

Table 4.6. PCR reagents used for the amplifications of markers D21S213, D21S219, D21S224, D21S263 and D21S272

Reagent	Volume (µl)	[Stock]	[Final]
Buffer (25 mM MgCl ₂ included)	2.5	10X	1X (2.5 Mm MgCl ₂)
dNTP	2.0	2.5 mM	0.2 Mm
Betaine	6.5	5M	1.3M
DMSO	0.32	100 per cent	1.28 per cent
Forward Primer	0.4	10 µM	0.16 µM
Reverse Primer	0.4	10 µM	0.16 µM
ExTaq Polymerase	0.2	5U/µl	1U/µl

The microsatellite marker D21S1270 was amplified with Touchdown PCR amplification protocol, as shown below, using specific primers (Table 3.7) and reagents (Table 4.7):

Initial denaturation:	94°C	4 minutes	
Hot start:	80°C	hold	
Denaturation:	94°C	30 seconds	} 5 cycles
Annealing:	55°C	30 seconds	
Extension:	72°C	30 seconds	
Denaturation:	94°C	30 seconds	} 5 cycles
Annealing:	54.8°C	30 seconds	
Extension:	72°C	30 seconds	
Denaturation:	94°C	30 seconds	} 10 cycles
Annealing:	54.4°C	30 seconds	
Extension:	72°C	30 seconds	
Denaturation:	94°C	30 seconds	} 10 cycles
Annealing:	54°C	30 seconds	
Extension:	72°C	30 seconds	
Denaturation:	94°C	30 seconds	} 10 cycles
Annealing:	53.6°C	30 seconds	
Extension:	72°C	30 seconds	
Final Extension:	72°C	8 minutes	

Table 4.7. PCR reagents used for the amplifications of marker D21S1270

Reagent	Volume (µl)	[Stock]	[Final]
Buffer	2.5	5X	1X
MgCl ₂	2.5	25 mM	2.5 mM
DMSO	0.32	100 per cent	1.28 per cent
dNTP	2.0	25 mM	0.2 mM
Forward Primer	0.5	20 µM	0.4 µM
Reverse Primer	0.5	20 µM	0.4 µM
GoTaq Polymerase	0.2	5U/µl	1U/µl

4.4.2. Determination of Fragment Sizes by GeneScan Analysis

In order to determine repeat genotypes for the selected microsatellite markers, all samples were subjected to GeneScan Analysis (ABI PRISM[®] 310 or ABI PRISM[®] 3130 XL Genetic Analyzer, Refgen Biyoteknoloji, Ankara).

GeneScan analysis software helps the calculation of sizes of PCR fragments via comparing their lengths with its size marker. PCR fragments were labelled with FAM at the 5' end. In every run, control samples were also used. Prior to running PCR products on ABI PRISM[®] 3130 XL Genetic Analyzer, all samples were treated with formamide or heat for denaturation. Each mixture consisted of 1 µl PCR product, 9.8 µl formamide and 0.5 µl size marker. The optimized injection time was 1.5 kV for 15 seconds and the injection voltage was 1.6 kV. A 500 bp size standart was used in each run. The data was retrieved as chromas or ABI PRISM Peak Scanner files when ABI PRISM[®] 310 or ABI PRISM[®] 3130 XL Genetic Analyzer were used, respectively.

4.5. Mutational Analysis of Autosomal Dominant and Nonconsanguineous Familial and Juvenile ALS Cases in the Turkish Cohort

Thus far, besides SOD1, six genes were shown to be responsible for autosomal dominant late-onset ALS. Among these, TDP-43, ANG and FUS were analyzed in this Turkish cohort.

Before the amplification of the indicated genes, genomic DNA was subjected to whole-genome amplification to obtain large quantities of DNA. For this purpose, REPLI-g Mini Kit protocol was used.

4.5.1. Amplification of Genomic DNA Using the REPLI-g Mini Kit

Before starting with the procedure, 5 µl DNA samples were loaded to 96-well plates. Buffer DLB was prepared by adding 500 µl of nuclease-free water to the tube. It was mixed thoroughly and centrifuged. The initial step was the preparation of buffers D1 and N1. Buffer D1 for seven reactions was prepared with 9 µl of reconstituted buffer DLB and 32 µl of nuclease-free buffer. Again for seven reactions, buffer N1 consisted of 12 µl of stop solution and 68 µl of nuclease-free water. Following the addition of 5 µl of buffer D1 into each well, plates were vortexed and centrifuged briefly. 10 µl of buffer N1 was added to each well and vortexed and centrifuged briefly. Meanwhile, it was important to thaw DNA polymerase on ice. Other components were thawed at room temperature. The master mix per sample was prepared on ice with the addition of 29 µl of REPLI-g mini

reaction buffer and 1 μ l of REPLI-g mini DNA polymerase. Samples were run on 0.8 per cent agarose gel. Agarose was dissolved in 1X TAE buffer by boiling it in a microwave. Then, the homogenous mixture was poured onto an electrophoresis plate and left to polymerize at room temperature. Before loading, 2 ng of DNA per sample was mixed with an equal volume of DNA loading buffer, including EtBr with a final concentration of 1 μ g/ml. 10 μ l of each sample was run on gel at 120 V for 15 minutes in 1X TAE buffer. The gel was observed under UV light and documented. Plates were incubated for 10-16 hours at 30°C. Amplified DNA was stored at -20°C.

4.5.2. PCR Amplifications of TDP-43, ANG and FUS

The amplification protocol for all genes required 10 ng DNA. The reagents are shown in Table 4.8. The primer sequences for TDP-43, ANG and FUS are as in Tables 3.8, 3.9 and 3.10, respectively. The protocol was as follows:

Initial denaturation:	95°C	3 minutes	} 35 cycles
Denaturation:	94°C	40 seconds	
Annealing:	58°C	40 seconds	
Extension:	72°C	40 seconds	
Final Extension:	72°C	10 minutes	

Table 4.8. PCR reagents used for the amplifications of TDP-43, FUS and ANG

Reagent	Volume (μ l)	[Stock]	[Final]
2X PCR PremixD buffer (containing MgCl ₂ and dNTP)	10 μ l	2X	1X
Forward Primer	1 μ l	10 μ M	0.1 μ M
Reverse Primer	1 μ l	10 μ M	0.1 μ M
Taq Polymerase	0.4 μ l	5U/ μ l	1.6 U/ μ l

4.5.3. DNA Sequencing of TDP-43, FUS and ANG

Sequencing of samples for TDP-43, ANG and FUS was performed by The W.M. Keck Foundation Biotechnology Resource Laboratory, New Haven, USA.

4.6. Whole Genome Genotyping of Turkish Familial and Juvenile ALS Cases

In order to detect DNA concentrations, 2 μ l of DNA was measured with NanoDrop. Elution buffer was used as blank. The quality of each sample was detected by running on 0.8 per cent agarose gel. Agarose was dissolved in 1X TAE buffer by boiling it in a microwave. Then, the homogenous mixture was poured onto an electrophoresis plate and left to polymerize at room temperature. Before loading, 2 ng of DNA per sample was mixed with an equal volume of DNA loading buffer, including EtBr with a final concentration of 1 μ g/ml. 10 μ l of each sample was run on gel at 120 V for 15 minutes in 1X TAE buffer. The gel was observed under UV light and documented. All sample were placed into a 96-well plate with a final concentration of 55 ng/ μ l. The plates were stored at 4°C until the next step.

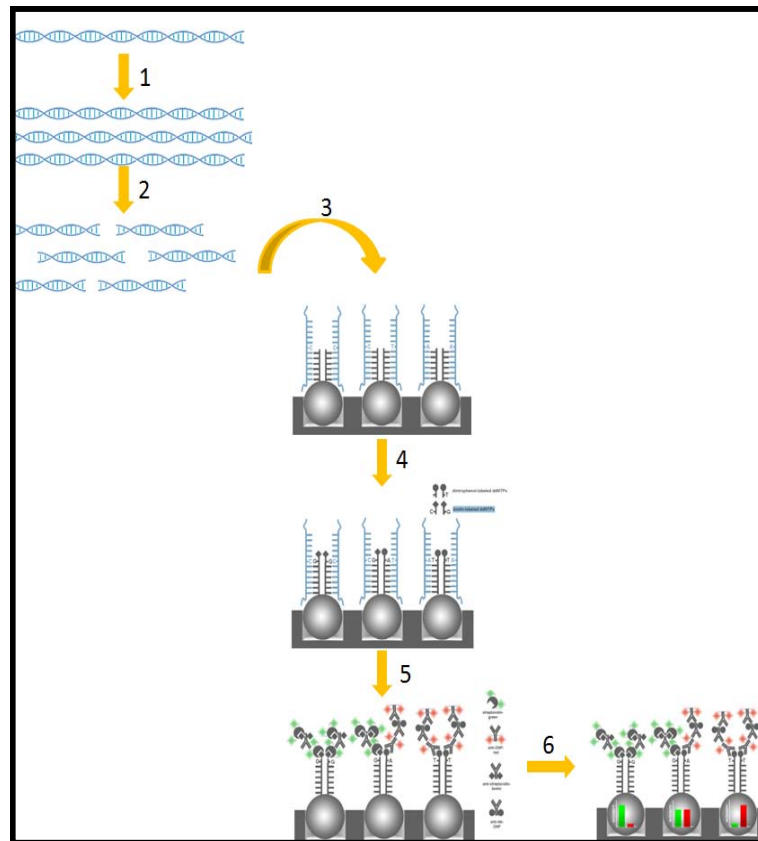


Figure 4.1. Steps of genotyping array. 1: whole-genome amplification; 2: fragmentation; 3: hybridization; 4: single base extension; 5: staining and 6: imaging (adapted from Illumina Whole-Genome Genotyping: Infinium[®] Assay Manual)

Illumina's Core BeadArray Technology is the most advanced technology used for the detection of whole-genome genotypes. BeadChips include 620,901 tagged SNPs derived from International HapMap Project. They also cover SNPs within 10kb of RefSeq genes, non-synonymous SNPs, ADME SNPs, and SNPs found in the MHC region. Besides being a powerful tool in the discovery of structural variations, they have an average of 15-18 fold redundancy which brings about an advantage in copy number measurements since it reduces overall noise.

On each bead, 50mer fragments are attached; on each chip, each bead is represented approximately 30 times for statistical significance. In an overall view, genomic DNA is firstly amplified in an isothermic reaction and then it is fragmented into 300-400 bp products (Figure 4.1). These fragments are transferred to BeadChips where they hybridize with their complement sequence. Then, a single base (dinitrophenol-labelled and biotin-labelled ddNTPs) is added to each bead strand so that during the staining process, these single bases can be recognized by specific primary and secondary antibodies. In the final stage, a laser system is used to excite the fluorophore of the single-base extension product on the beads. These signals can be detected by a scanner. Definite SNP genotypes are determined after data analysis using Illumina's genotyping analysis software. These experiments were performed in The W.M. Keck Foundation Biotechnology Resource Laboratory, New Haven, USA.

4.6.1. Amplification of DNA Samples

This step aims to amplify DNA samples. The principle is similar to conventional PCR. However, it differs in that the amplification occurs at a constant temperature. The procedure was as follows:

- In MSA1 plates, 20 μ l of MA1 was loaded to each well.
- 4 μ l of DNA and 4 μ l 0.1N NaOH were added.
- Plates were sealed with 96-well cap mat.
- Following vortex at 1600 rpm for 1 minute, plates were centrifuged at 280 xg for 1 minute.
- Samples were incubated for 10 minutes at room temperature.

- 75 µl MSM was added to each well.
- Plates were sealed with 96-well cap mat, vortexed at 1600 rpm for 1 minute and centrifuged at 280 xg for 1 minute.
- They were incubated in the Illumina Hybridization Oven overnight at 37°C.

4.6.2. Fragmentation of Amplified DNA

This step aims to fragment DNA enzymatically, using end-point fragmentation. This approach is more reliable in avoiding over-fragmentation problem. In the preparation step, the heat block was preheated to 37°C and FMS was thawed to room temperature, shaken gently and centrifuged at 280 xg.

The procedure was as follows:

- Plates were centrifuged at 50 xg for 1 minute.
- 50 µl of FMS was added to each well containing samples.
- Plates were sealed with 96-well cap mat, vortexed at 1600 rpm for 1 minute and centrifuged at 50 xg for 1 minute at 22°C.
- Sealed plates were placed on 37°C heat block for 1 hour.

4.6.3. Precipitation

In this step, 2-propanol and PM1 reagents were used to precipitate DNA. In the preparation step, PM1 was thawed to room temperature, shaken gently and centrifuged at 280 xg for 1 minute. The procedure was as follows:

- PM1 was added to each well, containing sample.
- Plates were sealed with 96-well cap mat, vortexed at 1600 rpm for 1 minute.
- Following incubation at 37°C for 5 minutes, plates were centrifuged at 50 xg for 1 minute at 22°C.
- 300µl of 100 per cent 2-propanol was added to each well.
- Plates were sealed with a new, dry cap mat.

- In order to mix the reagents, plates were inverted at least 10 times.
- They were incubated for 30 minutes at 4°C.
- Following centrifuge at 3000xg for 20 minutes at 4°C, plates were immediately removed.
- The next step was performed to avoid dislodging of the blue pellet. In case of delay, 20-minute centrifuge was performed before going on with the next steps.
- Cap mat was removed and supernatant was discarded by quickly inverting plates and tapping onto an absorbent pad.
- Tapping was performed firmly several times for 1 minute until no liquid was left in wells.
- Uncovered, inverted plates were left on the tube rack for 1 hour at room temperature until pallet was completely dry.

4.6.4. Resuspension of DNA

DNA present in pallet format should be resuspended. This was established by using RA1. In the preparation step, Illumina hybridization oven should be preheated to 48°C and RA1 should be thawed to room temperature. The following steps were as follows:

- RA1 was added to each well, containing DNA pellet.
- Plates were sealed with foil by firmly holding the heat-sealer sealing block down for 5 seconds.
- They were placed into the hybridization oven and incubated for 1 hour at 48°C.
- Finally, plates were vortexed at 1800 rpm for 1 minute and centrifuged at 280 ng.

4.6.5. Hybridization of DNA onto BeadChips

This step aims to transfer the fragmented, resuspended DNA onto BeadChips. In the preparation step, heat block and Illumina hybridization ovens were heated to 95°C and 48°C, respectively. The following steps were as follows:

- Hyb Chamber gaskets were placed into Hyb Chamber.
- 400 μ l of RA1 was added onto each of the 8 humidifying buffer reservoirs in each Hyb Chamber.
- They were closed firmly and were left on bench at room temperature until loading to BeadChips.
- Resuspended plates were placed on heat block for the denaturation of samples at 95°C for 20 minutes.
- BeadChips were removed from storage (2-8°C). However, they were not unpackaged until usage.
- Following incubation, plates were centrifuged at 280 xg.
- BeadChips were removed just prior to DNA loading.
- Each chip was placed in a Hyb Chamber insert, in the orientation that barcode symbol would match on the Hyb Chamber.
- 38 μ l of DNA was added into corresponding wells on BeadChips.
- BeadChip barcode should be labelled on lab tracking sheet and they were visually inspected to ensure that DNA samples were completely covered.
- Hyb Chamber inserts with BeadChips were loaded into Illumina Hyb Chamber. The barcode was placed over the ridges as indicated on the Hyb Chamber.
- Backside of lid was placed onto the Hyb Chamber, while front was brought down slowly because it was important not to dislodge inserts.
- Clamps on both sides of Hyb Chamber were tightly closed.
- Hyb Chamber was put into Illumina hybridization oven at 48°C in such an orientation that clamps face right and left side of oven.
- The incubation time was at least 16 hours, but not more than 24 hours.
- The plate was discarded.
- In order to resuspend XC4 reagent for Xstain HD BeadChip, 300 μ l of 100 per cent EtOH was added to XC4 bottle and was shaken vigorously for 15 seconds. It was left upright on bench overnight.
- It was important to resuspend the pellet completely. Thus, if any coating was observed, it was vortexed at 1625 rpm until total suspension.

4.6.6. Staining and Finalization of Genotyping

From this step on, the procedure was performed automatically by Tecan Freedom Eco Robot. The general flow of the procedure was washing away unhybridized and non-specifically hybridized DNA from chips, adding a single labelled base to beads, staining of primers, scanning and data analysis using Illumina's genotyping analysis software.

4.6.7. Evaluation of Genotyping Data

The final results were evaluated using the BeadStudio program, a program specifically designed for the analysis of BeadChip genotyping. The data was transferred to a text file. In the initial step, the efficiency of the experiment must be evaluated according to the 'B allele frequency' and 'Log R Ratio' values, using Illumina Genome Viewer.

B allele frequency, also referred as 'copy angle' or 'allelic composition', exhibits a rough representation of genotypes for an individual SNP which may be either AA, AB or BB (Figure 4.2). Therefore, a successful experiment is represented as three distinct bands, named as trimodal state.

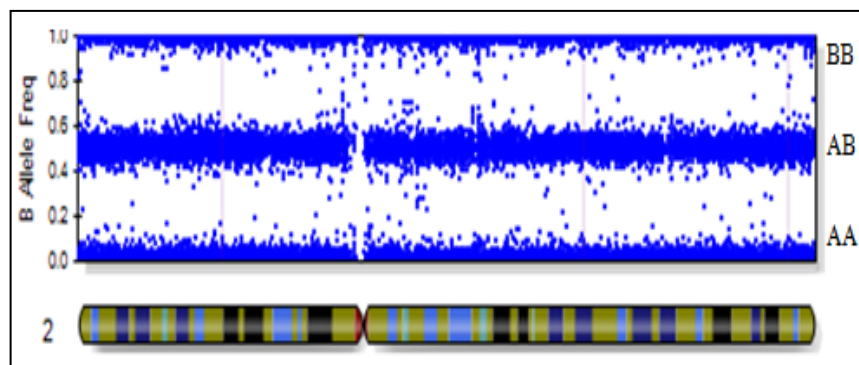


Figure 4.2. An example showing B allele frequency in chromosome 2

R measures the signal intensity for a locus. In this respect, $\log R$ is an indirect value of copy number for that locus (Gibbs *et al.*, 2006). It is based on normalized intensity of data. In this respect, the final $\log R$ ratio of a single sample is calculated with the below formula:

$$\log_2 R = \log_2 \text{sample} / \log_2 \text{control}$$

For an individual with normal number of alleles, the log R ratio is expected to be 0, mild fluctuations are overlooked (Figure 4.3). While an increase above 2 for this value may be an indicative of a duplication for that SNP, values below 2 are questioned for possible deletions. A significant region should have at least two consecutive SNPs with a change in log R ratio.

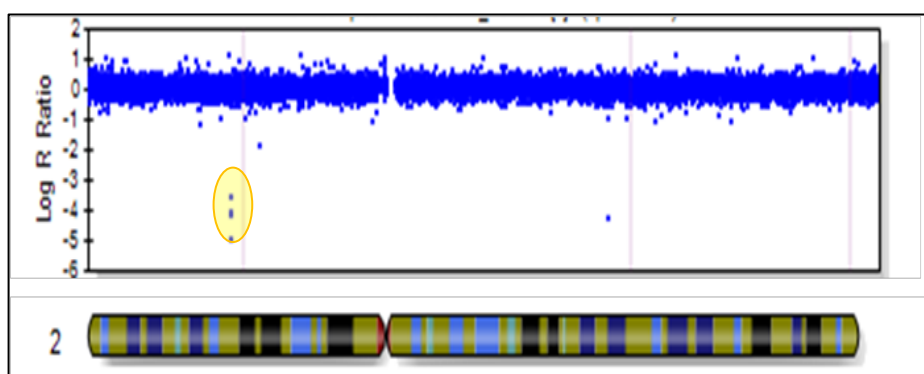


Figure 4.3. An example showing log R graph for chromosome 2. The yellow circle indicates three consecutive SNPs below threshold which may be a good candidate region.

In case of a deletion where only one copy is present, log R ratio is <1 as this value is directly determined by the DNA copy number. Also, B allele frequency becomes bimodal since only 'two genotypes are allowed' (Yau *et al.*, 2008). On the contrary, in case of copy number ≥ 3 , log R ratio becomes >1 and B allele frequency is represented with additional modes as a result of increased number of genotypes, such as AAA, AAB, ABB, etc. Basically, these two metrics produced by Illumina enables direct visualization of structural variations.

Once the samples were visually inspected for quality control for all chromosomes, further analysis were performed.

4.6.7.1. Loss-of-heterozygosity (LOH). Loss-of-heterozygosity (LOH) analysis aims to detect long stretches of chromosomal regions with a B allele frequency less than zero. In this study, blocks of 100 were chosen randomly by the program.

4.6.7.2. Copy number variation (CNV). Copy number variation analysis aims to detect any changes in the copy number within the genome. Basically, CN is determined by the combinatorial evaluation of CNV values and CNV confidence for chromosomal regions in each sample. While CNV value mostly represents an estimate copy number, CNV confidence is rather a relative score certifying the accuracy of the copy number estimate.

The exported reports were transferred to an excel file and were run in three different algorithms (PennCNV, QuidriSNP and Gnosis) which highly increased reliability. These algorithms were highly specific in detection of heterozygous deletions and duplications. Homozygous deletions were further analyzed by 'Homozygous Detector' program.

4.6.7.3. Further evaluation by PLINK. PLINK is an advanced program designed to perform a wide spectrum of GWA analysis from basic to complex in a computationally efficient manner (Purcell *et al.*, 2007). It has been developed by Shaun Purcell at the Center for Human Genetic Research (CHGR), Massachusetts General Hospital (MGH), and the Broad Institute of Harvard & MIT, with the support of others.

The initial step was the transfer of data in PLINK format by PLINK Input Report Plug-in v2.1 program. This program required a ped and a map file which included family data (family ID, sample ID, sex, relationship, etc) and SNP data (SNP ID, chromosomal location, size, etc), respectively. The selective parameters that were added for a more reliable analysis were:

- SNP call rate was adjusted to 100 per cent, meaning that only SNPs which were efficiently valued in all patients were chosen.
- Minimum allele frequency was determined as 0.05 per cent, indicating that only 5 per cent should have the minor allele.
- Hardy-Weinberg equilibrium was 0.001.
- Individual call rate was set to 97 per cent, indicating that at least 97 per cent of SNPs should have worked in each individual. Otherwise, that individual will be eliminated.

4.7. Special Focus on a Turkish Autosomal Recessive ALS Family: ALS252, ALS256 and ALS257

In order to determine ALS-specific homozygosity regions, the results of whole genome genotyping analysis were compared to 112 Turkish patients with cortical malformations. While some of these control cases belonged to consanguinous families, others were nonconsanguinous.

Five candidate genes which were suspected to play roles in ALS were selected for further analysis. This set of new candidate genes were proposed by Arthur L. Horwich (Eugene Higgins Professor of Genetics and Pediatrics at Yale School of Medicine) through personal communication of the collaborator of this study, Dr. Murat Gunel (Yale Medical School Department of Genetics).

4.7.1. PCR Amplifications of CPEB3, IL21, RAB27, UCHL3 and USP53

The amplification protocol for all genes required 10 ng DNA. The reagents are shown in Table 4.8. The primer sequences for CPEB3, IL21, RAB27, UCHL3 and USP53 are as in Tables 3.11 to 3.15, respectively. The protocol was as follows:

Initial denaturation:	95°C	3 minutes	
Denaturation:	94°C	40 seconds	} 35 cycles
Annealing:	58°C	40 seconds	
Extension:	72°C	40 seconds	
Final Extension:	72°C	10 minutes	

4.7.2. DNA Sequencing of CPEB3, IL21, RAB27, UCHL3 and USP53

The sequencing of samples for CPEB3, IL21, RAB27, UCHL3 and USP53 was been performed by The W.M. Keck Foundation Biotechnology Resource Laboratory, New Haven, USA.

4.7.3. Whole Human Exome Analysis

Whole human exome technology is a high-throughput next-generation resequencing which aims to identify functional variations that are responsible for many diseases. A single 2.1M array can include the entire human genome, consisting of ~180,000 coding exons of 18,673 protein-coding genes and 551 miRNA exons.

Basically, genomic DNA was first fragmented, followed by hybridization of common adaptors which contained universal priming sequences (Figure 4.4). Then, the sample was hybridized to NimbleGen 2.1M Human Exome Array. This array embedded ~385,000 ‘surface-tethered, single-stranded oligos with high sensitivity to regions of interest (Turner *et al.*, 2009). Unbound fragments were eliminated by washing step. Following the target fragment elution, amplification of exomes were established. The resulting PCR products were purified and subjected to DNA sequencing analysis on the Illumina platform. Quantitative PCR was performed to detect the relative fold enrichment of targeted sequences. To narrow down candidate genes, the results were filtered to eliminate sequences which are indicated in HapMap or SNP Database.

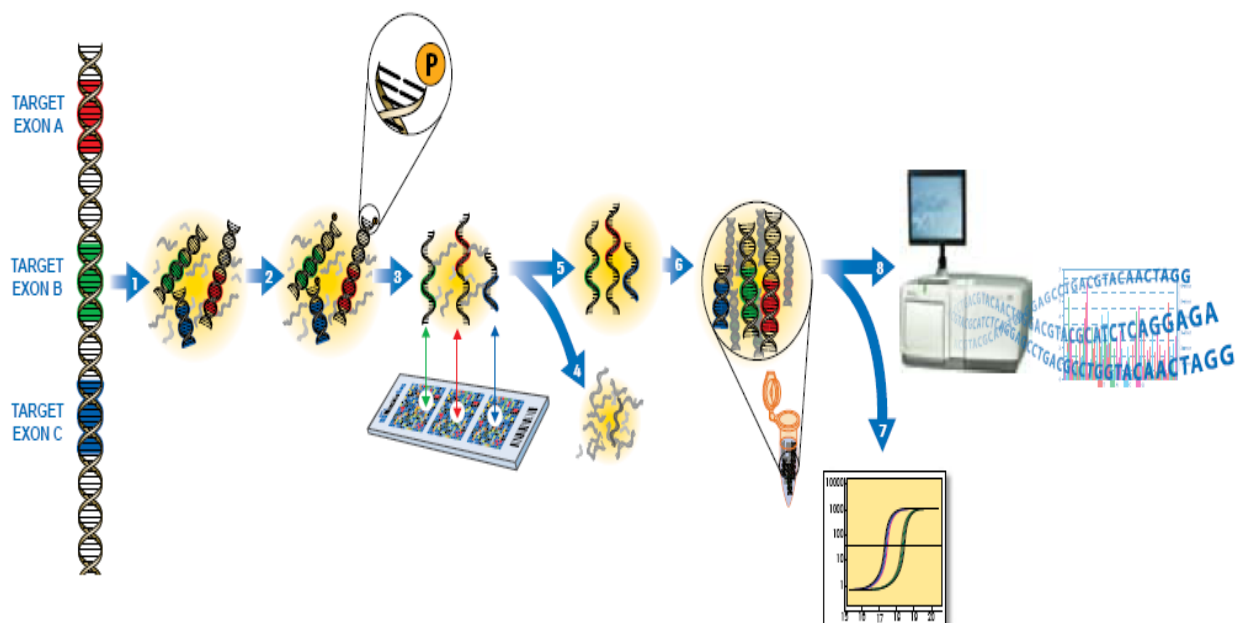


Figure 4.4. Schematic representation of whole exome sequencing (www.nimblegen.com)

4.8. Genome-wide Association (GWA) Study in SALS

4.8.1. Genotyping of samples

In the framework of this study, the expression profiles of five SNPs were investigated in 88 brain lysates of which 57 were from cerebellum and 32 from cortex. All cases were sporadic; they were diagnosed as probable or definite ALS. They were all Caucasian and of European-American descent. While 46 were male, 40 were female and two were unknown. The initial step was the identification of genotypes. The protocol was as follows:

- Final DNA concentration was adjusted to 2 ng/ μ l.
- In an Eppendorf tube, AmpliTaq Gold PCR Master mix was combined with probe.
- The content was mixed gently by hand.
- 2.5 μ l of mix was added to each well in an 384-well plate.
- 2.5 μ l of DNA was also added to each well and centrifuged briefly.
- For negative control, 2.5 μ l of dH₂O was tested in 6 wells; 2.5 μ l of mix was added onto these wells.
- Samples were run on thermocycler, as below:

95°C for 10 minutes	} 50 cycles
95°C for 15 seconds	
60°C for 1 minutes	

4.8.2. Detection of the Expression Levels of SNPs

4.8.2.1. Total RNA preparation. To determine total RNA concentration of each sample, 1.5 μ l of RNA was measured with NanoDrop. Elution buffer was used as blank. The quality of each sample was detected by running them on 1.25 per cent agarose gels. Agarose was dissolved in buffer by boiling it in a microwave. Then, the homogenous mixture was poured onto an electrophoresis plate and left to polymerize at room temperature. Before loading, 2 ng of RNA sample per sample was mixed with an equal volume of RNA loading buffer, including EtBr, with a final concentration of 1 μ g/ml.

Then, each tube was denaturated for 15 minutes at 65°C and placed immediately on ice. 10 µl of each sample was run on gel at 60 V for 2.5 hours in 1X MOPS buffer. The gel was observed under UV light and documented.

4.8.2.2. cDNA synthesis from total RNA. The master mix (Table 4.9) was prepared on ice with according to the following protocol:

- Master mix for each RNA sample was prepared separately, since RNA volumes differed and thus water volumes differed.
- Master mix was aliquoted to tubes and RNA (volume determined earlier for 0.5 µg total RNA) was added.
- Tubes were mixed by hand and then centrifuged.
- Samples were run on ‘cDNA-synthesis program’ on thermocycler; the program was as below:

25°C for 10 minutes

42°C for 50 minutes

85°C for 5 minutes

4°C hold

- 1 µl of E.coli RNase H was added to each reaction.
- Tubes were mixed by hand and then centrifuged.
- They were run on thermocycler at 37°C for 20 minutes.

Table 4.9. Reagents used in cDNA synthesis

Reagent	Volume (µl)	[Stock]	[Final]
RT Reaction Mix	10	2X	0.4X
RT Enzyme Mix	2	--	--
DEPC-treated H ₂ O	8-x (x: volume for 0.5 µg RNA)	--	--

4.8.2.3. Relative quantification of gene expression by qPCR. Quantitative polymerase chain reaction (qPCR) is a modification of the polymerase chain reaction which is used to

measure the quantity of complementary DNA that is present in a sample. The initial step was the preparation of qPCR master mix on ice (Table 4.10). This step must be performed separately for each target probe. It should be noted that ice bucket cover must be closed to protect thawed probes/controls from light exposure.

Table 4.10. Reagents of qPCR master mix

Reagent	Volume (μ l)
2X Platinum PCR Supermix	10
Target Probe (HS1135)	1
Endogenous Control (B2M)	1
MB Grade dH ₂ O	6

The steps of the protocol were as follows:

- In the previous step (Section 4.8.2.2), 20 μ l cDNA was produced. 60 μ l dH₂O was added to each well so that the samples were diluted.
- 2 μ l of cDNA template was put into a 384-well plate, containing qPCR master mix. It was important to have replicate sets for each sample.
- The plates were covered with translucent PCR sealing film, vortexed shortly at low speed and centrifuged.
- It was placed in TaqMan[®] 7900HT Sequence Detection System.

4.8.2.4. Running samples in TaqMan[®] 7900HT Sequence Detection System. TaqMan[®] 7900HT Sequence Detection System (SDS) aims to determine the quantity of expression of target genes, based on the fluorescent data from each amplicon. The data is displayed as either linear or logarithmic. Each run should include a calibrator, a sample used as the basis for comparison of expression results. For example, if an effect of a drug on expression level is investigated, then the calibrator is the untreated sample. Endogenous control is an RNA/DNA which is used for normalization of the amount of mRNA target for differences in the amount of total RNA, added to each reaction. Also, standards should be used in each run. These are generated from a biological sample, like a cell line, which simply expresses both target and reference genes.

The running of samples in TaqMan[®] 7900HT Sequence Detection System was as follows:

- Wells to be used were chosen, highlighted in trios and labelled.
- B2M was marked as endogenous control for each well.
- This data was saved as .SDS file.
- The analysis program was as below:

50°C for 2 minutes	} 40 cycles
95°C for 2 minutes	
95°C for 15 seconds	
60°C for 1 minute	

4.8.2.5. Evaluation of qPCR results. Quantitative PCR can be evaluated by two different analysis methods: absolute quantification is the measurement of the copy number of the transcript of interest, while relative quantification determines change in expression level of a target gene relative to a reference group (untreated control or a sample at time zero in a time-course study) (Livak *et al.*, 2001).

In this study, the relative quantification approach was performed. Each sample should be studied in replicates. In the final calculation, the expression level of a target gene is the average of its replicates. The ‘Threshold Cycle’ (C_T) is the cycle number at which sufficient amount of amplicons have been generated. It is important that C_T value is consistent within each replicate; standard deviation between each replicate should be <0.3 . PCR efficiency is formulated as:

$$\Delta C_T = C_{T\text{target}} - C_{T\text{reference}}$$

‘The Comparative C_T ($\Delta\Delta C_T$) Method’ is a similar approach to ‘Relative Standard Curve Method’, except for the use of arithmetic formulas for evaluation of data. A valid $\Delta\Delta C_T$ reflects the efficiency of target amplification relative to the efficiency of reference amplification.

$$\Delta\Delta C_T = C_{T\text{test sample}} - C_{T\text{calibrator}}$$

The software program displayed the standard curve as well as unknowns. The final calculations were presented as excel sheet. The statistical analysis was performed using GraphPad Prism 5 Program.

4.8.3. Western Blot Analysis

4.8.3.1. Preparation of cell lysates. The initial step of Western blot analysis was the preparation of cell lysates from brain samples. The steps were as follows:

- 2 ml of 0.5M of EDTA was added into 100 ml of RIPA buffer to make EDTA with a final concentration at 1mM.
- 10 μ l of protease inhibitor was added to 1 ml of RIPA buffer w/ 1 mM EDTA just before using for lysis (3 ml RIPA buffer was prepared for 4 unknowns).
- RIPA buffer w/ protease inhibitor was kept on ice before use.
- The culture medium was carefully removed from each flask.
- Each flask was washed with cold PBS twice. It was important to keep the scraper and 1.5 ml tube cold.
- 0.5 ml cold RIPA buffer was added to each 75cm² flask, containing 5 x 10⁶ HeLa cells.
- The flasks were kept on ice for 5 minutes, followed by swirling twice to spread RIPA buffer evenly during incubation (20 μ l of packed cells was equal to 5 x 10⁶ which was about 40 mg of cells).
- The lysate was mixed for 30 minutes at 4 °C on a nutator.
- After gathering the lysate to one side of the flask, it was transferred to 1.5 ml microtubes.
- The tubes were centrifuged in the microcentrifuge at 12,000 rpm for 20 minutes at 4 °C.
- The supernatant was transferred to a new tube and kept on ice for the quantification step.

4.8.3.2. Quantitative analysis of protein. Quantification of the extracted protein was performed using the BCA assay kit. The steps were as below:

- Six standards were prepared on a 96-well plate as shown in Table 4.11.

Table 4.11. Formulas for the dilutions of six standards

Standards	Final Concentration (mg/ml)	RIPA Buffer w/Protease (µl)	BSA Stock (µl)
Reference	0	50	0
1	0.025	43.75	6.25
2	0.5	37.5	12.5
3	0.75	31.25	18.75
4	1	25	25
5	1.5	12.5	37.5
6	2	0	50

- For each sample, 80 µl of BCA working reagent (WR) was prepared. The following formula was used for the calculation of total volume of WR needed:

$$(7 \text{ Standards} + 4 \text{ unknowns}) \times (2 \text{ replicates}) \times 80 \text{ µl} = 1760 \text{ µl of WR}$$

- For each unknown, 500 µl of Reagent A was mixed with 10 µl of Reagent B.
- 80 µl of WR reagent was added to each well on a 96-well PCR plate.
- 4 µl of each standard point and unknown sample replicate were pipetted.
- The PCR plate was sealed and incubated at 37 °C for 30 minutes.
- The tubes were cooled to room temperature.
- All samples should be tested on NanoDrop within 10 minutes.
- Before actual measurement in NanoDrop, dH₂O was used to initialize the instrument, and WR buffer was used as blank.
- Following the reading of the reference sample, six standards in replicates were tested.
- The unknown sample reading was adjusted according to standards.

- All lysates were frozen at -20 °C or -80 °C prior to polyacrylamide gel running.

4.8.3.3. Running lysates on polyacrylamide gel. All lysates were run on polyacrylamide gel (PAGE).

- The lysates were mixed with 4X Tris-Glycine SDS sample buffer and 2-mercaptaethanol. The volumes were as:

5 µl of 4X sample buffer + 1 µl of 20X 2-mercaptoethanol +15 µl of sample

- The protein marker was thawed in room temperature. It should not be heated!! 5 µl of marker was loaded to the gel.
- The samples were boiled at 100 °C for 5 minutes and kept at room temperature.
- 20 µl of each sample was loaded on the gel.
- 1000ml of 1X Tris-Glycine running buffer was prepared from 10X running buffer stock.
- 10 per cent Tris-Glycine gel (12-well with 1mm thickness) was warmed up at room temperature before using.
- After opening the gel package, the buffer inside the package was drained out.
- The gel cassette was rinsed with deionized water.
- First, the tape in the back of the gel was peeled off, and then the comb was pulled out.
- All wells were dried out and washed with 1X running buffer twice.
- They were filled with running buffer and all bubbles were removed.
- The minigel with Xcell Surelock systems was assembled as instructed.
- The upper chamber was filled with 200 ml of running buffer.
- The samples and the marker were loaded with special fine tips. If all lanes were not used, the remaining empty wells were filled with loading dye.
- The lower chamber was filled with 600 ml running buffer after sample loading.
- The gel was run at 125V for 1 hour 45 minutes (start: 30-40 mA; end: 8-12 mA).

4.8.3.4. Blotting. Following the dissociation of protein lysates on PAGE, the gel was transferred to membranes for Western blot analysis. The procedure was as follows:

- 500 ml transferred buffer was prepared with 20 ml of 25X of Tris-Glycine transfer buffer, 100 ml of methanol and 380 ml of ddH₂O.
- The PVDF membrane was first soaked into 2.5 ml of methanol for 2 minutes, followed by rinsing with dH₂O briefly and finally soaking into the transfer buffer. The membrane should not be touched with fingers at any point; forceps may be used.
- The blotting pads and filter paper were made wet with 400 ml transfer buffer just before use.
- The gel was removed from the cassette for transfer.
- The gel surface was pre-wetted with some transfer buffer.
- A pre-wet filter paper was placed on top of the gel. Then, the plate was turned over, so that the gel/filter paper was at the bottom.
- The plate was lifted off, while leaving the gel/filter on a plastic board.
- The top and bottom of the gel were cut off.
- The bubbles were removed from the gel/ membrane and gel/filter paper.
- The 'sandwich' structure was assembled, the layers were as follows: 2 blotting pads at the bottom, 1 pre-wet filter paper, gel, PVDF membrane, 1 filter paper, 3 blotting pads on top.
- The blot module was inserted into the gel box,
- Adequate amount of transfer buffer was added into the inner chamber to cover the pads. The chamber should not be overfilled.
- 650 ml of dH₂O was poured into the outer chamber.
- The gel was run at 25V for 2 hours (start current: 106 mA).

4.8.3.5. Blocking of the blots.

- Before the disassembly of the gel, 1X PBS and 3 per cent milk were prepared freshly.
- After transfer, the gel apparatus was turned such that the side of membrane with protein was up.

- The PVDF membrane was cut into two pieces. The top left corner on each piece was cut for orientation.
- It was rinsed in 50 ml PBS buffer twice.
- The transfer was blocked with 100 ml of PBS-3 per cent milk for 1 hour at room temperature while shaking slowly.

4.8.3.6. Primary antibody hybridization.

- 40 μ l of primary Ab was added to each 8 ml of PBS-3 per cent milk .
- The hybridization bags were prepared by sealing three sides.
- The blot was placed into each bag and 8 ml of primary Ab was poured in.
- The bags were taped to the clipboard and attached to nutator in the refrigerator and incubated for overnight at 4° C or 4 hours at room temperature.
- Blots were washed quickly in a container with PBST-0.05 per cent Tween 20 for 5 minutes 3 times.

4.8.3.7. Secondary antibody hybridization.

- The PVDF membrane was incubated with 50 ml PBS-3 per cent milk and 25 μ l 2nd antibody (1 to 4000 diluted) for 1 hour.
- It was washed in 50 ml of PBST-0.05 per cent Tween-20 for 5 minutes 3 times.
- The membrane was rinsed with PBS to remove extra Tween-20.
- For the detection of the protein on the blot by ‘west femto maximum sensitivity substrate’, the pieces of the membrane were lined up and placed in a small box and were treated with the working solution for 3 minutes.

4.8.3.8. Exposure of the blot.

- The membrane was transferred to a sheet protector and the cut blot pieces were lined up to the original orientation.
- Following the drying of the gel, it was wrapped properly.
- A blank paper was taped to the blot and exposed to film for 1 minute.

5. RESULTS

5.1. Mutation Analysis on Turkish SALS and FALS Patients: Investigation of SOD1 in the Turkish ALS Cohort

5.1.1. PCR Amplification of SOD1

All exons of the SOD1 gene of 198 Turkish ALS patients were amplified as described in Section 4.3.1.

5.1.2. DNA Sequencing Analysis of FALS Cases

5.1.2.1. N86S. In the wild-type sequence, SOD1/codon 86, located in exon 4, is AAT. DNA sequencing analysis of ALS191 revealed a homozygous AAT→AGT transition at this position, resulting in an asparagine to serine exchange in both alleles (Figure 5.1). This mutation is a previously described mutation to cause ALS (www.alsod.org).

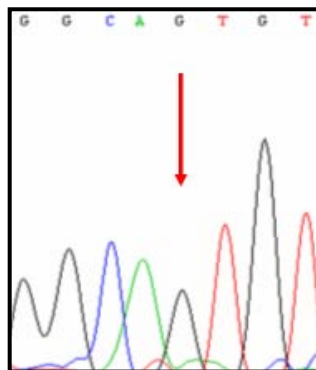


Figure 5.1. Chromatogram, showing the sequencing profiles of ALS191, carrying AAT→AGT transition in exon 4 position 86 (N86S)

The parents of the index case were first cousins. His first symptom was observed at the age of 28 which was weakness in his right shoulder. The clinical features extended to weakness in his right arm, right leg and left shoulder within a month. Due to a very progressive atrophy in legs and arms, he died within four months after diagnosis. There is

no apparent neurological disease running in the family, thus, the index patient was referred to us as ALS case.

Since the index case carried the mutation in a homozygous state, both of the parents were assumed to be carriers of the mutant allele. The presence of the mutation was confirmed in the father, but since the mother died at an early age, her DNA sample was not present. The pedigree was modified accordingly (Figure 5.2). The overall result of the analysis of the index case and his father indicate autosomal recessive inheritance of the N86S mutation in this family.

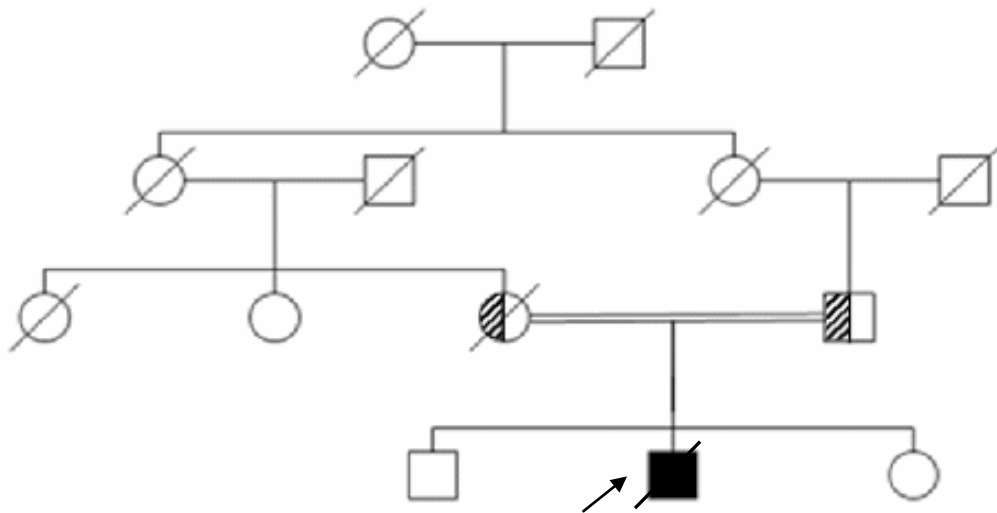


Figure 5.2. Pedigree of ALS191

5.1.2.2. H71Y. In the wild-type SOD1, codon 71, located in exon 3, is CAC. In a juvenile SALS patient, ALS226, CAC→TAC transition was detected, resulting in a histidine to tyrosine exchange (Figure 5.3). This is a mutation which has been already reported to cause ALS (www.alsod.org).

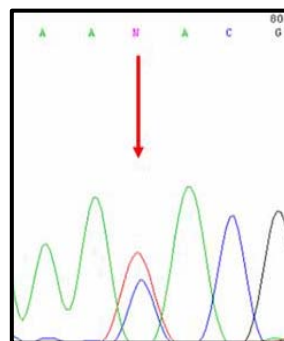


Figure 5.3. Chromatogram, showing the sequencing profile of ALS226, carrying CAC→TAC transition in exon 3 position 71 (H71Y)

The index patient was diagnosed with ALS at the age of 19. His initial symptom was weakness in his left leg which was followed by weakness in his right leg within a month. He was unable to walk by the end of two months due to a fast progressing atrophy in legs and arms. He died in less than one year.

DNA sequencing revealed the heterozygous presence of the H71Y mutation in this patient. This is indicative of the presence of this mutation in at least one of the index case's parents. Thus, other family members were also subjected to DNA sequencing for exon 3 (Figure 5.4). While his father and younger brother were carrying the mutant allele heterozygously, his mother and younger sister had normal alleles.

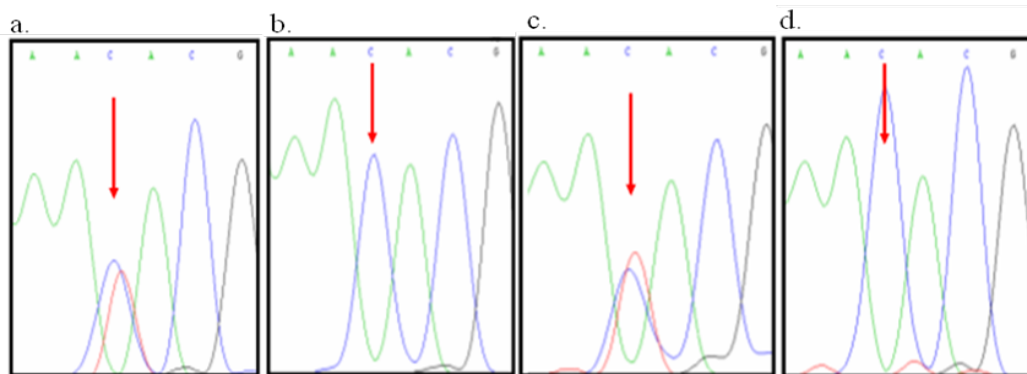


Figure 5.4. Chromatograms, showing the sequencing profiles of family members of ALS226, a. father, b. mother, c. older brother and d. younger sister.

The family tree according to the DNA sequencing analysis of exon 3 is below (Figure 5.5).

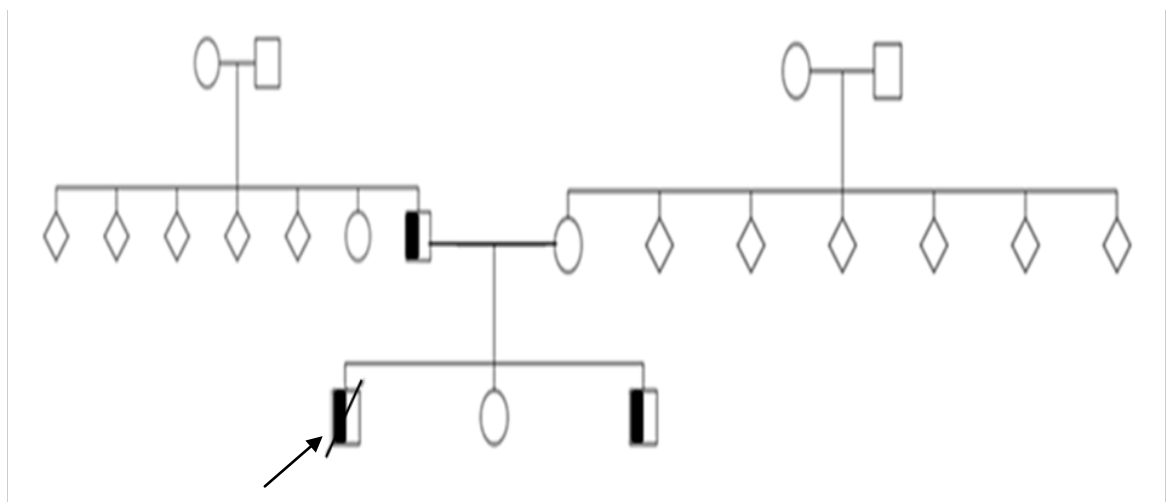


Figure 5.5. Family tree of ALS226

5.1.2.3. L144F. In the wild-type SOD1 sequence, codon 144, located in exon 5, is TTG. ALS61 was shown to have a TTG→TTC transversion at this position, resulting in the exchange of leucine to phenylalanine (Figure 5.6).

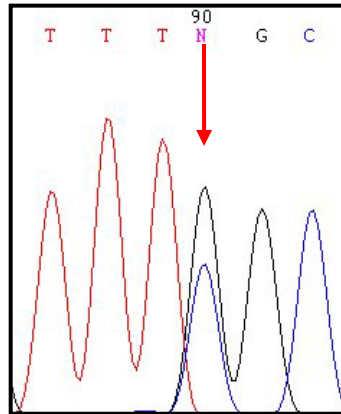


Figure 5.6. Chromatogram, showing the sequencing profile of ALS61, carrying TTG→TTC transversion in exon 4 position 144 (L144F)

ALS61 was diagnosed with ALS at the age of 52 (Figure 5.7). She is originally from the Balkan region. Her grandmother and uncle on fatherside, as well as her father and older brother, were diagnosed with ALS, indicative of dominant inheritance running through the fatherside. Her first symptoms were weakness in her legs and difficulty in walking. Recently, having the disease for over six years, she is still able to walk with cane and eat on her own, indicating a slow progression.

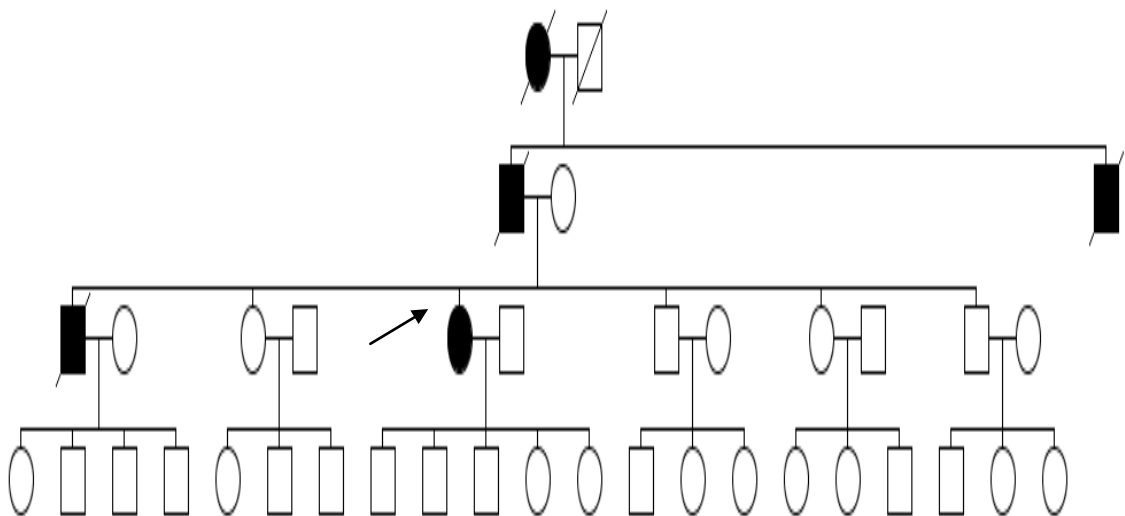


Figure 5.7. Family tree of ALS61

5.1.2.4. D90A. In the wild-type SOD1 sequence, codon 90 in exon 4 is GAC. DNA sequencing of ALS147 revealed a homozygous GAC→GCC transversion at this position which results in the exchange of aspartic acid to alanine (Figure 5.8).

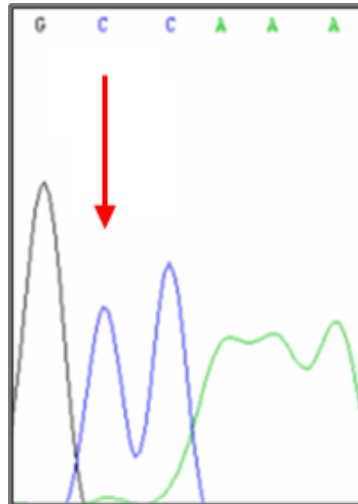


Figure 5.8. Chromatogram, showing the sequencing profile of ALS147, carrying GAC→GCC transversion in exon 4 position 90 (D90A)

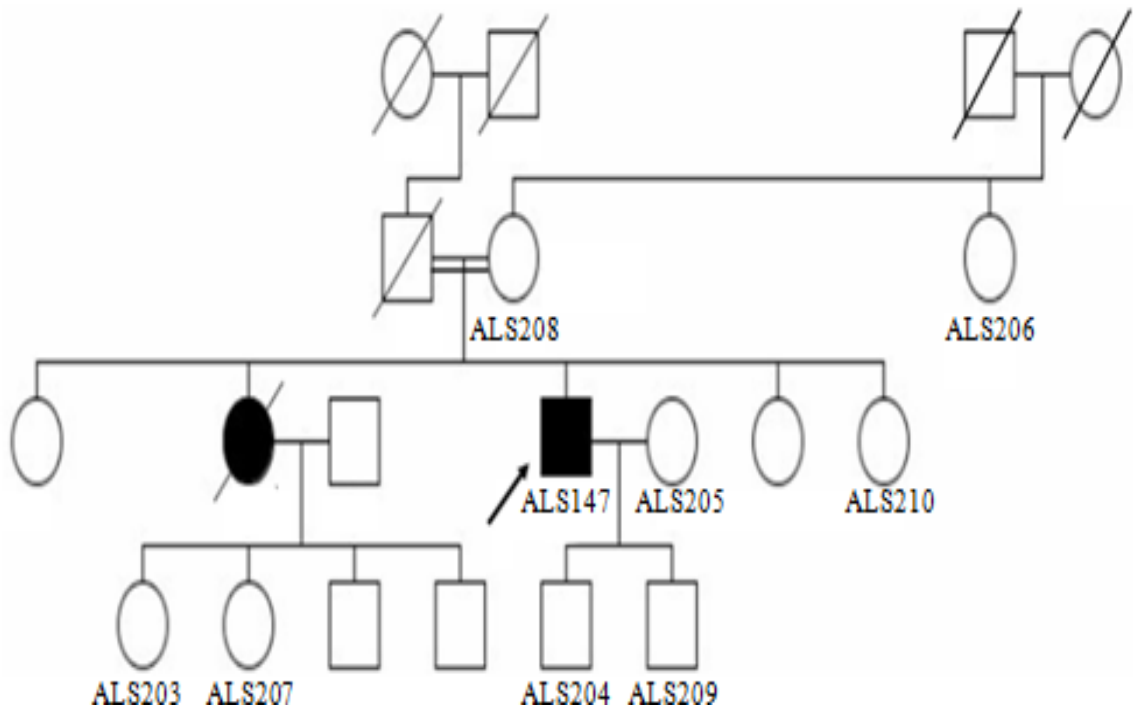


Figure 5.9. Family tree of ALS147

The patient was diagnosed with ALS at the age of 49 (Figure 5.9). His older sister had died from ALS, her sample was not available any more at the time of analysis. The initial symptoms of the index patient were weakness in his right leg, imbalance, difficulty in swallowing and depression. Recently, having the disease for five years, he can still walk with a cane, has increasing difficulty in swallowing, but can still eat soft food which are indicatives of slow progression.

The homozygous presence of D90A was found to be interesting, since it indicated an autosomal recessive inheritance pattern; available members of the family were subjected to further investigation (Section 5.2.1).

5.1.2.5. A4S and IVS-III-34 A→C transversion. In the wild-type SOD1 sequence, codon 4, located in exon 1, is GCC. ALS221 was shown to have a GCC → TCC transversion at this position, resulting in the exchange of alanine to serine (Figure 5.10a). The patient also carried IVS-III-34 A→C transversion (Figure 5.10b).

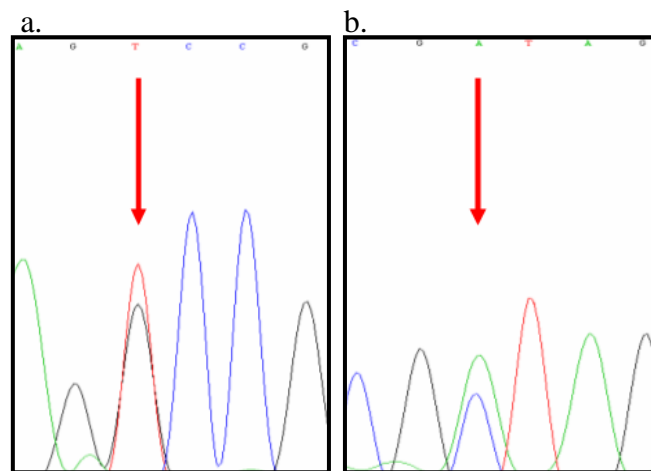


Figure 5.10. Chromatograms, showing the sequencing profile of ALS221, carrying both (a) the GCC → TCC transversion in exon 1 position 4 (A4S) and (b) the IVS-III-34 A→C transversion

IVS-III-34 is highly conserved in rodents (Figure 5.11). IVS-III-34 A→C was described as a rare polymorphism with a frequency of four per cent in normal controls (Siddique personal communication, Deng *et al.*, 1993).

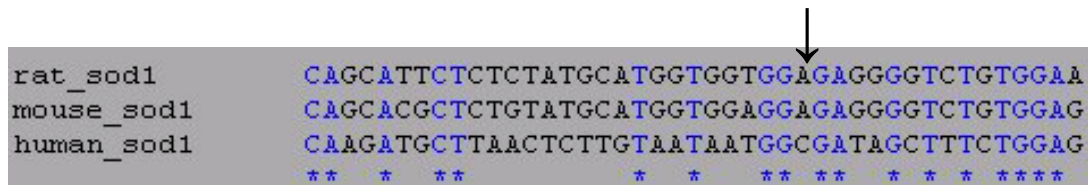


Figure 5.11. Multiple sequence alignment of a part of intron 3. The nucleotide in interest is indicated by the arrow, and (*) show the conserved regions.

5.1.2.6. IVS-III-34 A→C transversion. The rare polymorphism at position 34 in intron 3 was detected also in ALS215 in whom no SOD1 mutation was present (Figure 5.12).

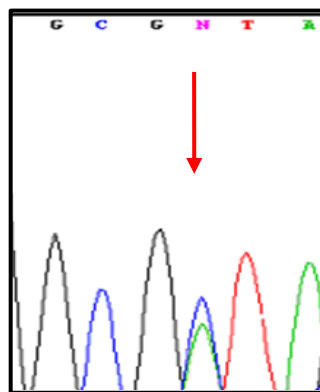


Figure 5.12. Chromatogram, showing the sequencing profile of ALS215, carrying the IVS-III-34 A→C transversion

The age of onset of the patient was 60. His father and younger sister were questioned for ALS, they both had passed away (Figure 5.13). He has been suffering from ALS for two years at the time of DNA analysis.

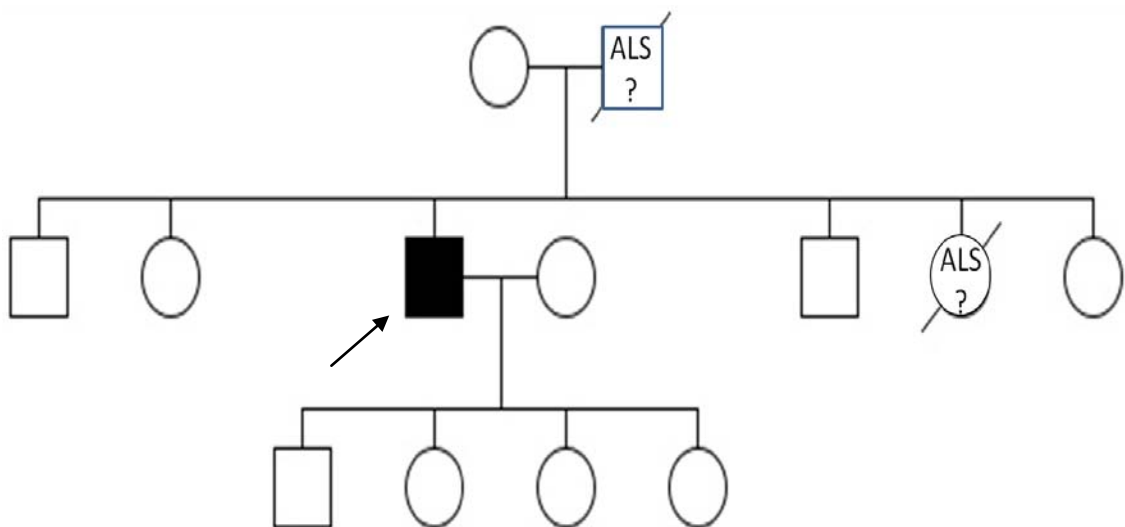


Figure 5.13. Family tree of ALS215

5.1.3. DNA Sequencing Analysis of SALS Cases

DNA sequencing of exon 3 revealed an A→C transversion at nucleotide position 34 in intron 3 of ALS patients 1, 40, 120, 122 and 242 in a heterozygote state (Figure 5.14).

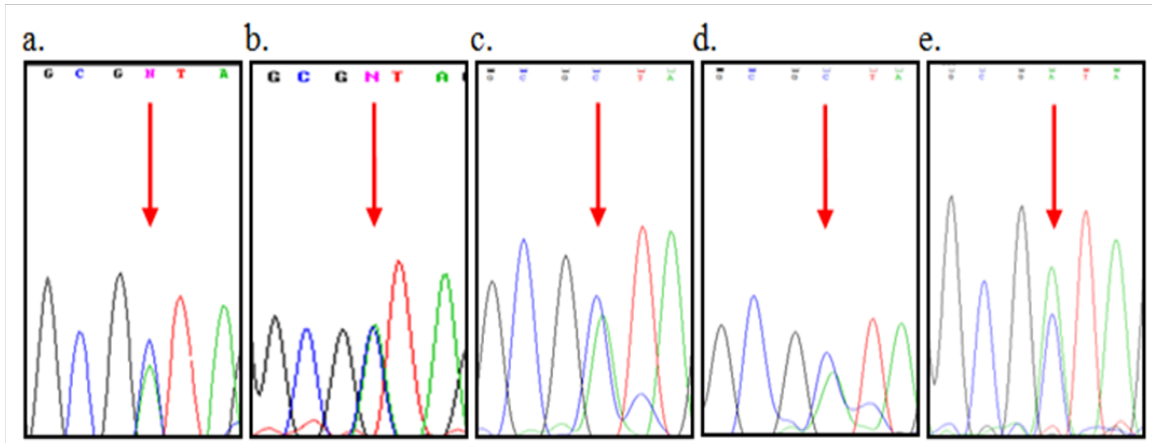


Figure 5.14. Chromatograms, showing the sequencing profiles of SALS patients with IVS-III-34 A→C transversion. a. ALS1, b. ALS40, c. ALS120, d. ALS122 and e. ALS242.

The family trees of individuals with IVS-III-34 A→C transversion are shown in Figures 5.15 through 5.19, respectively. Additionally, their brief clinical informations are presented in Table 5.1.

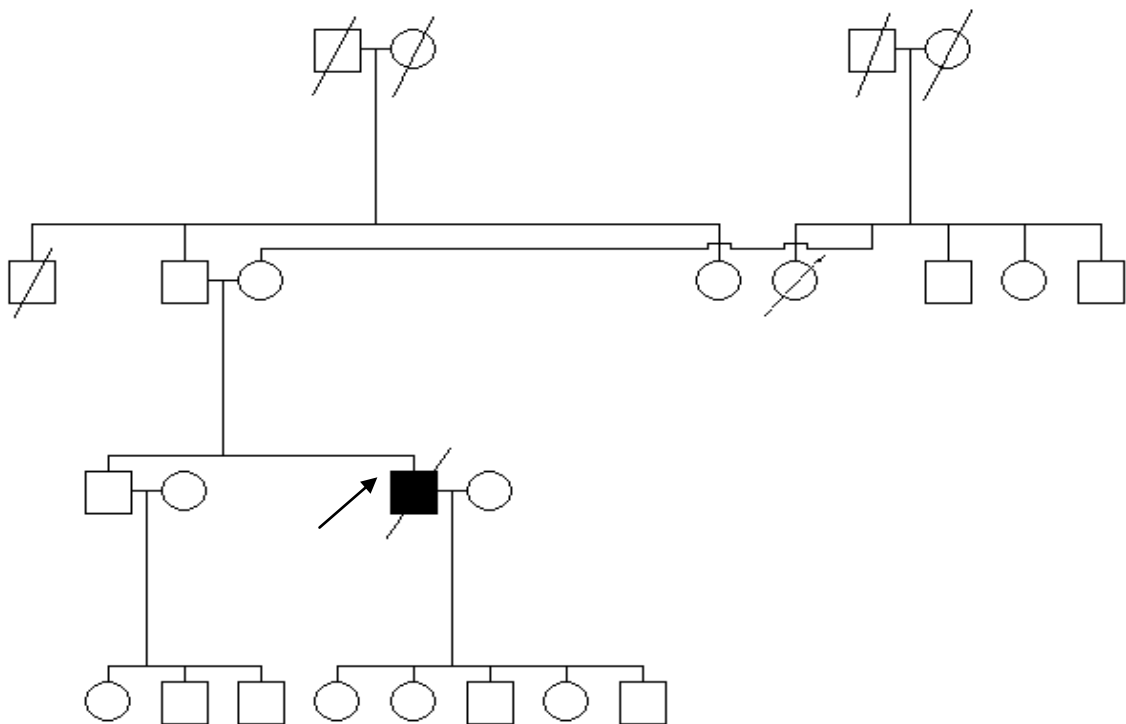


Figure 5.15. Family tree of ALS1

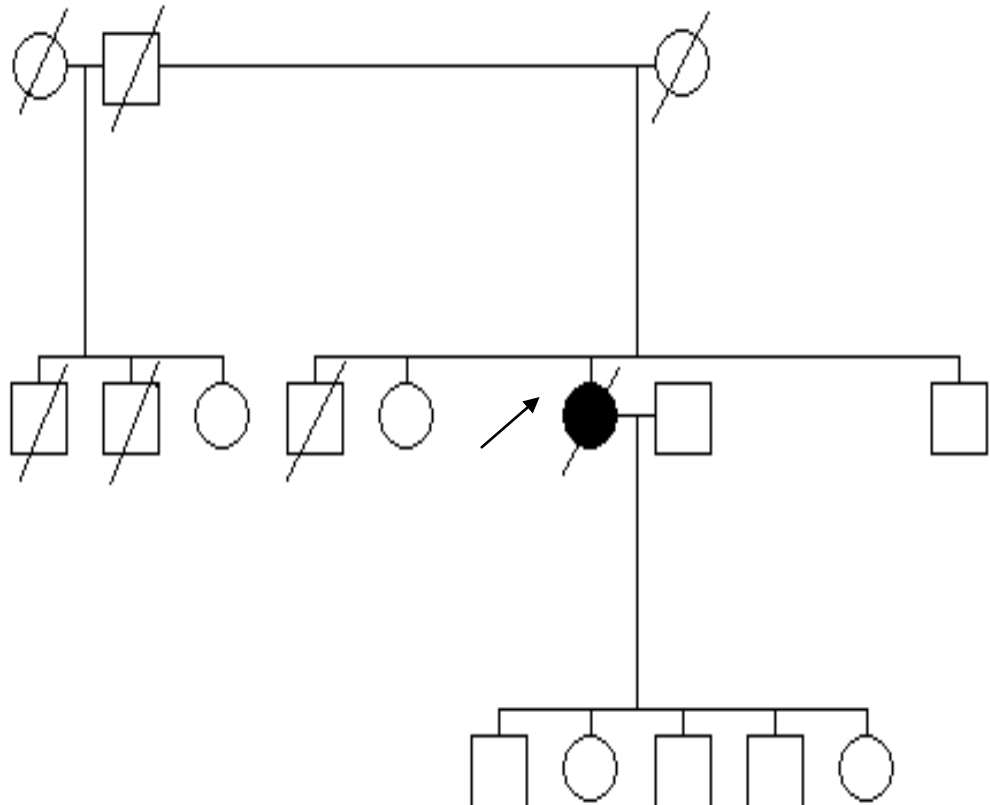


Figure 5.16. Family tree of ALS40

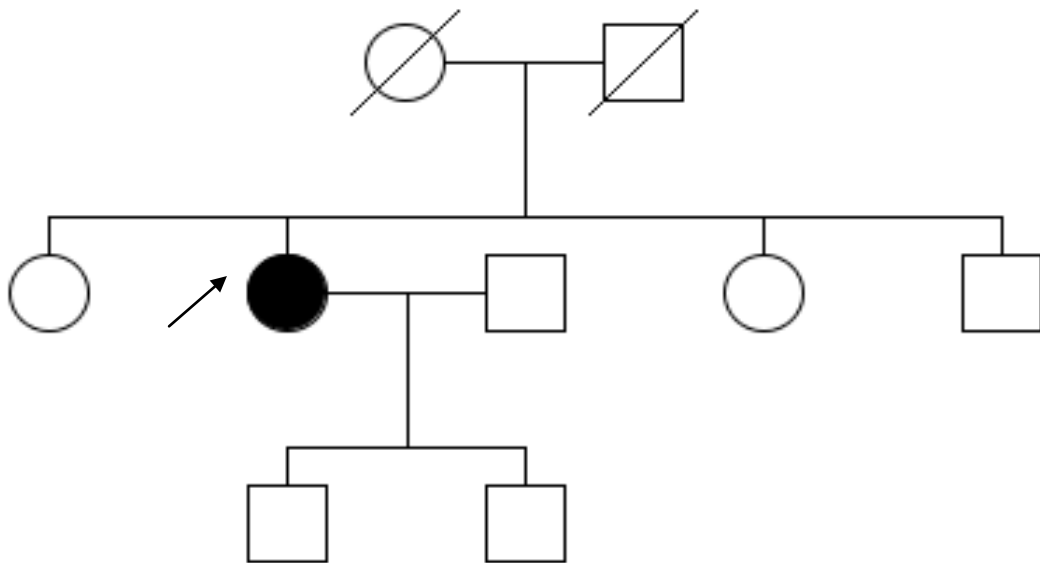


Figure 5.17. Family tree of ALS120

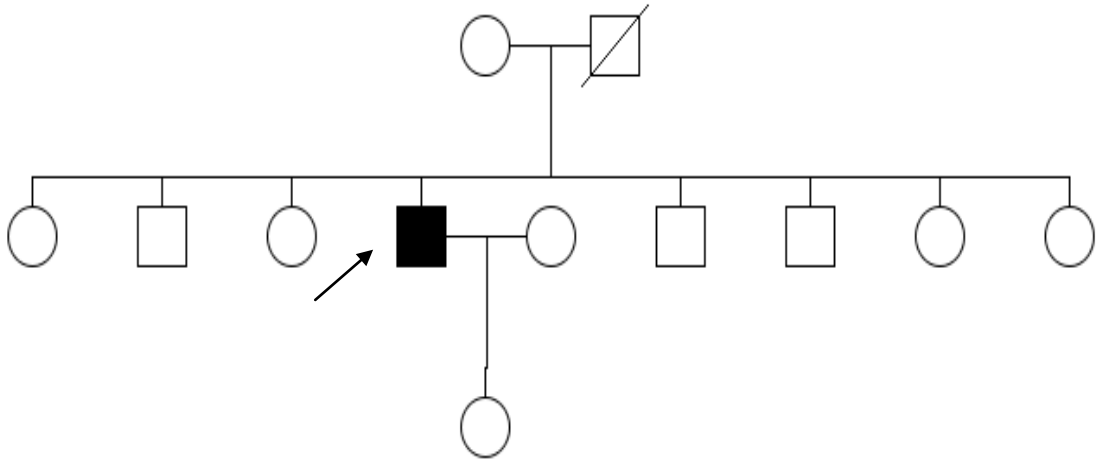


Figure 5.18. Family tree of ALS122

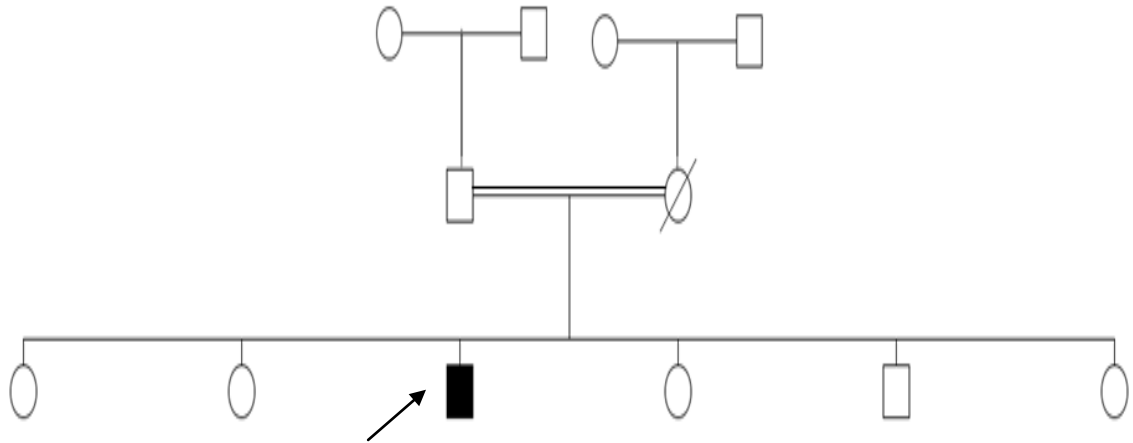


Figure 5.19. Family tree of ALS242

Table 5.1. Brief clinical information of SALS patients with IVS-III-34 A→C transversion

ALS ID	Age of Onset	Site of Onset	Inheritance Pattern
ALS1	49	Weakness in right arm	heterozygote
ALS40	68	Difficulculty in swallowing and talking	heterozygote
ALS120	48	Weakness in right arm	heterozygote
ALS122	32	Weakness in left hand and leg	heterozygote
ALS242	21	Bulbar onset	heterozygote

5.1.4. Overall results of SOD1 Analysis in the Turkish Cohort

All changes that have been detected in SOD1 analysis of ALS patients are compiled in Table 5.2.

Table 5.2. Overall representation of changes detected in SOD1 analysis

ALS ID	ALS Type	Defined Mutation/Polymorphism
ALS191	FALS	N86S
ALS226	FALS	H71Y
ALS61	FALS	L144F
ALS147	FALS	D90A
ALS221	FALS	A4V and IVS-III-34 A→C Polymorphism
ALS215	FALS	IVS-III-34 A→C Polymorphism
ALS1	SALS	IVS-III-34 A→C Polymorphism
ALS40	SALS	IVS-III-34 A→C Polymorphism
ALS120	SALS	IVS-III-34 A→C Polymorphism
ALS122	SALS	IVS-III-34 A→C Polymorphism
ALS242	SALS	IVS-III-34 A→C Polymorphism

5.2. Further Analysis of the D90A Mutation

5.2.1. DNA Sequencing of the Family Members of Patient ALS147

The replacement of aspartic acid with alanine in the SOD1-D90A mutation is represented with autosomal dominant inheritance in North American and in most European populations. The recessive inheritance has been associated only with Northern Scandinavia. Patient ALS147 originates from Muğla, in Southwestern Turkey, his parents are first cousins (Section 5.1.2.4). The recessive pattern of inheritance of D90A in this patient resembled that of Scandinavia. Accordingly, the presence of GAC→GCC transversion at codon 90 was investigated also in the family members of ALS147 (Figure 3.1). Informed consents were obtained from all analyzed subjects. Following PCR

amplification of exon 4, the family members of the index case were subjected to DNA sequencing (Figure 5.20).

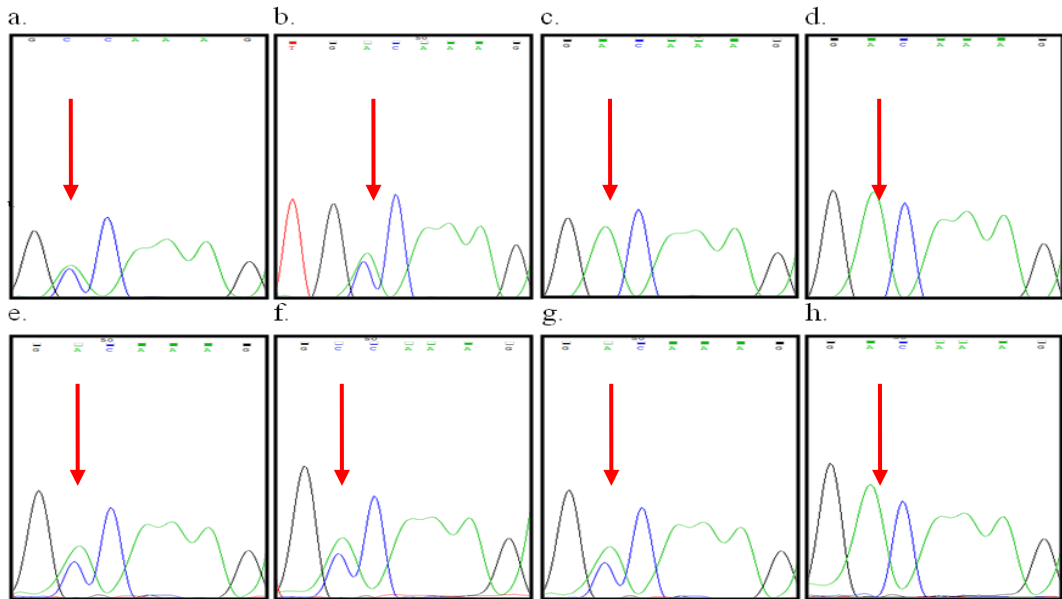


Figure 5.20. Chromatograms, showing the sequencing profiles of family members of ALS147. a. ALS203, b. ALS204, c. ALS205, d. ALS206, e. ALS207, f. ALS208, g. ALS 209 and h. ALS 210.

While his mother (ALS208), his two sons (ALS204 and ALS209) and two daughters of his older sister, who died of ALS (ALS203 and ALS207), were heterozygous carriers of the mutant allele, his aunt (ALS206), his younger sister (ALS210) and his wife (ALS205) had two wild-type alleles (Figure 5.21).

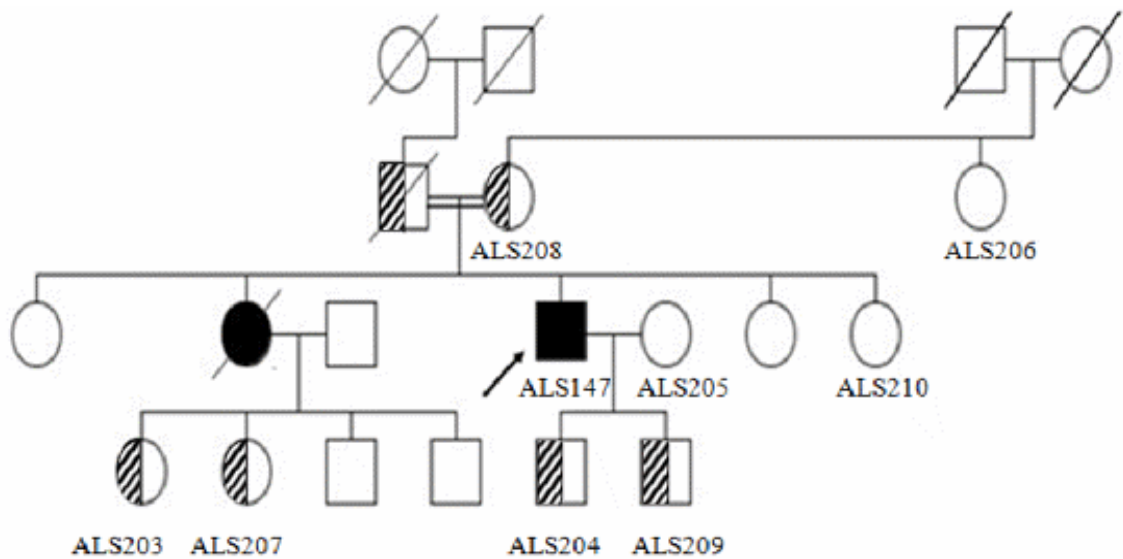


Figure 5.21. Revised pedigree of ALS147, according to the genotypes at position 90.

Shaded individuals are only carriers; they do not manifest ALS

5.2.2. Restriction Enzyme Analysis of D90A

The heterozygous presence of the D90A mutant allele in some family members of ALS147 was further confirmed by restriction enzyme analysis by *ItaI*. The specific cutting site of the restriction enzyme is indicated in Table 4.4. GAC→GGC transversion creates a digestion site for *ItaI*. The digestion of the PCR products with *ItaI* are indicated in Table 5.3. The agarose gel is shown in Figure 5.22.

Table 5.3. Fragment sizes from *ItaI* digestion of exon 4

Genotype of Alleles	Digested Product Sizes (bp)
Normal/Normal	147+92
Normal/D90A	147+92+76+68
D90A/D90A	92+76+68

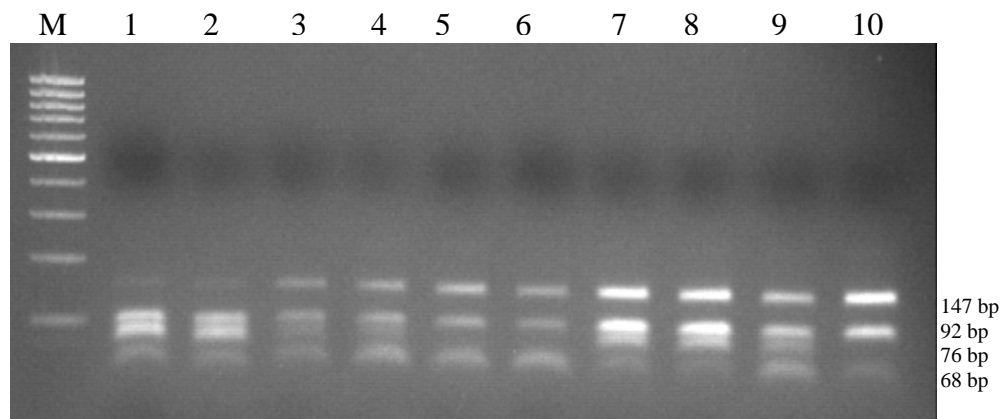


Figure 5.22. RE analysis of D90A mutation by *ItaI* of ALS147 and his family members. M: 100 bp ladder, lane 1-2: index case, lane 3: ALS203, lane 4: ALS204, lane 5: ALS205, lane 6: ALS206, lane 7: ALS208, lane 8: ALS208, lane 9: ALS209 and lane 10: ALS210.

The summarized results of the restriction enzyme analysis are shown in Table 5.4.

Table 5.4. Family members of ALS147 and their genotypes at position 90

ALS ID	Relation to ALS147	Genotype (according to presence of D90A allele)
ALS208	Mother	+/-
ALS203	Daughter of his older sister	+/-
ALS207	Daughter of his older sister	+/-
ALS204	Son	+/-
ALS209	Son	+/-
ALS206	Aunt	-/-
ALS210	His younger sister	-/-
ALS205	Wife	-/-

5.2.3. Haplotype Analysis of the D90A Family

Following the approval of recessive pattern in the family, the index case was subjected to haplotype analysis for a possible ancestral association with Scandinavian ethnicity.

5.2.3.1. PCR amplification of the microsatellite markers. The evolutionary linkage of the D90A mutation in the Turkish patient, to the Scandinavian patients was investigated by comparative Genescan analysis of the index case and his family members with 22 Scandinavian samples. For this purpose, six genetic markers were used (Table 5.5). All microsatellite markers were amplified as described in Section 4.4.1.

Table 5.5. The sizes of PCR products and corresponding repeat numbers for each markers

Marker	PCR Size (bp)	Repeat Number	Calculation of Sample Repeat Number
D21S213	147	13 TC	$(x-147) / 2$
D21S219	177	19 GT	$(x-177) / 2$
D21S224	133	18 CA	$(x-133) / 2$
D21S263	326	9 CA	$(x-326) / 2$
D21S272	175	9 CA	$(x-175) / 2$
D21S1270	139	21 CA	$(x-139) / 2$

5.2.3.2. Genescan analysis of the microsatellite markers. Genescan analysis revealed the fragment sizes for each sample. While a sharp single peak meant homozygosity of that allele, two peaks represented heterozygous state. Examples to homozygote and heterozygote patterns for D21S213, D21S219, D21S224, D21S263, D21S272 and D21S1270 microsatellite marker are shown in Figures 5.23 to 5.28, respectively.

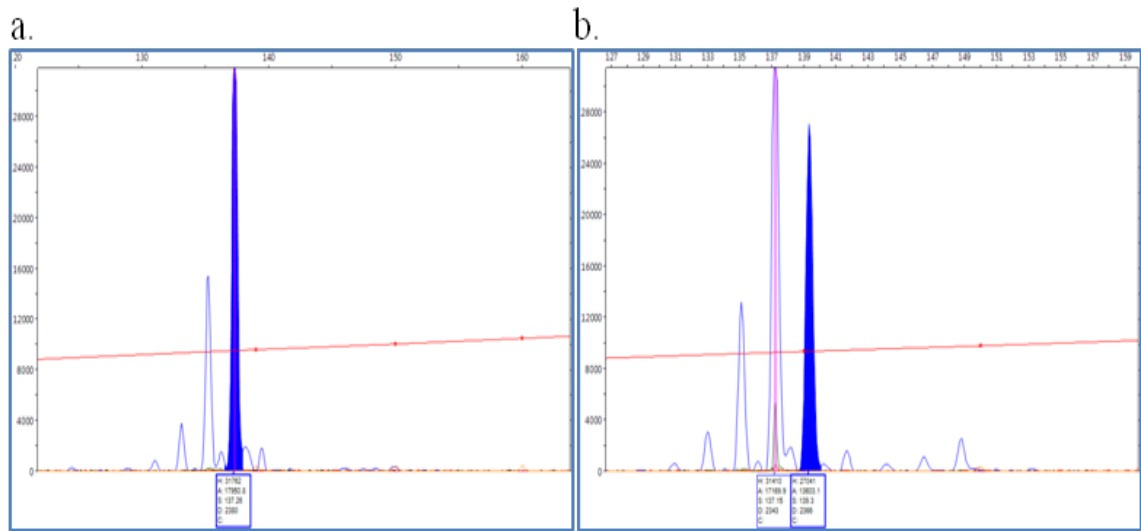


Figure 5.23. Genescan analysis for D21S213 (a) homozygous,
(b) heterozygous individual

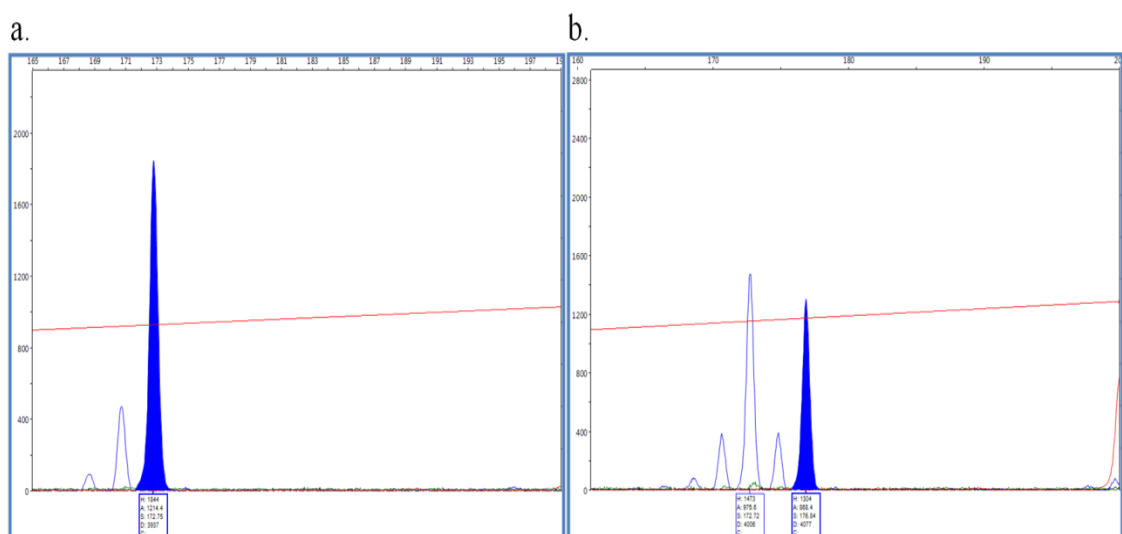


Figure 5.24. Genescan analysis for D21S219 (a) homozygous,
(b) heterozygous individual

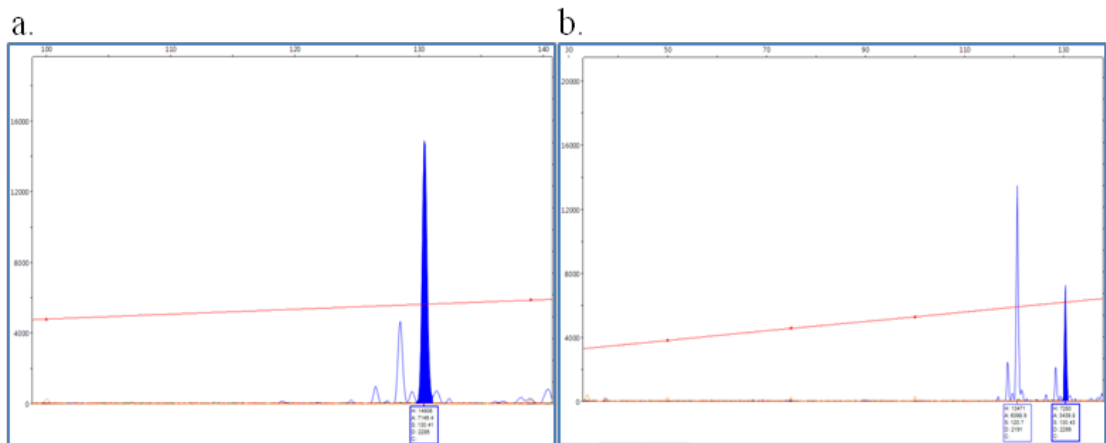


Figure 5.25. Genescan analysis for D21S224 (a) homozygous,
(b) heterozygous individual

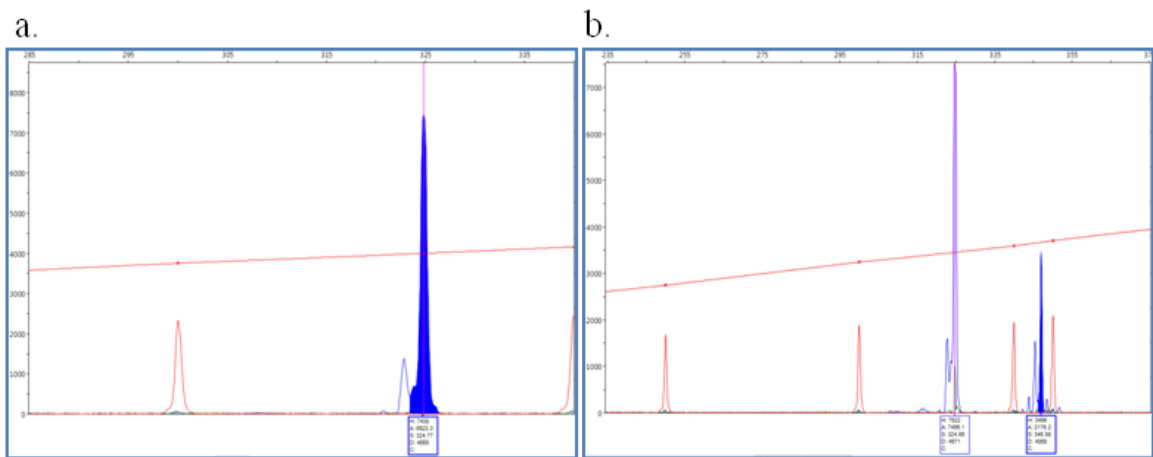


Figure 5.26. Genescan analysis for D21S263 (a) homozygous,
(b) heterozygous individual

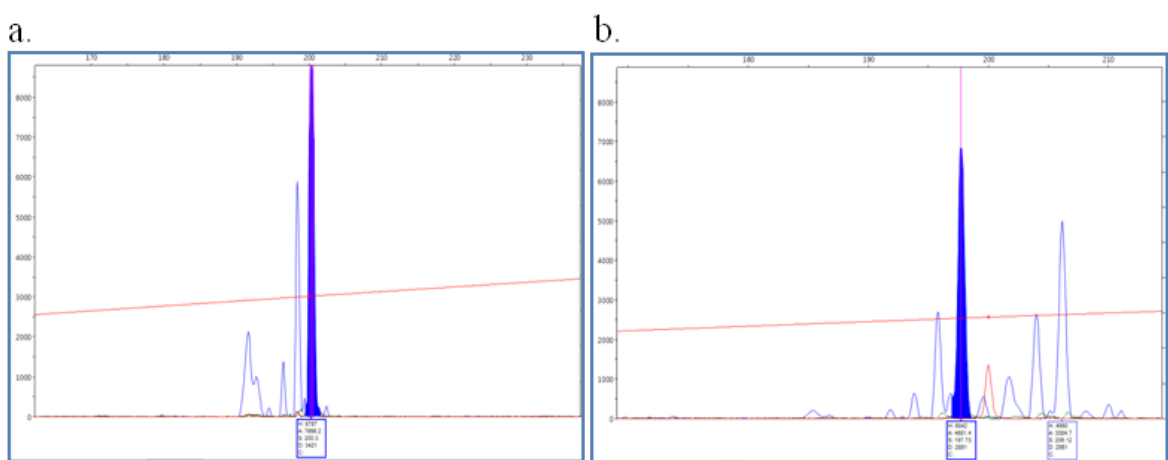


Figure 5.27. Genescan analysis for D21S272 (a) homozygous,
(b) heterozygous individual

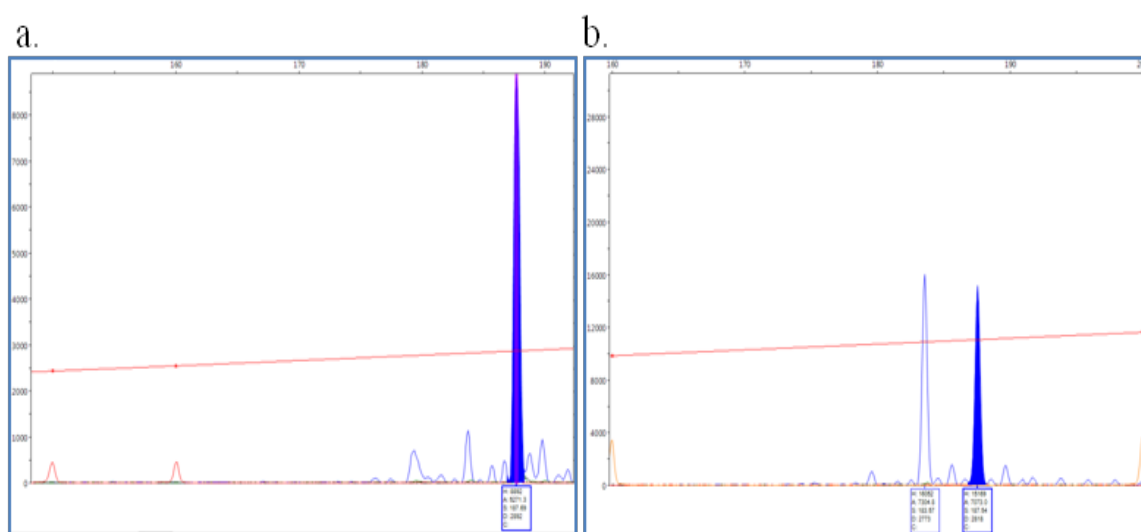


Figure 5.28. Genescan analysis for D21S1270 (a) homozygous,
(b) heterozygous individual

GeneScan analysis was applied to patient ALS147, his family members and 21 Scandinavian patients. The results of ALS147 and his family members are shown in Figure 5.29. The haplotype patterns of the homozygous index case at the six markers were compared to Scandinavian patients (Table 5.7).

Table 5.7. Haplotype blocks of patient ALS17 and Scandinavian patients. Red blocks indicate conserved Scandinavian-originated haplotype.

ALS147	463	727	789	1339	466	586	292	339	1546	1846	
15 15	15 15	15 15	15 15	15 15	15 17	15 16	15 15	15 16	15 13	15 13	
5 5	5 5	5 5	5 5	5 5	5 5	5 10	5 5	5 10	5 11	5 10	
4 4	4 4	4 4	4 4	4 4	4 4	4 4	4 3	4 4	4 1	4 4	
5 5	5 5	5 5	5 5	5 5	5 5	5 5	5 5	5 7	5 5	5 5	
15 15	15 15	15 15	15 15	15 15	15 15	15 15	15 15	15 15	15 15	15 10	
17 17	17 17	17 17	17 17	17 17	17 17	17 17	17 19	17 19	17 17	17 17	
ALS147	340	1950	1235	208	356	822	327	1609	578	6	3867
15 15	15 18	15 19	15 13	15 18	15 18	15 17	15 18	15 15	15 13	15 17	15 14
5 5	5 10	5 11	5 10	5 5	5 5	5 5	10 10	11 14	5 15	3 3	5 5
4 4	4 3	4 1	4 0	4 1	4 4	4 4	4 4	4 5	5 0	4 4	4 4
5 5	5 8	5 7	5 8	5 5	5 5	5 5	5 5	7 8	5 5	5 5	17 17
15 15	15 16	15 14	15 15	15 14	15 10	15 15	15 10	15 10	15 15	15 15	15 15
17 17	17 17	17 19	17 19	17 17	17 17	19 19	17 17	17 19	17 17	19 19	19 21

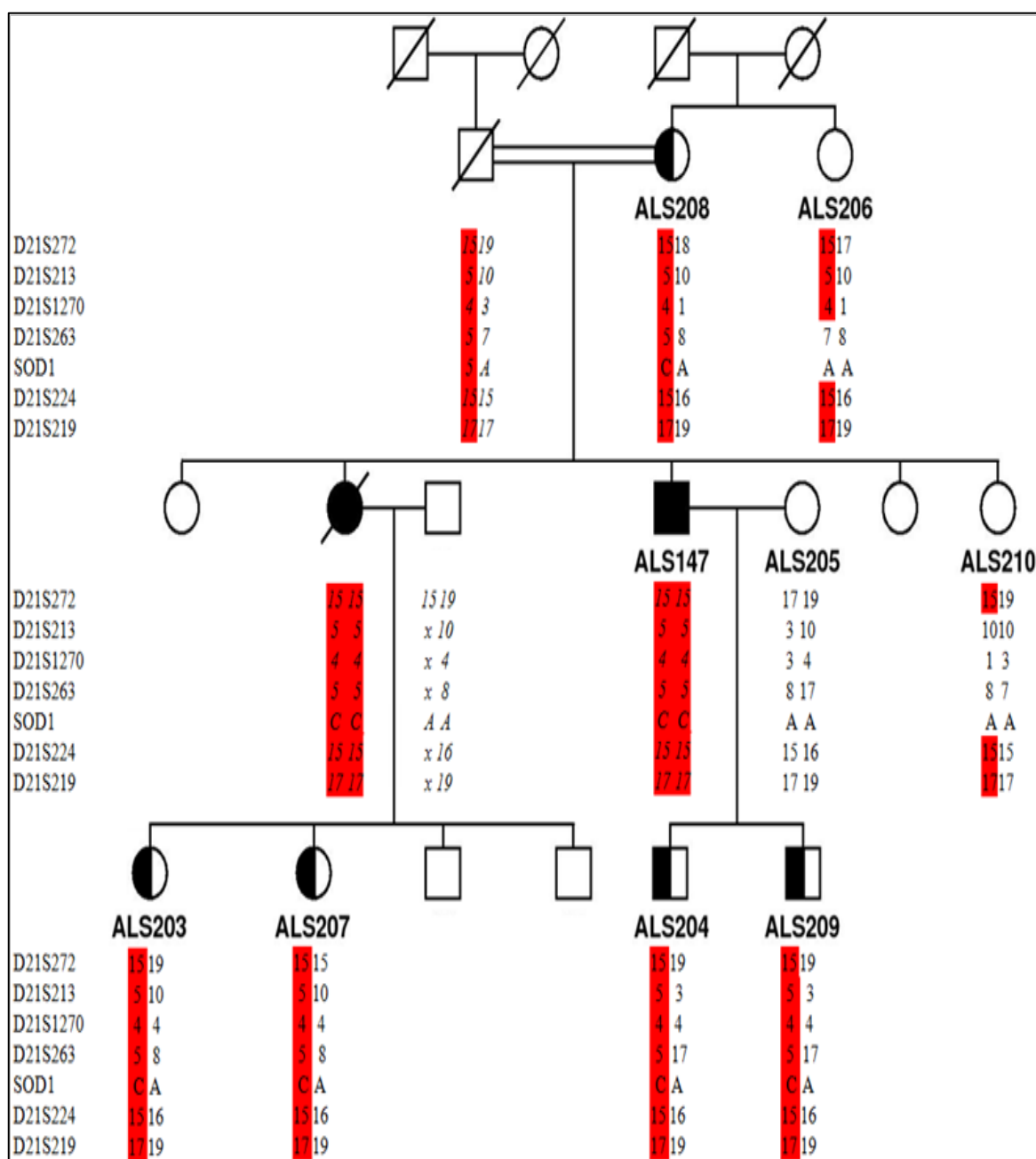


Figure 5.29. Pedigree and haplotypes of patient ALS147 and family members. Numbers indicate the repeat number for each microsatellite marker. D90A-associated haplotype is shown in red.

The haplotype analysis of the index case revealed the presence of identical haplotype blocks which were transmitted from his heterozygous parents. This pattern (15-5-4-5-15-17) is identical to Scandinavia, indicating a possible common ancestral relationship.

5.3. Further Mutational Analysis of ALS Cases in the Turkish Cohort

Nine autosomal dominant, ten familial and 13 juvenile cases who were negative for SOD1 were further investigated for possible mutations in TDP-43, ANG and FUS genes.

5.3.1. PCR Amplification and DNA Sequencing Analysis of TDP-43

The exons of the TDP-43 gene were amplified as described in Section 4.5.1. All familial, juvenile and autosomal dominant ALS cases under study were shown to have wild-type sequence in all exons of TDP-43.

5.3.2. PCR Amplification and DNA Sequencing Analysis of ANG

The exon of the ANG gene was amplified as described in Section 4.5.1. The products were subjected to DNA sequencing. Among 13 familial and juvenile cases, seven were shown to carry a GGT→GGG transversion at codon 11 (Figure 5.30). This is a previously reported polymorphism, rs11701, with an average heterozygosity of 0.187. Greenway *et al.* showed an increased risk for ALS in individuals carrying the mutated G allele when compared to wild-type T allele.

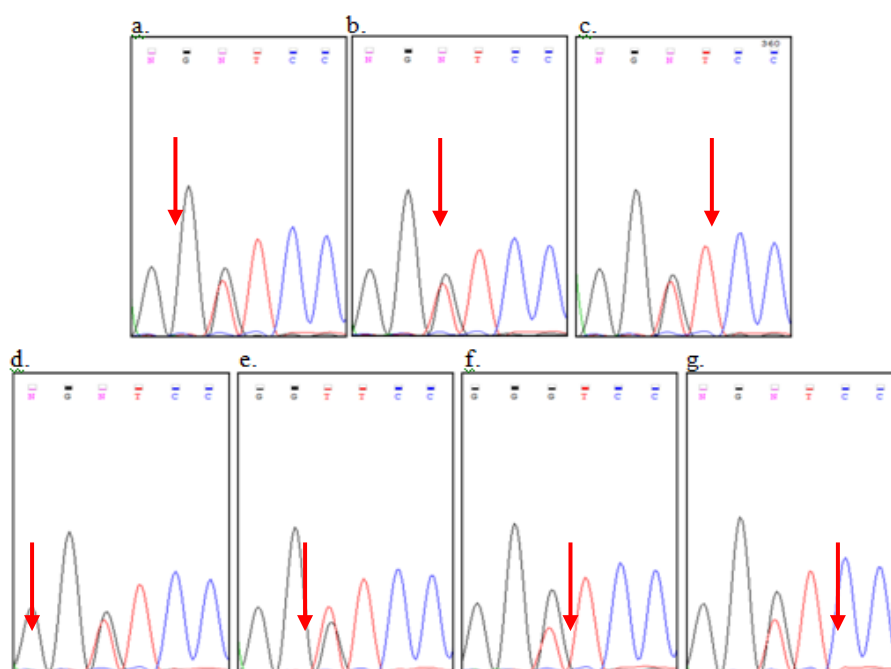


Figure 5.30. Chromatograms showing sequence profiles of patients carrying rs11701 in ANG. a. ALS86, b. ALS97, c. ALS135, d. ALS41, e. ALS202, f. ALS223 and g. ALS244

Among nine autosomal dominant cases, three individuals, two being from the same family, were shown to carry the same polymorphism (Figure 5.31)

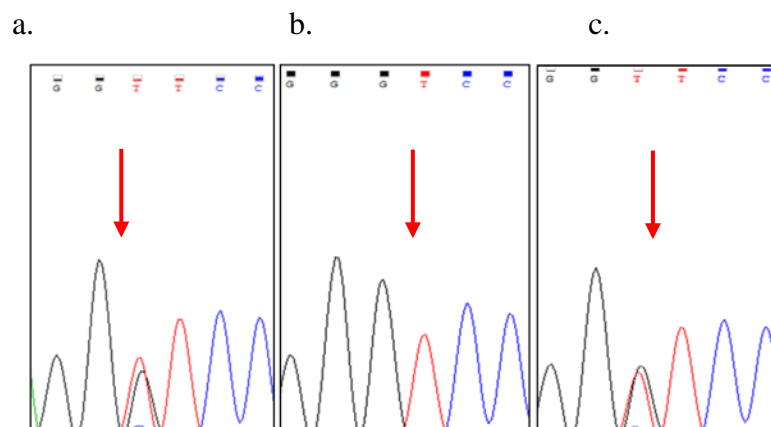


Figure 5.31. Chromatograms showing sequence profiles of patients carrying the rs11701 in ANG. a. ALS57 b. ALS59 and c. ALS220

The summary of the overall findings in the analysis of ANG gene is exhibited in Table 5.6

Table 5.6. Presentation of all SNPs identified in ANG in familial, juvenile and autosomal dominant ALS cases under study

ALS ID	Inheritance Pattern	Identified SNP	Nucleotide Change	Aminoacid Change	Location	Homozygous/Heterozygous
ALS86	Juvenile	rs11701	GGT→GGG	G→G	exon	heterozygous
ALS97	AR FALS	rs11701	GGT→GGG	G→G	exon	heterozygous
ALS135	Juvenile	rs11701	GGT→GGG	G→G	exon	heterozygous
ALS41	AR FALS	rs11701	GGT→GGG	G→G	exon	heterozygous
ALS202	FALS	rs11701	GGT→GGG	G→G	exon	heterozygous
ALS223	FALS	rs11701	GGT→GGG	G→G	exon	heterozygous
ALS244	FALS	rs11701	GGT→GGG	G→G	exon	heterozygous
ALS57	AD	rs11701	GGT→GGG	G→G	exon	heterozygous
ALS59	AD	rs11701	GGT→GGG	G→G	exon	homozygous
ALS220	AD	rs11701	GGT→GGG	G→G	exon	heterozygous

5.3.3. PCR Amplification and DNA Sequencing Analysis of FUS

All exons of the FUS gene were amplified as described in Section 4.5.1.

ALS97 was shown to carry a C→T transversion in the 5' untranslated region of the FUS gene (Figure 5.32). This seems to be a rare polymorphism, rs929867, with a frequency of 0.111.

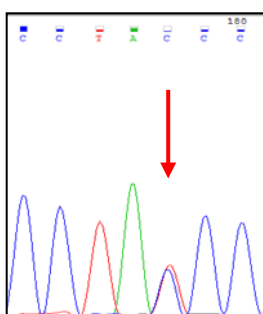


Figure 5.32. Chromatogram, showing the rs929867 in the FUS gene of ALS97

Among 13 FALS and juvenile cases, nine were shown to be carriers of a novel $\text{GTA} \rightarrow \text{GTG}$ transversion at codon 10 (Figure 5.33). This variation is silent on aminoacid level.

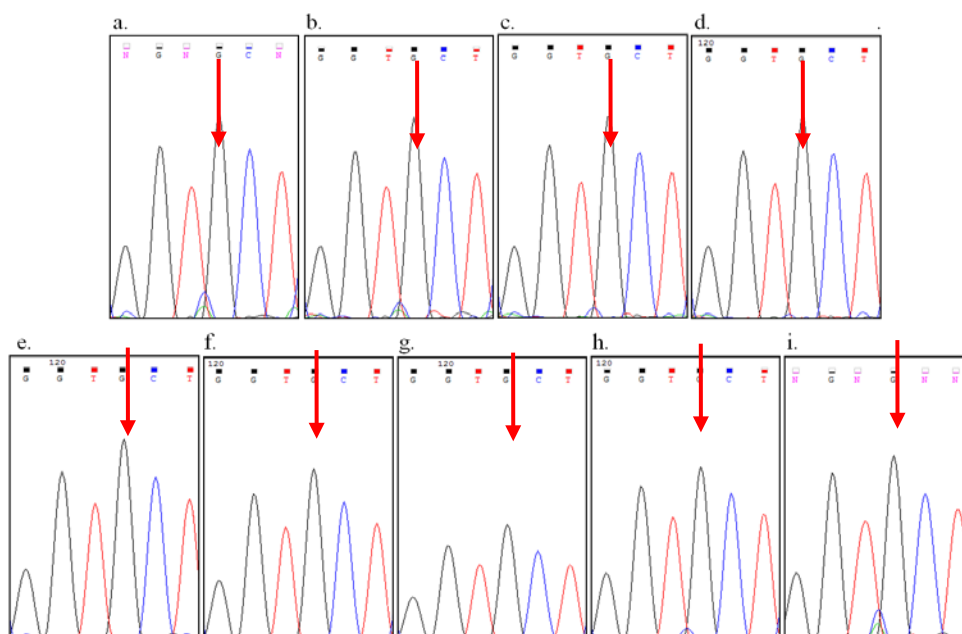


Figure 5.33. Chromatograms showing sequence profiles of patients carrying a novel $\text{GTA} \rightarrow \text{GTG}$ transversion at codon 10 of FUS. a. ALS85, b. ALS86, c. ALS227, d. ALS97, e. ALS135, f. ALS41, g. ALS173, h. ALS174, i. ALS189 and j. ALS202

Eleven cases were shown to carry a TAC→TAT change in exon 4 of the FUS gene at codon 97 (Figure 5.34). This is a common SNP, named rs1052352, with a frequency of 0.495.

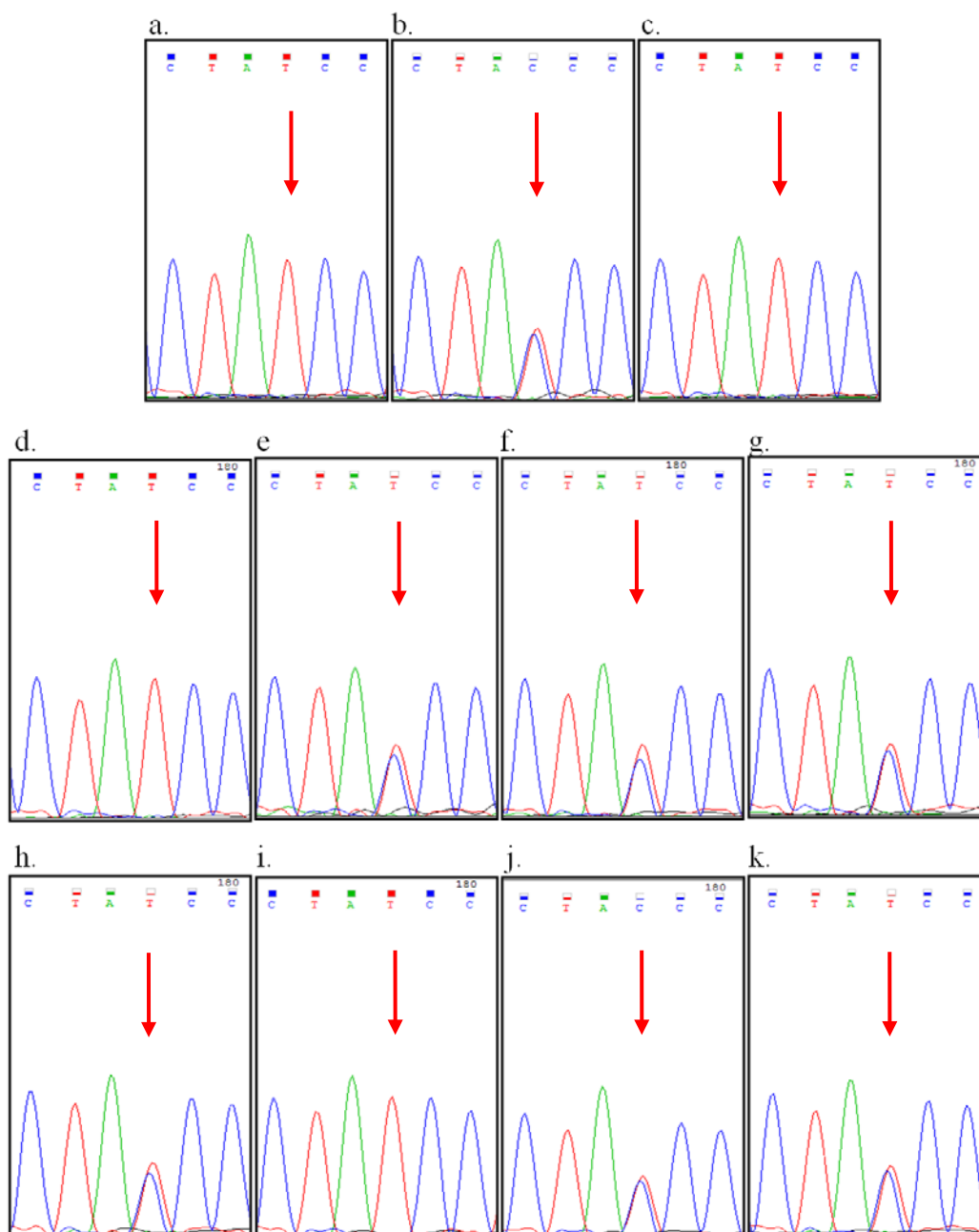


Figure 5.34. Chromatograms showing sequence profiles of patients carrying the rs1052352 in FUS. a. ALS85, b. ALS86, c. ALS227, d. ALS97, e. ALS135, f. ALS41, g. ALS174, h. ALS202, i. ALS223, j. ALS244 and k. ALS178

In the familial and juvenile ALS subgroup, GGC→GGA change at codon 49 was detected in seven cases (Figure 5.35). This is a rare polymorphism, rs741810, with an average heterozygosity of 0.29.

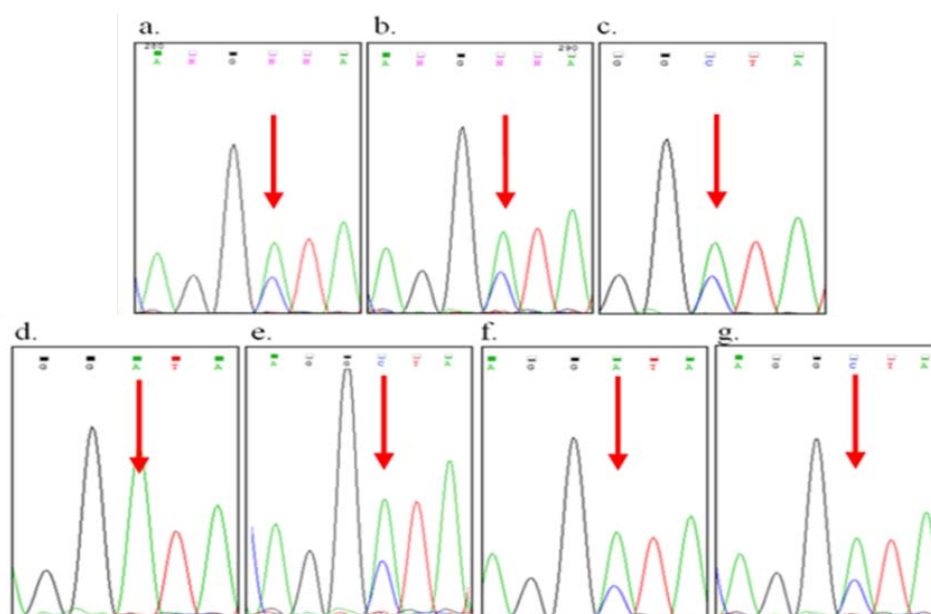


Figure 5.35. Chromatograms showing sequence profiles of patients carrying the rs741810 in FUS a. ALS86, b. ALS135, c. ALS41, d. ALS173, e. ALS174, f. ALS244 and g. ALS178

DNA sequencing of ALS178 revealed the presence of a novel C→T change in intron 5 (Figure 5.36).

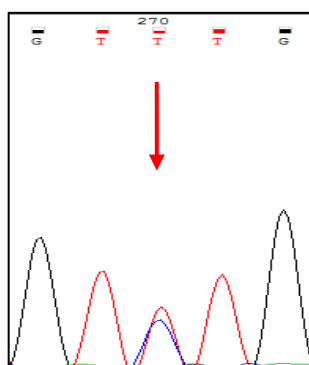


Figure 5.36. Chromatogram showing the sequence profile of ALS178 carrying a novel C→T change in intron 5 of FUS

Eight autosomal dominant cases were carriers of rs1052352, while five were of the rs741810 variation (Figures 5.37 and 5.38).

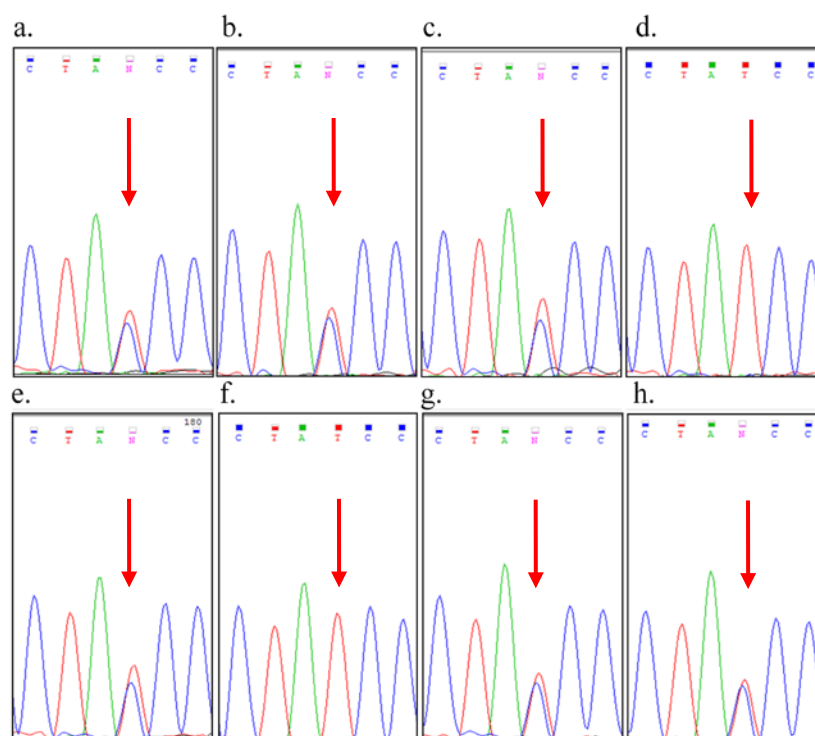


Figure 5.37. Chromatograms showing the sequence profiles of patients carrying the rs1052352 in FUS. a. ALS56, b. ALS57, c. ALS59, d. ALS220, e. ALS215, f. ALS184, g. ALS170 and h. ALS171

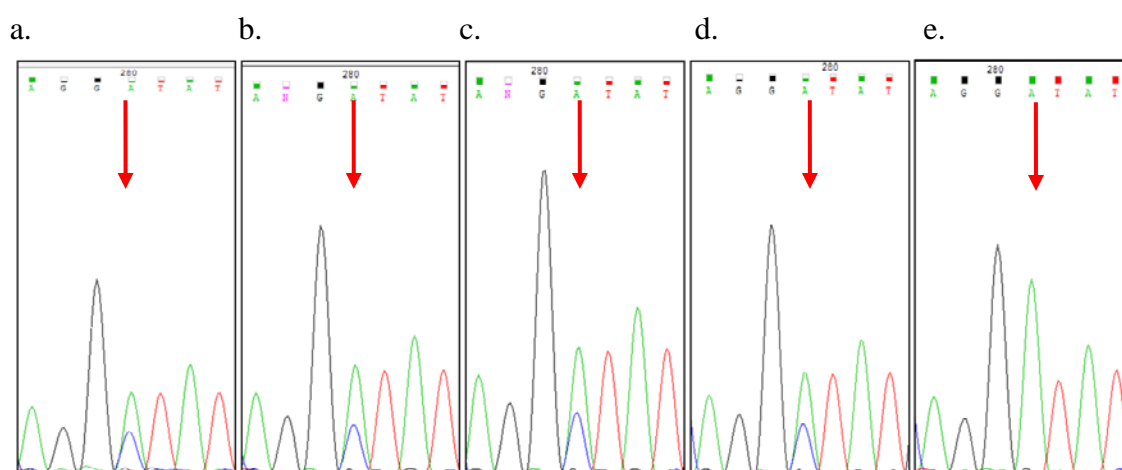


Figure 5.38. Chromatograms showing sequence profiles of patients carrying the rs741810 in FUS. a. ALS56, b. ALS59, c. ALS170, d. ALS171 and e. ALS172

ALS57 was shown to carry a T→C change in intron 3, a previously reported SNP, named rs73530283 (Figure 5.39).

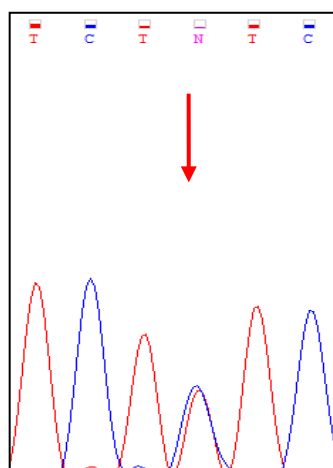


Figure 5.39. Chromatogram showing the sequence profile of ALS57 carrying rs73530283 in FUS

The overall presentation of all SNPs identified in FUS in familial and juvenile cases are compiled in Table 5.7, while autosomal dominant ALS cases are shown in Table 5.8

Table 5.7. Summary of SNPs identified in FUS in familial and juvenile ALS cases

ALS ID	Inheritance Pattern	Exon	Identified SNP	Nucleotide Change	A.acid Change	Location	Homozygous/Heterozygous
ALS97	AR FALS	1	rs929867	---	---	5'UTR	heterozygous
ALS85	Juvenile	1	novel	GTA→GTG	V→V	exon	homozygous
ALS86	Juvenile	1	novel	GTA→GTG	V→V	exon	homozygous
ALS227	FALS	1	novel	GTA→GTG	V→V	exon	homozygous
ALS97	AR FALS	1	novel	GTA→GTG	V→V	exon	homozygous
ALS135	Juvenile	1	novel	GTA→GTG	V→V	exon	homozygous
ALS41	Juvenile	1	novel	GTA→GTG	V→V	exon	homozygous
ALS173	AR FALS	1	novel	GTA→GTG	V→V	exon	homozygous
ALS174	AR FALS	1	novel	GTA→GTG	V→V	exon	homozygous
ALS189	AR FALS	1	novel	GTA→GTG	V→V	exon	homozygous
ALS202	FALS	1	novel	GTA→GTG	V→V	exon	homozygous
ALS86	juvenile	2; 3	rs741810	GGC→GGA	G→G	exon	heterozygous
ALS135	juvenile	2; 3	rs741810	GGC→GGA	G→G	exon	heterozygous
ALS41	AR FALS	2; 3	rs741810	GGC→GGA	G→G	exon	heterozygous
ALS173	AR FALS	2; 3	rs741810	GGC→GGA	G→G	exon	homozygous

Table 5.7. Summary of SNPs identified in FUS in familial and juvenile ALS cases
(continued)

ALS174	AR FALS	2; 3	rs741810	GGC→GGA	G→G	exon	heterozygous
ALS244	FALS	2; 3	rs741810	GGC→GGA	G→G	exon	heterozygous
ALS178	juvenile	2; 3	rs741810	GGC→GGA	G→G	exon	heterozygous
ALS85	juvenile	4	rs1052352	TAC→TAT	Y→Y	exon	homozygous
ALS86	juvenile	4	rs1052352	TAC→TAT	Y→Y	exon	heterozygous
ALS227	FALS	4	rs1052352	TAC→TAT	Y→Y	exon	homozygous
ALS97	AR FALS	4	rs1052352	TAC→TAT	Y→Y	exon	homozygous
ALS135	juvenile	4	rs1052352	TAC→TAT	Y→Y	exon	heterozygous
ALS41	juvenile	4	rs1052352	TAC→TAT	Y→Y	exon	heterozygous
ALS174	AR FALS	4	rs1052352	TAC→TAT	Y→Y	exon	heterozygous
ALS202	FALS	4	rs1052352	TAC→TAT	Y→Y	exon	heterozygous
ALS223	FALS	4	rs1052352	TAC→TAT	Y→Y	exon	heterozygous
ALS244	FALS	4	rs1052352	TAC→TAT	Y→Y	exon	heterozygous
ALS178	juvenile	4	rs1052352	TAC→TAT	Y→Y	exon	heterozygous
ALS178	juvenile	5	novel	---	C→T	Intron	heterozygous

Table 5.8. Summary of SNPs identified in FUS in autosomal dominant ALS cases

ALS ID	Inheritance Pattern	Exon	Identified SNP	Nucleotide Change	A.acid Change	Location	Homozygous/Heterozygous
ALS59	AD	2; 3	rs741810	GGC→GGA	G→G	exon	heterozygous
ALS170	AD	2; 3	rs741810	GGC→GGA	G→G	exon	heterozygous
ALS171	AD	2; 3	rs741810	GGC→GGA	G→G	exon	heterozygous
ALS172	AD	2; 3	rs741810	GGC→GGA	G→G	exon	homozygous
ALS57	AD	2; 3	rs73530283	T→C	--	intron	heterozygous
ALS56	AD	4	rs1052352	TAC→TAT	Y→Y	exon	heterozygous
ALS57	AD	4	rs1052352	TAC→TAT	Y→Y	exon	heterozygous
ALS59	AD	4	rs1052352	TAC→TAT	Y→Y	exon	heterozygous
ALS220	AD	4	rs1052352	TAC→TAT	Y→Y	exon	homozygous
ALS215	AD	4	rs1052352	TAC→TAT	Y→Y	exon	heterozygous
ALS184	AD	4	rs1052352	TAC→TAT	Y→Y	exon	homozygous
ALS170	AD	4	rs1052352	TAC→TAT	Y→Y	exon	heterozygous
ALS171	AD	4	rs1052352	TAC→TAT	Y→Y	exon	Heterozygous

5.4. Whole Genome Analysis of Turkish Familial and Juvenile ALS Cases

Familial and juvenile ALS cases, who did not have mutations in any of the genes under study, were subjected to whole genome analysis for the identification of new genes. The evaluation of the chip data in terms of B allele frequencies and log R ratio of each sample revealed success in 27 out of 28 samples. One sample, ALS132, was shown to be contaminated, determined by the presence of five distinct bands in B allele frequency graph in all chromosomes (Figure 5.40)

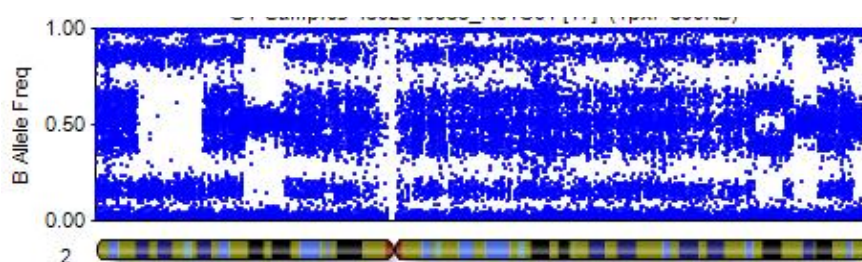


Figure 5.40. The B allele frequency analysis of chromosome 2 in ALS132

5.4.1. Chromosomal Regions with Duplications, Homozygous and Heterozygous Deletions

The samples were analyzed for loss of heterozygosity through the evaluation of CNV by both PLINK and BeadStudio programs. The change in the level of log R ratio reflects the type of change in the copy number. Examples to expected patterns for duplication, homozygous and heterozygous deletions are shown in Figures 5.41, 5.42 and 5.43, respectively.

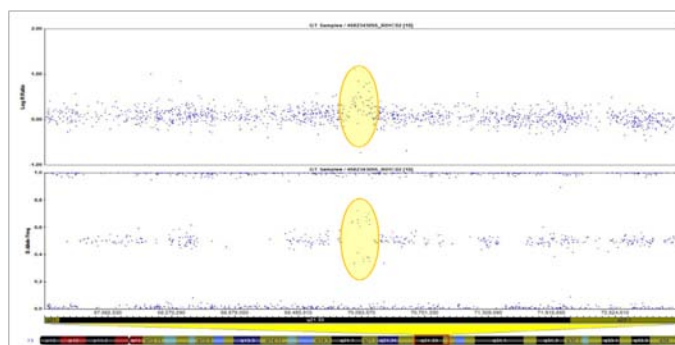


Figure 5.41. Changes in patterns of log R and B allele frequencies in duplication

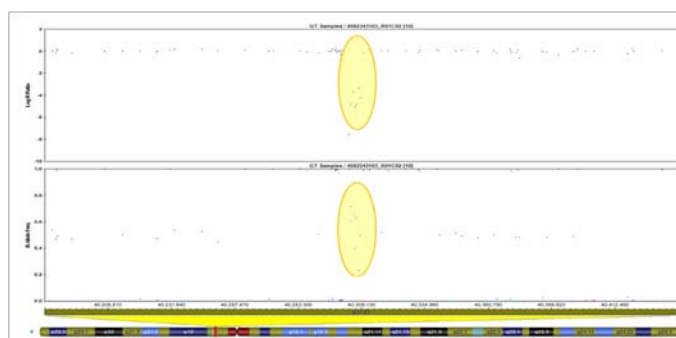


Figure 5.42. Changes in patterns of log R and B allele frequencies in homozygous deletion

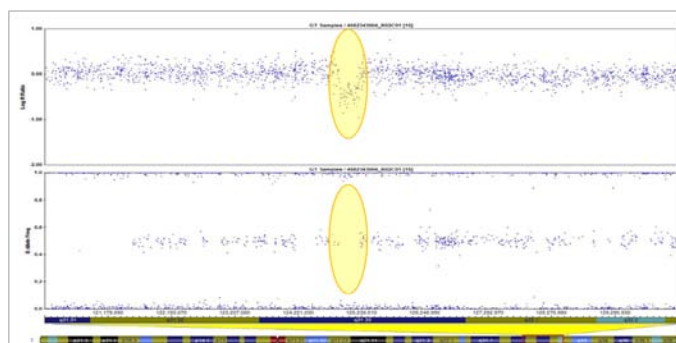


Figure 5.43. Changes in patterns of log R and B allele frequencies in heterozygous deletion

Among changes detected in the copy number, homozygous and heterozygous regions, which had not been published previously, were selected for further inspection (Table 5.9).

Table. 5.9. Unreported homozygous and heterozygous deletion regions that have been detected in familial and juvenile Turkish patient samples

ALS ID	Chrom	Loci Start	Loci Stop	Size (bp)	Type of Change	Location	Genes
ALS252	1	84719557	84733071	13514	Heterozygous	intron	DLG2
ALS256	1	84719557	84733071	13514	Heterozygous	intron	DLG2
ALS257	1	84719557	84733071	13514	Heterozygous	intron	DLG2
ALS135	13	49271585	49271799	214	Heterozygous	intergenic	--
ALS41	13	49271585	49271799	214	Heterozygous	intergenic	--
ALS155	13	49271585	49271799	214	Heterozygous	intergenic	--
ALS189	1	214199501	214203243	3742	Heterozygous	intron	USH2A
ALS173	1	214199501	214203243	3742	Heterozygous	intron	USH2A
ALS135	9	88015587	88029735	14148	Heterozygous	exon	C9orf153
ALS189	21	46391256	46427893	36637	Heterozygous	exon	C21orf56, FTCD
ALS173	6	100022903	100032890	9987	Heterozygous	exon	USP45
ALS49	11	1611186	1611326	140	Homozygous	intronic	HCCA2
ALS41	11	1611186	1611326	140	Homozygous	intronic	HCCA2

Table. 5.9. Unreported homozygous and heterozygous deletion regions that have been detected in familial and juvenile Turkish patient samples (continued)

ALS68	11	1611186	1611326	140	Homozygous	intronic	HCCA2
ALS256	12	111503947	111504440	493	Homozygous	intergenic	--
ALS257	12	111503947	111504440	493	Homozygous	intergenic	--
ALS49	4	19130834	19131054	220	Homozygous	intergenic	--
ALS167	4	19130834	19131054	220	Homozygous	intergenic	--
ALS68	4	19130834	19131054	220	Homozygous	intergenic	--
ALS96	4	19130834	19131054	220	Homozygous	intergenic	--
ALS133	4	19130834	19131054	220	Homozygous	intergenic	--
ALS85	4	19130834	19131054	220	Homozygous	intergenic	--
ALS97	4	19130834	19131054	220	Homozygous	intergenic	--
ALS227	4	19130834	19131054	220	Homozygous	intergenic	--
ALS252	4	19130834	19131054	220	Homozygous	intergenic	--
ALS46	4	19130834	19131054	220	Homozygous	intergenic	--
ALS178	4	19130834	19131054	220	Homozygous	intergenic	--
ALS155	4	19130834	19131054	220	Homozygous	intergenic	--
ALS202	4	19130834	19131054	220	Homozygous	intergenic	--
ALS46	21	46626358	46628866	2508	Homozygous	intron	PCNT
ALS46	6	90884890	90885603	713	Homozygous	intron	BACH2

Among detected homozygous and heterozygous regions, only three corresponded to coding regions in the genome. The first heterozygous region was located on chromosome 9 between positions 88,015,587 and 88,029,735 which corresponded to C9orf153, a hypothetical protein with an unidentified function. Previous Affimetrix studies showed no expression in brain. The notions of the absence of this region in any other ALS cases in the study, as well as its lack of expression in brain, eliminated this region from further analysis.

The second heterozygous deletion was on chromosome 6, between 100,022,903 and 100,032,890 bp. This region was within the coding region of Ubiquitin-Specific-Processing protease 45, USP45; it functions as a peptidase in the degradation of proteins. This region was observed in ALS189. Her two older sisters, ALS173 and ALS174, suffering from ALS, did not show homozygosity at this region. Thus, although the function might be relevant with ubiquitin-dependent degeneration observed in ALS, the region was also neglected.

The third heterozygous deletion was detected on chromosome 21, between 46,391,256 and 46,427,893 bp. There were two genes within the indicated region. The first one was formiminotransferase cyclodeaminase (FTCD). It is a bifunctional enzyme which leads 1-carbon units from formiminoglutamate (a component of the histidine degradation pathway) to the folate pool. GNF Expression Atlas 2 Data from U133A and GNF1H Chips exhibited scarce expression of the protein in brain.

The second gene within the region was C21orf56, a hypothetical protein. Affymetrix All Exon Microarrays analysis revealed the absence of expression in brain. The index case with the indicated heterozygous deletion was ALS173. Her two younger sisters also suffer from ALS; however, they were not homozygous at this region. Considering all, this region was eliminated from further study.

5.4.2. Detection of Homozygosity Regions

The proper evaluation of homozygosity regions obligates an absolute information on family history. Each sample registered to our laboratory was required to include patient's clinical picture as well as information about family history. However, information was not always complete or true. The consanguinity analysis performed on these samples has shown the real consanguinity pattern for all (Appendix D). The revised consanguinity results are as follows (Table 5.10).

Table 5.10. Revised consanguinity pattern of some ALS cases

ALS ID	Inheritance Pattern	Reported Consanguinity	Revised Consanguinity
ALS157	Juvenile	not reported	yes
ALS158	Juvenile	not reported	yes
ALS135	Juvenile	not reported	no
ALS175	FALS	No	yes
ALS155	Juvenile	not reported	yes
ALS97	AR FALS	not reported	no
ALS223	FALS	No	no

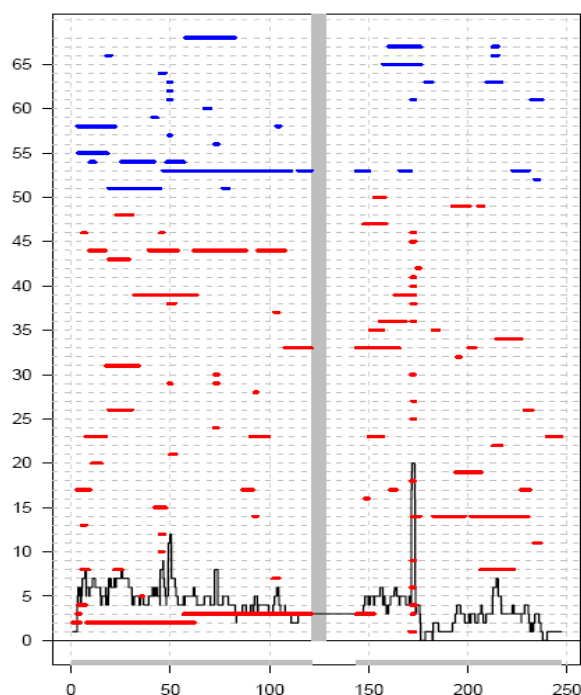


Figure 5.44. An example to ‘Homozygosity Mapping Graph’, showing homozygous regions of chromosome 1 in ALS and controls

Homozygous regions within the Turkish ALS samples were investigated. To determine ALS-specific regions, the results were compared with control samples. Overlapping regions between ALS cases and controls were eliminated. These results were displayed on ‘Homozygosity Mapping’ graphs. An example is shown in Figure 5.44. The x-axis shows the chromosomal location in mb, while each number on the y-axis represents an individual. Blue and red lines indicate ALS cases and controls, respectively. It should be noted that although the analysis involved 139 individuals in total (27 ALS and 112 controls), the y-axis number varies, since not all individuals have homozygosity for every chromosome. The grey zones correspond to centromeres which do not include any SNPs. In this study, the significance of detected homozygous regions was compared with 112 controls who were Turkish patients with cortical malformations (Appendix E).

5.5. Special Focus on a Turkish Recessive ALS Family:

ALS252, ALS256 and ALS257

A focused analysis, regarding the detection of homozygous regions, was performed on a recessive family with affected family members ALS252, ALS256 and ALS257.

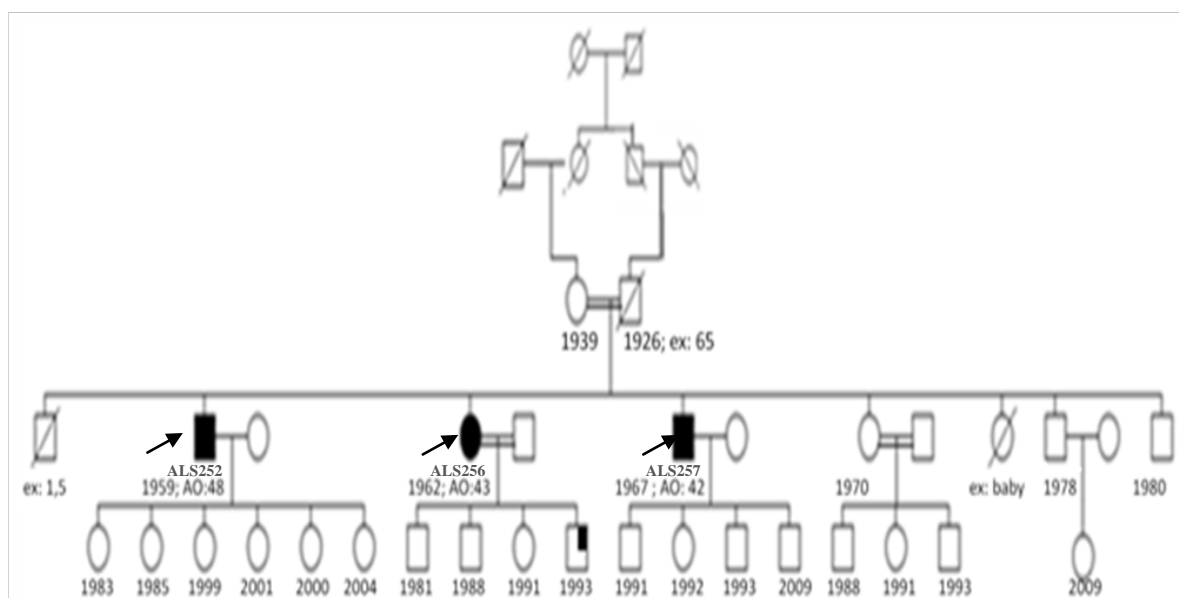


Figure 5.45. Family tree of ALS252, ALS256 and ALS257

The parents of these affected siblings are first cousins (Figure 5.45). The father suffered from asthma for a long time. He died at the age of 65; he showed no symptoms of any neurological defect. The first symptoms of the oldest index case, ALS252, appeared at the age of 48 with numbness first in distal extremities, followed by numbness in tongue. He can still walk on his own. ALS256 is married to her aunt's son (motherside). Her first symptoms occurred at the age of 43. Recently, she became committed to bed. Her youngest son is suffering from spasticity since birth. The youngest index case, ALS257, has been suffering from a similar disease since the age of 42. He is currently committed to bed, too.

Homozygous regions in the family were compared to homozygous regions in 112 controls, previously used in homozygosity mapping. The data interpreted from PLINK was displayed in 'Homozygosity Mapper' graphs. Regions below 1000 kb were neglected.

This inspection revealed 12 regions (Figures 5.46 to 5.54 and Table 5.11). Within these regions, there were 319 genes and 3279 coding regions. The intervals determined on chromosomes 10, 12 and 22 were highly observed in controls, thus were eliminated from further analysis. Also, two regions, chromosomes 9 and 18, were previously reported as linked to ALS (Hosler *et al.*, 2000, Hand *et al.*, 2002). They were named as ALS-FTD-2 and ALS3, respectively.

Table 5.11. Homozygosity regions common for samples ALS252, ALS256 and ALS257

Chrom #	Loci Start	Loci Stop	Size of Region (bp)	Type of Change	# of Genes within Region	# of Exons within Region
4	112.034.843	127.502.750	15.467.907	exon	78	796
4	183.284.897	185.253.393	1.968.496	exon	19	165
5	10.600.018	18.828.325	8.228.307	exon	23	365
7	154.553.069	154.973.454	420.385	exon	4	13
9	95.938.257	96.844.985	906.728	exon	16	85
10	73.157.023	74.341.617	1.184.594	exon	19	161
10	106.967.316	107.982.339	1.015.023	exon	2	10
12	32.976.840	34.008.675	1.031.835	exon	1	9
12	36.213.381	38.326.598	2.113.217	exon	8	93
13	73.984.888	78.632.888	4.648.000	exon	28	370
18	41.226.287	57.735.477	16.509.190	exon	98	943
22	29.856.811	30.899.263	1.042.452	exon	23	269

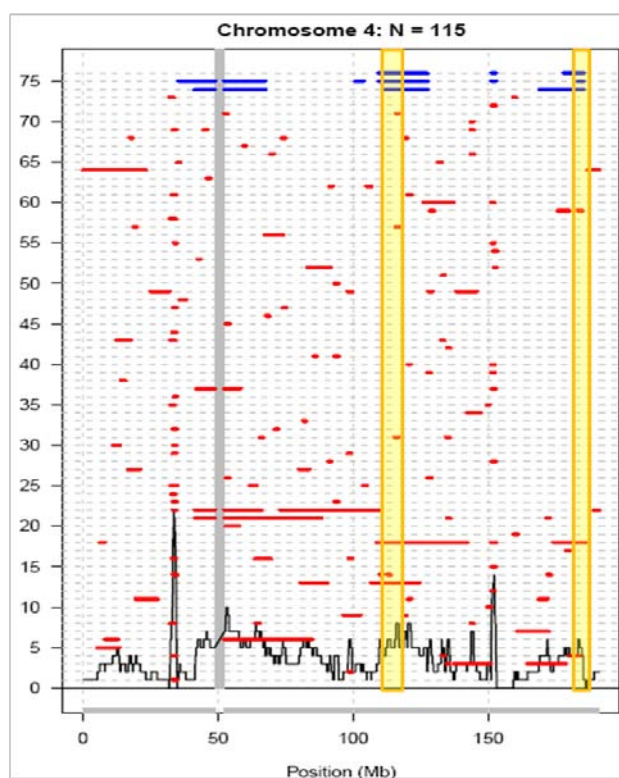


Figure 5.46. Homozygous regions on chromosome 4 for ALS252, ALS254, ALS257 and controls.

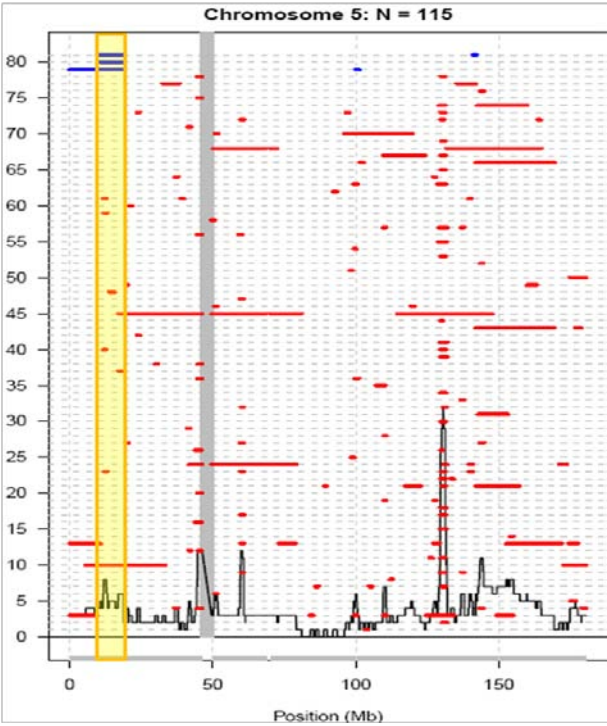


Figure 5.47. Homozygous regions on chromosome 5 for ALS252, ALS254, ALS257 and controls

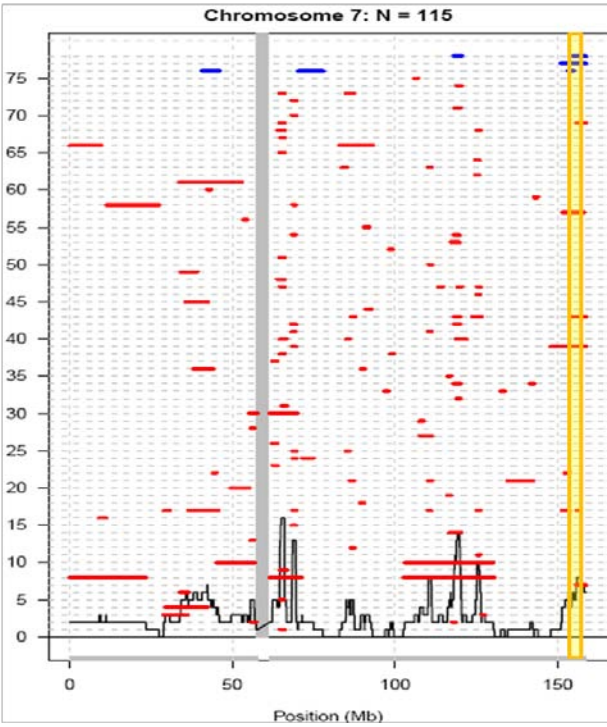


Figure 5.48. Homozygous regions on chromosome 7 for ALS252, ALS254, ALS257 and controls

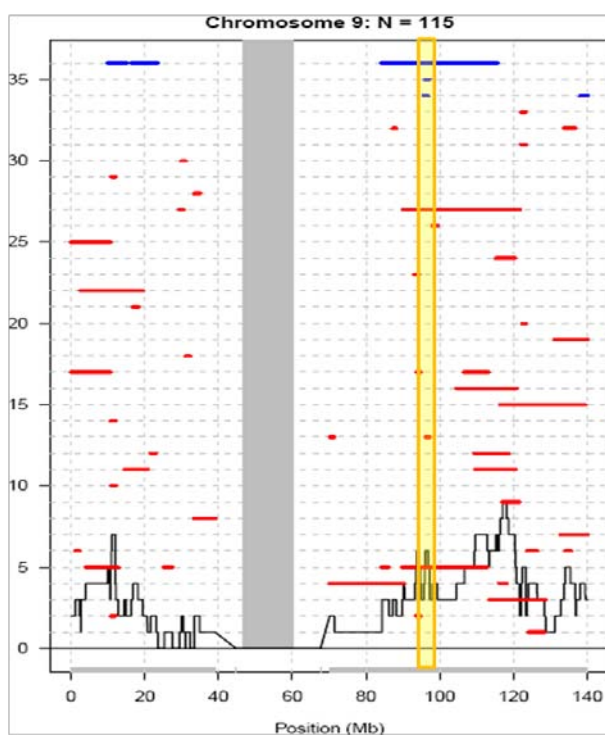


Figure 5.49. Homozygous regions on chromosome 9 for ALS252, ALS254, ALS257 and controls

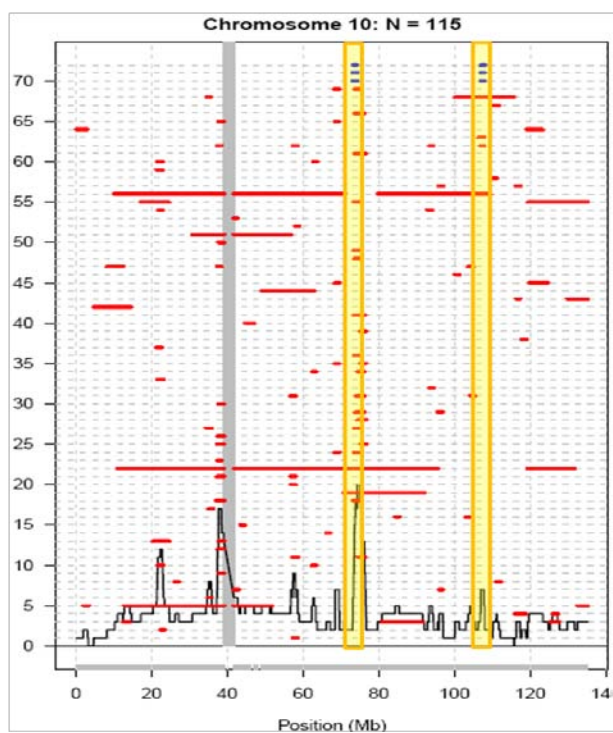


Figure 5.50. Homozygous regions on chromosome 10 for ALS252, ALS254, ALS257 and controls

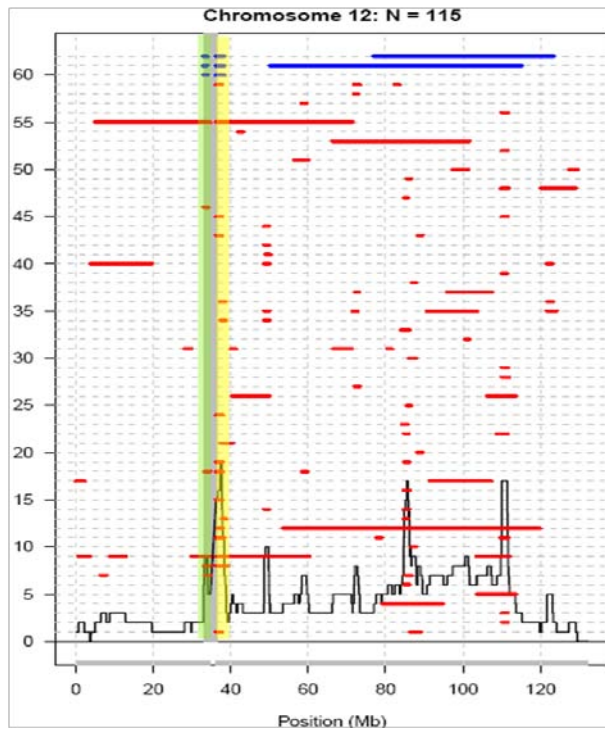


Figure 5.51. Homozygous regions on chromosome 12 for ALS252, ALS254, ALS257 and controls

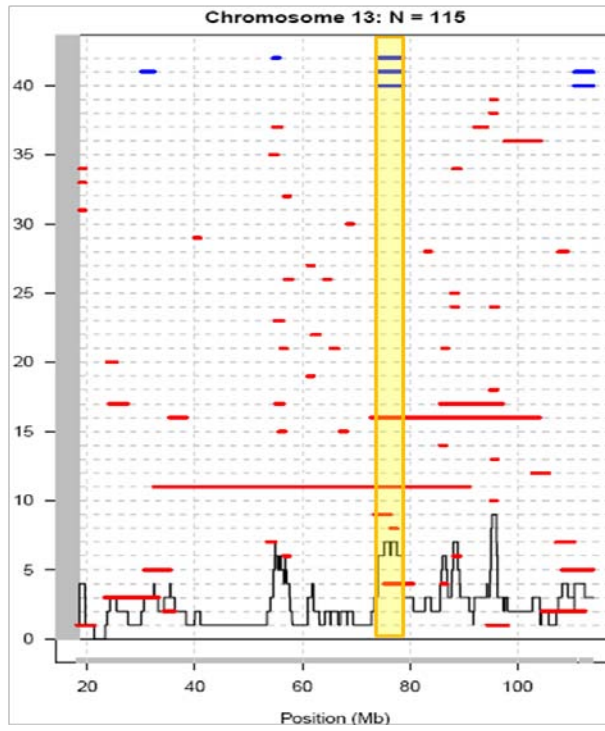


Figure 5.52. Homozygous regions on chromosome 13 for ALS252, ALS254, ALS257 and controls

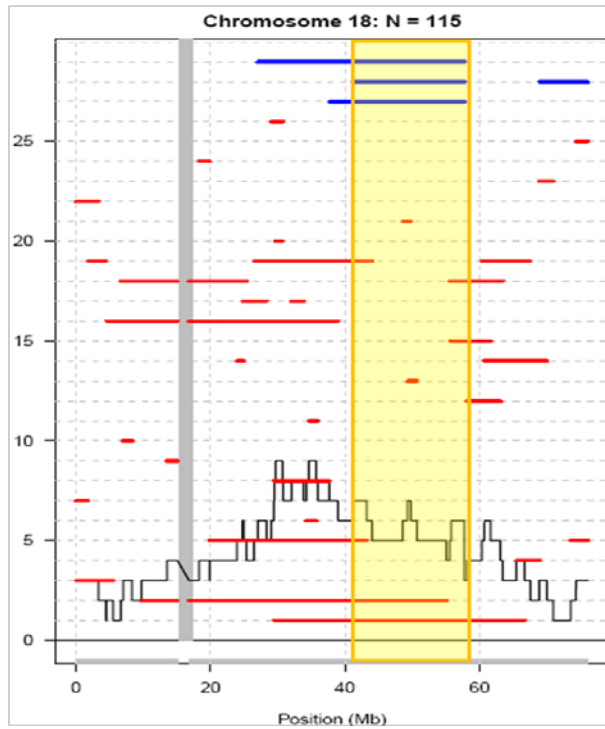


Figure 5.53. Homozygous regions on chromosome 18 for ALS252, ALS254, ALS257 and controls

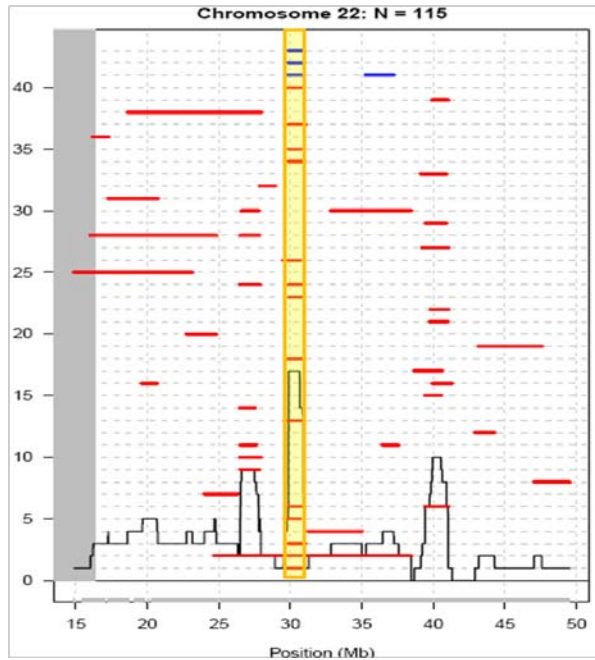


Figure 5.54. Homozygous regions on chromosome 22 for ALS252, ALS254, ALS257 and controls

After the elimination of several homozygosity regions, as indicated above, several candidate genes were selected for further analysis (Table 5.12). It should be noted that since some control samples belonged to consanguineous families, they embedded large regions of homozygosity. In this respect, if regions in the Turkish recessive family overlapped only with that of these individuals, the control individuals were neglected and the region was evaluated as significant.

Table 5.12. Candidate selected after the selective evaluation of homozygosity mapping

Gene	Full Name	Chromosomal Location
IL21	interleukin 21	chr4:123,753,315-123,761,661
UCHL3	ubiquitin carboxyl-terminal esterase L3	chr13:75,032,880-75,078,069)
USP53	ubiquitin specific protease 53	chr4:120,407,923-120,413,918
RAB27A	Ras-related protein Rab-27A	chr15: 55,495,164-55,582,001
CPEB3	cytoplasmic polyadenylation element binding	chr10:93,798,379-94,040,824

IL21, UCHL3 and USP53 were within homozygosity regions of all three siblings while missing in controls. RAB27A, a member of the RAS oncogene family, is a membrane-bound protein which may be involved in protein transport and GTPase-regulated signal transduction. CPEB, cytoplasmic polyadenylation element binding, is very highly expressed in brain. Although the definite function is unknown, it was suggested to be a prion required for memory storage (personal communications Dr. Murat Günel, Eric Kandel and Art Hortsitz, Yale University, Medical School).

5.6. Mutation Analyses of CPEB3, IL21, RAB27, UCHL3 and USP53 in a Recessive Turkish ALS Family

Patient ALS256, a representative of the same autosomal recessive family with three affected individuals (Section 5.5), was subjected to mutation screening for the candidate genes.

5.6.1. PCR amplification and DNA Sequencing of CPEB3

All exons of the CPEB3 gene were amplified as described in Section 4.5.1. ALS256 was shown to carry three variations in the CPEB3 gene. Among these, two were within the coding regions. rs3824734 is a fairly common polymorphism with a frequency of 0.408. It represents CCT→CCC transition at codon 86 in exon 1. The second SNP within the coding region was rs2676811. It results from the transition of TAC→TAT at position in exon 8. While the former was represented in a heterozygous manner, the latter was present homozygously. However, both were silent, since no change occurred in type of aminoacid.

The third variation was located at position 21 in intron 6. A→T transversion at this position was previously reported as a SNP with a frequency of 0.365, named rs1129578. All variations observed for this gene in ALS256 are displayed in Table 5.13.

Table 5.13. Variations observed in the CPEB3 gene of ALS256

Exon	Location	Identified SNP	Nucleotide Change	Aminoacid Change
Exon 1	Codon 86	rs3824734	CCT→CCC homozygous	none
Exon 8	Codon 573	rs2676811	TAC→TAT homozygous	none
Intron 6	21 bp before exon 7	rs1229578	A→G homozygous	--

5.6.2. PCR amplification and DNA Sequencing of USP53

All exons of the USP53 gene were amplified as described in Section 4.5.1. Several variations were detected in the USP53 gene.

Among these, only one variation was within the coding region. It was located at codon 724 in exon 15 where there was an ATG→ACG transition in a heterozygous manner. This results in a methionine to threonine exchange which is described as a tolerable state. One novel insertion was detected in intron 13 which was located 112 bp before the beginning of exon 14. Another novel variation was a deletion at position 17 in intron 14. Also, T→C transition at position 98 in intron 14 was a previously reported SNP,

termed rs11731675. Lastly, sequencing revealed the presence of homozygous A G transition at position 105 in intron 14 which has been named rs10006850. All variations observed for this gene in ALS256 are displayed in Table 5.14.

Table 5.14. Variations observed in the USP53 gene of ALS256

Exon	Location	Identified SNP	Nucleotide Change	Aminoacid Change
Exon 15	codon 724	novel	ATG→ACG heterozygous (tolerable)	M→T
Intron 13	112 bp before exon 14	novel	novel homozygous insertion	--
Intron 14	position 17	novel	novel homozygous deletion	--
Intron 14	position 98	rs11731675	T→C homozygous	--
Intron 14	position 105	rs10006850	G→A homozygous	--

5.6.3. PCR amplification and DNA Sequencing of UCHL3

All exons of the UCHL3 gene were amplified as described in Section 4.5.1. The investigation by DNA sequencing revealed two variations, both in the intron. The first variation lied within position 28 in intron 2. This was represented as a homozygous transition of C→T. It was reported as rs8192738 with a frequency of 0.486. The second variation was a T→A transversion in a homozygous state in intron 3 position 11. This was a previously reported common polymorphism (f: 0.485), named rs4884008. Also, a homozygous transition of G→A at position 108 in intron 7 was observed, named rs7330411. All variations observed for this gene in ALS256 are displayed in Table 5.15.

Table 5.15. Variations observed in the UCHL3 gene of ALS256

Exon	Location	Identified SNP	Nucleotide Change	Aminoacid Change
Intron2	position 28	rs8192738	C→T homozygous	--
Intron 3	position 11	rs4884008	T→A homozygous	--
Intron 7	position 108	rs7330411	G→A homozygous	--

5.6.4. PCR amplification and DNA Sequencing of RAB27

PCR amplification was performed for all exons of the RAB27 gene as described in Section 4.5.1. DNA sequencing analysis revealed a G→A transition in a homozygous state in the 5' untranslated region (Table 5.16). This was a previously reported polymorphism, named rs72742261.

Table 5.16. Variations observed in the RAB37 gene of ALS256

Exon	Location	Identified SNP	Nucleotide Change	Aminoacid Change
Exon 1	5' untranslated	rs72742261	G→A homozygous	--

5.6.5. PCR amplification and DNA Sequencing of IL21

All exons of the IL21 gene were amplified as described in Section 4.5.1.

Mutational analysis of IL21 in ALS256 revealed only a TGC→TGT transition at codon 43 in exon 3 in a homozygous manner. However, no change occurs in the protein, thus is only a silent change. It was a rare polymorphism with a frequency of 0.262. The variation observed for this gene in ALS256 is displayed in Table 5.17.

Table 5.17. Variations observed in IL21 gene of ALS256

Exon	Location	Identified SNP	Nucleotide Change	Aminoacid Change
Exon 3	Codon 43	rs4833837	TGC→TGT homozygous	C→C

5.7. Whole Human Exome Analysis of ALS256

ALS256 was also selected as a proxy for the identification of homozygous regions. The results of the whole exome analysis are shown in Table 5.18.

Table 5.18. Sequence changes detected in whole exome analysis

Chrom	Position	Base change	Gene full name	Status	A.acid change
4	122470104	CGG>TGG homozygous	pyroglutamylated Rfamide peptide receptor	coding-missense	R371W
6	10506712	TAC>TCC homozygous	transcription factor AP-2 α	coding-missense	Y407S
6	11822640	G>A heterozygous	chromosome 6 open reading frame 105	3UTR	
6	13819263	AAG>GAG homozygous	RAN binding protein 9	coding-missense	K152E
6	17710889	GTC>ATC heterozygous	family with sequence similarity 8, member A1	coding-missense	V268I
18	42267211	GGC>GCC homozygous	ring finger protein 165	coding-missense	G41A
18	42376722	GAC>GAA homozygous	lipoxygenase homology domains 1	coding-missense	D127E
18	42889008	A>G homozygous	haloacid dehalogenase-like hydrolase domain containing 2	3UTR	
18	43810098	CAC>CCC homozygous	zinc finger and BTB domain-containing 7C	coding-missense	H464P
18	45342673	C>G homozygous	lipase, endothelial	5UTR	
18	46060318	TGG>GGG homozygous	methyl-CpG binding domain protein 1	coding-missense	W15G
18	46060329	CTG>CCG homozygous	methyl-CpG binding domain protein 1	coding-missense	L11P
22	30347116	GAC>GGC homozygous	phosphatidylserine decarboxylase	coding-missense	D203G

Table 5.19. Overall representation of ALS genes analyzed

type of disorders	# families	# affected	# analyzed for SOD1	# analyzed for TDP-43	# analyzed for FUS	# analyzed for ANG	# analyzed for CNVs	# analyzed for Whole Exome Resequencing
FALS	22	29	29/29	9/29	9/29	9/29	15/29	1
JUVENILE	10	13	13/13	4/13	4/13	4/13	13/29	na
SALS	156	156	156/156	na	na	na	na	na
TOTAL	198	198	198/198	13/42	13/42	13/42	28	1

Table 5.20. Variations identified in SOD1, TDP-43, FUS and ANG

gene	mutations/SNPs	frequency in FALS	frequency in Juvenile	exon	nucleotide change	aminoacid change	type	effect
SOD1	N86S	1/29	0/29	4	AAT→A GT	Asn-Ser	missense	GOF
SOD1	H71Y	1/29	0/29	3	CAC→TAC	His-Tyr	missense	GOF
SOD1	L144F	1/29	0/29	5	TTG→TTC	Leu-Phe	missense	GOF
SOD1	D90A	1/29	0/29	4	GAC→GCC	Asp-Ala	missense	GOF
SOD1	A4S	1/29	0/29	1	GCC→TCC	Ala-Ser	missense	GOF
SOD1	IVS-III-34 A→C	2/29	0/29	intron 3	A→C	no change	polymorphism	no effect
TDP-43	none							
FUS	rs929867	1/24	0/13	5'UTR	---	---	---	---
FUS	novel	6/24	4/13	1	GTA→GTG	Val-Val	---	---
FUS	rs741810	8/24	4/13	2	GGC→GGA	Gly-Gly	---	---
FUS	rs1052352	14/24	5/24	4	TAC→TAT	Thy-Thy	---	---
FUS	novel	0/24	1/13	intron 5	---	---	---	---
ANG	rs11701	8/24	2/13	1	GGT→GGG	Gly-Gly	SNP	no effect

Table 5.21. Summary of unreported homozygous and heterozygous deletion regions detected via whole genome analysis of familial and juvenile cases

location	gene	chrom.	loci start	loci stop	size	change	frequency in FALS	frequency in Juvenile
intron	DLG2	1	84719557	84733071	13514	heterozygous	3/24	0/13
intragenic	---	13	49271585	49271799	214	heterozygous	1/24	2/13
intron	USH2A	1	214199501	214203243	3742	heterozygous	2/24	0/13
exon	C9orf153	9	88015587	88029735	14148	heterozygous	0/24	1/13
exon	C21orf56, FTCD	21	46391256	46427893	36637	heterozygous	1/24	0/13
exon	USP45	6	100022903	100032890	9987	heterozygous	1/24	0/13
intron	HCCA2	11	1611186	1611326	140	homozygous	2/24	1/13
intergenic	---	12	111503947	111504440	493	homozygous	2/24	0/13
intergenic	---	4	19130834	19131054	220	homozygous	6/24	7/13
intron	PCNT	21	46626358	46628866	2508	homozygous	1/24	0/13
intron	BACH2	6	90884890	90885603	713	homozygous	1/24	0/13

5.8. Genome-wide Association Study in Caucasian SALS Cases

In a large collaborative study in Cecil Day Lab at MGH in Boston, Landers and colleagues performed a genome-wide association study, using 279,217 SNPs on 1405 SALS samples (from Boston, National Institute of Neurological Disorders and Stroke (NINDS), Atlanta, France, London and Netherlands) and 1848 matching controls (Landers *et al.*, 2009). The study was performed with Illumina BeadArrays at the Broad Institute in Boston (Boston-Atlanta-London DNA set), the National Institutes of Health (Drs. A. Singleton and J. Hardy, NINDS/Coriell DNA set), the Centre National de Genotypage at Evry (French set) and at Rudolf Magnus Institute of Neuroscience, Utrecht (Netherlands set). The analysis was conducted by PLINK where all data of SALS cases and controls were considered as one. This approach increases the probability of pinpointing subtle associations in the presence of adequate number of cases and controls.

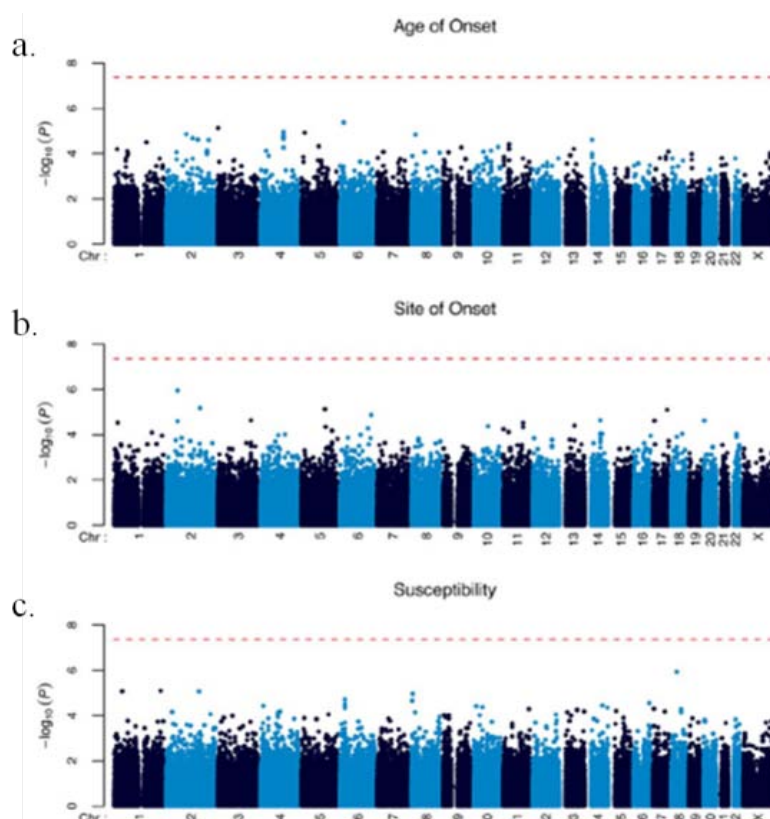


Figure 5.55. GWAS results according to site of onset, age of onset and survival. The cut-off value for Bonferroni significance is represented as the dotted red line (Landers *et al.*, 2009)

The results of SALS samples were evaluated according to four phenotypes: susceptibility, site of onset, age of onset and survival. No significant SNP was detected as associated to susceptibility, age of onset or site of onset (Figure 5.55). In a further effort, for susceptibility, when only SNPs with a p value $< 5 \times 10^{-4}$ were selected, which corresponded to 153 SNPs in total, still no significant variant was detected. Even previously reported variants in inositol-triphosphate receptor (ITPR2), DPP6 and FLJ10986 were not confirmed (Appendix F).

However, a different picture was observed for survival. The rs1541160 SNP revealed a significant value where the nominal and Bonferroni-corrected P values were 1.84×10^{-8} and 0.021, respectively (Figure 5.56a). Several SNPs around this region exhibited positive values, including four of the imputed SNPs (Figure 5.56b).

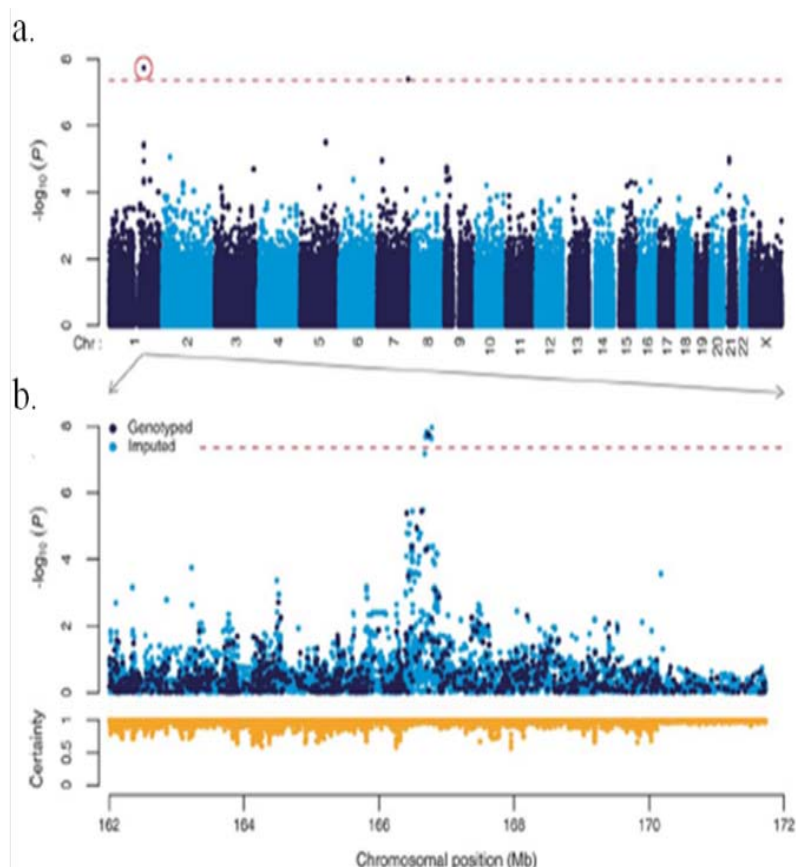


Figure 5.56. a. GWAS result on survival, b. a closer view of the rs1541160 region where dark points are SNPs within this study and light points are imputed SNPs (Landers *et al.*, 2009)

The significance of these results were further confirmed by pairwise linkage disequilibrium (LD) analysis for 50 SNPs located across this locus (Appendix G). When SALS cases with different genotypes at rs1541160 were compared in terms of survival, the presence of the CC genotype favored survival around 14 months when compared to the TT genotype (Figure 5.57).

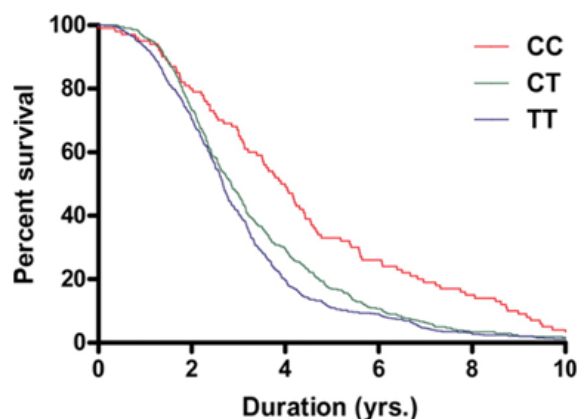


Figure 5.57. The effect of different alleles of rs1541160 on survival in SALS patients (Landers *et al.*, 2009)

SNP rs1541160 was localized within intron 8 of KIFAP3. The positive effect of the CC allele was investigated via sequencing of KIFAP3 in homozygous CC and TT individuals for the possible presence of a variant that may be in close LD with the SNP. Since no variations were detected in the coding regions of KIFAP3, the involvement of rs1541160 on survival was questioned for a possible change in the expression level of the protein in different genotypes.

The predicted changes in expression levels were also analyzed in SNPs with high scores in each category (Appendix H). This study has contributed to the investigation of gene expression analyses of KIFAP3, B4GALT6 and ADAMTS17 genes (Table 5.22).

Table 5.22. Three significant SNPs for susceptibility, survival and age of onset

Category	SNP	Gene	Chromosomal Location	p Value
Survival	rs1541160	KIFAP3	Chr 1: 168262426	1.84×10^{-8}
Susceptibility	rs10438933	B4GALT6	Chr 18: 27527127	1.18×10^{-6}
Age of Onset	rs931892	ADAMTS17	Chr 15: 96046836	5.33×10^{-5}

KIFAP3 is a regulator protein with two main functions: stimulation of GDP/GTP exchange reactions in small G-proteins (Rap1 and Rho) and inhibition of their interaction with the membrane. It is very highly expressed in all regions of the brain. B4GALT6, beta-1,4-galactosyltransferase6, is a lactosylceramide synthase which is an important component of glycolipid biosynthesis. It is very highly expressed in brain. While B4GALT6 exhibited a significant value in susceptibility, KIFAP3 was significant in survival (Table 5.28). The definite function of ADAMTS17 has not been identified yet, however, a statistically significant value was detected for a SNP in close proximity to the gene; thus, the expression profile of ADAMTS17 was also investigated.

The expression levels of each protein were questioned by real-time PCR with specific probes. Total RNA was isolated from both lymphoblastoid cell lines and brain tissues. The investigation of gene expression levels in individual regions included wild-type ancestral homozygotes, heterozygotes and derived allele homozygotes for each SNP.

5.8.1. The expression profile of B4GALT6

The expression level of B4GALT6 in SALS was compared within different genotypes in cortex (Figure 5.58) and cerebellum (Figure 5.59). There was no significant difference in expression between ancestral and derived homozygotes for this protein.

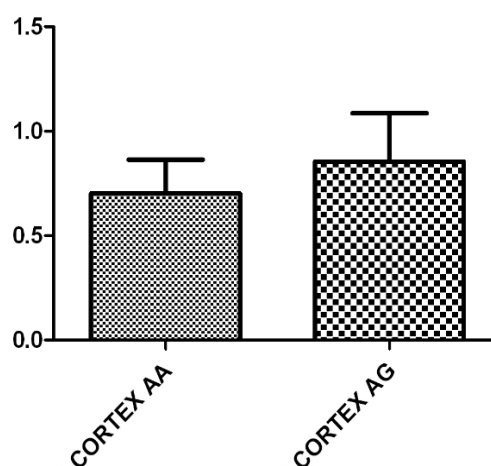


Figure 5.58. Hs00191135 expression in cortex, according to alleles

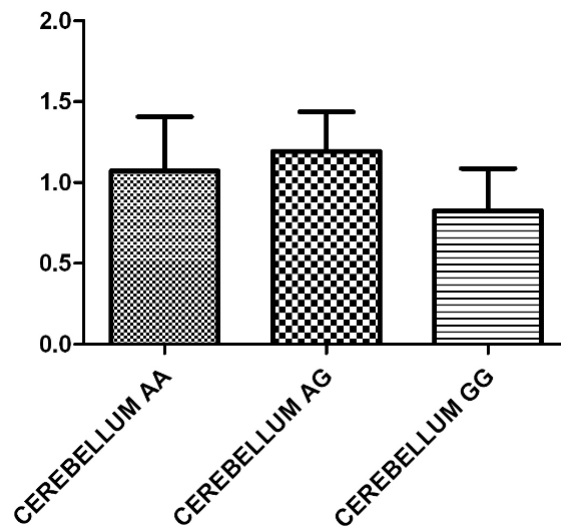


Figure 5.59. Hs00191135 expression in cerebellum, according to alleles

5.8.2. The expression profile of ADAMTS17

The expression of ADAMTS17 was investigated by probe Hs00330236. There was no significant change in brain for different genotypes (Figure 5.60).

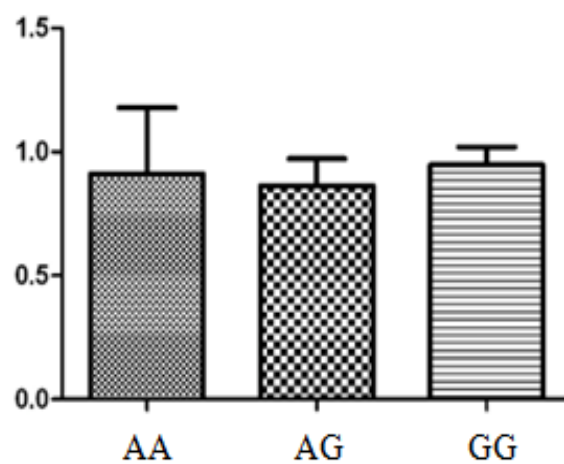


Figure 5.60. Hs00330236 expression in brain, according to alleles

When the same analysis was conducted on cortex only, AA exhibited an apparent difference in expression (Figure 5.61). However, this was due to small and unequal sample size. Thus, this result was considered not to be reliable.

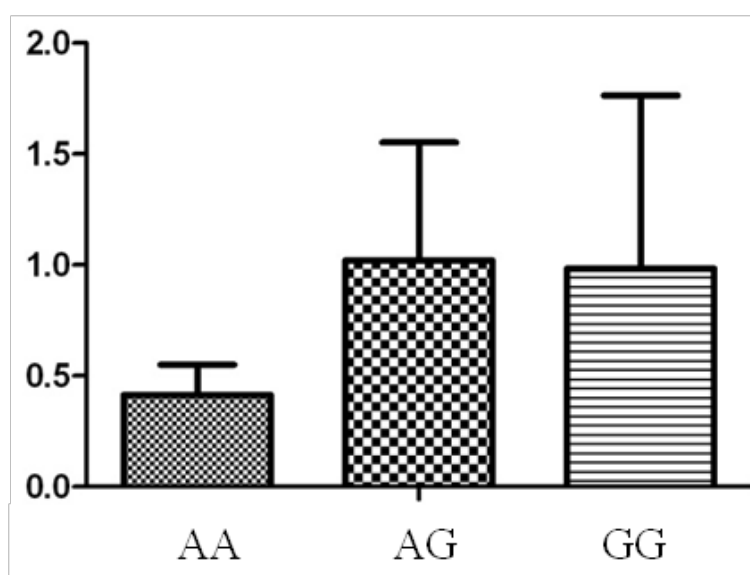


Figure 5.61. Hs00330236 expression in cortex, according to alleles

5.8.3. The expression profile of KIFAP3

5.8.3.1. Real-time PCR analysis. Using Hs00183973, a specific probe for KIFAP3, the relative expression levels of CC, CT and TT were compared both in cortex and cerebellum (Figures 5.62 and 5.63). In both regions, the expression level in CC was significantly reduced when compared to TT.

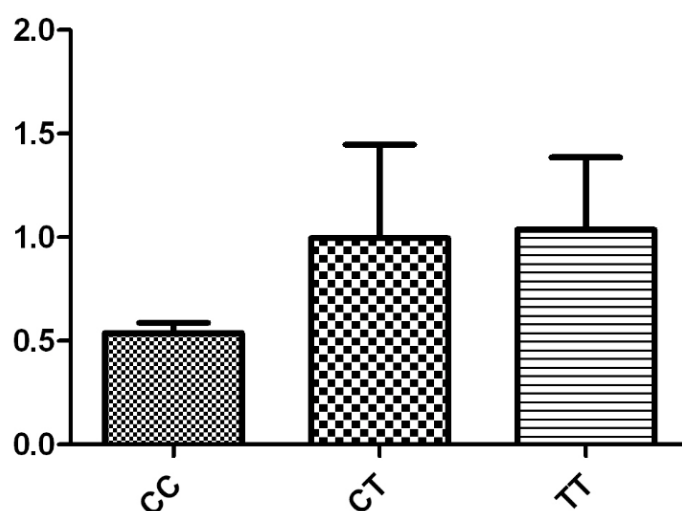


Figure 5.62. Hs00183973 expression in cortex, according to alleles

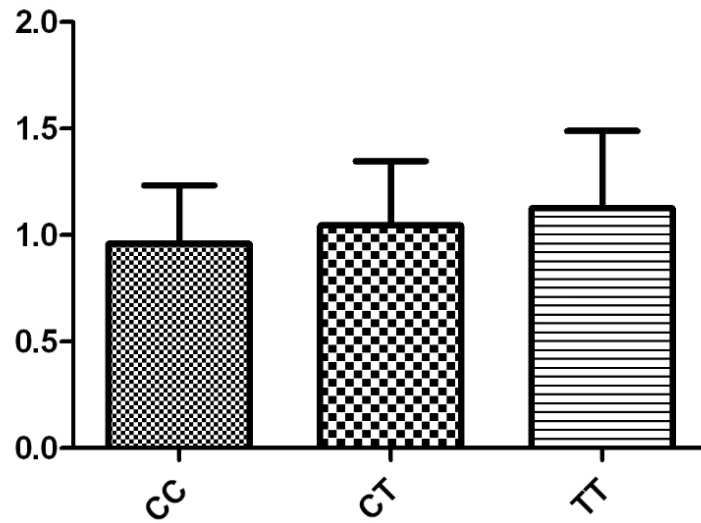


Figure 5.63. Hs00183973 expression in cerebellum, according to alleles

Like Hs00183973, Hs00946074 is also a probe, specific for KIFAP3; thus, it was used as a 'confirmation' probe for expression analysis. The decrease of KIFAP3 expression in the CC genotype was also reflected in the analysis of Hs00946074 in cortex and cerebellum (Figures 5.64 and 5.65).

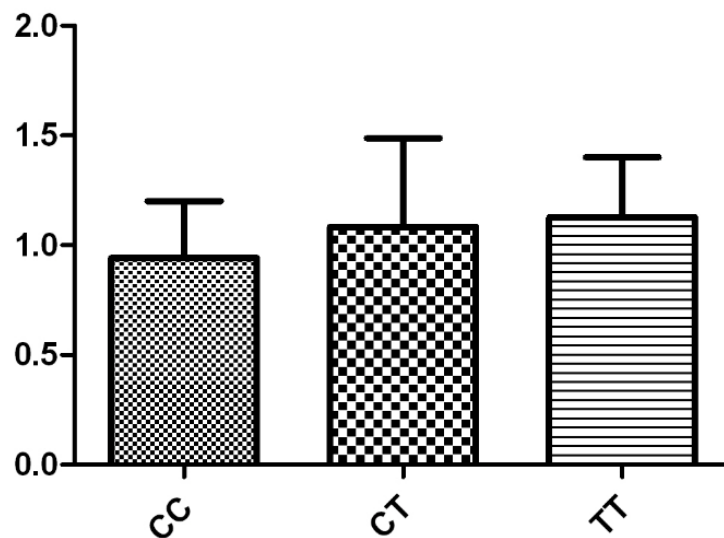


Figure 5.64. Hs00946074 expression in cortex, according to alleles

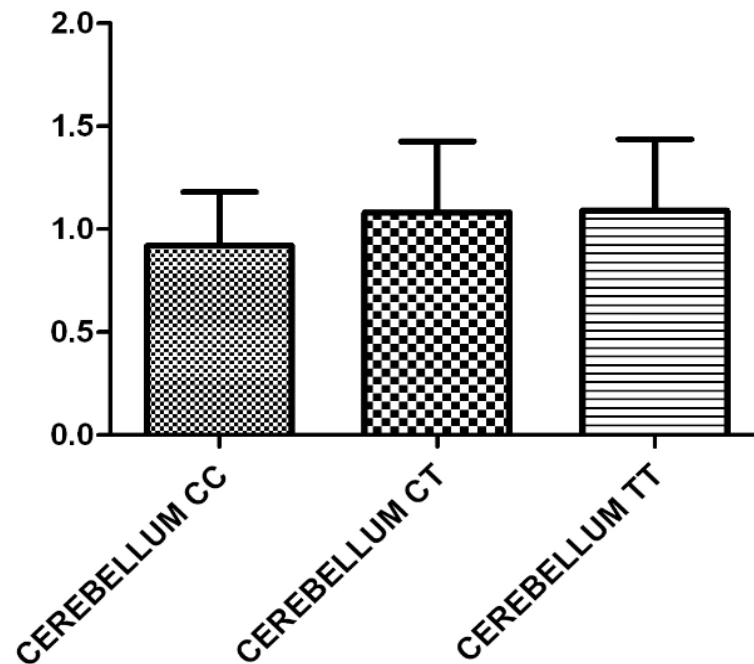


Figure 5.65. Hs00946074 expression in cerebellum, according to alleles

5.8.3.2. Western blot analysis of KIFAP3. The change in expression level was also questioned with Western blot analysis; the expression was investigated in 88 brain lysates (Figure 5.66).



Figure 5.66. Western blot analysis of KIFAP3 expression in association with rs1541160 genotype (Landers *et al.*, 2009)

Additional experiments at Cecil Day Lab confirmed the significant decrease of KIFAP3 protein level in CC homozygotes compared to TT. The results were also confirmed in occipital lobe samples (Figure 5.67).

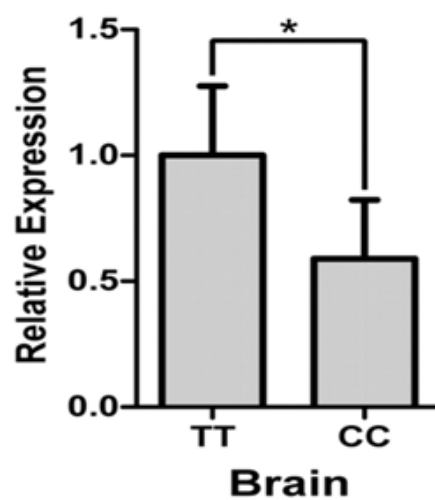


Figure 5.67. The relative expression of TT and CC genotypes for rs1541160 in occipital cortex (Landers et al., 2009)

6. DISCUSSION

ALS is a progressive neurodegenerative disease, predominantly initiated in mid-adult life and characterized by the selective death of motor neurons (Cleveland, 1999). The most predominant neuropathological changes are the appearance of abnormal mitochondrially-derived vacuoles and the fragmentation of Golgi apparatus, followed by the degeneration of motor neurons (Jaarsma *et al.*, 2001).

The most intriguing question is ‘why are motor neurons selectively prone to neurodegeneration in ALS?’ Several features of these cells are suggested for vulnerability:

- cell size and long axons
- high metabolic rate
- high energy demand
- specific features of motor neuron mitochondria
- NF content and the importance of proper intracellular filament structure and transport system
- relatively high expression of Ca⁺²-permeable AMPA receptors, lacking GluR2 subunit
- high expression of glutamate transporters in the proximity of vulnerable motor neuron groups
- low expression of Ca⁺²-binding proteins
- high expression of SOD1 (Shaw, 2005).

The mechanism by which mutations in SOD1, the predominant protein described in ALS, brings about motor neuron injury is not yet well understood, but is considered to be a toxic gain of function, rather than a loss of normal function. Two supporting findings are i. the identification of both decreased and normal levels of SOD1 dismutase activity in the case of SOD1 mutations and ii. the observation of ALS-like clinical phenotype in transgenic mice overexpressing FALS-linked mutations, while an unaffected clinical picture is present in mice overexpressing normal SOD1.

The combination of genetic, pathological and biochemical studies have brought out possible mechanisms that may provoke the disease or contribute to the disease:

- oxidative damage, an idea which emerged after the the identification of mutations in SOD1 as the primary cause in ALS,
- excitotoxic death due to glutamate, supported by the obstructive effect of riluzole via inhibition of glutamergic transmission,
- cytoskeletal abnormalities and transport defects, an idea supported by the abnormal accumulation of neurofilaments as a pathological finding and the detection of mutations in dynactin, an important regulator of retrograde transport,
- toxicity due to intracellular protein aggregation and failure in protein folding and ubiquitination mechanisms, common features of SOD1-linked ALS cases,
- the involvement of mitochondria, an idea dependent on the requirements of high energy levels of motor neurons and the neuropathological changes in mitochondria,
- the crosstalk between motor neurons and non-neuronal cells, where the inflammatory response generated by glial cells induces proinflammatory elements from neurons that induce glial cells back, and in the final stage cells are driven to apoptosis (Cozzolino, 2008, Lomen-Hoerth, 2008, Figure 6.1).

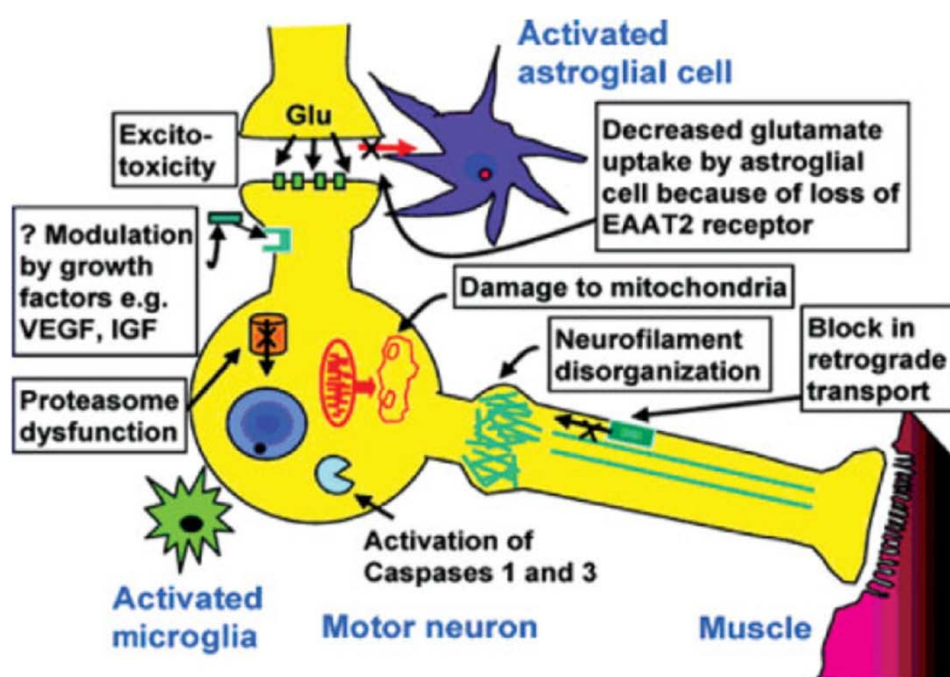


Figure 6.1. An overall representation of the proposed mechanisms in ALS

(Lomen-Hoerth, 2008)

Today, in the concept of understanding the pathogenesis of ALS, it seems more probable that the death of motor neurons is the result of the convergence of the factors, stated as ‘probable contributors’. However, it should be noted that the current knowledge on pathogenic mechanisms is mostly based on studies with mutant SOD1, which is responsible for only two per cent of all ALS cases. For the vast majority of patients, the primary cause of disease is unknown. Thus, there is a need to identify new genes associated with familial forms of ALS (Dion *et al.*, 2009)

6.1. Mutational Analysis of SOD1 in the Turkish ALS Cohort

This study included 198 Turkish ALS patients. Among these, 156 were sporadic, while 29 were familial and 13 juvenile. The percentages of FALS and SALS were 21 and 79 per cent, respectively, which are consistent with the values stated in literature (Figure 6.2).

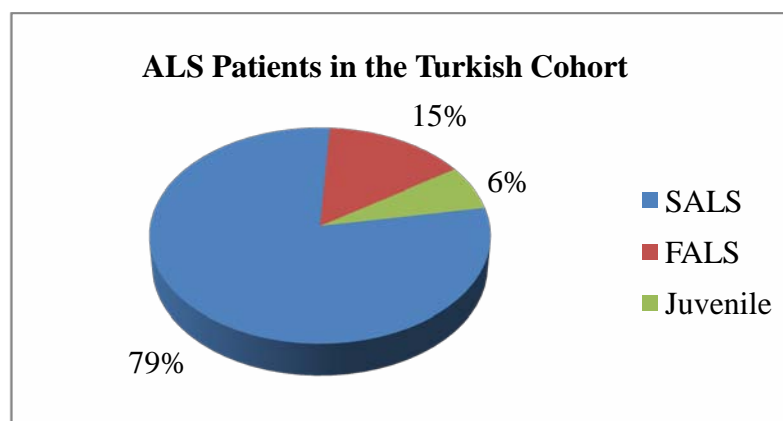


Figure 6.2. Distribution of Turkish ALS cases according to different subgroups

DNA sequencing analysis of SOD1 in the Turkish ALS cohort revealed five disease causing mutations in FALS cases. The number of FALS cases carrying SOD1 mutations (corresponding to 15.6 per cent of FALS cases and 2.5 per cent of all ALS cases) is in accordance with the literature, stating 20 per cent involvement of the gene in FALS and 2 per cent involvement in all ALS cases (Figure 6.3). Also, IVS-III-34 A→C transversion was observed in 2 FALS and 5 SALS cases, corresponding to 3.8 per cent in the study population. The frequency of IVS-III-34 A→C transversion in the Turkish control samples

was calculated as 3.4 per cent which was close to the reported percentage in literature (4 per cent) (Deng *et al.*, 1993).

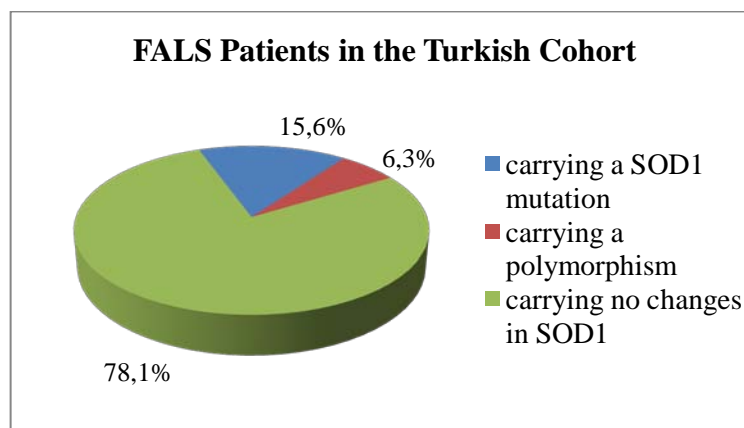


Figure 6.3. SOD1 gene analysis results of Turkish FALS cases

6.1.1. The N86S Patient

Among cases with SOD1 mutations, three were remarkable. The first interesting case was a FALS case who was diagnosed at the age of 28. He was shown to carry an AAT→AGT transition in exon 4 position 86 (N86S) in a homozygous state. This indicated that both of the parents should be carriers of the mutant allele. The mother died of cirrhosis at the age of 28; her DNA was not available at the time of analysis. The father is now 54 years old and normally would be expected to develop the disease.

This mutation was first defined in a Japanese family with two affected individuals who were heterozygous at this position. The father was diagnosed with ALS at the age of 56. He displayed only upper motor neuron symptoms and died within 4 years due to respiratory failure. Meanwhile, his daughter, who was diagnosed at the age of 36, suffered from lower limb weakness (lower motor symptoms), and general muscular atrophy occurred nine years after the first symptoms, indicative of a slow progression. She survived for 11 years (Kurahashi *et al.*, 1993). Another study reported a homozygous patient. She was diagnosed at the age of 13 with lower limb weakness. The disease progressed rapidly. She died within 14 weeks of diagnosis due to respiratory failure. Similar to the index case of this study, her parents were heterozygous carriers with no disease phenotype (Hayward *et al.*, 1998). Overall, there seems to be incomplete penetrance in the clinical representation

of the disease among ALS cases with N86S mutation, probably depending on the presence of the mutant allele in homo- or heterozygous state, as well as on the initial site of onset.

SOD1 mutations have been linked to autosomal dominant inheritance. Only few mutations are known to be represented both dominantly and recessively (Andersen *et al.*, 1995). In this context, N86S has been represented recessively in this family which brings about the presence of heterogeneity in the mode of transmission.

Considering a toxic gain of function of SOD1 mutants, a double dose of the mutant protein would be expected to result in a more severe phenotype. The clinical picture of the index case is consistent with this assumption. However, the absence of disease phenotype in N86S heterozygotes is still interesting, since arginine at this position displays an important role in both the protein structure and function. Codon 86 is located within the β 5-strand. A beta barrel is a large beta-sheet which twists and coils to form a closed structure, so that the first strand is hydrogen-bonded to the last. Meaning, it is responsible for the establishment of the electrostatic guidance channel, which guides O_2^- to Cu^{+2} -containing active site. In this respect, the presence of a mutation at this position would be expected to disrupt the proper structure of the active channel, leading to deficiency in the dismutase activity.

Interestingly, in literature, N86S mutant has been reported as having a wild-type-like structure where no change in stability or metal coordination properties is observed (Shaw *et al.*, 2006). Previous reports have shown that it does not affect the enzymatic activity of SOD1. However, this mutant still aggregates more rapidly than wild-type SOD1 in cell cultures and *in vitro* (Bergemalm *et al.*, 2006).

The contradiction of having a native-state-like stability and being more prone to aggregation may be reasoned as the occurrence of aggregation directly from native/-like state. If so, the conformational changes which lead to aggregation of the mutant protein may happen after the formation of native-like oligomers. Changes like decrease in net charge may contribute to formation of oligomers. It is probable that the native-like mutant SOD1 aggregates may be nontoxic structures which encourage formation of toxic SOD1 aggregates.

N86S is represented with a rapid disease progression in less than three years (Hayward *et al.*, 1996). The index case died within 4 months after diagnosis, which is consistent with the previously reported N86 homozygous patient profile. Rapid disease progression in C6F and A4V have previously been related to higher rates of ubiquitination of the mutant proteins. However, whether this applies to mutants at codon 86 is to be determined.

A further understanding may be obtained by assessing the sequence variations in the noncoding regions of SOD1 of the index case and his father. For example, SOD1 protein is vulnerable to alternative splicing defects, since it contains a high number of GC motifs, especially in intron 1. Thus, a sequence variation in the index case may result in the abnormal splicing of mutant SOD1, leading to reduction in transcription of the mutant protein. In a recent study, a patient with homozygous deletion at position 27 exhibited an ALS phenotype, while eight heterozygous relatives were phenotypically normal. The mutation at this site was shown to decrease transcription of the protein. Such a reduction may also explain the phenotypic heterogeneity in our N86S family (Dion *et al.*, 2009).

6.1.2. The H71Y Patient

The second interesting case was also a FALS patient who carried a heterozygous CAC→TAC transition at position 71 in exon 3, resulting in H71Y mutant SOD1. Exon 3 of SOD1 has been special in that only recently mutations have been identified in this region. Until then, two possibilities were suggested as to explain the absence of disease-causing mutations: i. mutations in exon 3 would be lethal in utero, thus no individual was born with a mutation at this site (Siddique *et al.*, 1996) or alternatively ii. it would be represented in a benign fashion which indicated that exon 3 integrity was necessary for the toxic effect of SOD1 (Orrell *et al.*, 1997).

While residues 58-63 within exon 3 structurally construct the symmetrical region 3, residues 56-79 are responsible for Zn⁺² binding. His71 is specifically one of the zinc ligands (Getzoff *et al.*, 1999). Zn⁺² is required for the stability of SOD1 structure, pH of the dismutation reaction, as well as the rapid dissociation of the H₂O₂ produced. Thus, as implicated in the peroxidase hypothesis, the change in the Zn⁺² binding capacity can result

in the destabilization of the protein backbone where Cu^{+2} located at the active site becomes more accessible to H_2O_2 . This causes an excess generation of hydroxyl radicals in cells, resulting in oxidative damage.

The investigation of the mutation in other family members of this patient revealed the heterozygous presence of the mutant allele in his father and younger brother, while his mother and younger sister carried normal alleles. When the facts that the disease was represented with very fast progression at a very early age, and that the father is still phenotypically normal, are considered, it can be proposed that there has been an increase in penetrance. However, it is still interesting to observe normal state in heterozygotes when the structural and functional importance of position 71 are considered. As implicated for the FALS case with the N86S mutation, it would also be important to search for the presence of possible sequence variations that may lead to phenotypic heterogeneity in this family.

6.1.3. The D90A Patient

The patient carried a homozygous $\text{GAC} \rightarrow \text{GCC}$ transversion at position 90 in exon 4, resulting in the D90A mutant SOD1. His older sister died of ALS, so a family inheritance can be mentioned. The homozygous representation of the disease in the index case indicated that both parents should be carriers of the mutant allele. It has been previously shown that D90A mutation represents mainly an autosomal dominant inheritance pattern in non-Scandinavian populations, while autosomal recessive inheritance is pronounced in Scandinavian populations. The inheritance pattern within this family resembled that of Scandinavian patients.

Also, the clinical picture was in concordance with the literature: while autosomal dominant D90A cases in non-Scandinavian populations show a diversity in phenotype, autosomal recessive cases in Scandinavia exhibit a uniform clinical picture with always limb onset and slow progression. Our index case can still eat and walk on his own after having the disease for five years, thus can be defined as slowly progressing.

D90 is located nearby a β -barrel on the periphery of SOD1; it has little influence on dimer-dimer interaction or the catalytic activity, it is a highly conserved position. Interestingly, another mutation at the same position (D90V) is dominantly-inherited which disproves the implication of an unimportant position.

Diverse clinical picture and mode of transmission have been suggestive of a possible protective factor in heterozygote D90A-SOD1 individuals in Scandinavian populations, a statement which has not been proven thus far. Considering the similarity of the index case with Scandinavian recessive pattern, the index case and his family members were further subjected to haplotype analysis for a possible ancestral relationship.

6.2. Haplotype Analysis of the Turkish ALS Patient with the Homozygous D90A Mutation

Linkage analysis relies on 'the tendency of genes, located at specific loci, to segregate together due to their physical proximity on a single chromosome' (Strachan and Read, 1999). In this respect, linkage analysis can be defined as a study aiming establishment of linkage between genes. This approach also applies to studies of association between populations. The investigation of similar haplotypes across individuals supplies a powerful data for unraveling the migration of civilizations.

In this line, considering the special mode of transmission of D90A in the index case, the patient's sample was subjected to haplotype analysis with 21 Scandinavian cases, using six markers which were proximal to SOD1. The haplotype pattern of the index case was identical to the conserved Scandinavian haplotype, implying a common ancestry.

Scandinavian populations, mainly Finland and Northern Sweden, are homozygous and genetically different from most European populations (Nevanlinna *et al.*, 1972, Andersen *et al.*, 1996). Thus, the haplotype around D90A is unique for this mutation and the mode of inheritance.

Andersen *et al.* showed the overrepresentation of highly conserved haplotypes of D90A homozygotes and heterozygotes in Scandinavian population which converged as

they approached to SOD1. This had been the indicative of a common founder 20,000 years ago in Eurasia. Considering the pattern of inheritance and the clinical representation of the disease in homozygotes and heterozygotes, the appearance of a second modifying factor was suggested to occur in B.C. 1,500. in Finland which had been distributed throughout the world by migrations (Parton *et al.*, 2002).

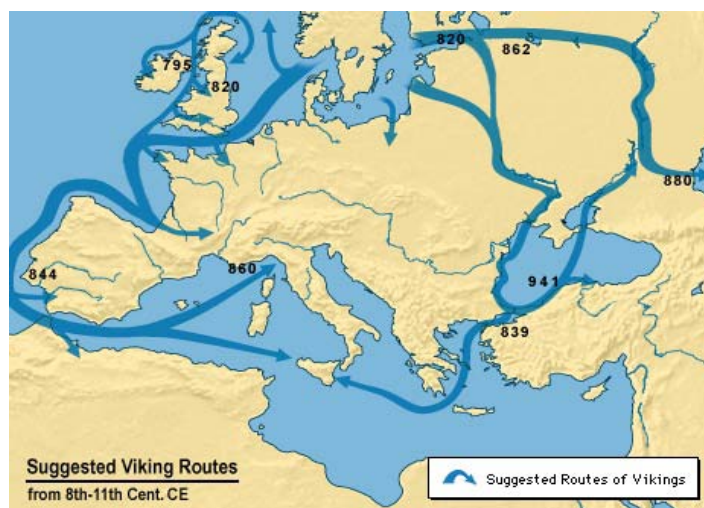


Figure 6.4. Suggested migration routes of Vikings (www.designsofwonder.com)

Inbreeding of Scandinavian populations within themselves led to higher allele frequency (2.5 per cent) in Finland and North Sweden while the frequency gradually decreased southwestly in Europe (Westray in the Orkney Isles: 1.5 per cent, 0.3 per cent in England) (Själänder *et al.*, 1995, Al-Chalabi *et al.*, 1998).

The phylogeographic analysis of lineages proposed the migration of Vikings from Scandinavia to all over Europe, including Constantinople (Figure 6.4). From there, they diverged into two routes; one to Northern Turkey and the other one to Western Turkey. The family of this study originates from Muğla, a city among the suggested settlement areas of Vikings, which supports the possible ancestral relationship (Al-Chalabi *et al.*, 1998).

6.3. Investigation of Mutations in Other ALS Genes

Recently, different genes have been defined as responsible for ALS (Table 1.1). Following the subcategorization of the Turkish ALS cohort, autosomal dominant cases as

well as nonconsanguineous familial and juvenile cases, who were negative for SOD1 mutations, were analyzed for possible mutations in the TDP-43, FUS and ANG genes.

No mutations were identified in any of the cases under study. Several SNPs have been detected some of which were novel (Tables 5.8, 5.10 and 5.11). The contribution of TDP-43, FUS and ANG to ALS genetics is a total of ~10 per cent of FALS cases. When nine AD cases are considered, the absence of a mutation was acceptable since the sample size was very small (Section 6.4).

Several evidences are present as to the low penetrance in ALS. Considering the literature-stated influence of susceptibility factors and environment in representation of disease phenotype as well as the observation of increase in penetrance in a FALS case within this study, a total of 13 nonconsanguineous FALS and juvenile cases were also considered for mutation screening in TDP-43, FUS and ANG. However, it is more likely that a mutation with low penetrance skips a generation in nonconsanguineous families with respect to consanguineous families; chances are fairly low in the latter; thus, consanguineous FALS and juvenile cases were eliminated. These genes have been related with autosomal dominant inheritance. Normally, FALS and juvenile cases within this study were represented recessively. Thus, the absence of any mutations in nonconsanguineous FALS and juvenile cases was not surprising.

In conclusion, the mutational analyses of TDP-43, FUS and ANG could not explain disease state in FALS, juvenile and autosomal dominant cases in the Turkish cohort under study, indicating new gene/genes as responsible.

6.4. The Discrimination of SALS and FALS Is Not Always Straightforward but Important For The Geneticist

Since the distinction between SALS and FALS patients is not always clear, in the framework of this study, several SALS patients have been referred to our center erroneously as sporadic (isolated) cases. However, it is important to discriminate between familial and sporadic ALS, to be able to properly counsel patients and to choose the correct molecular strategy. If it can be ascertained that no first and second degree relative has

(had) ALS, and both parents of the patient have become older than 75 years, the patient can be considered as sporadic. Some labs do not perform further testing at this stage any more. If the parents are younger than 75 years or have died at an earlier age, the patient should be more carefully inspected; especially, recessive inheritance in case of consanguineous parents should not escape attention. In general, in the framework of this thesis, also SALS patients were subjected to SOD1 analysis to exclude SOD1 mutations.

In familial cases, we first have tested for SOD1 mutations. If absent, TDP-43, FUS and angiogenin were screened for, but the yield of testing is generally low. It is of prime importance to explain in detail the significance of not finding a mutation in these genes to the patients and their families. In most instances, the patients and families conclude from the absence of a mutation in these genes that they do not have the disease at all, or they do not have its familial form, which is misleading (van Damme and Robberecht, 2009).

6.5. Whole Genome Genotyping of Familial and Juvenile ALS Cases in the Turkish Cohort

The whole genome analyses of Turkish familial and juvenile cases, who tested negative for SOD1, TDP-43, FUS and ANG, projected several regions with genomic variations. Among these, only three were within coding regions of the genome. However, these regions did not reveal any change in other affected individuals of the same families, thus they were considered insignificant and neglected.

Identification of genes in rare recessive diseases is very difficult because of the deficits in families with more than one affected individual. In this respect, homozygosity mapping has been a great tool, since even families with single affected individuals are informative. It is based on retrieving genomic information from inbred affected individuals for the identification of a region in the genome where they are all homozygous. The disease locus is expected to be highly linked to this homozygous region. These inbred individuals have probably inherited two identical by descent disease alleles from both their parents (Seelow *et al.*, 2009). Homozygosity mapping has a high power such that a single affected individual whose parents are first cousins provides the same power of linkage compared to a family with three affected sibs (Génin *et al.*, 1998). Starting from early 80s,

this approach has been used for the mapping of many rare recessive diseases, including Friedreich Ataxia with selective vitamin E deficiency on chromosome 8, Tunisian autosomal recessive Duchenne-like muscular dystrophy on chromosome 22 and several others (Hamida *et al.*, 1993; Othmane *et al.*, 1992).

Considering the advantages of homozygosity mapping, FALS and juvenile ALS cases were subjected to this analysis. To further narrow down the candidate regions, the same approach was performed on a recessive Turkish family with three affected sibs (ALS252, ALS256 and ALS257). This family was preselected as a proxy because: i. they belonged to a consanguineous family, ii. among six siblings, three had been diagnosed with probable ALS which is a high number in a recessive picture and iii. their ages of onset and symptoms were identical which is very rarely observed in ALS, where phenotype differs even within affected family members.

In the framework of this study, several homozygous regions were identified which pointed out new candidate genes within regions of interest. Although these regions included many genes, five were chosen as a start. While IL21, UCHL3 and USP53 were within homozygosity regions of all three siblings, and absent in controls, RAB27A and CPEB, were not within the detected regions. The two latter proteins were shown to be important players in ALS mouse models and *C. elegans* models (unpublished data, Art Horwich, Yale University Medical School). The proxy case, ALS256, was questioned for possible mutations in the candidate genes. However, no disease-causing mutations were identified in any of these genes.

At this point, the search for disease-related genes in these cases requires additional mutational analyses of new candidate genes which lie within the detected homozygosity regions.

Homozygosity mapping was also applied to patients ALS157 and ALS158, who were two brothers with juvenile onset and consanguinity. These regions may be compared with control samples and new candidate genes may be chosen for mutation analysis (Appendix K).

6.6. Whole Exome Resequencing

Today, the significance of genetic variants in the phenotypic representation of Mendelian and non-Mendelian diseases is undeniable. The genetic base of ~2,600 Mendelian diseases has been identified; most are caused by rare mutations which alter proteins' functions. This has been an important observation which encouraged the establishment of robust sequencing of coding regions, a newly-developed technology, named 'whole exome analysis'. As the name implies, the basic principle is sequencing only the exons within the genome. This has several advantages:

- Majority of variants has been shown to alter protein-coding sequences. In this respect, splice acceptor and donor sites have been included to this strategy.
- Unlike noncoding regions where variants exhibit neutral or weak effects, most of the rare nonsynonymous variants are believed to be deleterious. Thus, the exome includes a highly-enriched part of the genome with variants exhibiting large effects (Ng *et al.*, 2009).
- It is time-saving with respect to PCR-based methods, since it dramatically reduces the number of DNA sequencing which also reflects to cost-saving.
- It enables high specificity and sensitivity with capture design algorithm.
- Built-in control probes are used to achieve optimal performance.

Utilization of whole exome resequencing is especially more advantageous in rare autosomal recessive disorders because:

- Since they are autosomal recessive, the causative variants are unlikely to be present as SNPs in general population.
- Unlike autosomal dominant cases, only few genes in any affected individual have two or more rare nonsynonymous variants.

A successful application of whole exome resequencing in defining candidate genes involves the detection of coding variants in cases, followed by comparison of the new findings with genetic variation databases and utilization of control samples via the same approach for elimination of common variants (Figure 6.5).

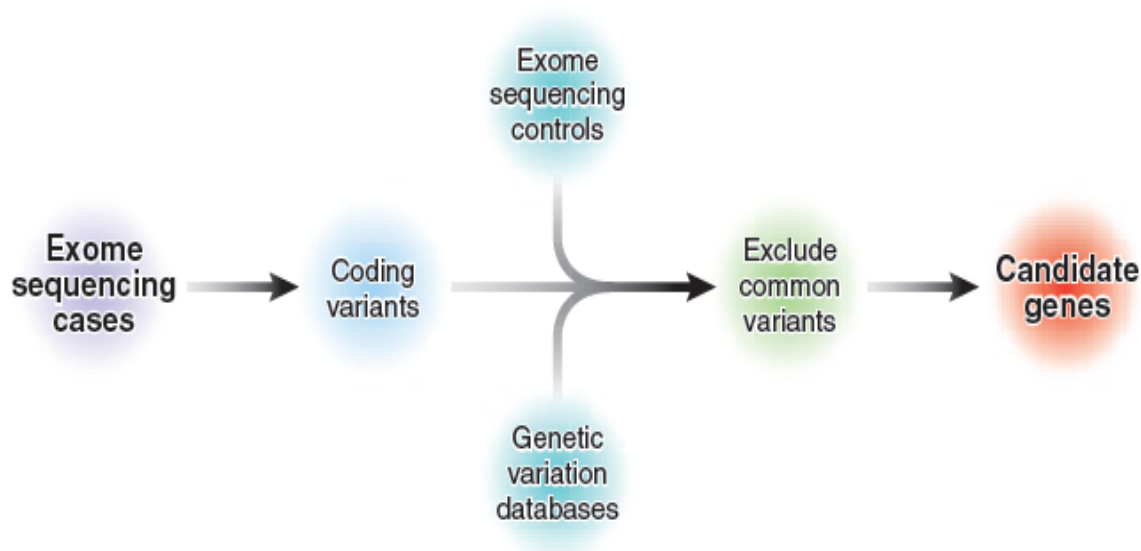


Figure 6.5. A stepwise approach from whole exome resequencing to determine possible candidate genes (Biesecker, 2010)

In the framework of this study, the same patient, ALS256, was assessed by both genotyping and whole exome sequencing. Thus, the candidate regions determined in genotyping were further narrowed down via comparison with the findings of the whole exome analysis.

In the genotyping analysis, very large segments of homozygosity regions are detected which include hundreds of genes. The researcher is supposed to make educated guess to continue with further investigation. In this study, candidate genes were selected according to brain expression levels or being suggested players in ALS pathogenesis. On the other hand, the results of the whole exome analysis pinpoints specific changes which emphasizes the advantages of this new technology in terms of its efficiency and specificity.

The whole exome analysis of our patient revealed 13 sequence changes located on chromosomes 4, 6, 18 and 22. Among these sequence changes, nine were also within the homozygous regions detected in the genotyping analysis of the same index case, which increased the importance of these regions.

Interestingly, ALS3, an autosomal dominant adult subtype of ALS, was linked to chromosome 18q21. However, no definite location has been identified yet. The genes

defined in whole exome analysis of the patient are all expressed in brain, some are even found in large quantities. Although the patient in this study seems to present an autosomal recessive inheritance pattern, the changes in genes identified via whole exome resequencing may actually be the gene that lies within the ALS3 locus. Thus, further analysis of these sequence variations may be important in the identification of ALS3 gene.

At this point, a further step should include the confirmation of detected changes by Sanger sequencing. Meanwhile, two other siblings should also be analyzed. If any of these changes are involved in ALS, they should also be present in all three siblings. If any change is shown to be significant in this family, then the same region should be investigated in control samples. Only then, the sequence variation can be stated as a mutation.

6.7. Genome-wide Association Study in Caucasian SALS Cases

The aetiology of ALS is multifactorial; there is a complex interplay between many pathological and genetic factors. The underlying cause of ALS remains unknown. Although the familial form comprises only 10 per cent of cases, SOD1, the major protein in FALS, is commonly used in genetic studies, basically due to the clinical and pathological similarities of SOD1-linked FALS and SALS. Identification of novel genes responsible for the remaining ALS cases may lead to a greater understanding of mechanisms of cell death in all forms of the disease.

6.7.1. Linkage Analysis

Linkage analysis is a conventional method used for the identification of genes in monogenic disorders which requires a precise genetic model, gene frequencies and penetrance of each genotype (Figure 6.6). Today, it serves as a way of gene-hunting and genetic testing. Many linkage analysis studies have been performed in ALS. Several genes/loci have been identified, some of which have been investigated within the framework of this study.

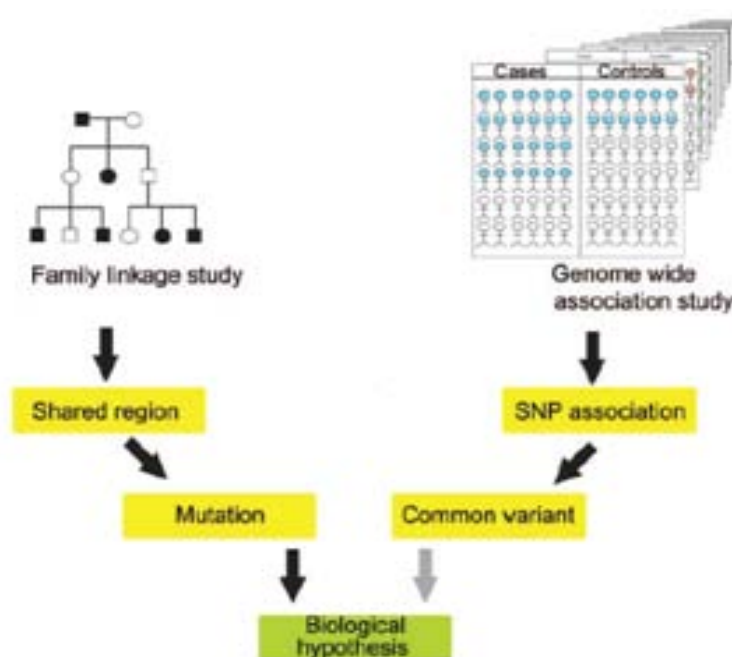


Figure 6.6. Schematic representation of different approaches used in the identification of new disease genes (adapted from Mullen *et al.*, 2009)

However, linkage is a specific genetic relationship between loci; it creates associations within families, but not among unrelated individuals. In this respect, the picture becomes more complicated in complex disorders, like ALS, where clinical picture differs between individuals with the same mutation or even between members of the same family. It is specifically hard to collect samples from multiple families where the same mutant gene is represented with overlapping phenotype. Also, the method is problematic and insufficient due to the: i. late onset and age-dependent penetrance of the disease, ii. relatively short survival of affected individuals and iii. difficulty of obtaining large pedigrees with several affected individuals (Strachan and Read, 1999). Meanwhile, in complex diseases, like ALS, the disease phenotype is believed to be the consequence of multiple different alleles of multiple genes in combination with environmental factors. Thus, since no single gene is concerned, conventional linkage approach is not effective (Mullen *et al.*, 2009).

6.7.2. Genome-wide Association Studies

In accordance, genome-wide association approach is highly favored, since this approach does not require the presence of many affected individuals from the same family

which is a great advantage for late-onset diseases, like ALS. It mainly depends on the idea that two unrelated individuals in the same population, who have the same disease allele, most probably inherited the disease from a common ancestor, so they probably share the same loci, close to this disease allele because of low recombination rates between close chromosomal regions. So, association study actually is a kind of linkage analysis in the population, considering individuals as part of a large family (Strachan and Read, 1999).

Association is simply a statistical statement about the co-occurrence of alleles and phenotypes. In this respect, association studies aim to identify a combination of mutations or polymorphisms that segregate with a certain gene and that cause changes in expression or function of that gene. While such changes do not reveal a disease phenotype on their own, co-occurrence with a mutation in the disease-related gene results in a disease phenotype. Such a phenomenon is named as susceptibility. These susceptibility genes may be of great importance in the explanation of phenotypic differences between patients with the same mutation or that of patients within the same family (Cardon *et al.*, 2001).

In ALS, usually, progression rate is linear for a given individual; however, it may vary greatly among different patients where a large spectrum from 1 year to >10 years may be observed. Such a diversity may be the result of a dosage effect, the 'relative potency of a specific underlying pathogenic factor' or disease-modifying factors. Thus, many association studies have been conducted in ALS in search of possible genes/modifier factors (Ravits *et al.*, 2009).

In a small number of SALS patients, a set of mutations in the NF-H gene was found (Table 6.1). Single cases have been reported with a mutation in EAAT2, cytochrome c and APEX nuclease genes (Hand *et al.*, 2002). Apo E has been studied as a candidate risk factor gene. While two groups have reported an increased risk of developing bulbar onset ALS in the presence of the Apo E4 allele, other groups were unable to confirm this result. Deletions in the SMN2 gene were shown to be more frequent in ALS patients with respect to controls. Furthermore, a mutation in leukemia inhibitory factor (LIF) has been reported in a set of ALS patients, but not in controls (Robberecht, 2000).

Table 6.1. Susceptibility and modifier genes in SALS (adapted from Özoğuz *et al.*, 2004).

Gene	Gene Name	Chromosomal Region	Possible Mechanism
NF-H	Neurofilament heavy chain	22q12.2	degradation of NF integrity
NF-L	Neurofilament light chain	8p21	degradation of NF integrity
PRPH	Peripherin	12q12-12	degradation of NF integrity
EAAT2	Glutamate transporter	11p13	decrease in expression
AMPA	Glutamate receptor	5p33	mistakes in RNA editing
APEX	Apurinic apirimidic endonuclease	14q11-12	decrease in enzyme level
CYP2D6	Cytochrome P450	22q13.1	polymorphic changes
COX1	Cytochrome C oxidase subunit-1	mtDNA	mutations
SOD2	Manganese superoxide dismutase	6q25	decrease in enzyme level
ApoE	Apolipoprotein E	19q13.2	E4 allele
CNTF	Ciliar neurotrophic factor	11q12.2	decrease in expression
SMN2	Survival motor neuron	5q13	decrease in copy number
LIF	Leukemia inhibitor factor	22q12	mutations
PSEN1	Presenillin-1	14q24.3	allele 2
VEGF	Vascular endothelial growth factor	6p12	promotor polymorphisms
HFE	Hfe (Hemachromatose protein)	6p21.3	mutations

Following the completion of the Human Genome Project, the most intriguing topic has been the investigation of i. functions, regulations and interactions of different genes and their roles in cellular processes and ii. variations in gene expression in different cell types in health and disease states. In this respect, the most attractive approach has been microarray technology which enables the analysis of the expression of many genes in a single experiment quickly and efficiently.

6.7.3. Gene Expression Analysis

Three studies have been published, regarding the use of gene expression microarray technology in ALS. The first paper published in this manner by Yoshihara used cDNA microarray to monitor 'differential expression of inflammation- and apoptosis-related genes in spinal cords of a mutant SOD1 transgenic mouse model of familial amyotrophic lateral sclerosis' (Yoshihara *et al.*, 2002). The results revealed an up-regulation of genes involved in both of these pathways in the presymptomatic stage prior to motor neuron death, suggesting the involvement of inflammatory response as an important component. In 2003, Dangond *et al.* used oligonucleotide-microarray system to determine the

expression level of ~6800 genes from postmortem spinal cord gray matter in ALS patients and controls (Dangond *et al.*, 2004). Alterations in genes involved in mitochondrial function, oxidative stress, excitotoxicity and apoptosis were shown which were important findings since these are the basic proposed mechanisms in ALS pathology. The third study investigated the gene expression profiles of degenerating spinal motor neurons obtained from autopsies of SALS patients. In concordance with the first study, there was a significant up-regulation in the expression of genes associated with cell death activation and a distinct down-regulation in the expression of genes associated with cell death inhibition (Jiang *et al.*, 2005). Overall, these results may be of great importance in determining the genes leading to neurodegeneration and neuronal death.

An interesting study by Strunk *et al.* had focused on the possible mechanisms to explain variable phenotypes in *Egfr^{tm1Mag}* homozygous embryos (Strunk *et al.*, 2004) Via the microarray system, it was shown that the variation was due to the action of the modifier genes. It would be interesting to use the same system in ALS since even patients of the same family with the same SOD1 mutation can exhibit significant phenotypic differences (Siddique *et al.*, 1996). SNPs detected in association studies can be questioned using oligonucleotide chips. The frequency of each SNP can be calculated for both patients and controls. Statistically significant values would point out SNPs that may be important as modifiers.

6.7.4. The Effect of Reduced Expression of KIFAP3 On Survival In SALS Patients

In this respect, this study has been a contributor to a large collaborative study where Caucasian SALS cases were investigated for possible variants that modified susceptibility, age of onset, site of onset and survival of the disease. The initial part of the genome-wide association study performed by Landers *et al.* had identified candidate SNPs. Within the framework of this thesis, KIFAP3, B4GALT6 and ADAMTS17, which exhibited suspected effects on survival, susceptibility and age of onset, respectively, were questioned for possible changes in the expression levels. Among these, only rs1541160, located in intron 8 of the KIFAP3 gene, displayed a significant advantage of CC homozygotes in survival of about 14 months when compared to TT homozygotes. While no variation in KIFAP3 sequence was detected in any of CC or TT homozygotes, expression studies

revealed that the positive effect on survival was related to reduced levels of expression of CC homozygotes with respect to TT homozygotes. These findings were further confirmed by Western blot analysis.

6.7.4.1. The parameters that provided success in this GWA study. The success of this study depends on several powers which overcome the burdens of GWA studies. First of all, for the detection of a true association, a minimum of 250 case-controls are necessary; otherwise small sample size would lead to false-negative results because of reduced statistical power. It has been proven that while a study of 1000 cases and 1000 controls provide 1 per cent power in the identification of a variant with a risk impact of 1.3, this value increases up to 98 per cent when 5000 cases and 5000 controls are involved. This study employed ~1400 ALS cases and ~1800 controls which increased the efficiency.

The second handicap in GWA analysis is differences in genetic contributions to the disease in sample group. In this respect, it is important to study cases which have been precisely defined with clinical examination. The phenomenon, named as population stratification, defines the presence of differences in allele frequencies of subgroups in the same population. Different ethnic groups may carry different allele frequencies as a result of natural selection, migration patterns and random effects, like natural disasters. In this respect, a false-positive association can be defined, if the control groups are not chosen from the same ethnic origin. This study has overcome this burden by employing European Caucasians SALS cases and matching controls. Also, several other evidences were indicative of the absence of stratification effects for rs1541160. These were:

- When analyzed individually, it revealed a significant P value in all populations, but Atlanta, which had the lowest sample size (n:90) (Appendix J).
- For quality control, a sensitivity analysis was performed, where each of the four populations were eliminated in each equation. If a single population was to have an overall impact on the occurrence of significance, then its elimination would be expected to give an insignificant value. However, it was consistently significant in all.

- Hardy-Weinberg testing was performed which exhibited rs1541160 as in equilibrium in each population under study. Also, the population allele frequencies were similar which further confirmed the reliability of the result.

6.7.4.2. KIFAP3 in axonal transport. The involvement of axonal transport due to motor protein defects has been detected in several neuropathies, like distal spinobulbar muscular atrophy, hereditary spastic paraplegia and Charcot-Marie Tooth, where mutations occur in p150glued subunit of dynactin, KIF5A and KIF1B β , respectively. Since disruption of axonal caliber and perturbations of axonal transport have been suggested among possible mechanisms in ALS, the involvement of KIAP3 becomes more valid (Magrané *et al.*, 2009).

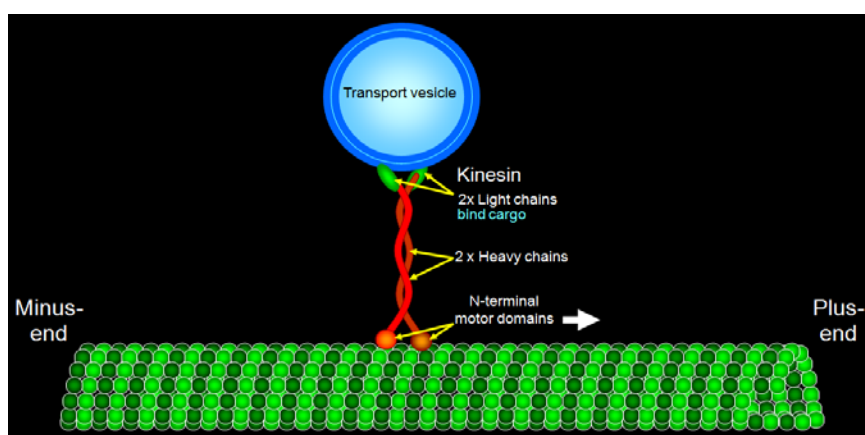


Figure 6.7. Kinesin and representation of anterograde transport (www.biology.utah.edu)

Kinesins are motor proteins which are involved in intracellular transport (Figure 6.7). They transport cargo along microtubules while utilizing ATP to establish conformational changes that generate motile force (Hirokawa *et al.*, 2008). Kinesin superfamily has been categorized into 15 groups according to their phylogenetic analysis (Miki *et al.*, 2001). Among these, the kinesin II complex is composed of the interaction of KIF3A with KIF3B or KIF3C. KIFAP3 is a motor protein which forms a trimeric motor complex with KIF3A and KIF3B. This complex plays a role in axonal elongation, an essential process in brain wiring (Yamazaki *et al.*, 1996, Hirokawa *et al.*, 2000). The 40-amino acid repeat region on KIFAP3 interacts with the tail domains of KIF3 and its cargos. KIF3 is mostly responsible for the transport of fodrin-associated vesicles. These vesicles

may bear necessary plasma membrane components for tips of neurites (Takeda *et al.*, 2000).

In accordance with the study that this thesis had been a part of, a recent study by Pantelidou *et al.* demonstrated that there was no significant downregulation of KIF3A in cortex of SALS cases. However, the upregulation of KIFAP3 was an early event both in human brain samples (Pantelidou *et al.*, 2007) and transgenic mouse models (Dupuis *et al.*, 2000). Also, in a SOD1-mutant mice model, Tateno *et al.* showed a reduction in the transport of choline acetyltransferase in motor axons at the pre-onset stage. Such a reduction was correlated with misfolded mutant SOD1. Moreover, this burden was overcome by the overexpression of KIFAP3, indicating that mutant SOD1 sequestered KIFAP3 in aggregates and defects in ChAT transport was crucial in the dysfunction of ALS (Tateno *et al.*, 2009).

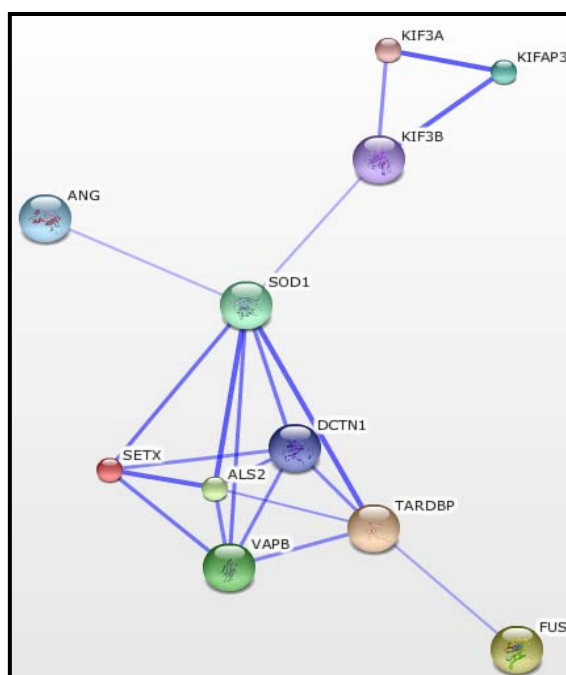


Figure 6.8. Schematic representation of protein interactions of KIFAP3 and ALS genes
(www.string.embl.de)

However, the mechanisms underlying these consequences are unclear, since there is no direct interaction of KIFAP3 with SOD1 or any other previously defined ALS genes (Figure 6.8). Since 14-month advantage in survival cannot be underestimated in a disease, where the mean survival is ~3-5 years and only a few susceptibility factors have been

identified, the next aim should be the identification of underlying mechanisms. Only then, an effective approach can be established for drug therapy.

6.8. Concluding Remarks

In the framework of this study, the molecular genetics of FALS and SALS was investigated from both overlapping and differing perspectives. Besides DNA sequencing analysis for several previously defined ALS genes, three recent approaches in molecular genetics were conducted for the identification of new ALS genes. Among these, the genotyping study, performed on familial and juvenile Turkish ALS cases, could not define a new gene/locus, mainly due to its small sample size. As the sample size increases, the overlapping homozygosity regions will be narrowed down. This will decrease the number of genes within the candidate regions. Thus, rather than making educated guess from hundreds of genes, there will be less to choose among. In this respect, a further step in the genotyping approach should be employing more familial cases; consanguineous families would be more useful. This will definitely enhance the chance of pinpointing new genes in ALS.

This is the first study in an ALS cohort which utilized the whole exome resequencing for the identification of new ALS genes. In a more generalized manner, there are only three publications reporting the identification of new genes with this methodology (Choi *et al.*, 2009, Horswell *et al.*, 2009, Ng *et al.*, 2009). Thus, this study is also important in being among one of the first publications including the utilization of this methodology. The detected specific variations, which should be tested for further confirmation, point out the advanced specificity and efficiency of this method. In near future, this approach is expected to replace many methods in search of new genes due to its highly computerized system and widespectrum search.

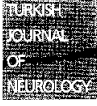
GWA study in Caucasian SALS cases aimed to identify variants which would influence phenotype (age of onset, site of onset, survival and susceptibility). Much has been expected from the genotyping and GWA approaches as to 'unlock' the mystery of many complex diseases. Although they have been improved greatly, thus far they have succeeded in the identification of different common variants associated with only 20 per

cent of diseases in total, due to the reasons mentioned above. In this respect, the defined variant is precious. The result should be evaluated for the possible effect mechanism which may lead to a therapeutic strategy.

To the best of our knowledge, this is the largest, if not the single molecular study investigating the molecular pathology of ALS in Turkey. It is the first attempt to gain insights into ALS pathogenesis through genetic and high-throughput genomic investigations of Turkish ALS patients. We hope that in this context, this thesis will contribute to the establishment of high-throughput methodologies described in this study in Turkey, and to the understanding of the complex pathology of ALS. This will hopefully pave the ways for the long-awaited molecular therapies in ALS.

APPENDIX A: PRODUCTS OF THIS THESIS

T Ü R K
N Ö R O L O J İ
D E R G İ S İ



Nörolojide Genetik / *Genetics in Neurology*

Türk Nöroloji Dergisi 2005; Cilt:11 Sayı:2 Sayfa:1-20

Amiyotrofik Lateral Skleroz'un Moleküler Biyolojisi / *Molecular Biology of Amyotrophic Lateral Sclerosis*

Aslıhan Özoğuz, R. Mine Güzel, A. Nazlı Başak
Boğaziçi Üniversitesi Moleküler Biyoloji ve Genetik Bölümü, İSTANBUL

ÖZET
Amiyotrofik Lateral Skleroz'un Moleküler Biyolojisi adlı derleme yazısı üç ana bölümden oluşmaktadır.
Birinci bölümde Amiyotrofik Lateral Skleroz'un (ALS) tarihçesi, kliniği ve genetiği tartışılmıştır. Amiyotrofik Lateral Skleroz hastalığı ailesel ve sporadik olmak üzere iki büyük gruba ayrılır. Ailesel ALS'de, hem dominant, hem resesif geçiş görülür. Burada tanımlanan genlere ilaveten özellikle sporadik ALS'de de rol oynadığı düşünülen yatkınlık genleri vardır. ALS araştırmalarında önemli bir dönüm noktası, genetik geçişli ALS olgularının %20'sine Süperoksit Dismutaz1 (SOD1) genindeki mutasyonların neden olduğunun anlaşılmasıdır. Ailesel ALS ve Sporadik ALS klinik ve patolojik özellikleri açısından benzerlik gösterdiği için, ALS patogeneziye yönelik çalışmalar, hastalıkta çok önemli bir rol oynadığı bilinen SOD1 proteini ve patolojisi üzerine yoğunlaşmıştır.
İkinci bölümde SOD1 geni ve proteini üzerine yapılan çalışmalar ve özellikle de moleküler patogenezdaki olası mekanizmalar açıklanmıştır.
Üçüncü bölümde ise, ALS araştırmalarındaki güncel durum tartışılmıştır.
Özet olarak, ALS'de tedavi olanakları halen genetik ve patogenez mekanizmalardaki ilerlemeye oranla her ne kadar geri kalmışsa da, RNA Interference ve kök hücre gibi son gelişmeler iyimser olma nedenleridir.

ABSTRACT
Molecular Biology of Amyotrophic Lateral Sclerosis
This review paper on the Molecular Biology of Amyotrophic Lateral Sclerosis consists of three main parts.
In the first part, history, clinical features and genetics of ALS have been discussed. ALS can be considered under two main groups: familial and sporadic ALS. Familial ALS, in turn, is classified into two main groups according to its inheritance pattern, dominant FALS and recessive FALS. In addition to the genes which give rise to FALS, also in SALS patients, several genes have been identified. A landmark discovery in ALS research is the identification of mutations in the Superoxide Dismutase1 (SOD1) gene as the primary cause of 20% of instances of familial ALS. Since FALS and SALS are clinically indistinguishable and pathologically very similar, research on the molecular pathogenesis of ALS has concentrated on the SOD1 protein and its pathology.
In the second part of this review, research on SOD1 gene and protein has been compiled, with a special emphasis on the possible mechanisms playing a role in the molecular pathogenesis.
In the third part of this review, state-of-the-art research on ALS has been discussed.
In summary, although therapy development is currently lagging behind the elucidation of the genetic and pathogenic mechanisms involved in ALS, there is enough reason to be optimistic. RNA Interference and stem cell research are promising new approaches in the creation of effective therapies for ALS.

Anahtar Kelimeler: ALS, SOD1 geni, SOD1 proteini, moleküler patogenez

Keywords: ALS, SOD1 gene, SOD1 protein, molecular pathogenesis

Figure A.1. Review article on the genetics of ALS

Reduced expression of the *Kinesin-Associated Protein 3 (KIFAP3)* gene increases survival in sporadic amyotrophic lateral sclerosis

John E. Landers^{a,1}, Judith Melki^{b,2}, Vincent Meininger^c, Jonathan D. Glass^d, Leonard H. van den Berg^e, Michael A. van Es^f, Peter C. Sapp^{g,1}, Paul W. J. van Vught^h, Diane M. McKenna-Yasekⁱ, Hylke M. Blauw^j, Ting-Jan Cho^k, Meraida Polak^l, Lijia Shi^m, Anne-Marie Willsⁿ, Wendy J. Broom^o, Nicola Ticozzi^{p,q}, Vincenzo Silani^r, Aslihan Ozoguz^h, Ildefonso Rodriguez-Leyva^s, Jan H. Veldink^t, Adrian J. Ivinson^u, Christiaan G. J. Saris^v, Betsy A. Hosler^w, Alayna Barnes-Nessa^x, Nicole Couture^y, John H. J. Wokke^z, Thomas J. Kwiatkowski, Jr.^{aa}, Roel A. Ophoff^{ab}, Simon Cronin^{ac}, Orla Hardiman^{ad}, Frank P. Diekstra^{ae}, P. Nigel Leigh^{af}, Christopher E. Shaw^{ag}, Claire L. Simpson^{ah}, Valerie K. Hansen^{ai}, John F. Powell^{aj}, Philippe Corcia^{ak}, François Salachas^{al}, Simon Heath^{am}, Pilar Galan^{an}, Franck Georges^{ao}, H. Robert Horvitz^{ap}, Mark Lathrop^{aq}, Shaun Purcell^{ar}, Ammar Al-Chalabi^{as}, and Robert H. Brown, Jr.^{at,1,3}

^aCecil B. Day Neuromuscular Research Laboratory, Massachusetts General Hospital-East, Building 114, Navy Yard, Charlestown, MA 02129; ^bLaboratoire de Neurogénétiq ue Moléculaire, Institut National de la Santé et de la Recherche Médicale U-798, Université d'Evry et Paris 11, 2 rue Gaston Crémieux, CP5724, 91057 Evry France; ^cFédération des maladies du système nerveux, Assistance Publique—Hôpitaux de Paris, Hôpital de la Salpêtrière, 75651 Paris, France; ^dDepartment of Neurology, Emory University, Atlanta, GA 30322; Departments of ^eNeurology and ^fMedical Genetics, Rudolf Magnus Institute of Neuroscience, University Medical Center Utrecht, 3584 CK, Utrecht, The Netherlands; ^gHoward Hughes Medical Institute, Department of Biology, Massachusetts Institute of Technology, Cambridge, MA 02139; ^hDepartment of Neurology and Laboratory of Neuroscience, 'Dino Ferrari' Center, University of Milan Medical School—Istituto Di Ricovero e Cura a Carattere Scientifico Istituto Auxologico Italiano, 20149 Milan, Italy; ⁱDepartment of Molecular Biology and Genetics, Neurodegeneration Research Laboratory, Bogazici University, Istanbul, Turkey; ^jFaculty of Medicine, Universidad Autonoma de San Luis Potosí, San Luis Potosí, México S.L.P., CP 78210; ^kHarvard NeuroDiscovery Center, Harvard Medical School, Boston, MA 02115; ^lNeuropyschiatric Institute, University of California, Los Angeles; ^mDepartment of Neurology, Beaumont Hospital, Dublin 9, Ireland; ⁿMedical Research Council Centre for Neurodegeneration Research, Department of Clinical Neuroscience, PO43, Institute of Psychiatry, King's College London, London SE5 8AF, United Kingdom; ^oService de Neurologie, Centre Hospitalier Universitaire Bretonneau, 37044 Tours, France; ^pCentre National de Génotypage, Institut Génomique, Commissariat à l'Énergie Atomique, 91057 Evry, France; ^qUnité de Recherche en Épidémiologie Nutritionnelle, l'UFV Santé/Médecine et Biologie Humaine, 74 rue Marcel Cachin, 93017 Bobigny, France; and ^rCenter for Human Genetics Research, Massachusetts General Hospital, Richard B. Stulman Research Building, CP2N-6254, 185 Cambridge Street, Boston, MA 02114

Edited by David E. Housman, Massachusetts Institute of Technology, Cambridge, MA, and approved April 1, 2009 (received for review December 22, 2008)

Amyotrophic lateral sclerosis is a degenerative disorder of motor neurons that typically develops in the 6th decade and is uniformly fatal, usually within 5 years. To identify genetic variants associated with susceptibility and phenotypes in sporadic ALS, we performed a genome-wide SNP analysis in sporadic ALS cases and controls. A total of 288,357 SNPs were screened in a set of 1,821 sporadic ALS cases and 2,258 controls from the U.S. and Europe. Survival analysis was performed using 1,014 deceased sporadic cases. Top results for susceptibility were further screened in an independent sample set of 538 ALS cases and 556 controls. SNP rs1541160 within the *KIFAP3* gene (encoding a kinesin-associated protein) yielded a genome-wide significant result ($P = 1.84 \times 10^{-9}$) that withstood Bonferroni correction for association with survival. Homozygosity for the favorable allele (CC) conferred a 14.0 months survival advantage. Sequence, genotypic and functional analyses revealed that there is linkage disequilibrium between rs1541160 and SNP rs522444 within the *KIFAP3* promoter and that the favorable alleles of rs1541160 and rs522444 correlate with reduced *KIFAP3* expression. No SNPs were associated with risk of sporadic ALS, site of onset, or age of onset. We have identified a variant within the *KIFAP3* gene that is associated with decreased *KIFAP3* expression and increased survival in sporadic ALS. These findings support the view that genetic factors modify phenotypes in this disease and that cellular motor proteins are determinants of motor neuron viability.

genome-wide association study | single nucleotide polymorphism

Amyotrophic lateral sclerosis (ALS) is an age-dependent, degenerative disorder of motor neurons (1) that typically develops in the 6th decade and is uniformly fatal, usually within 5 years (2). Approximately 10% of ALS cases are dominantly inherited (3); 20% of these are caused by mutations in the gene encoding copper/zinc superoxide dismutase 1 (*SOD1*) (4); mutations in the *TARDBP* gene (5, 6) account for ~5% of cases. Rare familial cases arise from mutations in genes encoding the vesicle-associated membrane associated protein B (7), alsin (a RAB5-guanine nu-

cleotide exchange factor) (8, 9), senataxin (10) or dynactin (11). Recently, we reported that ~5% of familial ALS cases are due to mutations in the *FUS/TLS* gene (12, 13) whose product binds DNA and RNA, as does *TARDBP*. The cause of sporadic ALS is thought to be multifactorial, with environmental, infectious and genetic etiologies. Reported associations with variants in diverse genes (14–25) have proven difficult to replicate. Advances in the technology for large-scale genotyping of single nucleotide polymorphisms (SNPs) have facilitated unbiased, genome-wide association studies. Examples include the identification of IL2RA and IL7RA variants as risk factors for multiple sclerosis (26–28) and the recent reports of 6 new gene regions associated with type 2 diabetes (29–35). To test the hypothesis that commonly occurring genetic

Author contributions: J.E.L., J.M., V.M., J.D.G., L.H.v.d.B., M.A.v.E., P.C.S., P.W.J.v.V., D.M.M.-Y., H.M.B., T.-J.C., M.P., L.S., A.-M.W., W.J.B., N.T., V.S., A.O., I.R.-L., J.H.V., A.J.I., C.G.J.S., B.A.H., J.H.J.W., R.A.O., S.C., O.H., F.P.D., P.N.L., C.E.S., C.L.S., V.K.H., J.F.P., P.C., S.H., P.G., F.G., H.R.H., M.L., S.P., A.A.-C., and R.H.B. designed research; J.E.L., M.A.v.E., P.C.S., P.W.J.v.V., D.M.M.-Y., H.M.B., T.-J.C., M.P., L.S., A.-M.W., W.J.B., N.T., V.S., A.O., I.R.-L., J.H.V., C.G.J.S., B.A.H., A.B.-N., N.C., T.J.K., R.A.O., S.C., O.H., F.P.D., C.L.S., V.K.H., J.F.P., P.C., F.S., S.H., P.G., F.G., H.R.H., M.L., S.P., A.A.-C., and R.H.B. performed research; J.M., V.M., J.D.G., L.H.v.d.B., W.J.B., I.R.-L., A.J.I., P.N.L., C.E.S., J.F.P., S.P., A.A.-C., and R.H.B. contributed new reagents/analytic tools; J.E.L., J.M., V.M., L.H.v.d.B., M.A.v.E., P.C.S., P.W.J.v.V., D.M.M.-Y., H.M.B., T.-J.C., M.P., L.S., A.-M.W., W.J.B., N.T., V.S., A.O., I.R.-L., J.H.V., C.G.J.S., B.A.H., A.B.-N., N.C., J.H.J.W., T.J.K., R.A.O., S.C., O.H., F.P.D., P.N.L., C.E.S., C.L.S., V.K.H., J.F.P., P.C., F.S., S.H., P.G., F.G., H.R.H., M.L., S.P., A.A.-C., and R.H.B. analyzed data; and J.E.L., S.P., A.A.-C., and R.H.B. wrote the paper.

The authors declare no conflict of interest.

This article is a PNAS Direct Submission.

Freely available online through the PNAS open access option.

To whom correspondence should be addressed at the present address: Department of Neurology, University of Massachusetts Medical School, Worcester, MA 01605. E-mail: john.landiers@umassmed.edu.

¹Present address: Department of Human Genetics, Hadassah University Hospital, P.O. Box 12000, 91120 Jerusalem, Israel.

²A.A.-C. and R.H.B. contributed equally to this work.

This article contains supporting information online at www.pnas.org/cgi/content/full/0812937106/DCSupplemental.

Figure A.2. Research article on a collaborative GWA study of Caucasian SALS cases by Landers *et al.*, PNAS, Vol. 106, No. 22, pp. 9004-9009. The contribution of this thesis includes work performed in Cecil Day Laboratory

APPENDIX B: PATIENT REGISTRY FORM FOR ALS

ALS HASTA BİLGİLERİ

Adı / Soyadı :

Cinsiyeti :

Doğum yılı / yeri :

Hastalık başlangıç yaşı / yılı :

Hastalığın başlangıç bölgesi : (ilk belirtiler nerede görüldü?)

Bulbar Kol Bacak

Son klinik bulgular :

Bulbar tutulum

Kolda tutulum

Bacakta tutulum

Tipik klinik var yok

Baska hastalık olabilir evet hayır

Aile Öyküsü (aile ağacı) :

Akraba evliliği :

Özgeçmiş (hastalık, travma, toksinler,vs):

Adres / telefon :

Gönderen Doktor / Klinik :

Telefon / Fax :

E-mail :

**APPENDIX C: REVISED EL ESCORIAL CRITERIA
FOR ALS DIAGNOSIS**

Table C. El Escorial criteria used for the diagnosis of ALS

Clinically Definite ALS	Evidence of UMN plus LMN signs in the bulbar region and in at least two spinal region, or
	The presence of UMN signs in two spinal regions and LMN signs in three spinal regions
Clinically Probable ALS	Evidence of UMN plus LMN signs in at least two regions with some UMN signs rostral to LMN signs
Probable, laboratory supported ALS	Clinical evidence of UMN and LMN signs in only one region, or
	UMN signs alone in one region and LMN signs defined by EMG criteria in at least two muscles of different root and nerve origin in two limbs
Possible ALS	UMN plus LMN in only one region,
	UMN signs alone in two or more regions, or
	LMN signs found alone to rostral to UMN signs

APPENDIX D: IMBREEDING COEFFICIENCIES OF TURKISH FALS AND JUVENILE CASES

Table D. Inbreeding coefficient results of FALS and juvenile cases.

Bold are revised according to testing results

ALS ID	Inbreeding Coefficient	Consanguineous
ALS133	0.1426	yes
ALS85	0.01011	no
ALS86	0.01103	no
ALS49	0.07037	yes
ALS157	0.06536	yes
ALS158	0.07189	yes
ALS227	0.0002633	no
ALS46	0.1359	yes
ALS97	- 0.01515	no
ALS135	0.007394	no
ALS68	0.08477	yes
ALS41	-0.003509	no
ALS96	0.089	yes
ALS173	-0.01142	no
ALS174	-0.009857	no
ALS189	-0.007787	no
ALS202	-0.0002427	no
ALS223	0.02124	yes
ALS252	0.08403	yes
ALS257	0.06218	yes
ALS256	0.1114	yes
ALS244	-0.01092	no
ALS175	0.0637	yes
ALS178	0.003622	no
ALS150	0.09264	yes
ALS155	0.1114	yes
ALS167	0.03435	yes

**APPENDIX E: REGIONS OF HOMOZYGOSITY IN FALS,
JUVENILE ALS CASES AND CONTROLS**

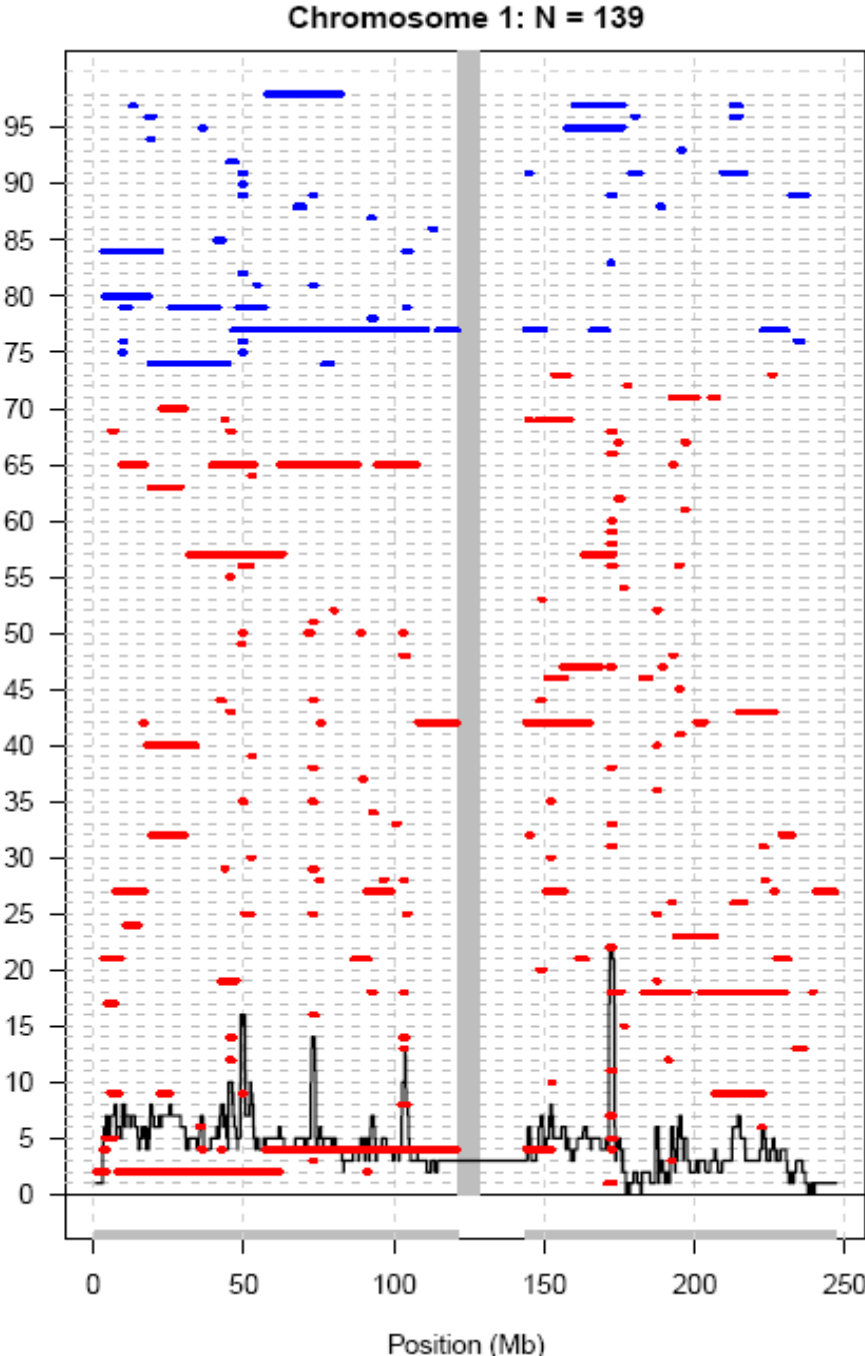


Figure E.1. Homozygous regions in chromosome 1 for FALS, juvenile cases and controls

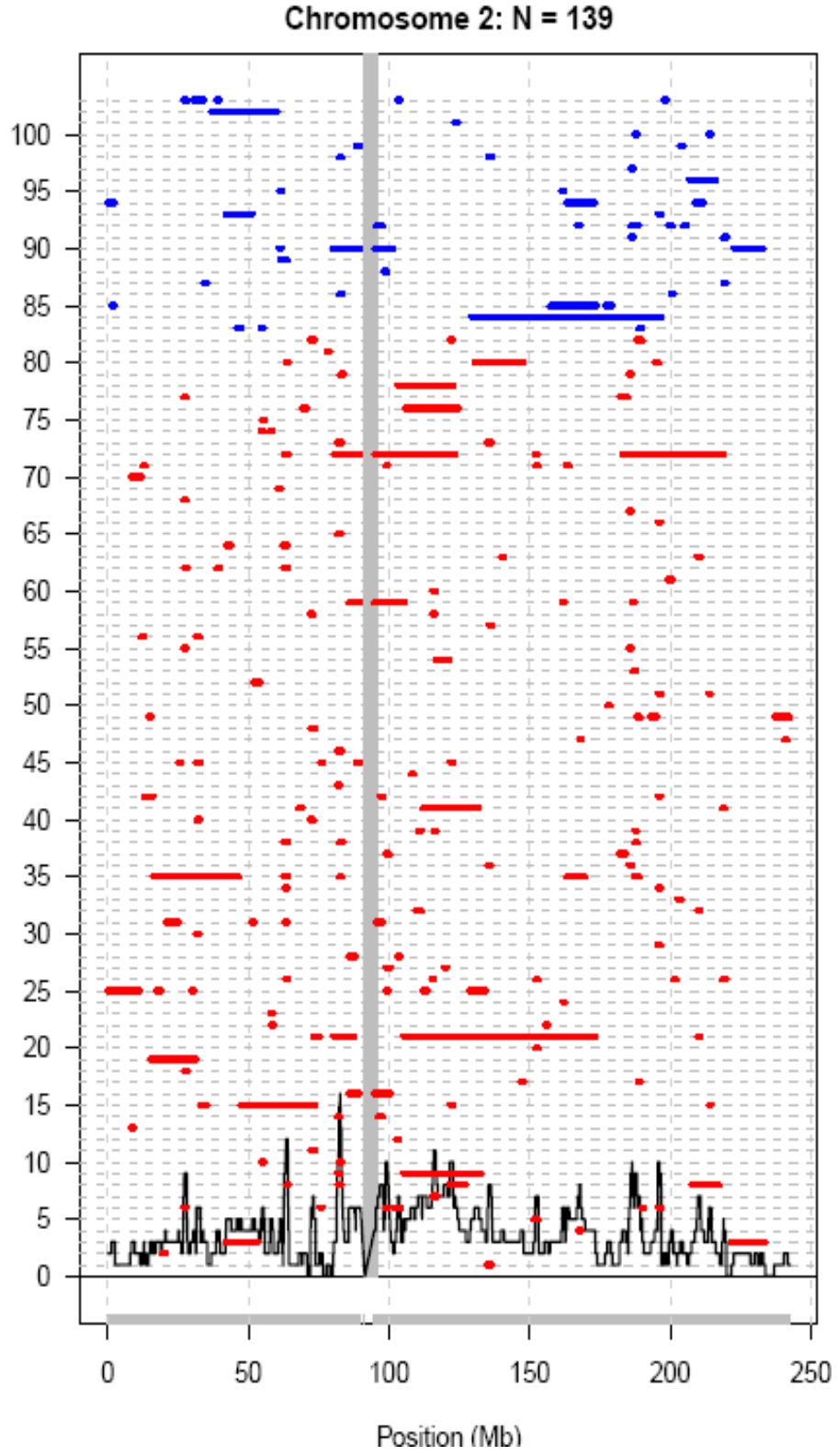


Figure E.2. Homozygous regions in chromosome 2 for FALS, juvenile cases and controls

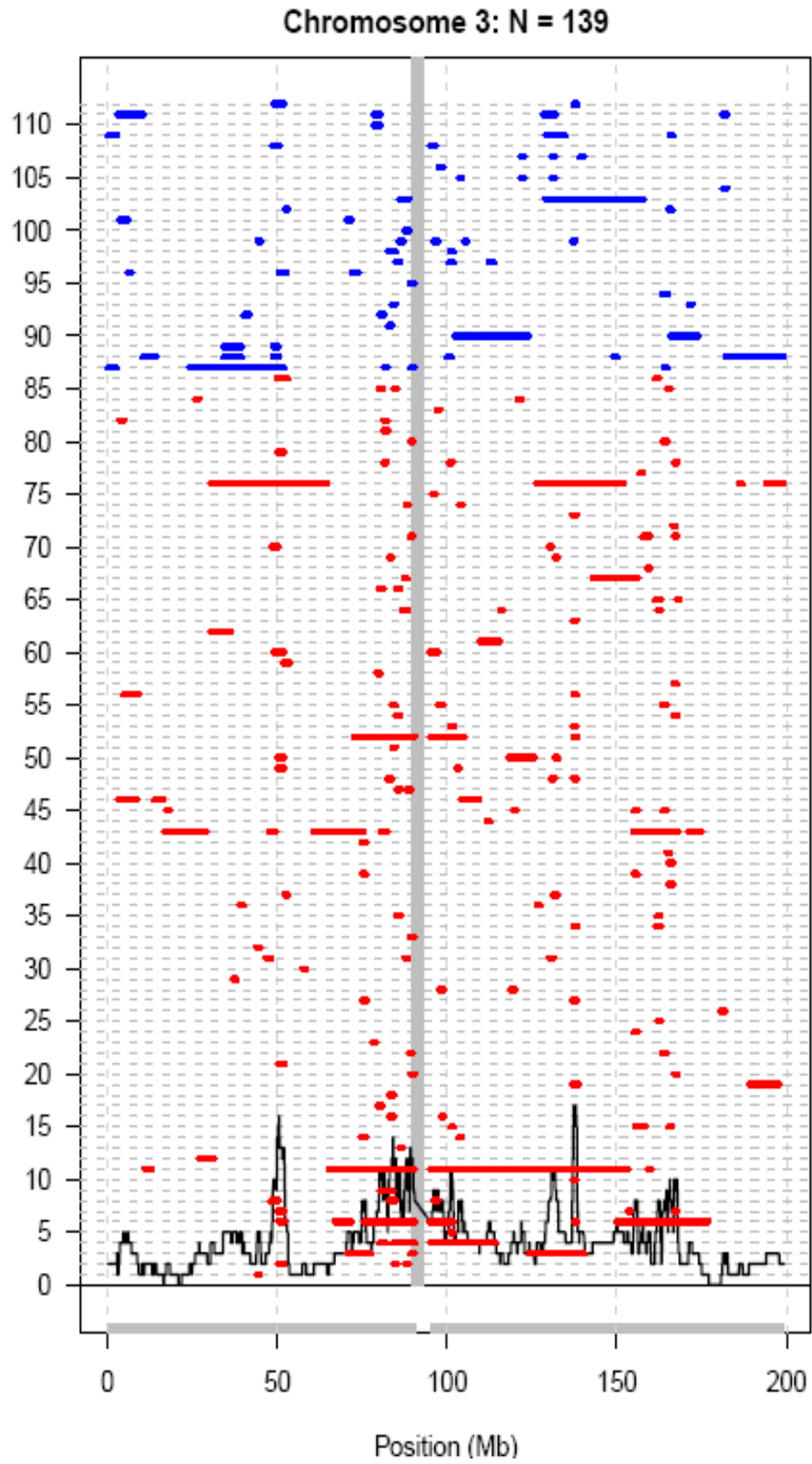


Figure E.3. Homozygous regions in chromosome 3 for FALS, juvenile cases and controls

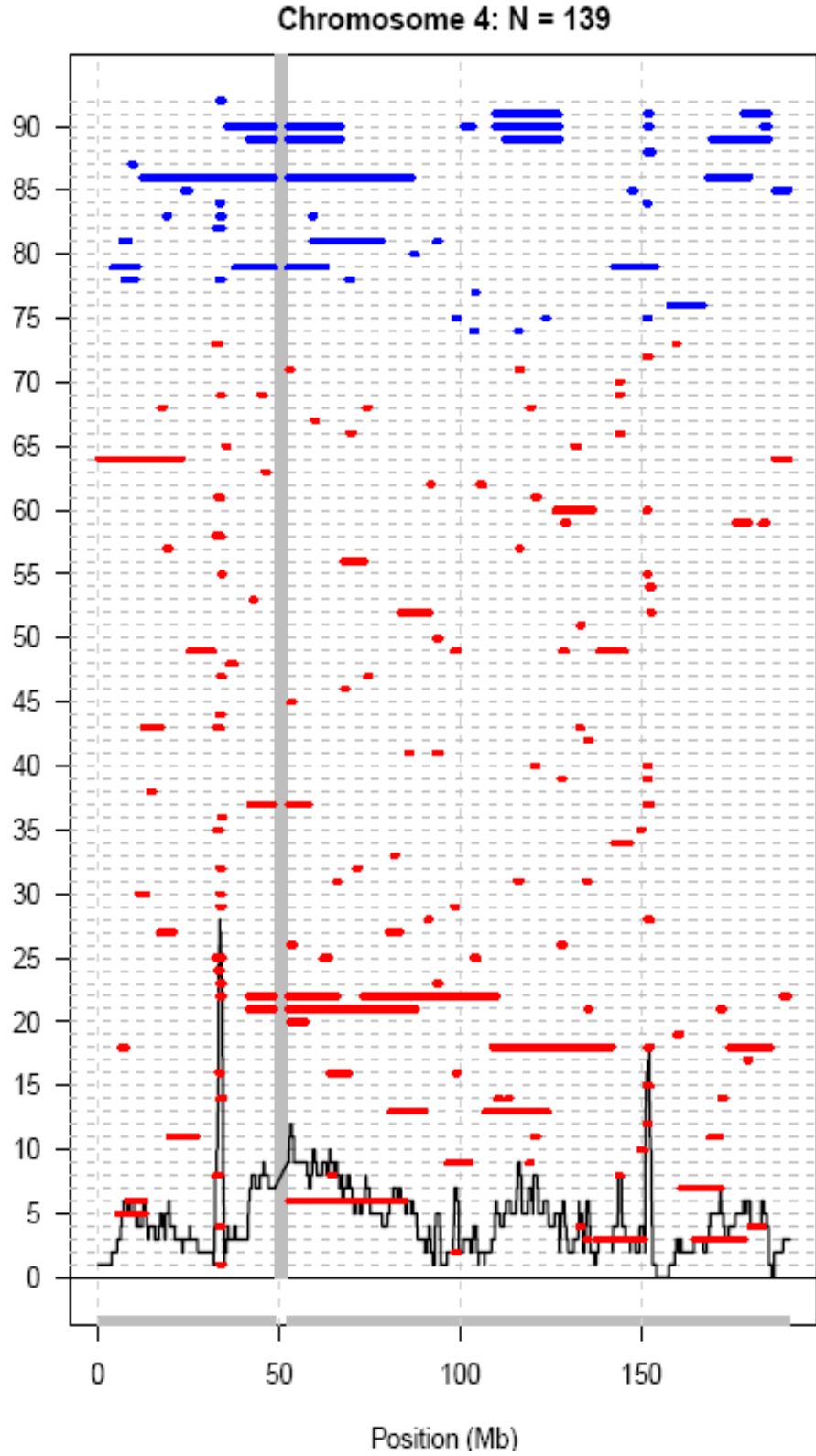


Figure E.4. Homozygous regions in chromosome 4 for FALS, juvenile cases and controls

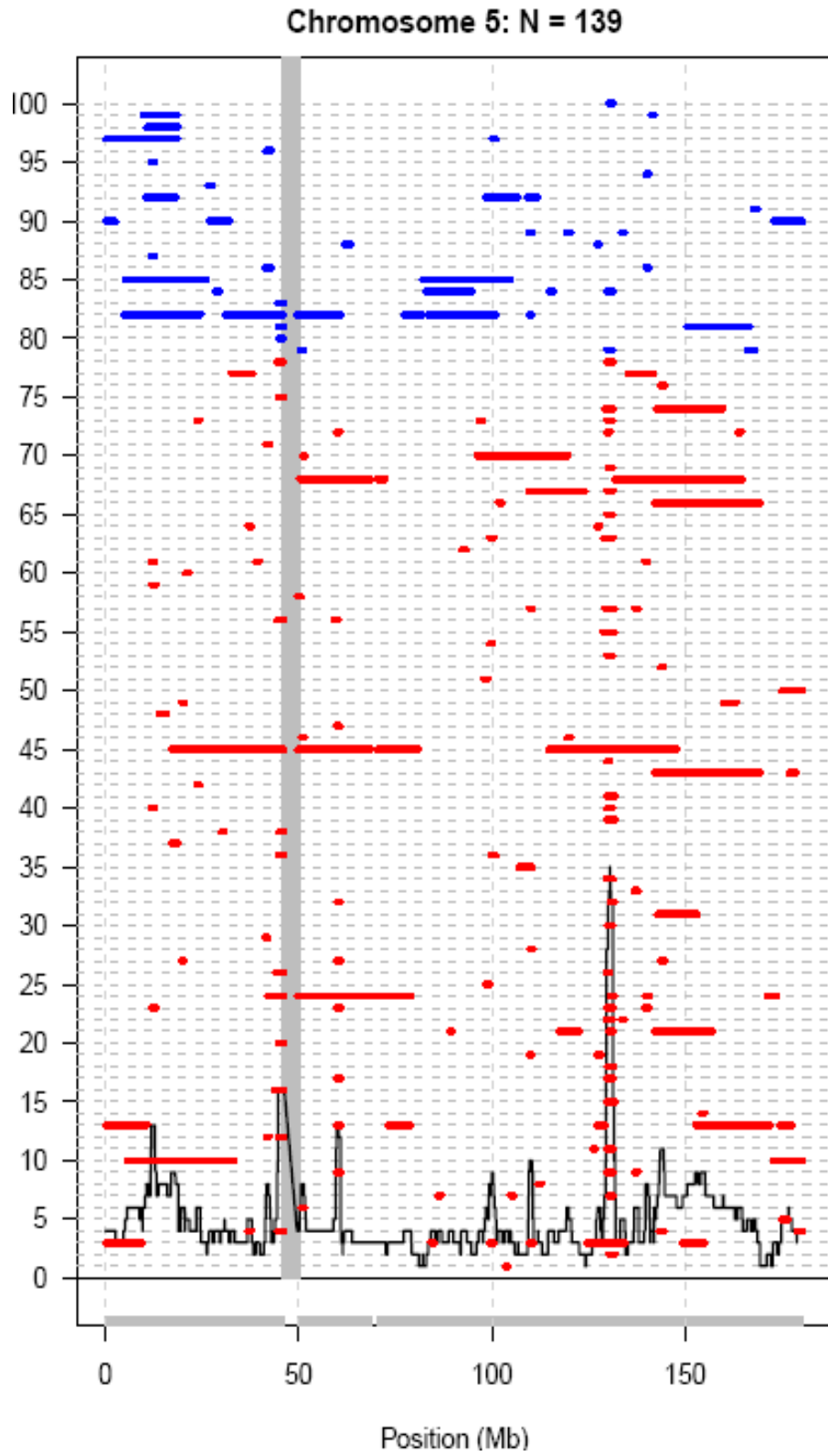


Figure E.5. Homozygous regions in chromosome 5 for FALS, juvenile cases and controls

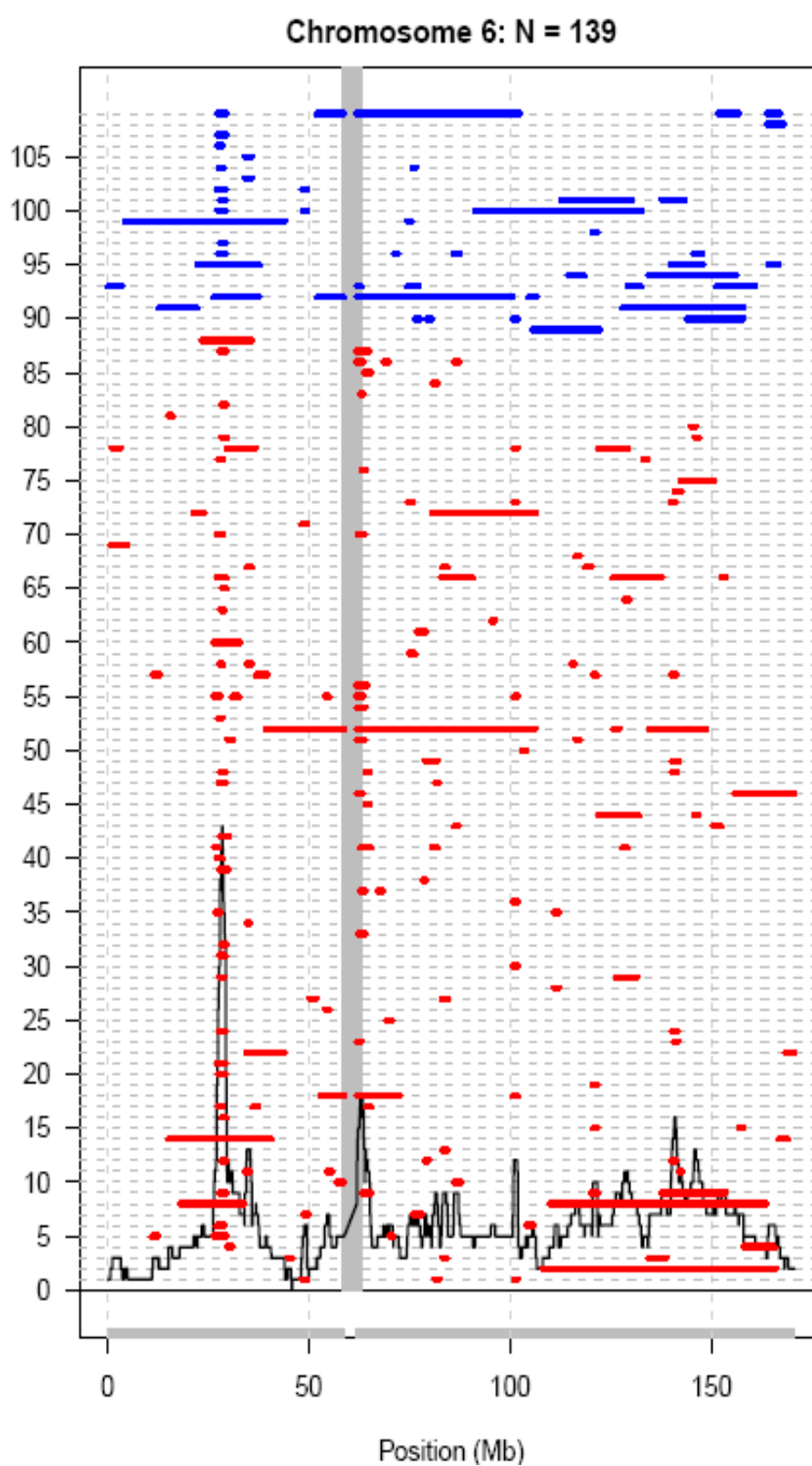


Figure E.6. Homozygous regions in chromosome 6 for FALS, juvenile cases and controls

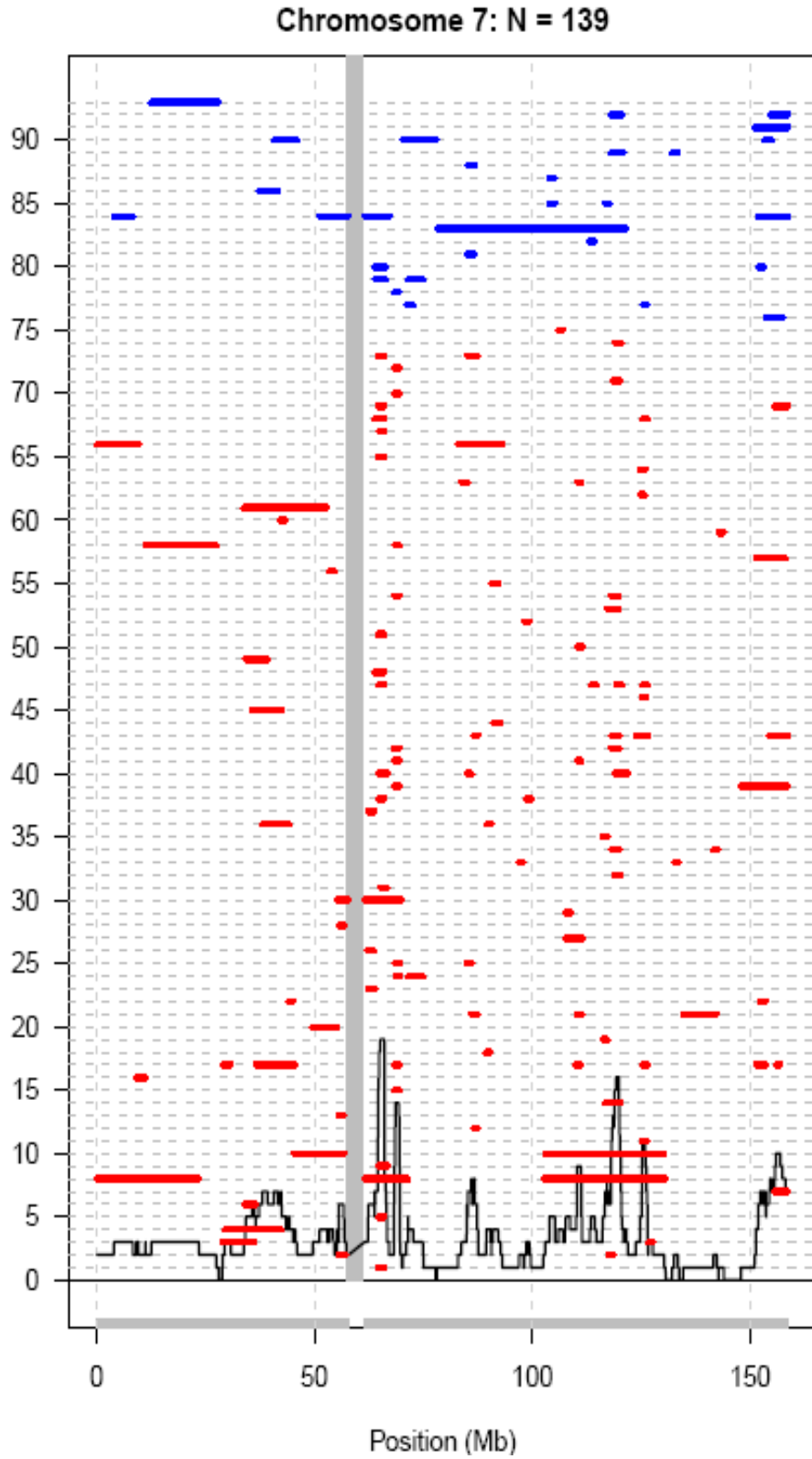


Figure E.7. Homozygous regions in chromosome 7 for FALS, juvenile cases and controls

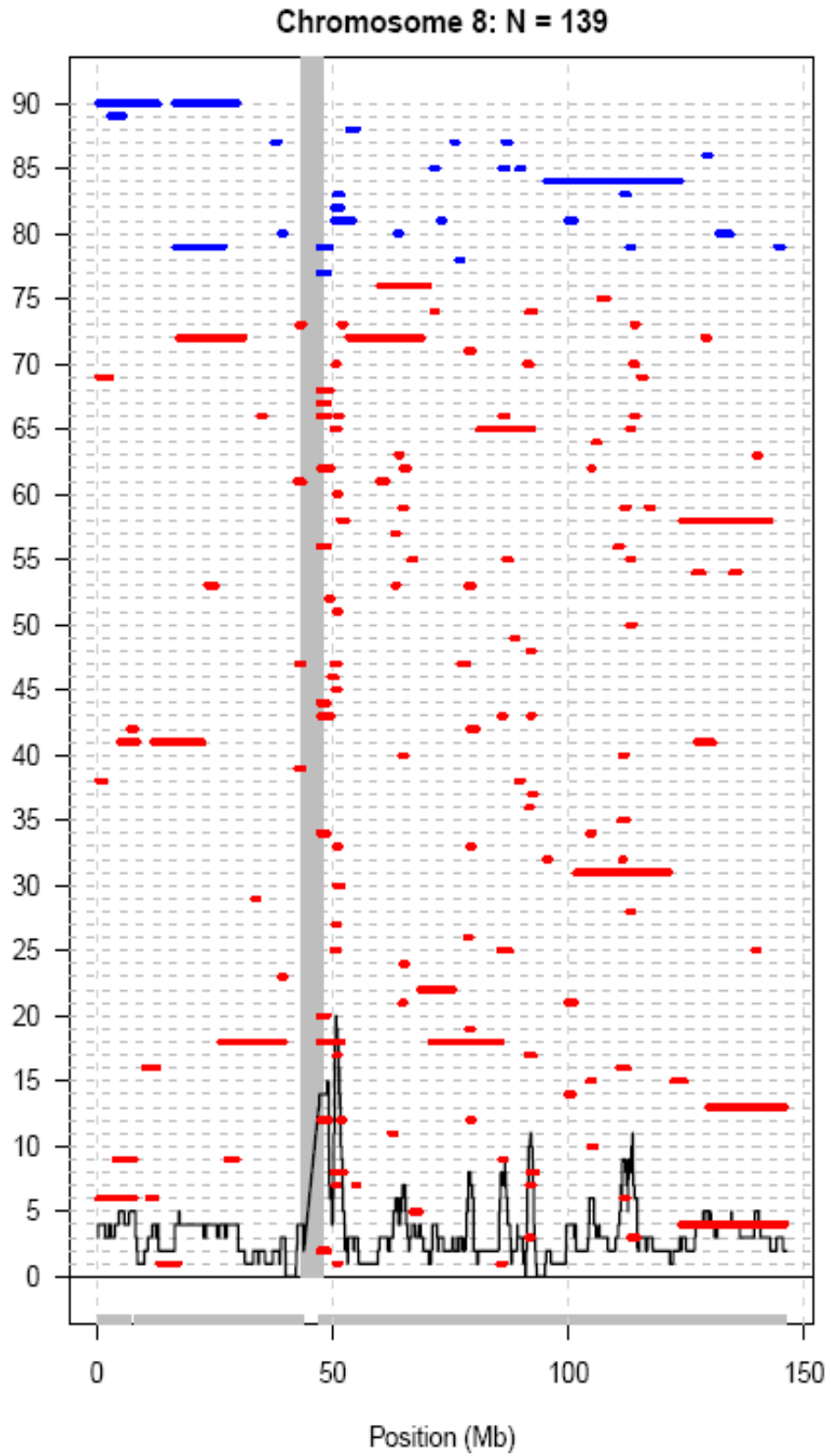


Figure E.8. Homozygous regions in chromosome 8 for FALS, juvenile cases and controls

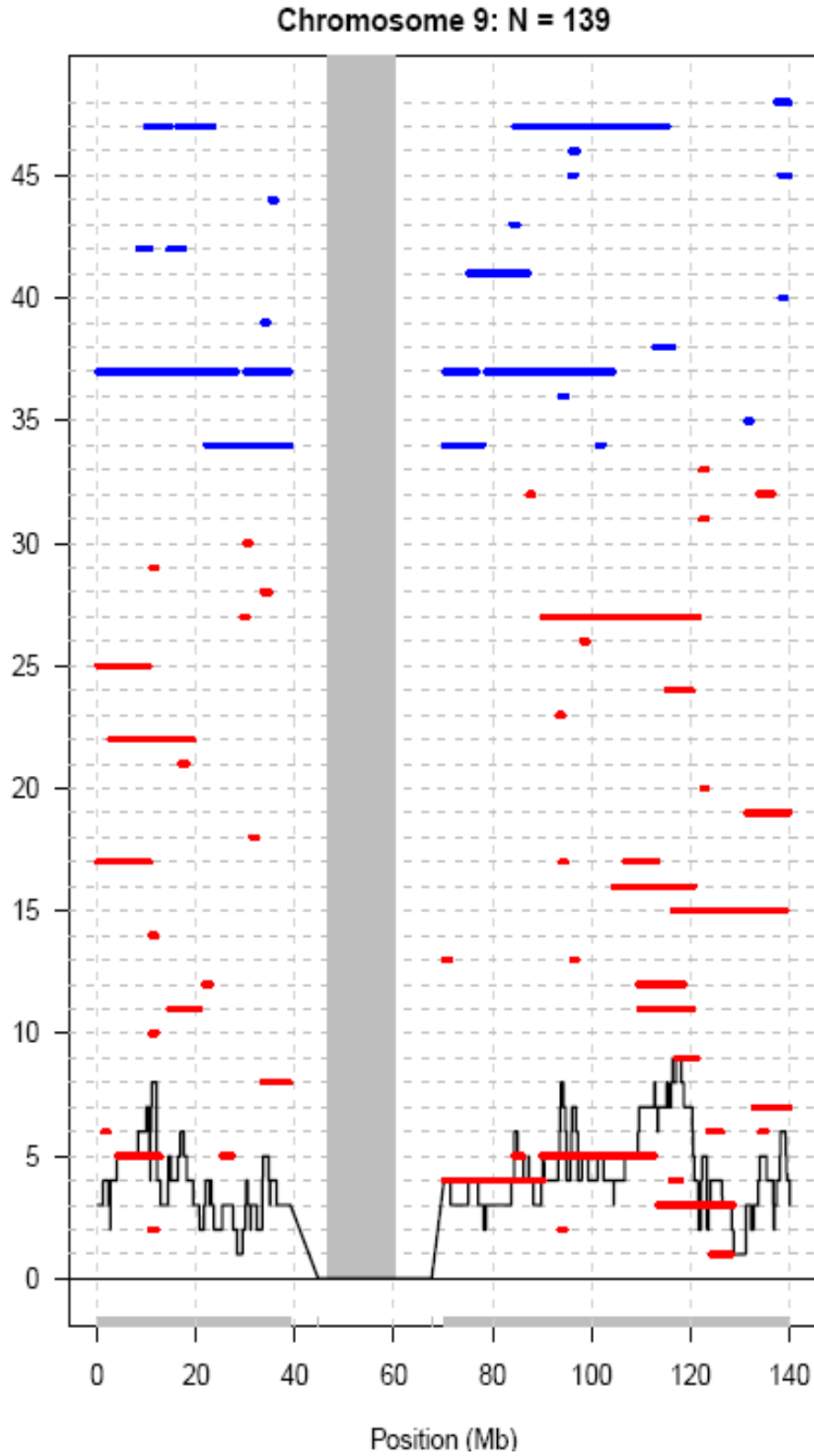


Figure E.9. Homozygous regions in chromosome 9 for FALS, juvenile cases and controls

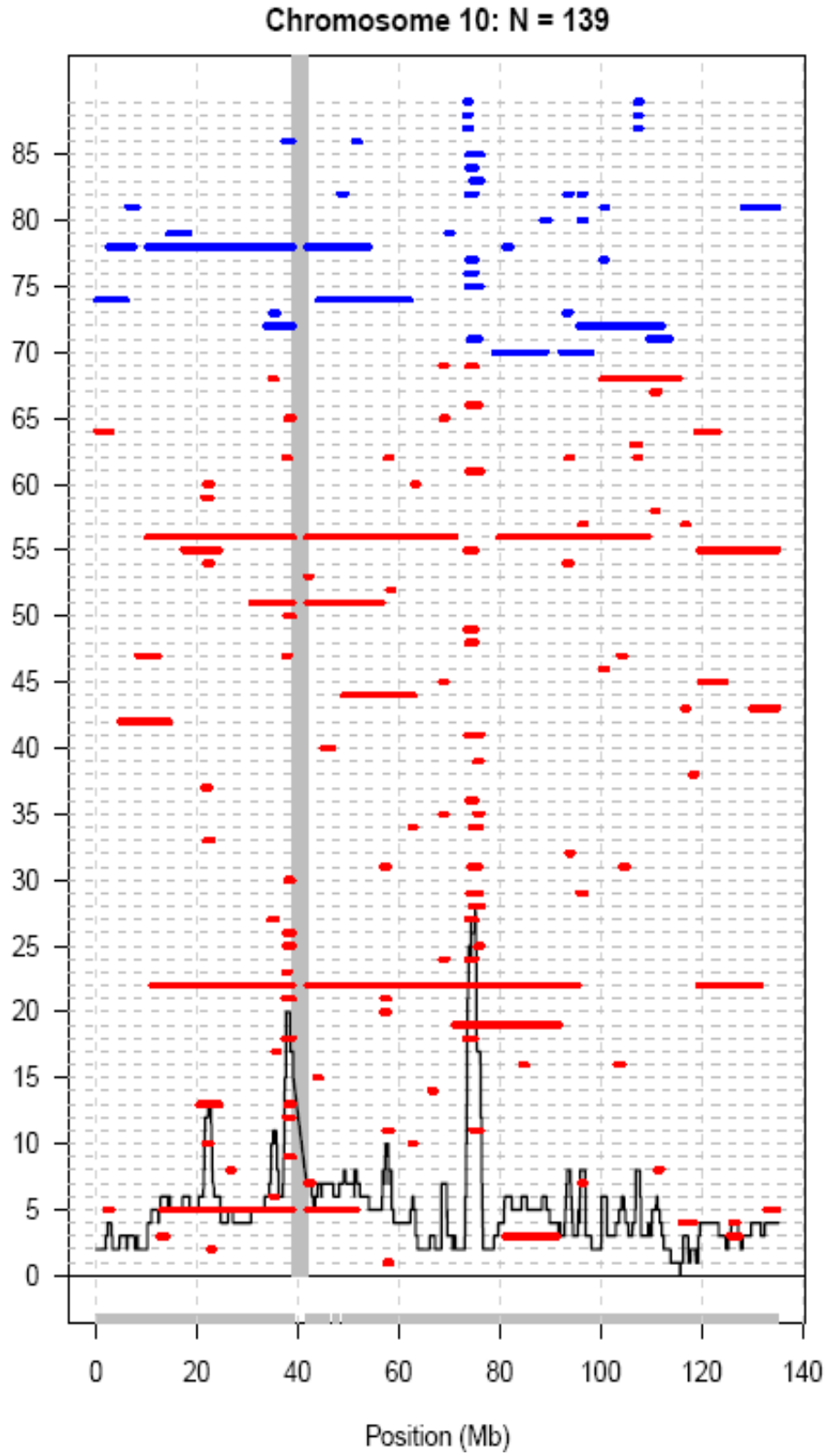


Figure E.10. Homozygous regions in chromosome 10 for FALS, juvenile cases and controls

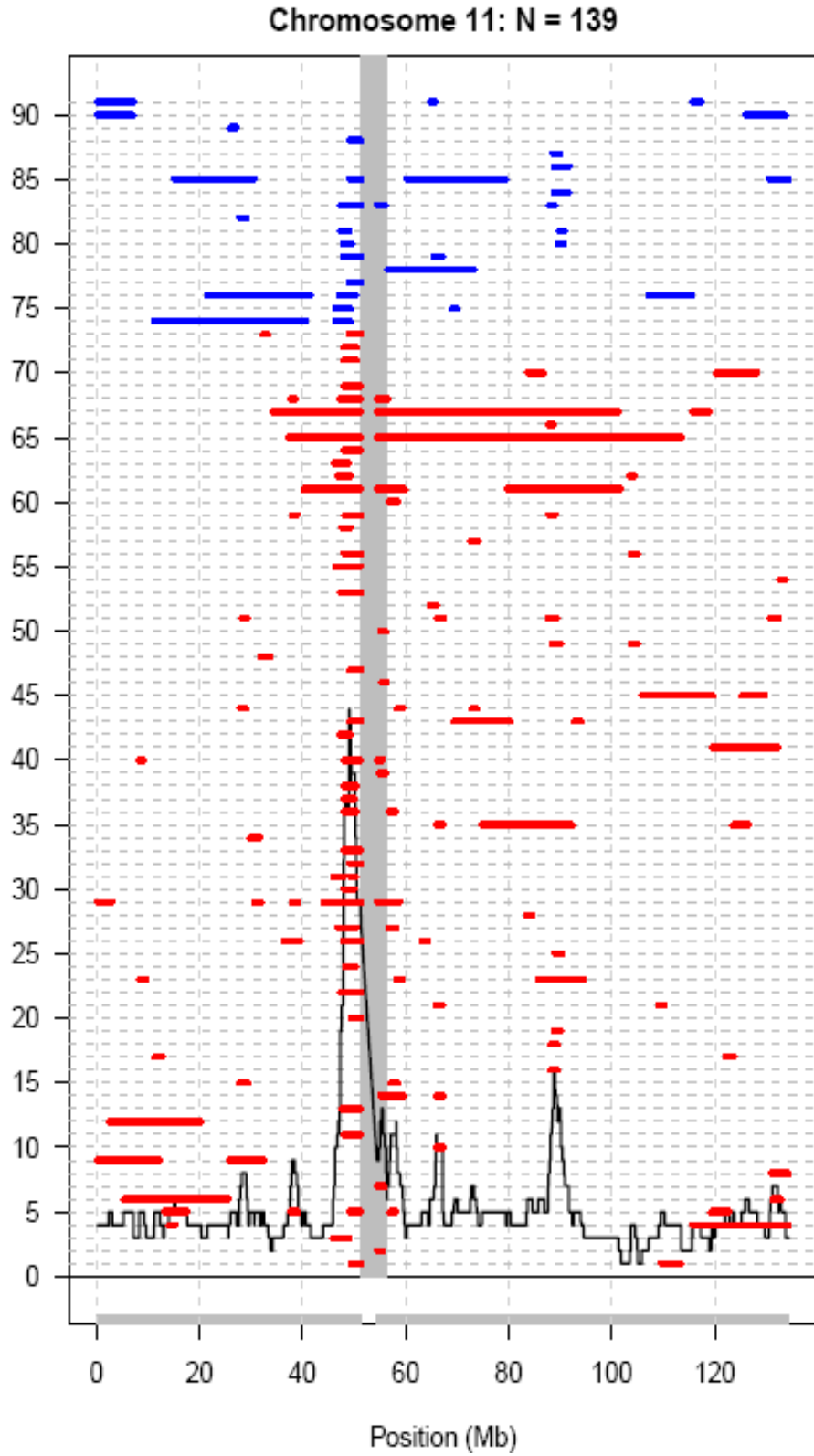


Figure E.11. Homozygous regions in chromosome 11 for FALS, juvenile cases and controls

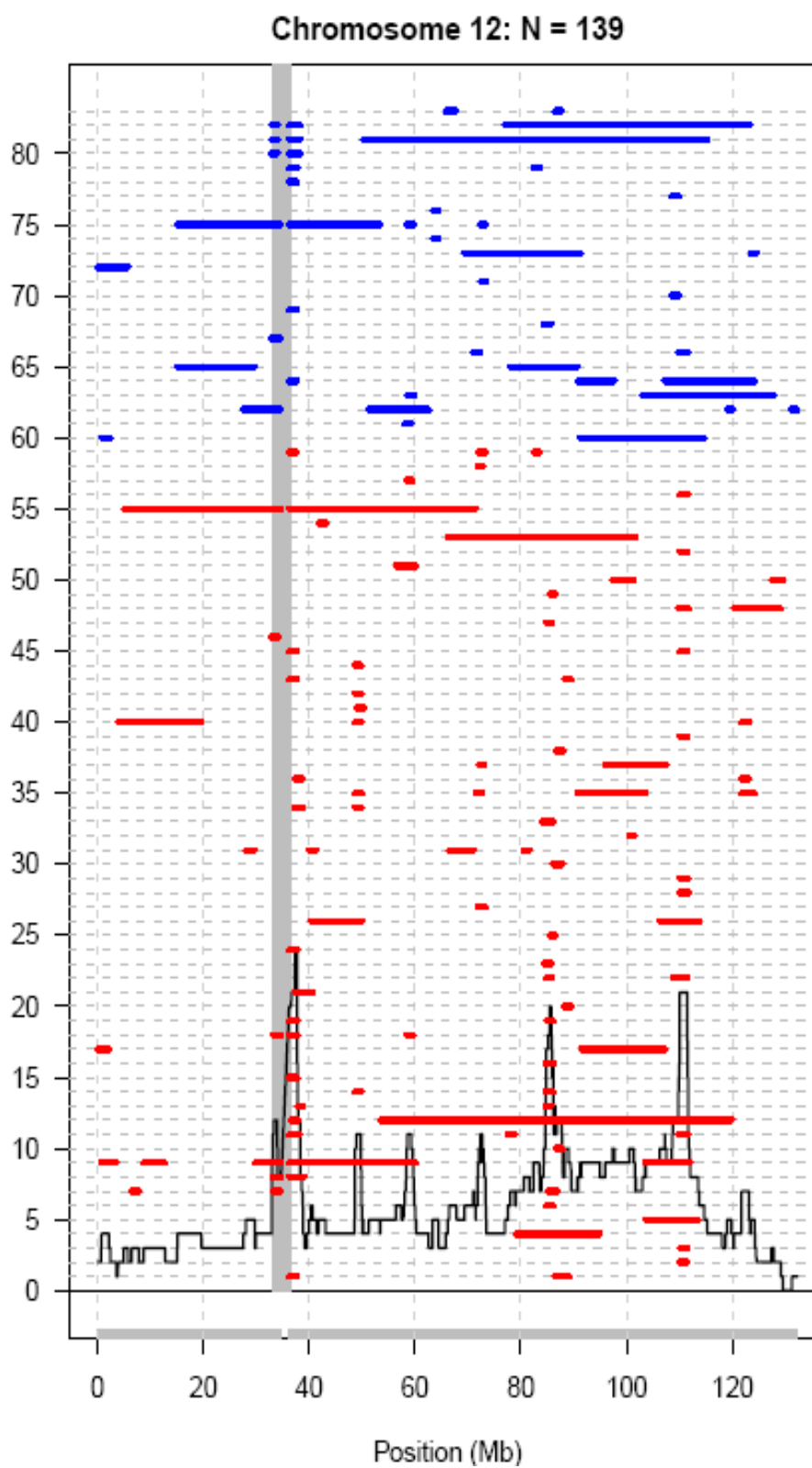


Figure E.12. Homozygous regions in chromosome 12 for FALS, juvenile cases and controls

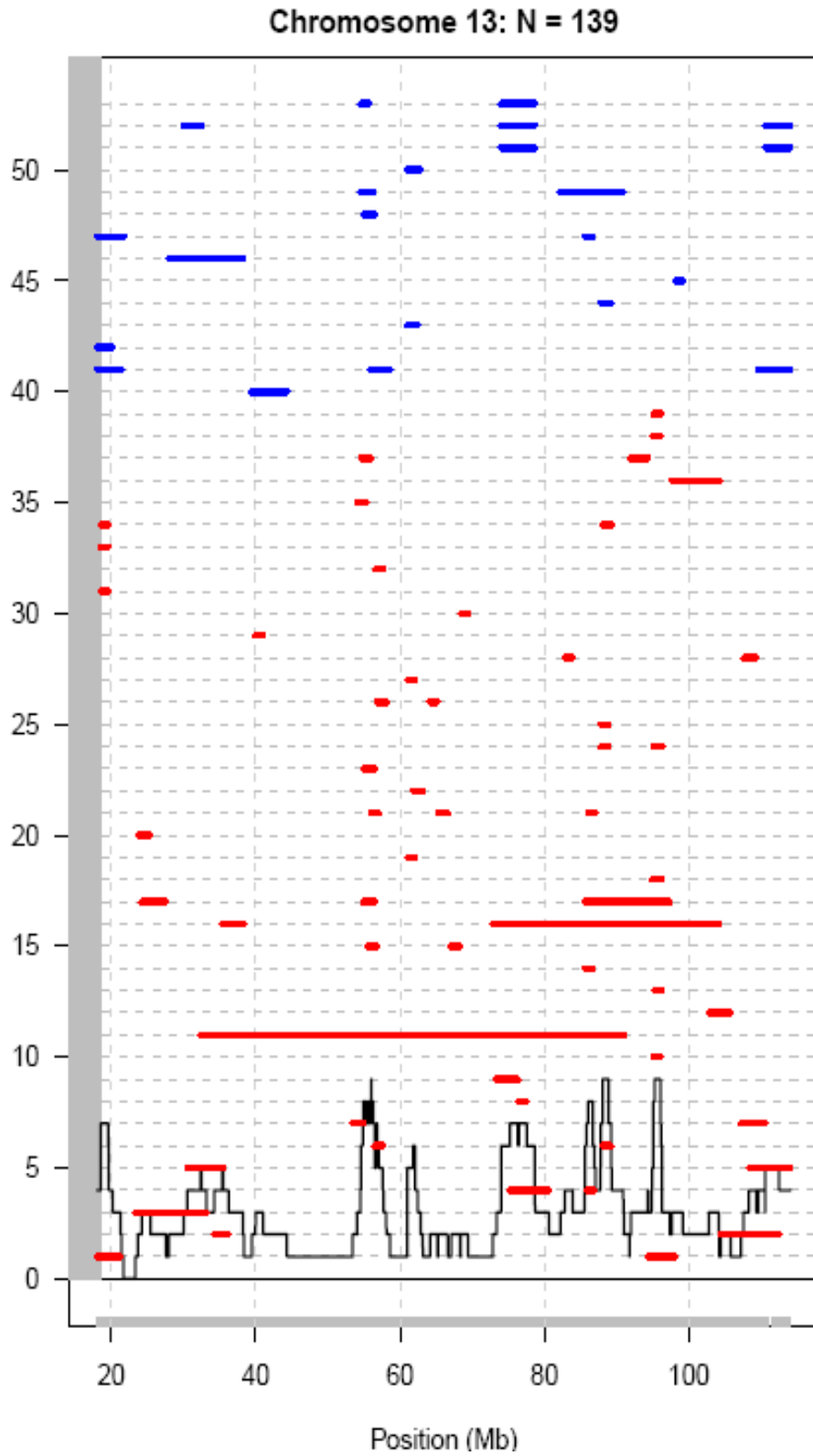


Figure E.13. Homozygous regions in chromosome 13 for FALS, juvenile cases and controls

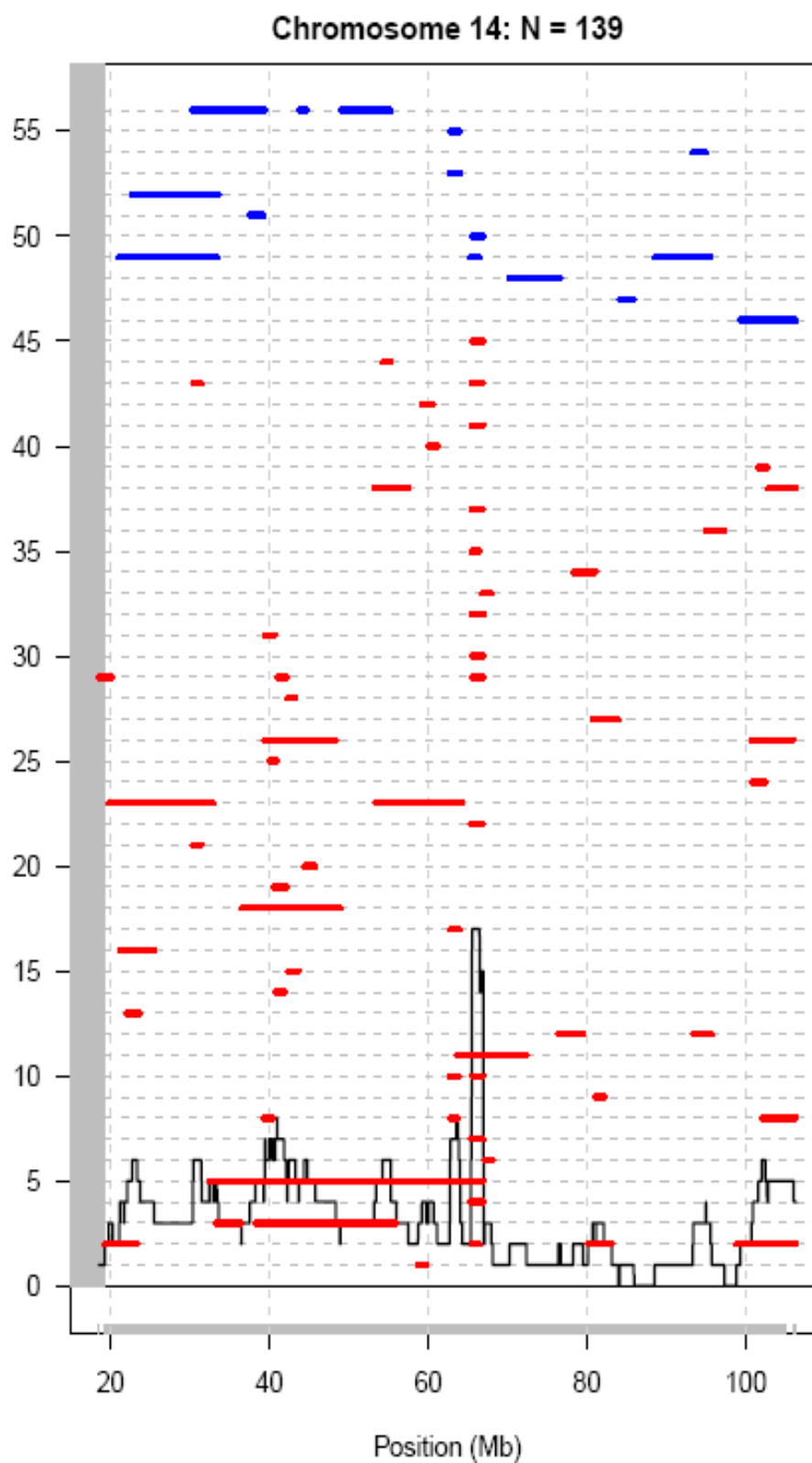


Figure E.14. Homozygous regions in chromosome 14 for FALS, juvenile cases and controls

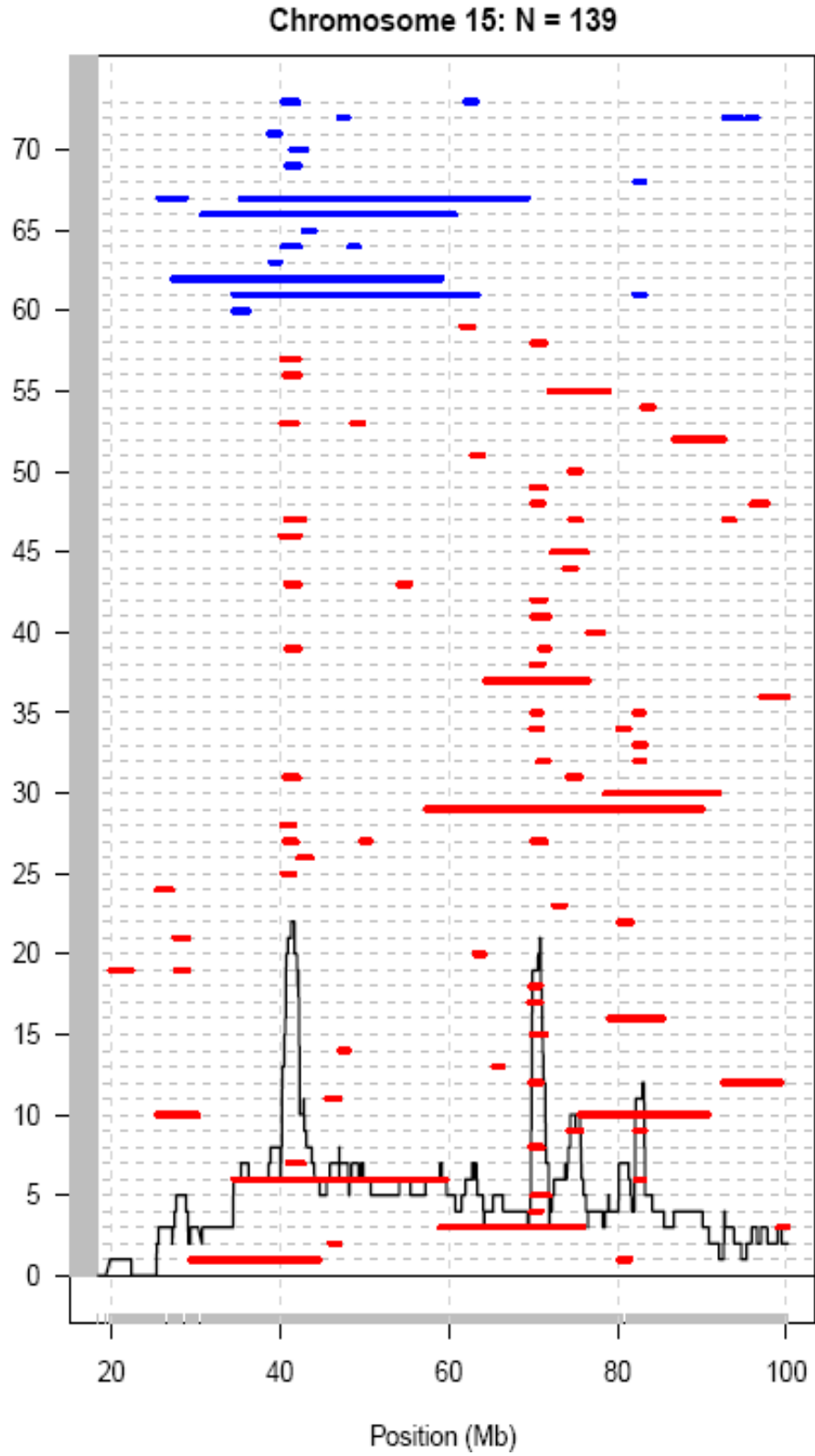


Figure E.15. Homozygous regions in chromosome 15 for FALS, juvenile cases and controls

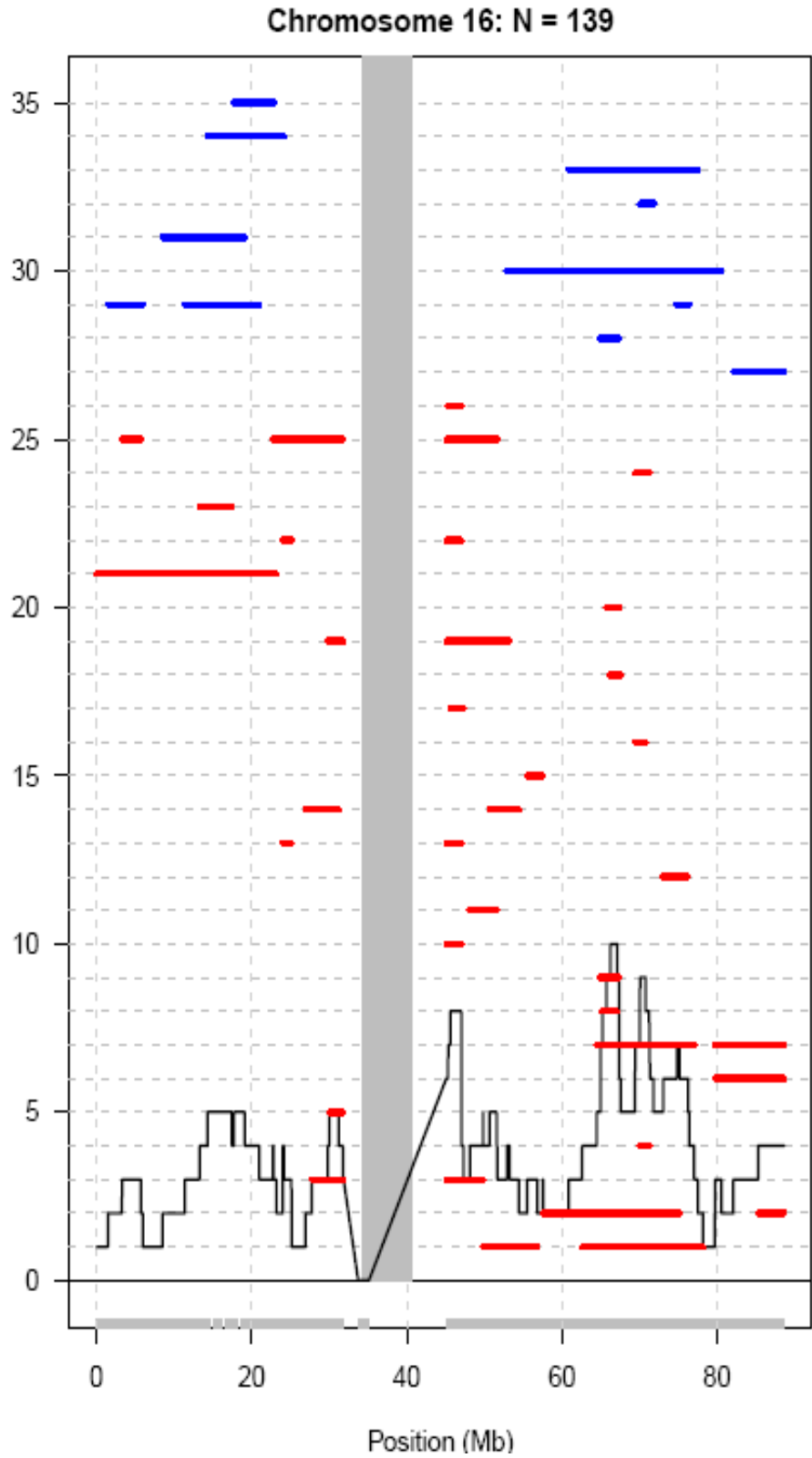


Figure E.16. Homozygous regions in chromosome 16 for FALS, juvenile cases and controls

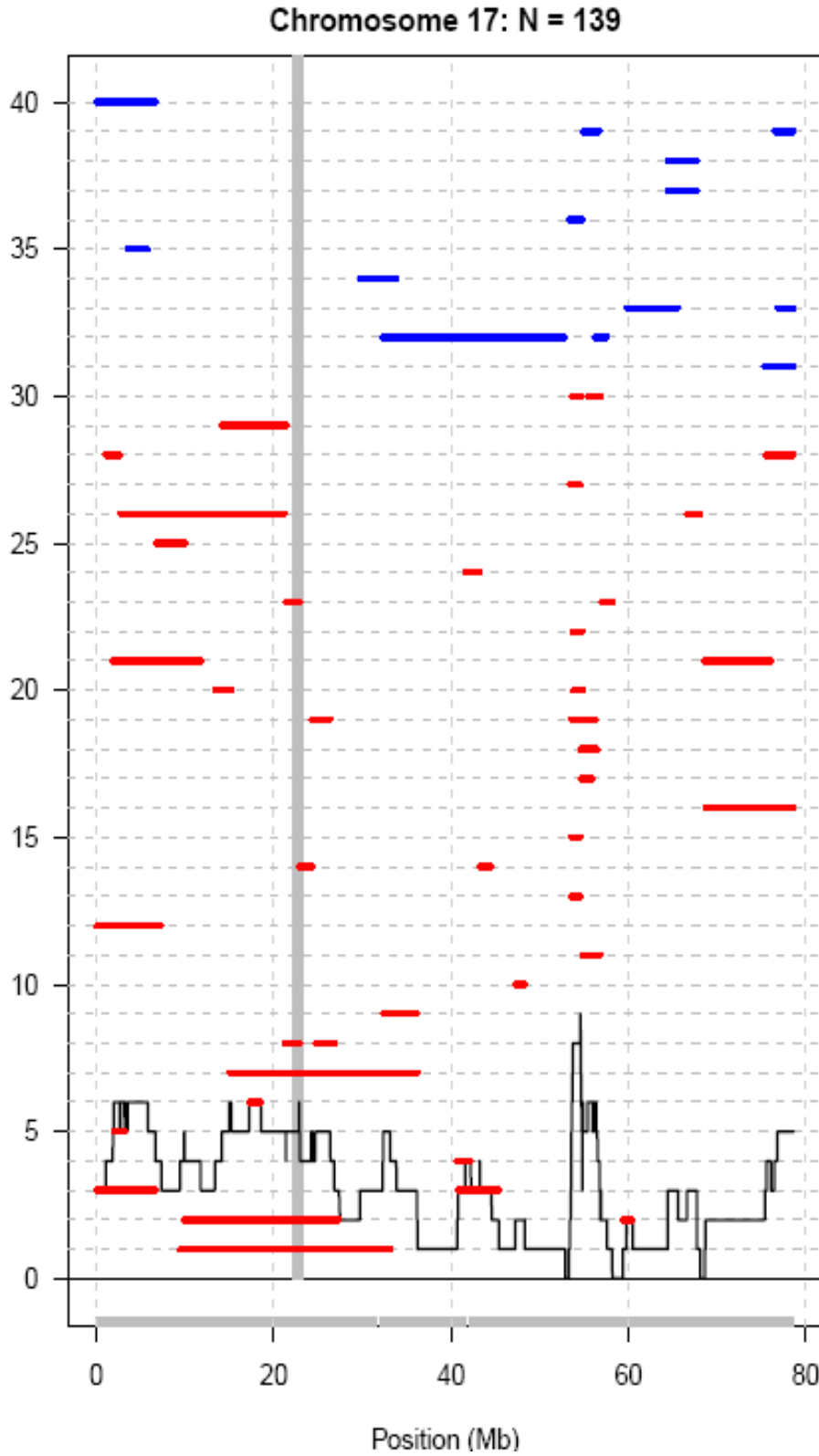


Figure E.17. Homozygous regions in chromosome 17 for FALS, juvenile cases and controls

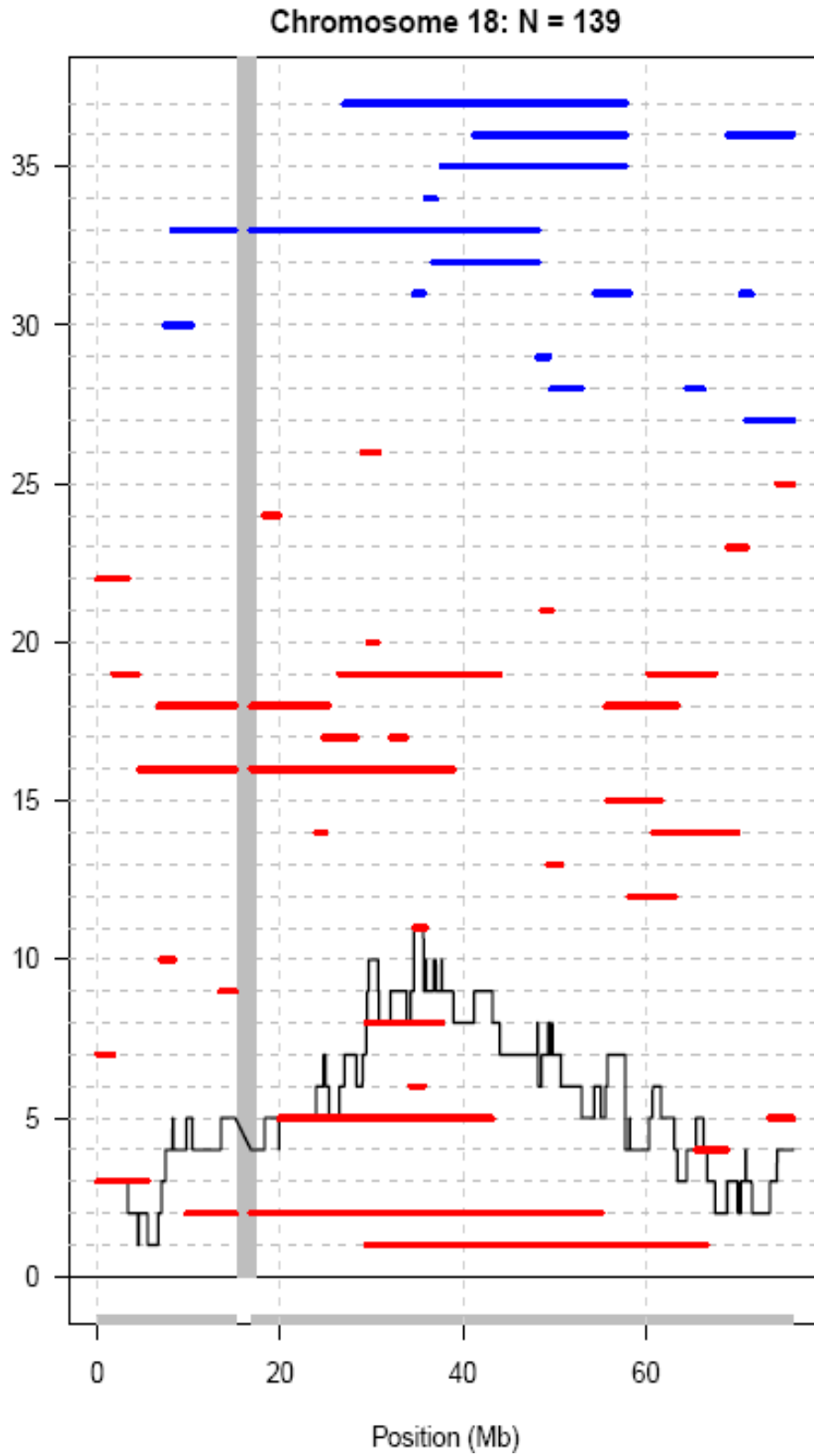


Figure E.18. Homozygous regions in chromosome 18 for FALS, juvenile cases and controls

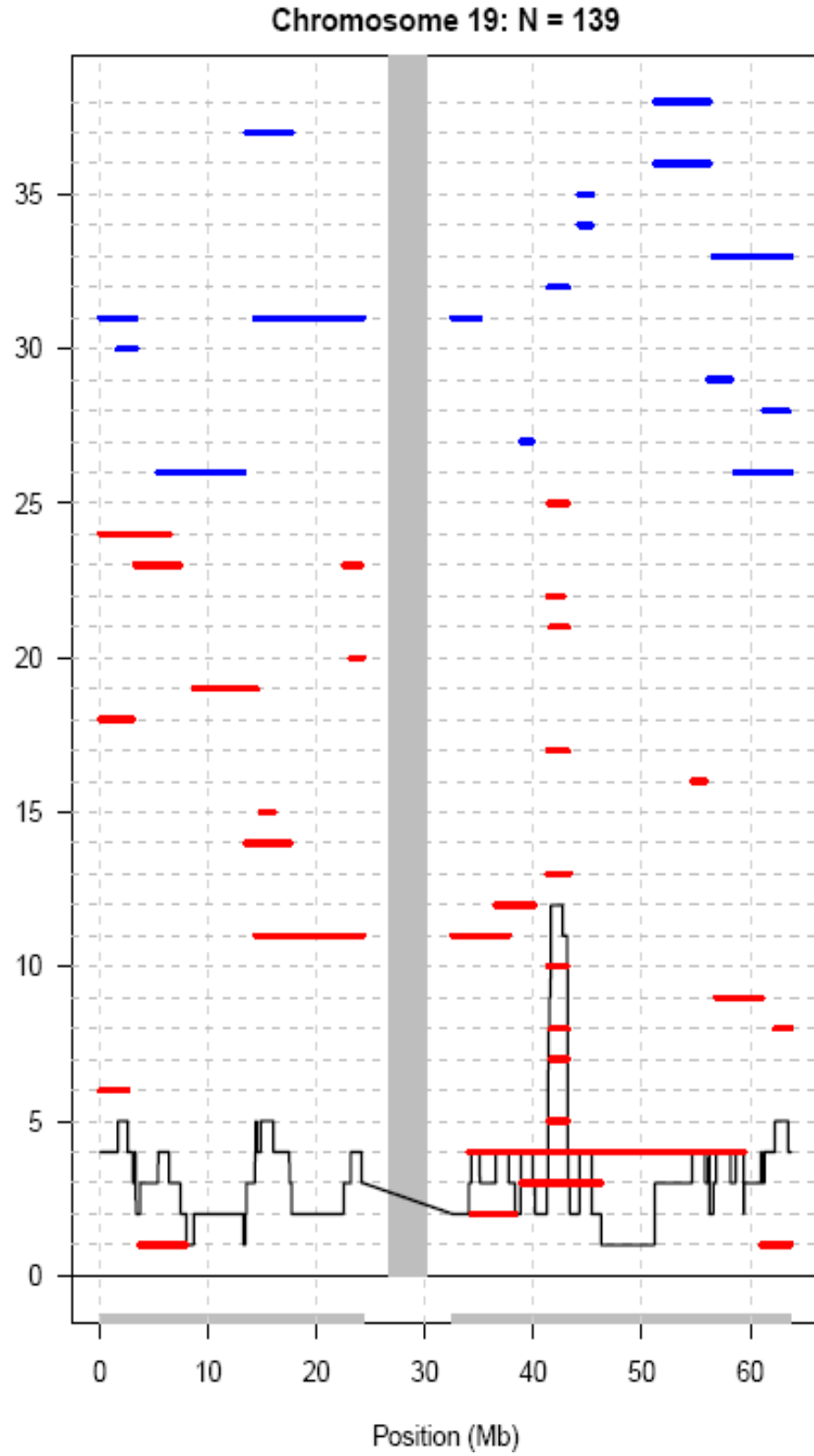


Figure E.19. Homozygous regions in chromosome 19 for FALS, juvenile cases and controls

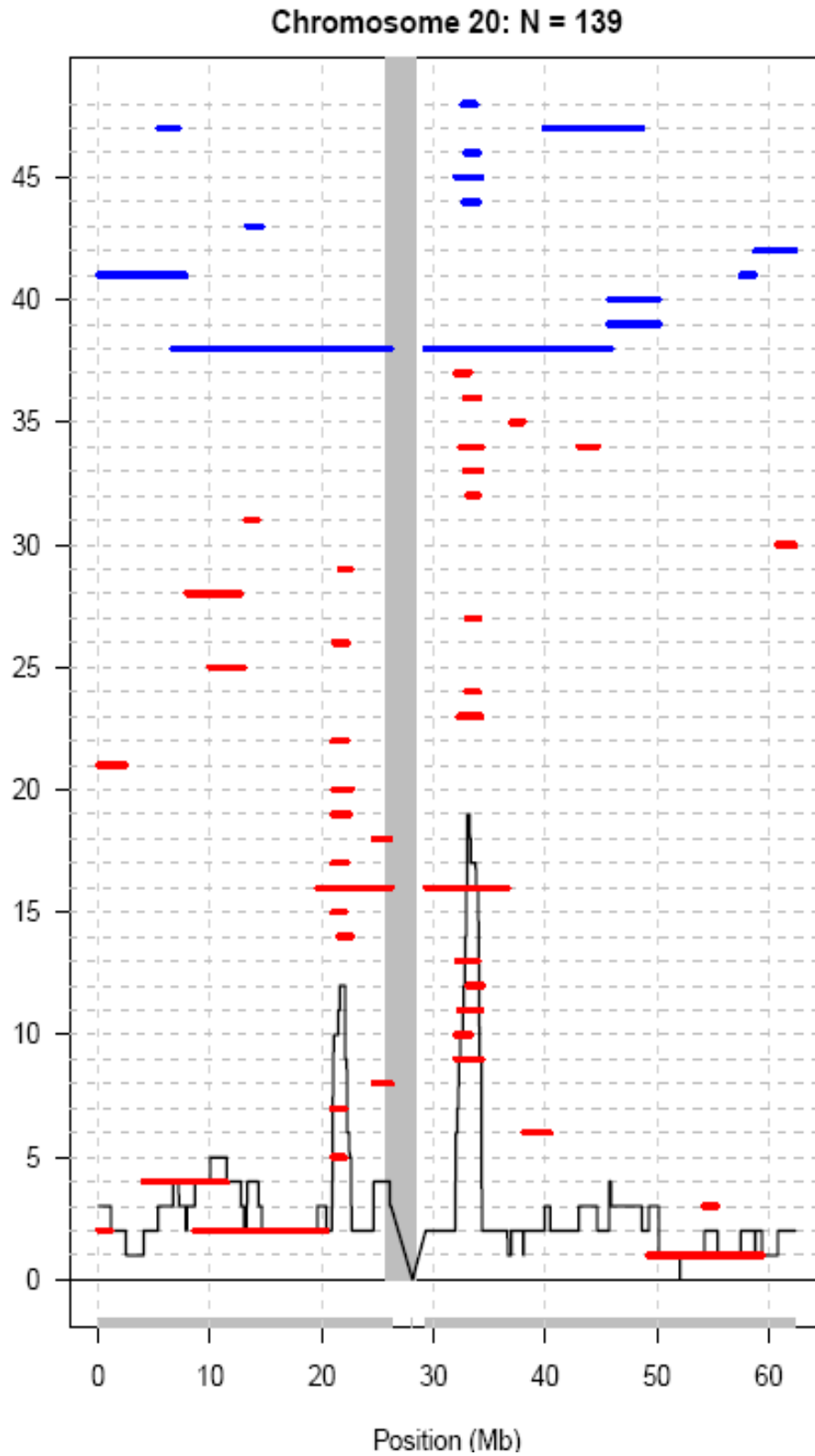


Figure E.20. Homozygous regions in chromosome 20 for FALS, juvenile cases and controls

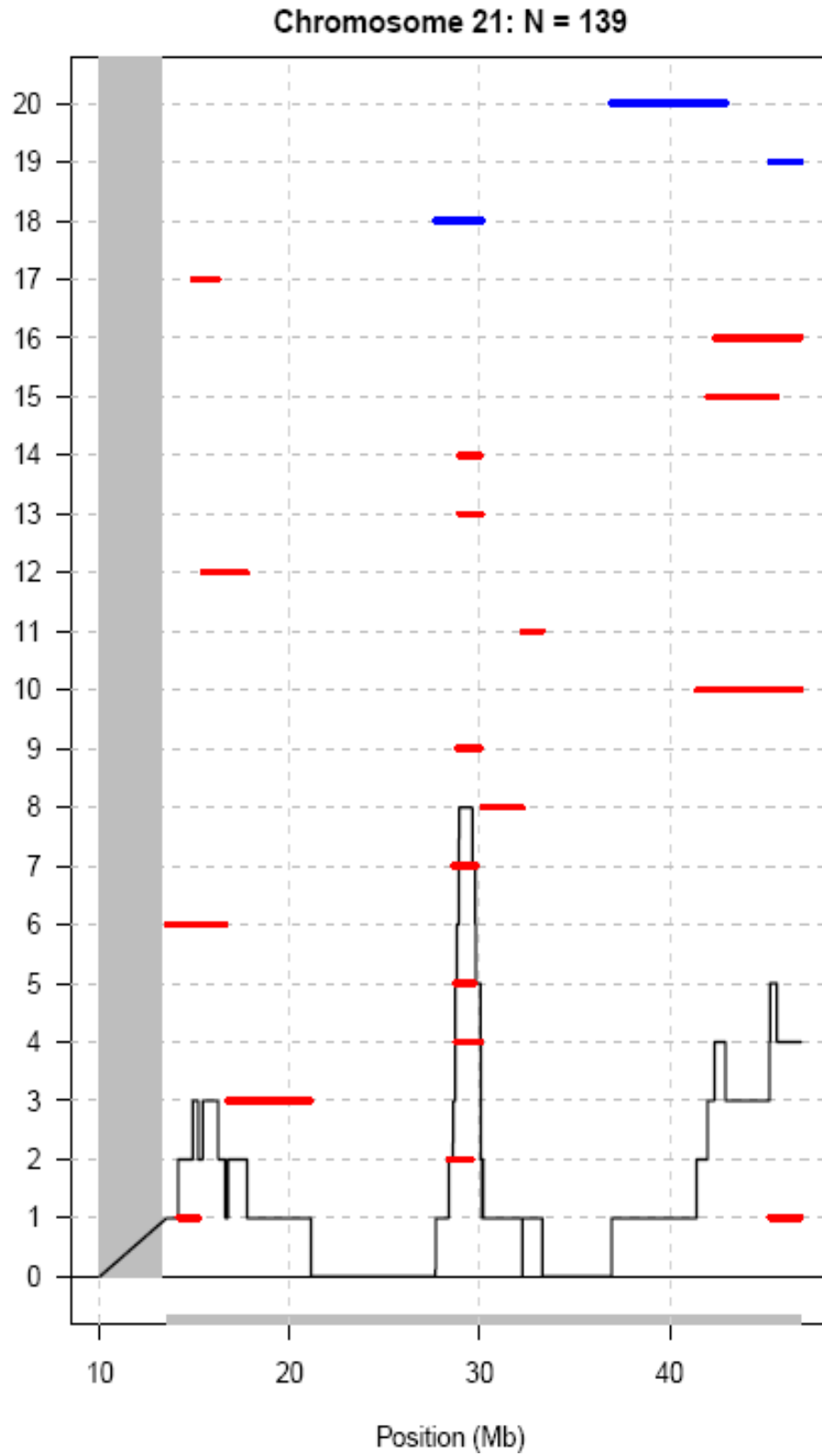


Figure E.21. Homozygous regions in chromosome 21 for FALS, juvenile cases and controls

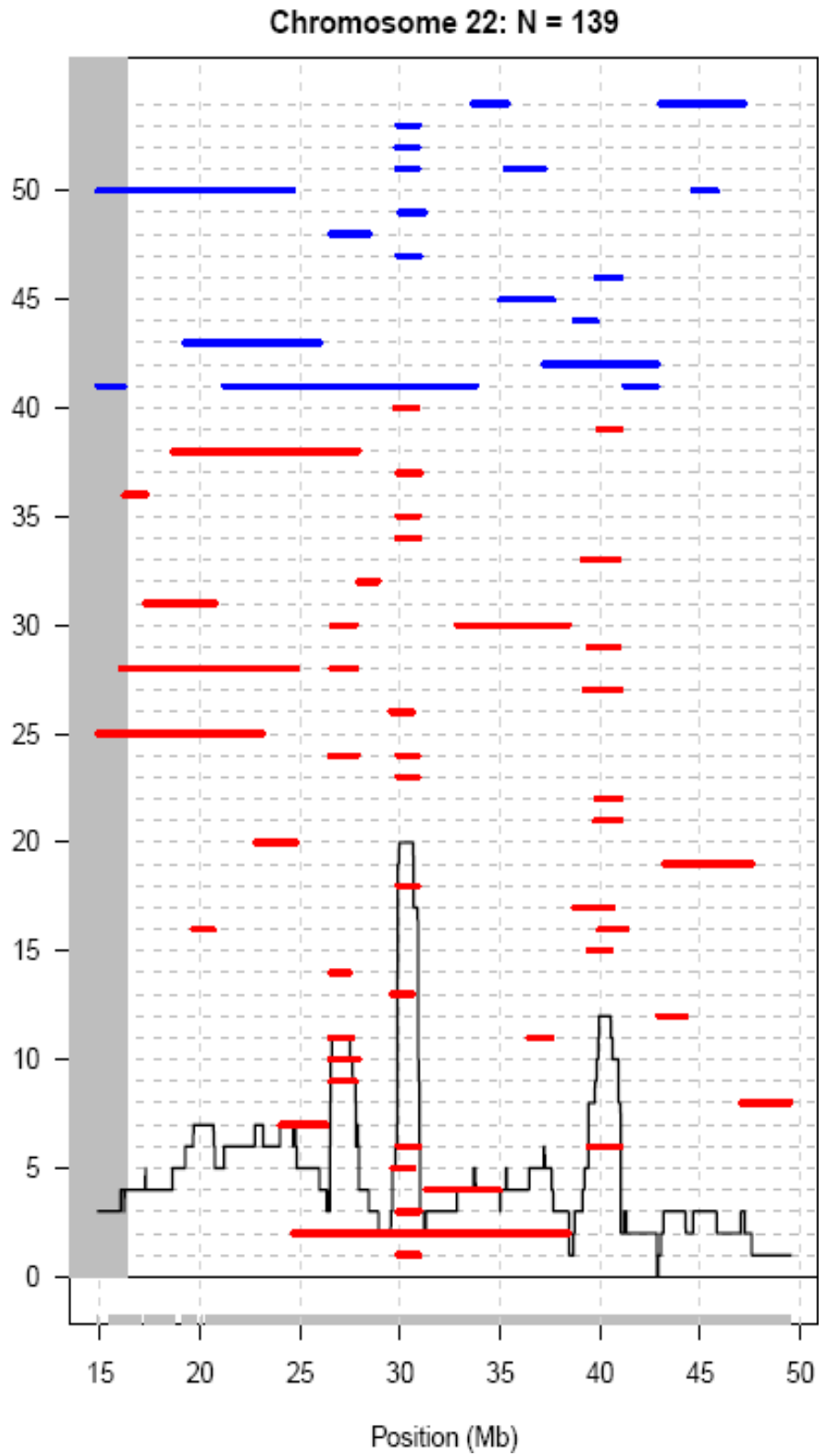


Figure E.22. Homozygous regions in chromosome 22 for FALS, juvenile cases and controls

APPENDIX F: P VALUES FOR PREVIOUSLY REPORTED SNPS

	Chromosome	SNP	Position	P-value	Reported P-value
DPP6	7	rs10263063	153,817,459	0.5094	5.40E-08
	7	rs2087720	153,828,605	0.6732	
	7	rs10232716	153,833,116	0.9814	
	7	rs11763727	153,836,224	0.3727	
	7	rs10239794	153,836,827	0.3136	
	7	rs10260404	153,841,731	0.0122	
	7	rs1388543	153,847,279	0.3168	
	7	rs1552734	153,854,974	0.1965	
	7	rs7803828	153,856,588	0.1804	
	7	rs10232522	153,864,625	0.5625	
	7	rs902743	153,879,201	0.1240	
FLJ10986	1	rs3850543	59,426,218	0.9748	1.80E-05
	1	rs12044604	59,427,090	0.9360	
	1	rs12752853	59,441,293	0.8558	
	1	rs12402265	59,463,190	0.7608	
	1	rs7540474	59,466,058	0.9289	
	1	rs7531917	59,467,199	0.7296	
	1	rs6700125	59,475,385	0.0993	
	1	rs6683082	59,480,913	0.4245	
	1	rs11207432	59,487,861	0.5098	
	1	rs751101	59,501,930	0.3682	
	1	rs333683	59,504,431	0.4884	
	1	rs835365	59,529,637	0.3108	
ITPR2	12	rs1532720	26,494,667	0.2681	3.28E-06
	12	rs2344158	26,499,020	0.2042	
	12	rs7975290	26,505,185	0.9933	
	12	rs4964001	26,516,433	0.2275	
	12	rs11048545	26,523,863	0.8932	
	12	rs2306677	26,527,853	0.0430	
	12	rs1825478	26,529,224	0.3056	
	12	rs4964002	26,531,824	0.0428	
	12	rs905298	26,533,200	0.0728	
	12	rs1393413	26,549,435	0.0448	
	12	rs2220188	26,549,746	0.0366	

Figure F. P values for three hits which were previously reported as significant in susceptibility. The hits and 10 surrounding SNPs are shown (Landers *et al.*, 2009)

APPENDIX G: LINKAGE DISEQUILIBRIUM PLOT FOR rs1541160

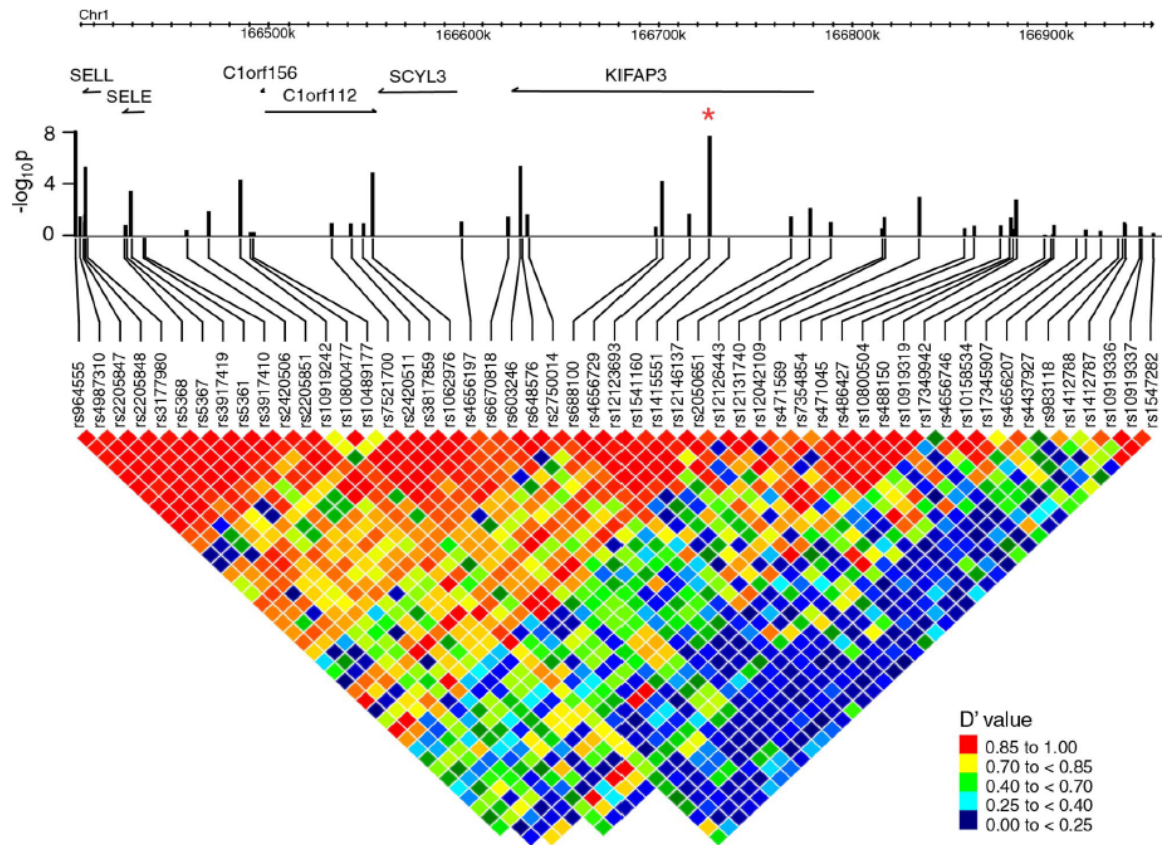


Figure G. Linkage disequilibrium plot of rs151160. Pairwise linkage disequilibrium values (D') for each SNP spanning rs151160 are represented with colors; the color key is at the right bottom. An asterisk indicate rs151160 (Landers et al., 2009)

APPENDIX H: SNPs WITH BEST P VALUES IN THE FOUR TESTED CATEGORIES

Susceptibility	SNP	Chromosome	Position	Raw P	Corrected P	Nearest Gene	Freq. Case	Freq. Cont.	OR	Alleles
	rs10438933	18	27527127	1.18E-06	1	B4GALT6	0.155	0.124	1.296	A>G
	rs16856202	1	228461886	7.98E-06	1	DISC1	0.020	0.038	0.499	A>C
	rs873917	1	39801888	8.37E-06	1	NT5C1A	0.316	0.285	1.162	G>T
	rs10192369	2	161206395	8.53E-06	1	RBMS1	0.512	0.473	1.170	C>T
	rs10503354	8	5940352	1.09E-05	1	MCPH1	0.134	0.166	0.773	G>A
Site of Onset	SNP	Chromosome	Position	Raw P	Corrected P	Nearest Gene	Freq. Limb	Freq. Bulbar	OR	Alleles
	rs7577894	2	55920555	1.13E-06	1	EFEMP1	0.386	0.471	0.708	T>C
	rs13015447	2	167203485	6.71E-06	1	SCN7A	0.344	0.425	0.709	T>G
	rs7702057	5	115755737	7.60E-06	1	SEMA6A	0.033	0.066	0.488	C>A
	rs8066857	17	68207698	8.11E-06	1	SLC39A11	0.172	0.235	0.676	C>T
	rs3734803	6	151961759	1.37E-05	1	C6orf97	0.177	0.243	0.669	C>T
Age of Onset	SNP	Chromosome	Position	Raw P	Corrected P	Nearest Gene	Regr. Coeff.	Standard Error	R ²	Alleles
	rs697739	6	16850012	4.14E-06	1	ATXN1	-2.036	0.4409	0.0097	G>A
	rs2619566	3	2599938	7.42E-06	1	CNTN4	-3.032	0.6746	0.0107	A>G
	rs1486860	4	113751047	1.12E-05	1	ALPK1	1.833	0.4161	0.0082	T>C
	rs2451852	5	16642040	1.20E-05	1	FLJ20152	-2.503	0.5702	0.0097	T>C
	rs2055593	2	98450631	1.39E-05	1	CNGA3	-2.136	0.4903	0.0103	G>A
Survival	SNP	Chromosome	Position	Raw P	Corrected P	Nearest Gene	Regr. Coeff.	Standard Error	R ²	Alleles
	rs1541160	1	166727460	1.84E-08	0.021	KIFAP3	0.582	0.1026	0.0293	T>C
	rs855913	7	148641310	4.02E-08	0.046	ZNF746	1.079	0.1951	0.0279	C>A
	rs11241713	5	123147464	3.17E-06	1	CSNK1G3	0.786	0.1677	0.0202	G>T
	rs648576	1	166631085	3.63E-06	1	KIFAP3	0.490	0.1052	0.0198	C>T
	rs3177980	1	166408144	4.10E-06	1	SELL	0.509	0.1098	0.0248	A>G

Figure H. SNPs with best P values in the four tested categories (Landers et al., 2009)

APPENDIX I: SENSITIVITY ANALYSIS OF rs1541160

Stage 2 Population	Stage 1 P-value	Stage 1 Rank	Stage 2 P-value	Stage 1 Sample Size	Stage 2 Sample Size	Stage 2 Median Surv. CC	Stage 2 Median Surv. TT	% Survival Increase (CC vs. TT)
Atlanta	2.89E-07	1st	0.079	924	90	4.00	2.77	44.40%
Boston	5.50E-06	5th	8.86E-04	616	398	4.27	2.93	45.73%
London	4.00E-06	5th	1.42E-03	804	210	4.66	2.61	78.54%
Netherlands	2.60E-07	1st	0.022	698	316	2.82	2.34	20.51%
United States	7.70E-05	31st	5.55E-05	526	488	4.23	2.85	48.42%
Europe	5.55E-05	20th	7.70E-05	488	526	3.39	2.42	40.08%
Total		1.84E-08			1014	3.96	2.67	46.44%

Figure I. Sensitivity analysis of rs151160 within the populations under study

APPENDIX J: HOMOZYGOSITY REGIONS IN ALS157 AND ALS158

Table J. Homozygosity regions of ALS157 and ALS158

ALS ID	Chromosome	Start Position	End Position
ALS158	1	9462280	10565380
ALS157	1	9462280	10565380
ALS158	1	48965981	50414531
ALS157	1	48965981	50414531
ALS157	1	233816201	235863460
ALS158	2	45871727	47702540
ALS158	2	54266043	55549628
ALS157	2	129199576	196857742
ALS158	2	188847730	190065687
ALS158	3	10170485	14386659
ALS158	3	33938575	39584795
ALS157	3	33938575	39584795
ALS158	3	48566485	50500021
ALS157	3	48566485	50500021
ALS158	3	99791605	101331030
ALS158	3	148975529	150130883
ALS158	3	182006645	199308268
ALS158	4	98456113	99660372
ALS158	4	123127576	124297420
ALS158	4	151323320	152389749
ALS157	4	157699524	167236114
ALS158	5	44649728	46322869
ALS157	5	44649728	46322869
ALS157	5	150496699	166972188
ALS157	6	12704984	22160404
ALS158	6	76525835	77633774
ALS158	6	79453687	80470921

Table J. Homozygosity regions of ALS157 and ALS158 (continued)

ALS ID	Chromosome	Start Position	End Position
ALS158	6	100868398	102115516
ALS157	6	127939998	158113713
ALS158	6	144072186	158113713
ALS157	7	71150234	72727355
ALS157	7	125388765	126404106
ALS158	7	153759222	157471022
ALS157	8	76388731	77540500
ALS158	9	131231273	132261749
ALS157	10	73841644	76238263
ALS158	10	78837467	89250313
ALS158	10	92072230	98245941
ALS157	10	109476001	113869784
ALS158	11	11183154	40652704
ALS158	11	46290815	49347195
ALS157	11	46290815	49347195
ALS157	11	69009256	70065899
ALS157	12	27609825	34711193
ALS157	12	51335846	62627372
ALS158	12	58107233	59307512
ALS157	12	119025953	120174181
ALS157	12	131268822	132288869
ALS157	13	18045562	20152518
ALS158	13	18045562	21369401
ALS158	13	55896819	58616916
ALS158	13	109667423	114108295
ALS158	14	84165788	85918211
ALS157	15	34446939	36265550
ALS158	16	82129738	88677423
ALS157	17	75368668	78653169
ALS157	19	38828497	39926175

REFERENCES

- Abrahams, S., P. N. Leigh and L. H. Goldstein, 2005, "Cognitive Change in ALS- A Prospective Study", *Neurology*, Vol. 64, pp. 1222-1226.
- Ahmed, M. S., W. Y. Hung., J. Zu, P. Hockberger and T. Siddique, 2000, "Increased Reactive Oxygen Species in Familial Amyotrophic Lateral Sclerosis with Mutations in SOD1", *Journal of Neurological Sciences*, Vol. 176, pp. 88-94.
- Al-Chalabi, A., P. M. Andersen, B. Chioza, C. Shaw, P. C. Sham, W. Robberecht, G. Matthijs, W. Camu, S. L. Marklund, L. Forsgren, G. Rouleau, N. G. Laing, P. V. Hulse, T. Siddique, P. N. Leigh and J. F. Powell, 1998, "Recessive Amyotrophic Lateral Sclerosis Families with the D90A SOD1 Mutation Share a Common Founder: Evidence for a Linked Protective Factor", *Human Molecular Genetics*, Vol. 7, pp. 2045-2050.
- Al-Chalabi, A., P. N. Leigh, I. P. Blair, G. Nicholson, J. de Belleruche, J. M. Gallo, C. C. Miller and C. E. Shaw, 2009, "Mutations in FUS, an RNA Processing Protein, Cause Familial Amyotrophic Lateral Sclerosis Type 6", *Science*, Vol. 323, pp. 1208-1211.
- Alexianu, M. E., M. Kozovska and S. H. Appel, 2001, "Immune Reactivity in a Mouse Model of Familial ALS Correlates With Disease Progression", *Neurology*, Vol. 57, pp. 1282-1289.
- Andersen, P. M., L. Forsgren, M. Binzer, P. Nilsson, V. Ala-Hurula, M. L. Keranen, L. Bergmark, A. Saarinen, T. Haltia, I. Tarvainen, E. Kinnunen, B. Udd and S. L. Marklund, 1996, "Autosomal Recessive Adult-onset Amyotrophic Lateral Sclerosis Associated With Homozygosity For Asp90Ala CuZn-superoxide Dismutase Mutation: A Clinical and Genealogical Study of 36 Patients", *Brain*, Vol. 119, pp. 1153-1172.

- Bär, P. R., 2000, "Motor Neuron Disease in Vitro: The Use of Cultured Motor Neurons to Study Amyotrophic Lateral Sclerosis", *European Journal of Pharmacology*, Vol. 405, pp. 285-295.
- Barry, D. M., S. Millicamps, J. P. Julien and M. L. Garcia, 2007, "New movements in neurofilament transport, turnover and disease", *Experimental Cell Research*, Vol. 313, pp. 2110-2120.
- Beckman, G. and A. Pakarinen, 1973, "Superoxide Dismutase: A Population Study", *Human Heredity*, Vol. 23, pp.346-351.
- Beckmann, J. S., X. Estivill and S. E. Antonarakis, 2007, "Copy Number Variants And Genetic Traits: Closer To The Resolution Of Phenotypic To Genotypic Variability", *Nature Reviews Genetics*, Vol. 8, pp. 639-646.
- Ben Hamida, M., C. Ben Hamida, M. Zouari, S. Belal and F. Hentati, 1996, "Limb-girdle Muscular Dystrophy 2C: Clinical Aspects", *Neuromuscular Disorders*, Vol. 6, pp. 493-494.
- Ben Hamida, M., S. Belal, G. Sirugo, C. Ben Hamida, K. Panayides, P. Ionannou, J. Beckmann, J. L. Mandel, F. Hentati and M. Koenig, 1993, "Friedreich's Ataxia Phenotype Not Linked To Chromosome 9 and Associated With Selective Autosomal Recessive Vitamin E Deficiency In Two Inbred Tunisian Families", *Neurology*, Vol. 43, pp. 2179-2183.
- Bendotti, C. and M. T. Carri, 2004, "Lessons from Models of SOD1-linked Familial ALS", *Trends in Molecular Medicine*, Vol.10, pp. 393-400.
- Bergemalm, D., P. A. Jonsson, K. S. Graffmo, P. M. Andersen, T. Brännström, A. Rehnmark and S. L. Marklund, 2006, "Overloading of Stable and Exclusion of Unstable Human Superoxide Dismutase-1 Variants In Mitochondria of Murine Amyotrophic Lateral Sclerosis Models", *Journal of Neuroscience*, Vol. 26, pp. 4147-4154.

- Bertram, L. and R. E. Tanzi, 2005, "The Genetic Epidemiology of Neurodegenerative Disease", *The Journal of Clinical Investigation*, Vol. 115, pp. 1449.
- Biesecker, L. G., 2010, "Exome Sequencing Makes Medical Genomics a Reality", *Nature Genetics*, Vol. 42, pp. 13-14.
- Blauw, H. M., J. H. Veldink, M. A. van Es, P. W. van Vught, C. G. J. Saris, B. van der Zwaag, L. Franke, J. P. H. Burbach, J. H. Wokke, R. A. Ophoff, L. H. van den Berg, 2008, "Copy Number Variation In Sporadic Amyotrophic Lateral Sclerosis: A Genome-wide Screen", *Lancet Neurology*, Vol. 7, pp. 319-326.
- Boillé S., C. V. Velde and D. W. Cleveland, 2006, "ALS: A Disease of Motor Neurons and Their Nonneuronal Neighbors", *Neuron*, Vol. 52, pp. 39-59.
- Brannstrom, T., K. Ernhill, S. Marklund and P. Nilsson, 1998, "Transgenic Mice Homozygous for the Asp90Ala Human SOD-1 Mutation Develop ALS Clinically and Histologically", *The Society for Neuroscience*, pp. 188.1.
- Broom, W. J., C. Russ, P. C. Sapp, D. McKenna-Yasek, B. A. Hosler, P. M. Andersen and R. H. Brown Jr., 2006, "Variants in Candidate ALS Modifier Genes Linked to Cu/Zn Superoxide Dismutase Do Not Explain Divergent Survival Phenotypes", *Neuroscience Letters*, Vol. 392, pp. 52-57.
- Broom, W. J., D. V. Johnson, M. Garber, P. M. Andersen, N. Lennon, J. Landers, C. Nusbaum, C. Russ and R. H. Brown Jr., 2009, "DNA Sequence Analysis of the Conserved Region Around the SOD1 Gene Locus in Recessively Inherited ALS", *Neuroscience Letters*, Vol. 463, pp. 64-69.
- Brown, R. H. D., W. Robberecht, 2000, "Amyotrophic Lateral Sclerosis: Pathogenesis", *Seminars in Neurology*, Vol. 21, pp. 131-139.
- Brown, R. H., 1998, "SOD1 Aggregates in ALS: Cause, Correlate or Consequence?", *Nature Medicine*, Vol. 4, pp. 1362-1364.

- Bruijn, L.I., T. M. Miller and D. W. Cleveland, 2004, "Unraveling the Mechanisms Involved in Motor Neuron Degeneration in ALS.", *Annual Review of Neuroscience*, Vol. 27, pp. 723-749.
- Bryan J. T. and A. B. Singleton, 2009, "What's the FUS!", *Lancet Neurology*, Vol. 8, pp. 418-419.
- Buratti E and F. E. Baralle, 2001, "Characterization and Functional Implications of the RNA Binding Properties of Nuclear Factor TDP-43, a Novel Splicing Regulator of CFTR Exon 9", *The Journal of Biological Chemistry*, Vol. 276, pp. 36337-36643.
- Buratti E. and F. E. Baralle, 2009, "The Molecular Links Between TDP-43 Dysfunction and Neurodegeneration", *Advances in Genetics*, Vol. 66, pp. 1-34.
- Burkhardt, J. K., C. J. Echeverri, T. Nilsson and R. B. Vallee, 1997, "Overexpression of the Dynamitin (p50) Subunit of the Dynactin Complex Disrupts Dynein-dependent Maintenance of Membrane Organelle Distribution", *Journal of Cellular Biology*, Vol. 139, pp. 469-484.
- Cardon L. R and J. I. Bell, 2001, "Association Study Design for Complex Disorders", *Nature Review Genetics*, Vol. 2, pp.91-99.
- Chanock, S. J., T. Manolio, M. Boehnke, E. Boerwinkle, D. J. Hunter, G. Thomas, J. N. Hirschhorn, G. Abecasis, D. Altshuler, J. E. Bailey-Wilson, L. D. Brooks, L. R. Cardon, R. Lon, M. Daly, P. Donnelly, J.F. Fraumeni Jr., N.B.Freimer, D. S. Gerhard, C. Gunter, A. E. Guttmacher, M. S. Guyer, E. L. Harris, J. Hoh, R. Hoover, C. A. Kong, K. R. Merikangas, C. C. Morton, L. J. Palmer, E. G. Phimister, J. P. Rice, J. Roberts, C. Rotimi, M. A. Tucker, K. J. Vogan, S. Wacholder, E. M. Wijsman and D. M. Winn, 2007, "Replicating Genotype-phenotype Associations", *Nature*, Vol. 447, pp. 655-660.

- Charcot, J. M. and A. Joffroy, 1869, “Deux Cas D’atrophie Musculaire Progressive avec Lesions de la Substance Grise et des Faisceaux Antero-lateraux de la Moelle Epiniere”, *Archives of Physiology Neurology Pathology*, Vol. 2, pp. 744-754.
- Choi, M, U. I. Scholl, W. Ji, T. Liu, I. R. Tikhonova, P. Zumbo, A. Nayir, A. Bakkaloğlu, S. Ozen, S. Sanjad, C. Nelson-Williams, A. Farhi, S. Mane, R. P. Lifton, 2009, “Genetic Diagnosis by Whole Exome Capture and Massively Parallel DNA Sequencing”, *Proceedings of the National Academy of Sciences of the United States of America*, Vol. 106, pp. 19096-101.
- Chou, L. S., C. S. J. Liu, B. Boese, X. Zhang and R. Mao, 2009, “DNA Sequence Capture and Enrichment by Microarray Followed by Next-Generation Sequencing for Targeted Resequencing: Neurofibromatosis Type 1 Gene as a Model”, *Clinical Chemistry*, Vol. 56, pp. 1-11.
- Cindy, V. L. and P. Verstreken, 2006, “Mitochondria at the Synapse”, *Neuroscientist*, Vol. 12, pp. 291-299.
- Clement, A. M., M. D. Nguyen, E. A. Roberts, M. L. Garcia, S. Boillée, M. Rule, A. P. McMahon, W. Doucette, D. Siwek, R. J. Ferrante, R. H. Brown Jr., J. P. Julien, L. S. Goldstein and D. W. Cleveland, 2003, “Wild-type Nonneuronal Cells Extend Survival of SOD1 Mutant Motor Neurons in ALS Mice”, *Science*, Vol. 302, pp. 113-117.
- Cleveland, D. W. and J. R. Rothstein, 2001, “From Charcot to Lou Gehrig: Deciphering Selective Motor Neurons in ALS”, *Nature Reviews Neuroscience*, Vol. 2, pp. 806-814.
- Cleveland, D. W., 1999, “From Charcot to SOD1: Mechanisms of Selective Motor Neuron Death in ALS”, *Neuron*, Vol. 24, pp. 515-520.
- Cluskey, S. and D. B. Ramsden, 2001, “Mechanisms of Neurodegeneration in Amyotrophic Lateral Sclerosis”, *Molecular Pathology*, Vol. 54, pp. 386-392.

- Cole, N., T. Siddique, 1999, "Genetic Disorders of Motor Neurons", *Seminars in Neurology*, Vol. 19, pp. 407-418.
- Cook C., Y. J. Zhang , Y.F. Xu , D. W. Dickson and L. Petrucelli, 2008, "TDP-43 in Neurodegenerative Disorders", *Expert Opinion on Biological Therapy*, Vol. 8, pp. 969-978.
- Corrado, L., A. Ratti, C. Gellera, E. Buratti, B. Castellotti, Y. Carlomagno, N. Ticozzi, L. Mazzini, L. Testa, F. Taroni, F. E. Baralle, V. Silani and S. D'Alfonso, 2009, "High Frequency of TARDBP Gene Mutations in Italian Patients with Amyotrophic Lateral Sclerosis", *Human Mutations*, Vol. 30, pp. 688-694.
- Cote, F., J. F. Collard and J. P. Julien, 1993, "Progressive Neuronopathy in Transgenic Mice Expressing the Human Neurofilament Heavy Gene: a Mouse Model of Amyotrophic Lateral Sclerosis", *Cell*, Vol. 73, pp. 35-46.
- Couillard-Després, S., Q. Zhu, P. C. Wong, D. L. Price, D. W. Cleveland and J. P. Julien, 1998, "Protective Effect of Neurofilament Heavy Gene Overexpression in Motor Neuron Disease Induced by Mutant Superoxide Dismutase", *Proceedings of the National Academy of Sciences of the United States of America*, Vol. 95, pp. 9626-9630.
- Coyle, J. T. and P. Puttfarcken, 1993, "Oxidative Stress, Glutamate and Neurodegenerative Disorders", *Science*, Vol. 262, pp. 689-695.
- Cozzolino, M., A. Ferri, and M. T. Carri, 2008, "Amyotrophic Lateral Sclerosis: From Current Developments in the Laboratory to Clinical Implications", *Antioxidants & Redox Signaling*, Vol. 10, pp. 405-443.
- Dangond, F., D. Hwang, S. Camelo, Piera Pasinelli, M. P. Frosch, G. Stephanopoulos, R. H. Brown, Jr. and S. R. Gullans, 2003, "Molecular Signature of Late-stage Human ALS Revealed by Expression Profiling of Postmortem Spinal Cord Gray Matter", *Physiological Genomics*, Vol. 16, pp. 229-239.

- Deitch, J., G. M. Alexander, L. D. Vallea and T. D. Heinma-Patterson, 2002, "GLT-1 Glutamate Transporter Levels are Unchanged in Mice Expressing G93A Human Mutant SOD1", *Journal of the Neurological Sciences*, Vol. 193, pp. 117-126.
- Deng, H. X., A. Hentati, J. A. Tainer, Z. Iqbal, A. Cayabyab, W. Y. Hung, E. D. Getzoff, P. Hu, B. Herzfeldt, R. P. Roos, C. Warner, G. Deng, E. Soriano, C. Smyth, H. E. Parge, A. Ahmed, A. D. Roses, R. A. Hallewell, M. A. Pericak-Vance, T. Siddique, 1993, "Amyotrophic Laterla Sclerosis and Structurel Defects in Cu, Zn Superoxide Dismutase", *Science*, Vol. 261, pp. 1047-1051.
- Dion, P. A., H. Daoud and G. A. Rouleau, 2009, "Genetics of Motor Neuron Disorders: New Insights Into Pathogenic Mechanisms", *Nature Reviews Genetics*, Vol. 10, pp. 769-782.
- Dunckley, T., M. J. Huentelman, D. W. Craig, J. V. Pearson, S.Szelinger, K. Joshipura, R. F. Halperin, C. Stamper, K. R. Jensen, D. Letizia, S. E. Hesterlee, A. Pestronk, T. Levine, T. Bertorini, M. C. Graves, T. Mozaffar, C. E. Jackson, P. Bosch, A. McVey, A. Dick, R. Barohn, C. Lomen-Hoerth, J. Rosenfeld, D. T. O'Connor, K. Zhang, R. Crook, H. Ryberg, M. Hutton, J. Katz, E. P. Simpson, H Mitsumoto, R. Bowser, R. G. Miller, S. H. Appel and D. A. Stephan, 2007, "Whole-Genome Analysis of Sporadic Amyotrophic Lateral Sclerosis", *The New England Journal of Medicine*, Vol. 23, pp. 775- 788.
- Dupuis, L., M. de Tapia, F. René, B. Lutz-Bucher, J. W. Gordon, L. Mercken, L. Pradier and J. P. Loeffler, "Differential Screening of Mutated SOD1 Transgenic Mice Reveals Early Up-regulation of a Fast Axonal Transport Component in Spinal Cord Motor Neurons", *Neurobiology of Disease*, Vol. 7, pp. 274-285.
- Easton, D. F., K. A. Pooley, A. M. Dunning, P. D. Pharoah, D. Thompson, D. G. Ballinger, J. P. Struewing, J. Morrison, H .Field, R .Luben, N .Wareham, S .Ahmed, C. S. Healey, R. Bowman; SEARCH collaborators, K. B. Meyer, C. A. Haiman, L. K. Kolonel, B. E. Henderson, L. Le Marchand, P. Brennan, S. Sangrajrang, V. Gaborieau, F. Odefrey, C. Y. Shen, P. E. Wu, H. C. Wang, D .Eccles, D. G. Evans, J.

- Peto, O. Fletcher, N. Johnson, S. Seal, M. R. Stratton, N. Rahman, G. Chenevix-Trench, S. E. Bojesen, B. G. Nordestgaard, C. K. Axelsson, M. Garcia-Closas, L. Brinton, S. Chanock, J. Lissowska, B. Peplonska, H. Nevanlinna, R. Fagerholm, H. Eerola, D. Kang, K. Y. Yoo, D. Y. Noh, S. H. Ahn, D. J. Hunter, S. E. Hankinson, D. G. Cox, P. Hall, S. Wedren, J. Liu, Y. L. Low, N. Bogdanova, P. Schürmann, T. Dörk, R. A. Tollenaar, C. E. Jacobi, P. Devilee, J. G. Klijn, A. J. Sigurdson, M. M. Doody, B. H. Alexander, J. Zhang, A. Cox, I. W. Brock, G. MacPherson, M. W. Reed, F. J. Couch, E. L. Goode, J. E. Olson, H. Meijers-Heijboer, A. van den Ouweland, A. Uitterlinden, F. Rivadeneira, R. L. Milne, G. Ribas, A. Gonzalez-Neira, J. Benitez, J. L. Hopper, M. McCredie, M. Southey, G. G. Giles, C. Schroen, C. Justenhoven, H. Brauch, U. Hamann, Y. D. Ko, A. B. Spurdle, J. Beesley, X. Chen; kConFab; AOCs Management Group, A. Mannermaa, V. M. Kosma, V. Kataja, J. Hartikainen, N. E. Day, D. R. Cox and B. A. Ponder, 2007, "Genome-wide Association Study Identifies Novel Breast Cancer Susceptibility Loci.", *Nature*, Vol. 447, pp. 1087-93.
- Elliott, J. L., 2001, "Zinc and Copper in the Pathogenesis of Amyotrophic Lateral Sclerosis", *Progress Neuro-Psychopharmacology and Biological Psychiatry*, Vol. 25, pp. 1169-1185.
- Esterez, A. G. and J. Jordan, 2002, "Nitric Oxide and Superoxide, A Deadly Cocktail", *Annals New York Academy Sciences*, Vol. 962, pp. 207-211.
- Figlewicz, D. A., A. Krizus, M. G. Martinoli, V. Meininger, G. A. Rouleau and J. P. Julien, 1994, "Variants of the Heavy Neurofilament Subunit are Associated With the Development of Amyotrophic Lateral Sclerosis", *Human Molecular Genetics*, Vol. 3, pp. 1757-1761.
- Frayling, T. M., 2007, "Genome-wide Association Studies Provide New Insights Into Type 2 Diabetes Aetiology", *Nature Reviews Genetics*, Vol. 8, pp. 657-662.
- Fukada, Y., K. Yasui, M. Kitayama, K. Doi, T. Nakano, Y. Watanabe and K. Nakashima, 2007, "Gene Expression Analysis of the Murine Model of Amyotrophic Lateral

- Sclerosis: Studies of the Leu126delTT Mutation in SOD1”, *Brain Research*, Vol. 1160, pp. 1-10.
- Gal, J., K. R. Strom, F. Zhang and H. Zhu, 2007, “p62 Accumulates and Enhances Aggregate Formation in Model Systems of Familial Amyotrophic Lateral Sclerosis”, *Journal of Biological Chemistry*, Vol. 282, pp. 11068-11077.
- Génin, E., A. A. Todorov and F. Clerget-Darpoux, 1998, “Optimization of Genome Search Strategies For Homozygosity Mapping: Influence Of Marker Spacing On Power And Threshold Criteria For Identification Of Candidate Regions”, *Annals of Human Genetics*, Vol. 62, pp. 419-429.
- Getzoff, E. D., J. A. Tainer, M. M. Stempien, G. I. Bell, R. A. Hallewell, 1989, “Evolution of CuZn Superoxide Dismutase And The Greek Key β -barrel Structural Motif”, *Proteins*, Vol. 5, pp. 322-336.
- Gibbs, J. R. and A. Singleton, 2006, “Application of Genome-Wide Single Nucleotide Polymorphism Typing: Simple Association and Beyond”, *Public Library of Science Genetics*, Vol. 2, pp. 1511-1517.
- Gong, Y. H., A. S. Parsadarian, A. Andreeva, W. D. Snider and J. L. Elliott, 2000, “Restricted Expression of G86R Cu/Zn Superoxide Dismutase in Astrocytes Results in Astrocytosis but Does Not Cause Motoneuron Degeneration”, *Journal of Neuroscience*, Vol. 20, pp. 660-665.
- Gonzalez de Aguilar, J. L., A. Echaniz-Laguna, A. Fergani, F. René, V. Meininger, Epiniere”, *Archives of Physiology Neurology Pathology*, Vol. 2, pp. 744-754.
- Greenway, M. J., P. M. Andersen, C. Russ, S. Ennis, S. Cashman, C. Donaghy, V. Patterson, R. Swingler, D. Kieran, J. Prehn, K. E. Morrison, A. Green, K. R. Acharya, R. H. Brown Jr. and O. Hardiman, 2006, “ANG Mutations Segregate With Familial And ‘Sporadic’ Amyotrophic Lateral Sclerosis”, *Nature Genetics*, Vol. 38, pp. 410-413.

- Gwinn, K., R. A. Corriveau, H. Mitsumoto, K. Bednarz, R. H. Brown Jr., M. Cudkowicz, P. H. Gordon, J. Hardy, E. J. Kasarskis, P. Kaufmann, R. Miller, E. Sorenson, R. Tandan, B. J. Traynor, J. Nash, A. Sherman, M. D. Mailman, J. Ostell, L. Bruijn, V. Cwik, S. S. Rich, A. Singleton, L. Refolo, J. Andrews, R. Zhang, R. Conwit and M. A. Keller, for The ALS Research Group, 2007, "Amyotrophic Lateral Sclerosis: An Emerging Era of Collaborative Gene Discovery", *PloS One*, Vol. 2, pp. e1254.
- Hand, C. K. and G. A. Rouleau, 2002, "Familial Amyotrophic Lateral Sclerosis", *Muscle and Nerve*, Vol. 25, pp. 135-159.
- Hand, C. K., J. Khoris, F. Salachas, F. Gros-Louis, A. A. Simoes Lopes, V. Mayeux-Portas, C. G. Brewer, R. H. Brown Jr., V. Meininger, W. Camu, G. A. Rouleau, 2002, "A Novel Locus For Familial Amyotrophic Lateral Sclerosis, On Chromosome 18q", *American Journal of Human Genetics*, Vol. 70, pp. 251-256.
- Hardiman, O, 2004, "A Novel Candidate Region for ALS on Chromosome 14q11.2", *Neurology*, Vol. 63, pp. 1936-1938.
- Harris, H., D. A. Hopkinson and E. B. Robson, 1974, "The Incidence of Rare Alleles Determining Electrophoretic Variants: Data on 43 Enzyme Loci", *Human Genetics*, Vol. 37, pp. 237-253.
- Hayward, C. and D. J. H. Brock, 1998, "Homozygosity For Asn86Ser Mutation in the CuZn-superoxide Dismutase Gene Produces a Severe Clinical Phenotype in a Juvenile Onset Case of Familial Amyotrophic Lateral Sclerosis", *Journal of Medical Genetics*, Vol. 35, pp. 174-176.
- Hayward, C., R. A. Minns, R. J. Swingler and D. J. H. Brock, 1997, "A Juvenile Onset Case of Familial Amyotrophic Lateral Sclerosis Associated with Homozygosity for a Mutation in the CuZn-Superoxide Dismutase Gene.", *In Proceedings of the 8th International Symposium on ALS/MND*, Abstract Booklet, pp. 109 (abstract).

- Heath, P.R. and P. J. Shaw, 2002, "Update on the Glutamatergic Neurotransmitter System and the Role of Excitotoxicity in Amyotrophic Lateral Sclerosis", *Muscle & Nerve*, Vol. 26, pp. 438-458.
- Henrichsen, C. N., E. Chaignat and A. Reymond, 2009, "Copy Number Variants, Diseases and Gene Expression", *Human Molecular Genetics*, Vol. 18, pp. R1–R8.
- Hervias, I., M. F. Beal and G. Manfredi, 2006, "Mitochondrial Dysfunction And Amyotrophic Lateral Sclerosis", *Muscle & nerve*, Vol. 33, pp. 598-608.
- Hirokawa, N, 2000, "Stirring Up Development With the Heterotrimeric Kinesin KIF3", *Traffic*, Vol. 1, pp. 29-34.
- Hirokawa, N. and Y. Noda, "Intracellular Transport and Kinesin Superfamily Proteins, KIFs: Structure, Function and Dynamics", *Physiological Reviews*, Vol. 88, pp. 1089-1118.
- Horswell, S. D., Ringham H. E. and C. C. Shoulders, 2009, "New Technologies for Delineating and Characterizing the Lipid Exome: Prospects for Understanding Familial Combined Hyperlipidemia", *Journal of Lipid Research*, Vol. 50, pp. S370-S375.
- Hosler, B. A., T. Siddique, P. C. Sapp, W. Sailor, M. C. Huang, A. Hossain, J. R. Daube, M. Nance, C. Fan, J. Kaplan, W. Y. Hung, D. McKenna-Yasek, J. L. Haines, M. A. Pericak-Vance, H. R. Horvitz and R. H. Brown Jr., 2000, "Linkage Of Familial Amyotrophic Lateral Sclerosis With Frontotemporal Dementia To Chromosome 9q21-q22", *JAMA*, Vol. 284, pp. 1664-1669.
- Hunter, D. J., D. Altshuler and D. J. Rader, 2008, "From Darwin's Finches To Canaries In The Coal Mine- Mining The Genome For New Biology", *New England Journal of Medicine*, Vol. 358, pp. 2760-2763.

- Ionita-Laza, I., A. J. Rogers, C. Lange, B. A. Raby and C. Lee, 2009, "Genetic Association Analysis Of Copy Number Variation (CNV) In Human Disease Pathogenesis", *Genomics*, Vol. 93, pp. 22-26.
- Jaarsma, D., F. Rognoni, W. Duijn, H. W. Verspaget, E. D. Haasdijk and J. C. Holstege, 2001, "CuZn Superoxide Dismutase (SOD1) Accumulates in Vacuolated Mitochondria in Transgenic Mice Expressing Amyotrophic Lateral Sclerosis-Linked SOD1 Mutations", *Acta Neuropathologica*, Vol. 102, pp. 293-305.
- Johnson, G. C., L. Esposito, B. J. Barratt, A. N. Smith, J. Heward, G. Di Genova G, H. Ueda, H. J. Cordell, I. A. Eaves, F. Dudbridge, R. C. Twells, F. Payne, W. Hughes, S. Nutland, H. Stevens, P. Carr, E. Tuomilehto-Wolf, J. Tuomilehto, S. C. Gough, D. G. Clayton and J. A. Todd, 2001, "Haplotype Tagging for the Identification of Common Disease Genes", *Nature Genetics*, Vol. 29, pp. 233-237.
- Johnston, J. A., M. E. Illing and R. R. Kopito, 2002, "Cytoplasmic Dynein/dynactin Mediates the Assembly of Aggresomes", *Cell Motility and Cytoskeleton*, Vol. 53, pp. 26-38.
- Jonsson, P. A., A. Bäckstrand, P. M. Andersen, J. Jacobsson, M. Parton, C. Shaw, R. Swingler, P. J. Shaw, W. Robberecht, A. C. Ludolph, T. Siddique, V. I. Skvortsova and S. L. Marklund, 2002, "CuZn-Superoxide Dismutase in D90A Heterozygotes From Recessive and Dominant ALS Pedigrees", *Neurobiology of Disease*, Vol. 10, pp. 327-333.
- Jonsson, P. A., K. S. Graffmo, P. M. Andersen, S. L. Marklund and T. Brännström, 2009, "Superoxide Dismutase in Amyotrophic Lateral Sclerosis Patients Homozygous for the D90A Mutation", *Neurobiology of Disease*, Vol. 36, pp. 421- 424.
- Jonsson, P. A., A. Bäckstrand, P. M. Andersen, J. Jacobsson, M. Parton, C. Shaw, R. Swingler, P. J. Shaw, W. Robberecht, A. C. Ludolph, T. Siddique, V. I. Skvortsova and S. L. Marklund, 2002, "CuZn-superoxide Dismutase in D90A Heterozygotes

From Recessive and Dominant ALS Pedigrees”, *Neurobiology of Disease*, Vol. 10, pp. 327-33.

Jonsson, P. A., K. S. Graffmo, T. Brannstrom, P. Nilsson, P. M. Andersen and S. L. Marklund, “Motor Neuron Disease in Mice Expressing the Wild Type-like D90A Mutant Superoxide Dismutase-1”, *Journal of Neuropathology & Experimental Neurology*, Vol. 65, pp. 1126-1136.

Julien, J. P. and J. M. Beaulieu, 2000, “Cytoskeletal Abnormalities in Amyotrophic Lateral Sclerosis: Beneficial or Detrimental Effects?”, *Journal of Neurological Sciences*, Vol. 180, pp. 7-14.

Julien, J. P., 2001, “Amyotrophic Lateral Sclerosis: Unfolding the Toxicity of the Misfolded”, *Cell*, Vol. 104, pp. 581-591.

Julien, J. P., 2007, “ALS: Astrocytes Move in as Deadly Neighbors”, *Nature Neuroscience*, Vol. 10, pp. 535- 537.

Kang, J. H. and W. S. Eum, 2000, “Enhanced Oxidative Damage by the Familial Amyotrophic Lateral Sclerosis-Associated Cu,Zn-Superoxide Dismutase Mutants”, *Biochimica et Biophysica Acta*, Vol. 1524, pp. 162-170.

Kieran, D. M., M. Greenway, O. Hardiman and J. Prehn, 2005, “The Effects of Angiogenin on Motor Neuron Degeneration”, *Amyotrophic Lateral Sclerosis and Other Motor Neuron Disorders*, Vol. 6, pp. 42-45.

Kishikawa, H., D. Wu and G. Hu, 2008, “Central & Peripheral Nervous Systems Targeting Angiogenin in Therapy of Amyotrophic Lateral Sclerosis”, *Expert Opinion on Therapeutic Targets*, Vol. 12, pp. 1229-1242.

Klein RJ, C. Zeiss, E. Y. Chew, C. Zeiss, E. Y. Chew, J. Y. Tsai, R. S. Sackler, C. Haynes, A. K. Henning, J. P. SanGiovanni, S. M. Mane, S. T. Mayne, M. B. Bracken, F. L.

- Ferris, J. Ott, C. Barnstable and J. Hoh, 2005, "Complement Factor H Polymorphism in Age related Macular Degeneration.", *Science*, Vol. 308, pp. 385-359.
- Kong, J., Z. Xu, 1998, "Massive Mitochondrial Degeneration in Motor Neurons Triggers the Onset of Amyotrophic Lateral Sclerosis in Mice Expressing a Mutant SOD1", *The Journal of Neuroscience*, Vol. 18, pp. 3241-3250.
- Kurahashi, K., T. Okushima, K. Kimura, S. Narita and M. Matsunaga, 1993, "Different Phenotype and Clinical Course in a Family with Motor Neurone Disease", *Medical Journal of Aomori City Hospital*, Vol. 38, pp. 142-146.
- Kwong, J. Q., M. F. Beal and G. Manfredi, 2006, "The Role of Mitochondria in Inherited Neurodegenerative Diseases", *Journal of Neurochemistry*, Vol. 97, pp. 1659-1675.
- Lacomblez, L, G. Bensimon, P. N. Leigh, P. Guillet, L. Powe, S. Durrleman, J. C. Delumeau and V. Meininger, 1996, "A confirmatory Dose-ranging Study of Riluzole in ALS. ALS/Riluzole Study Group-II", *Neurology*, Vol. 47, pp. S242-S250.
- Laird, F. M., 2005, " Neuronal Expression of an ALS-associated Mutation Dynactin P150 Glued in Mice Causes Motor Neuron Disease", *Amyotrophic Lateral Sclerosis and Other Motor Neuron Disorders*, Vol. 6, pp. 22-23.
- Lambrechts, D., P. Lafuste, P. Carmeliet and E. M. Conway, "Another Angiogenic Gene Linked To Amyotrophic Lateral Sclerosis", *Trends in Molecular Medicine*, Vol.12, pp. 345-347.
- Landers, J. E., J. Melki, V. Meininger, J. D. Glass, L. H. van den Berg, M. A. van Es, P. C. Sapp, P. W. J. van Vught, D. M. McKenna-Yasek, H. M. Blauw, T. Cho, M. Polak, L. Shi, A. M. Wills, W. J. Broom, N. Ticozzi, V. Silani, A. Ozoguz, I. Rodriguez-Leyva, J. H. Veldink, A. J. Iverson, C. G. J. Saris, B. A. Hosler, A. Barnes-Nessa, N. Couture, J. H. J. Wokke, T. J. Kwiatkowski, Jr., R. A. Ophoff, S. Cronin, O. Hardiman, F. P. Diekstra, P. N. Leigh, C. E. Shaw, C. L. Simpson, V. K. Hansen, J. F. Powell, P. Corcia, F. Salachas, S. Heath, P. Galan, F. Georges, H. R. Horvitz, M.

- Lathrop, S. Purcell, A. Al-Chalabi and R. H. Brown, Jr, 2009, “Reduced Expression of the Kinesin-Associated Protein 3 (KIFAP3) Gene Increases Survival in Sporadic Amyotrophic Lateral Sclerosis” *Proceedings of the National Academy of Sciences of the United States of America*, Vol. 106, pp. 9004–9009.
- Lederer, C. W., A. Torrisi, M. Pantelidou, N. Santama and S. Cavallaro, 2007, “Pathways and Genes Differentially Expressed in the Motor Cortex of Patients with Sporadic Amyotrophic Lateral Sclerosis”, *BMC Genomics*, Vol. 8, pp. 26.
- Lee, M. K., J. R. Marszalek and D. W. Cleveland, 1994, “A Mutant Neurofilament Subunit Causes Massive, Selective Motor Neuron Death: Implications For The Pathogenesis of Human Motor Neuron Disease”, *Neuron*, Vol. 13, pp. 975-988.
- Lenaz, G., 1998, “Role of mitochondria in oxidative stress and ageing”, *Biochimica et Biophysica Acta*, Vol. 1366, pp.53-67.
- Lin C.L., L. A. Bristol, L. Jin, M. Dykes-Hoberg, T. Crawford, L. Clawson and J. D. Rothstein, 1998, “Aberrant RNA Processing in a Neurodegenerative Disease: The Cause for Absent EAAT2, a Glutamate Transporter, in Amyotrophic Lateral Sclerosis.”, *Neuron*, Vol. 20, pp. 589-602.
- Liochev, S. and I. Fridovich, 2003, “Mutant Cu, Zn Surepoxide Dismutase and Familial Amyotrophic Lateral Sclerosis: Evaluation of Oxidative Hypotheses”, *Free Radical Biology & Medicine*, Vol. 34, pp. 1383-1389.
- Lobsiger C. S. and D. W. Cleveland, 2007, “Glial Cells as Intrinsic Components of Non-cell-autonomous Neurodegenerative Disease.”, *Nature Neuroscience*, Vol. 10, pp. 1355-1360.
- Loeffler, J. P. and L. Dupuis, 2007, “Amyotrophic Lateral Sclerosis: All Roads Lead to Rome”, *Journal of Neurochemistry*, Vol. 101, pp. 1153-1160.

- Magrané J. and G. Manfredi, 2009, "Mitochondrial Function, Morphology, and Axonal Transport in Amyotrophic Lateral Sclerosis", *Antioxidant Redox Signalling*, Vol. 11, pp. 1615-1626.
- Manfredia, G. and X. Zuoshang, 2005, "Mitochondrial dysfunction and its role in motor neuron degeneration in ALS", *Mitochondrion*, Vol. 5, pp. 77-87.
- Maragakis, N. J. and J. D. Rothstein, 2001, "Glutamate Transporters in Neurologic Disease", *Archives of Neurology*, Vol. 58, pp. 365-370.
- Maragakis, N.J., M. Dykes-Hoberg, and J. D. Rothstein, 2004, "Altered Expression of the Glutamate Transporter EAAT2b in Neurological Disease.", *Annals of Neurology*, Vol. 55, pp. 469-477.
- Marinou, M. Sabatelli, A. Conte, J. Mandrioli, P. Sola, F. Salvi, I. Bartolomei, G. Siciliano, C. Carlesi, R. W. Orrell, K. Talbot, Z. Simmons, J. Connor, E. P. Piro, T. Dunkley, D. A. Stephan, D. Kasperaviciute, E. M. Fisher, S. Jabonka, M. Sendtner, M. Beck, L. Bruijn, J. Rothstein, S. Schmidt, A. Singleton, J. Hardy and B. J. Traynor, 2009, "A Two-stage Genome-wide Association Study of Sporadic Amyotrophic Lateral Sclerosis", *Human Molecular Genetics*, Vol. 18, pp. 1524-1532.
- McCarroll, S. A. and David M Altshuler, 2007, "Copy-number Variation and Association Studies of Human Disease", *Nature Genetics Supplement*, Vol. 39, pp. 537-542.
- McCarroll, S. A., 2008, "Extending Genome-wide Association Studies To Copy Number Variation", *Human Molecular Genetics*, Vol. 17, pp. R135-R142.
- McPherson, R., A. Pertsemlidis, N. Kavaslar, A. Stewart, R. Roberts, D. R. Cox, D. A. Hinds, L. A. Pennacchio, A. Tybjaerg-Hansen, A. R. Folsom, E. Boerwinkle, H. H. Hobbs and J. C. Cohen, 2007, "A Common Allele on Chromosome 9 Associated with Coronary Heart Disease", *Science*, Vol. 8, pp.1488- 1491.

- Meininger, C. J., R. S. Marinos, K. Hatakeyama, R. Martinez-Zaguilan, J. D. Rojas, K. A. Kelly and G. Wu, 2000, "Impaired Nitric Oxide Production in Coronary Endothelial Cells of the Spontaneously Diabetic BB Rat is Due to Tetrahydrobiopterin Deficiency.", *Biochemical Journal*, Vol. 349, pp. 353-356.
- Mendonca, D. M. F., L. Chimelli, and A. M. B. Martinez, 2006, "Expression of Ubiquitin and Proteasome in Motorneurons and Astrocytes of Spinal Cords from Patients with Amyotrophic Lateral Sclerosis", *Neuroscience Letters*, Vol. 404, pp. 315-319.
- Menzies, F. M., M. R. Cookson, R. W. Taylor, D. M. Turnbull, Z. M. Chrzanowska-Lightowlers, L. Dong, D. A. Figlewicz and P. J. Shaw, 2002, "Mitochondrial Dysfunction in a Cell Culture Model of Familial Amyotrophic Lateral Sclerosis", *Brain*, Vol. 125, pp. 1522-1533.
- Menzies, F. M., P. G. Ince and P. J. Shaw, 2002, "Mitochondrial Involvement in Amyotrophic Lateral Sclerosis", *Neurochemistry International*, Vol. 40, pp. 543-551.
- Menzies, F. M., P. G. Ince and P. J. Shaw, 2002, "Mitochondrial Involvement in Amyotrophic Lateral Sclerosis", *Neurochemistry International*, Vol. 40, pp. 543-551.
- Miki, H., M. Setou, K. Kaneshiro and N. Hirokawa, 2001, "All Kinesin Superfamily Protein, KIF, Genes in Mouse and Human", *Proceedings of the National Academy of Sciences of the United States of America*, Vol. 98, pp. 7004-7011.
- Morohoshi, F., Y. Ootsuka, K. Arai, H. Ichikawa, S. Mitani, N. Munakata and M. Ohki, 1998, "Genomic Structure of The Human RBP56/hTAFII68 and FUS/TLS Genes", *Gene*, Vol. 221, pp. 191-198.
- Morrison, B. M., I. W. Shu, A. L. Wilcox, J. W. Gordon and J. H. Morrison, 2000, "Early and Selective Pathology of Light Chain Neurofilament in the Spinal Cord and Sciatic Nerve of G86R Mutant Superoxide Dismutase Transgenic Mice", *Experimental Neurology*, Vol. 165, pp. 207-220.

- Mougeot, J. L., S. Richardson-Milazi and B. Rix Brooks, 2009, "Whole-genome Association Studies of Sporadic Amyotrophic Lateral Sclerosis: Are Retroelements Involved?", *Trends in Molecular Medicine*, Vol.15, pp. 148- 158.
- Mullen, S. A., D. E. Crompton, P. W. Carney, I. Helbig and S. F. Berkovic, 2009, "A Neurologist's Guide to Genome-wide Association Studies", *Neurology*, Vol. 72, pp. 558-565.
- Neusch, C., M. Bahr and C. Schneider-Gold, 2007, "Glia Cells in Amyotrophic Lateral Sclerosis: New Clues to Understanding an Old Disease?", *Muscle Nerve*, Vol. 35, pp. 712-724.
- Nevanlinna, H. R., 1972, "The Finnish Population Structure: A Genetic and Genealogical Study", *Hereditas*, Vol. 71, pp.195-236.
- Ng, S. B., E. H. Turner, P. D. Robertson, S. D. Flygare, A. W. Bigham, C. Lee, T. Shaffer, M. Wong, A. Bhattacharjee, E. E. Eichler, M. Bamshad, D. A. Nickerson and J. Shendure, 2009, "Targeted Capture and Massively Parallel Sequencing of 12 Human Exomes", *Nature*, Vol. 461, pp. 272-276.
- Ng, S. B., K. J. Buckingham, C. Lee, A. W. Bigham, H. K. Tabor, K. M. Dent, C. D. Huff, P. T. Shannon, E. W. Jabs, D. A. Nickerson, J. Shendure and M. J. Bamshad, 2009, "Exome Sequencing Identifies the Cause of a Mendelian Disorder", *Nature Genetics*, Vol. 13, pp. 1-7.
- Orrell, R. W., S. L. Marklund and J. S. deBellerocche, 1997, "Familial ALS Is Associated With Mutations in All Exons of SOD1: A Novel Mutation In Exon 3 (Gly72Ser)", *Journal of the Neurological Sciences*, Vol. 153, pp. 46-49.
- Özoğuz, A., R. M. Güzel and A. N. Başak, 2005, "Amiyotrofik Lateral Skleroz'un Moleküler Biyolojisi", *Türk Nöroloji Dergisi*, Vol 11/2, pp. 1-20.

- Pantelidou, M., S. E. Zographos, W. L. Carsten Lederer, T. Kyriakides, M. W. Pfaffl and N. Santamaa, 2007, "Differential Expression of Molecular Motors in the Motor Cortex of Sporadic ALS", *Neurobiology of Disease*, Vol. 26, pp. 577-589.
- Parton, M. J., W. Broom, P. M. Andersen, A. Al-Chalabi, P. N. Leigh, J. F. Powell and C. E. Shaw; D90A SOD1 ALS Consortium, 2002, "D90A-SOD1 Mediated Amyotrophic Lateral Sclerosis: A Single Founder for All Cases With Evidence for a Cis-acting Disease Modifier in the Recessive Haplotype", *Human Mutation: Mutation in Brief*, Vol. 20, pp. 473-481.
- Pasinelli, P. and R. H. Brown, 2006, "Molecular Biology of Amyotrophic Lateral Sclerosis: Insights From Genetics", *Nature Review Neurology*, Vol. 7, pp. 710-723.
- Pearson, T.A. and T. A. Manolio, 2008, "How to interpret a genome-wide association study", *JAMA*, Vol. 299, pp. 1335-44.
- Pesiridis, G. S., M. Virginia, Y. Lee and J. Q. Trojanowski, 2009, "Mutations in TDP-43 Link Glycine-rich Domain Functions to Amyotrophic Lateral Sclerosis", *Human Molecular Genetics*, Vol. 18, pp. R156-R162.
- Pramatarova, A., J. Laganier, J. Roussel, K. Brisebois and G. Rouleau, 2001, "Neuron-Specific Expression of Mutant Superoxide Dismutase 1 in Transgenic Mice Does not Lead to Motor Impairment", *Journal of Neuroscience*, Vol. 21, pp. 3369-3374.
- Puls, I., C. Jonnakuty, B. H. La Monte, E. L. Holzbaur, M. Tokito, E. Mann, M. K. Floeter, K. Bidus, D. Drayna, S. J. Oh, R. H. Brown JR., C. L. Ludlow and K. H. Fischbeck, 2003, "Mutant Dynactin in Motor Neuron Disease", *Nature Genetics*, Vol. 33, pp. 455-456.
- Purcell, S., B. Neale, K. Todd-Brown, L. Thomas, M. A. R. Ferreira, D. Bender, J. Maller, P. Sklar, P. I. W. de Bakker, M. J. Daly and Pak C. Sham, 2007, "PLINK: A Tool Set for Whole-Genome Association and Population-based Linkage Analyses", *The American Journal of Human Genetics*, Vol. 81, pp. 559-575.

- Ravits, J. M. and A. R. La Spada, 2009, "ALS Motor Phenotype Heterogeneity, Focality, and Spread", *Neurology*, Vol. 73, pp. 805-811.
- Ravits, J., P. Paul and C. Jorg, 2007, "Focality of Upper and Lower Motor Neuron Degeneration at the Clinical Onset of ALS", *Neurology*, Vol. 68, pp. 1571-1575.
- Reich, D. E. and E. S. Lander, 2001, "On the Allelic Spectrum of Human Disease", *Trends in Genetics*, Vol. 17, 502-510.
- Reich, D. E., S. F. Schaffner, M. J. Daly, G. McVean, J. C. Mullikin, J. M. Higgins, D. J. Richter, E. S. Lander and D. Altshuler, "Human Genome Sequence Variation and the Influence of Gene History, Mutation and Recombination", *Nature Genetics*, Vol. 32, pp. 135-142.
- Reynolds, I. J., 1999, "Mitochondrial Membrane Potential and the Permeability Transition in Excitotoxicity", *Annals of the New York Academy of Sciences*, Vol. 893, pp. 33-41.
- Robberecht, W., 2000, "Genetics of Amyotrophic Lateral Sclerosis", Vol. 247, Suppl. 6, pp.VI/2-VI/6.
- Robberecht, W., T. Aguirre, L. Van Den Bosch, P. Tilkin, J.J. Cassiman and G. Matthijs, 1996, "D90A Heterozygosity in the SOD1 Gene is Associated with Familial and Apparently Sporadic Amyotrophic Lateral Sclerosis", *Neurology*, Vol. 47, pp. 1336-1339.
- Roman G.C., 1996, "Neuroepidemiology of Amyotrophic Lateral Sclerosis: Clues to Etiology and Pathogenesis.", *Journal of Neurology, Neurosurgery and Psychiatry*, Vol. 61, pp. 131-137.
- Rosen, D.R., T. Siddique, D. Patterson, d. a. Figlewicz, P. Sapp, A. Hentati, D. Donaldson, J. Goto, J. P. O'Regan, H. -X. Deng, Z. Rahmani, A. Krizus, D. Mckenna-Yasek, A.

- Cayabyab, S. M. Gaston, R. Berger, R. E. Tanzi, J. J. Halperin, B. Herzfeldt, R. V. den Bergh, W.-Y Hung, T. Bird, G. Deng, D. W. Mulder, 1993, "Mutations in Cu/Zn Superoxide Dimutase Gene are Associated with Familial Amyotrophic Lateral Sclerosis", *Nature*, Vol. 362, pp. 59-62.
- Ross C. A. and A. P. Michelle, 2005, "What is the Role of Protein Aggregation in Neurodegeneration?", *Nature Reviews*, Vol. 6, pp. 891-898.
- Rowland, L. P. and N. A. Shneider, 2001, "Amyotrophic Lateral Sclerosis", *The New England Journal of Medicine*, Vol. 344, pp. 1688-1700.
- Sasaki, S. and M. Iwata, 1996, "Impairment of Fast Axonal Transport In The Proximal Axons of Anterior Horn Neurons in Amyotrophic Lateral Sclerosis", *Neurology*, Vol. 47, pp. 535-540.
- Schymick, J. C., S. W. Scholz, H. C. Fung, A. Britton, S. Arepalli, J. R. Gibbs, F. Lombardo, M. Matarin, D. Kasperaviciute, D. G. Hernandez, C. Crews, L. Bruijn, J. Rothstein, G. Mora, G. Restagno, A. Chiò, A. Singleton, J. Hardy and B. J. Traynor, 2007, "Genome-wide Genotyping in Amyotrophic Lateral Sclerosis and Neurologically Normal Controls: First Stage Analysis and Public Release of Data", *Lancet Neurology*, Vol. 6, pp. 322- 328.
- Sebat, J., B. Lakshmi, J. Troge, J. Alexander, J. Young, P. Lundin, S. Månér, H. Massa, M. Walker, M. Chi, N. Navin, R. Lucito, J. Healy, J. Hicks, K. Ye, A. Reiner, T. C. Gilliam, B. Trask, N. Patterson, A. Zetterberg and M. Wigler, 2004, "Large-scale Copy Number Polymorphism in the Human Genome", *Science*, Vol. 305, pp. 525-528.
- Seelow, D., M. Schuelke, F. Hildebrandt and P. Nürnberg, 2009, "HomozygosityMapper- An Interactive Approach To Homozygosity Mapping", *Nucleic Acids Research*, Vol. 37, pp. W593-W599.

- Sham, P. C., S. S. Cherny, P. Y. P. Kao, Y. Q. Song, D. Chan and K. M. C. Cheung, 2008, "Whole-genome Association Studies of Complex Diseases", *Current Orthopaedics*, Vol. 22, pp. 251- 258.
- Shaw B. F. and J. S. Valentine, 2007, "How do ALS-associated mutations in Superoxide Dismutase 1 Promote Aggregation of the Protein?", *Trends in Biochemical Sciences*, Vol. 32, pp. 78-85.
- Shaw, P. J., 2001, "Genetic Inroads in Familial ALS", *Nature Genetics*, Vol. 29, pp. 103-104.
- Shi, J., Y. Wang and W. Huang, 2009, "Development and Application of Genotyping Technologies", *Science in China Series C Life Sciences*, Vol. 52, pp. 17-23.
- Siddique, T. and H. X. Deng, 1996, "Genetics of Amyotrophic Lateral Sclerosis", *Human Molecular Genetics*, Vol. 5, pp. 1465-1470.
- Siddique, T., D. Nijhawan, A. Hentati, 1996, "Molecular Genetic Basis of Familial ALS", *Neurology*, Vol. 47, pp. 27-35.
- Siddique, T., H. X. Deng, 1996, "Genetics of Amyotrophic Lateral Sclerosis", *Human Molecular Genetics*, Vol. 5, pp. 1465-1470.
- Simpson C. L. and A. Al-Chalabi, 2006, "Amyotrophic Lateral Sclerosis as a Complex Genetic Disease", *Biochimica et Biophysica Acta*, Vol. 1762, pp. 973-985.
- Sjalander, A., G. Beckman, H. X. Deng, Z. Iqbal, J. A. Tainer and T. Siddique, 1997, "The D90A Mutation Results in a Polymorphism of Cu, Zn Superoxide Dismutase that is Prevalent in Northern Sweden and Finland", *Human Molecular Genetics*, Vol. 4, pp.1105-1108.
- Slegers, K. and C. van Broeckhoven, 2009, "Rogue Gene in the Family", *Nature*, Vol. 458, pp. 415-417.

- Staats, K. A. and L. Van Den Bosch, 2009, "Astrocytes in Amyotrophic Lateral Sclerosis: Direct Effects on Motor Neuron Survival", *Journal of Biological Physics*, Vol. 35, pp. 337-346.
- Strom, A. L., G. Jozsef, P. Shi, E. J. Kasarskis, L. J. Hayward and H. Zhu, 2008, "Retrograde Axonal Transport and Motor Neuron Disease", *Journal of Neurochemistry*, Vol. 106, pp. 495-505.
- Strong, M. J., 2003, "The Basic Aspects of Therapeutics in Amyotrophic Lateral Sclerosis", *Pharmacology and Therapeutics*, Vol. 98, pp. 379-414.
- Strunk, K. E., V. Amann and D. W. Threadgill, 2004, "Phenotypic Variation Resulting From a Deficiency of Epidermal Growth Factor Receptor in Mice Is Caused by Extensive Genetic Heterogeneity That Can Be Genetically and Molecularly Partitioned", *Genetics*, Vol. 167, 1821-1832.
- Subramaniam, J.R., W.E. Lyons, J. Liu, T.B. Bartnikas, J. Rothstein, D.L. Price, D.W. Cleveland, J.D. Gitlin and P.C. Wong, 2002, "Mutant SOD1 Causes Motor Neuron Disease Independent of Copper Chaperone-mediated Copper Loading", *Nature Neuroscience*, Vol. 5, pp. 301-307.
- Takeda, S., H. Yamazaki, D. H. Seog, Y. Kanai, S. Terada, N. Hirokawa, 2000, "Kinesin Superfamily Protein 3 (KIF3) Motor Transports Fodrin-associating Vesicles Important for Neurite Building", *Journal of Cell Biology*, Vol. 148, pp. 1255-1265.
- Tateno, M., H. Sadakata, M. Tanaka, S. Itohara, R. M. Shin, M. Miura, M. Masuda, T. Aosaki, M. Urushitani, H. Misawa and R. Takahashi, 2004, "Calcium-permeable AMPA Receptors Promote Misfolding of Mutant SOD1 Protein and Development of Amyotrophic Lateral Sclerosis in a Transgenic Mouse Model", *Human Molecular Genetics*, Vol. 13, pp. 2183-2196.

- Tateno, M., S. Kato, T. Sakurai, N. Nukina, R. Takahashi and T. Araki, 2009, "Mutant SOD1 impairs axonal transport of choline acetyltransferase and acetylcholine release by sequestering KAP3", *Human Molecular Genetics*, Vol. 18, pp. 942-955.
- Taylor, J. P., F. Tanaka, J. Robitschek, C. M. Sandoval, A. Taye, S. Markovic-Plese and K. H. Fischbeck, 2003, "Aggresomes Protect Cells by Enhancing the Degradation of Toxic Polyglutamine-containing Protein", *Human Molecular Genetics*, Vol. 12, pp. 749-757.
- Ticozzi N., V. Silani, A.L. LeClerc, P. Keagle, C. Gellera, A. Ratti, F. Taroni, T.J. Kwiatkowski JR., D.M. McKenna-Yasek, P.C. Sapp, R.H. Brown, JR., D. Phil and J.E. Landers, 2009, "Analysis of FUS Gene Mutation in Familial Amyotrophic Lateral Sclerosis within an Italian Cohort", *Neurology*, Vol. 73, pp.1-6.
- Tourenne, C. L. and D. W. Cleveland, 2009, "Rethinking ALS: The FUS about TDP-43", *Cell*, Vol. 20, pp. 1001-1004.
- Traynor, B. J. and A. Singleton, 2007, "Genome-wide Association Studies and ALS: Are We There Yet?", *Neurology*, Vol. 6, pp. 841-843.
- Turner, E. H., S. B. Ng, D. A. Nickerson and J. Shendure, 2009, "Methods for Genomic Partitioning", *The Annual Review of Genomics and Human Genetics*, Vol. 10, pp. 263-284.
- Urushitani M., J. Kurisu, K. Tsukita, and R. Takahashi, 2002, "Proteasomal Inhibition by Misfolded Mutant Superoxide Dismutase 1 Induces Selective Motor Neuron Death in Familial Amyotrophic Lateral Sclerosis.", *Journal of Neurochemistry*, Vol. 83, pp. 1030-1042.
- Valentine, J. S., P. J. Hart and E. B. Gralla, 1999, "Copper-zinc Superoxide Dismutase and ALS", *Advances in Experimental Medicine and Biology*, Vol. 448, pp.193-203.

- van Damme, P., L. Van Den Bosch, E. Van Houtte, G. Callewaert and W. Robberecht, 2002, "GluR2-dependent Properties of AMPA Receptors Determine the Selective Vulnerability of Motor Neurons To Excitotoxicity", *Journal of Neurophysiology*, Vol. 88, pp. 1279-1287.
- van Damme, P. and W. Robberecht, 2009, "Recent Advances in Motor Neuron Disease", *Current Opinion in Neurology*, Vol. 22, pp. 486-492.
- van Den Bosch, L. and W. Robberecht, 2008, "Crosstalk Between Astrocytes and Motor Neurons: What is The Message?", *Experimental Neurology*, Vol. 211, pp. 1-6.
- van Den Bosch, L. and W. Robberecht, 2008, "Crosstalk between astrocytes and motor neurons: What is the message?", *Experimental Neurology*, Vol. 211, pp. 1-6.
- van Den Bosch, L., P. Van Damme, E. Bogaert and W. Robberecht, 2006, "The Role of Excitotoxicity in the Pathogenesis of Amyotrophic Lateral Sclerosis", *Biochimica et Biophysica Acta*, Vol. 1762, pp. 1068-1082.
- van Es, M. A., J. H. Veldink, C. G. J. Saris, H. M. Blauw, P. W. J. van Vught, A. Birve, R. Lemmens, H. J. Schelhaas, E. J. N. Groen, M. H. B. Huisman, A. J. van der Kooi, M. de Visser, C. Dahlberg, K. Estrada, F. Rivadeneira, A. Hofman, M. J. Zwarts, P. T. C. van Doormaal, D. Rujescu, E. Strengman, I. Giegling, P. Muglia, B. Tomik, A. Slowik, A. G. Uitterlinden, C. Hendrich, S. Waibel, T. Meyer, A. C. Ludolph, J. D. Glass, S. Purcell, S. Cichon, M. M. Nöthen, H. E. Wichmann, S. Schreiber, S. H. H. M. Vermeulen, L. A. Kiemeny, J. H. J. Wokke, S. Cronin, R. L. McLaughlin, O. Hardiman, K. Fumoto, R. J. Pasterkamp, V. Meininger, J. Melki, P. N. Leigh, C. E. Shaw, J. E. Landers, A. Al-Chalabi, R. H. Brown Jr., W. Robberecht, P. M. Andersen, R. A. Ophoff and L. H. van den Berg, 2009, "Genome-wide Association Study Identifies 19p13.3 (UNC13A) And 9p21.2 As Susceptibility Loci For Sporadic Amyotrophic Lateral Sclerosis", *Nature Genetics*, Vol. 41, pp. 1083-1088.
- van Es, M. A., P. W. J. van Vught, H. M. Blauw, L. Franke, C. G. J. Saris, L. van Den Bosch, S. W. de Jong, V. de Jong, F. Baas, R. van't Slot, R. Lemmens, H. J.

- Schelhaas, A. Birve, K. Slegers, C. van Broeckhoven, J. C. Schymick, B. J. Traynor, J. H. J. Wokke, C. Wijmenga, W. Robberecht, P. M. Andersen, J. H. Veldink, R. A. Ophoff and L. H. van den Berg, 2008, "Genetic Variation in DPP6 is Associated with Susceptibility to Amyotrophic Lateral Sclerosis", *Nature Genetics*, Vol. 40, pp. 29-31.
- van Es, M. A., P. W. J. van Vught, J. H. Veldink, P. M. Andersen, A. Birve, R. Lemmens, S. Cronin, A. J. van Der Kooi, M. de Visser, H. J. Schelhaas, O. Hardiman, I. Ragoussis, D. Lambrechts, W. Robberecht, J. H. J. Wokke, R. A. Ophoff and L. H. van den Berg, 2009, "Analysis of FGGY as A Risk Factor for Sporadic Amyotrophic Lateral Sclerosis", *Amyotrophic Lateral Sclerosis*, Vol. 10, pp. 441- 447.
- van Es, M. A., P. W. Van, H. M. Blauw, L. Franke, C. G. Saris, P. M. Andersen, L. van Den Bosch, S. W. de Jong, R. van't Slot, A. Brive, R. Lemmens, V. de Jong, F. Baas, H. J. Schelhaas, K. Slegers, C. van Broeckhoven, J. H. J. Wokke, C. Wijmenga, W. Robberecht, J. H. Veldink, R. A. Ophoff and L. H. Van den Berg, 2007, "ITPR2 as a Susceptibility Gene in sporadic Amyotrophic Lateral Sclerosis: A Genome-wide Association Study", *Lancet Neurology*, Vol. 6, pp. 869- 877.
- Vance, C., B. Rogelj, T. Hortobágyi, K. J. De Vos, A. L. Nishimura, J. Sreedharan, X. Hu, B. Smith, D. Ruddy, P. Wright, J. Ganesalingam, K. L. Williams, V. Tripathi, S. Al-Saraj, A. Al-Chalabi, P. N. Leigh, I. P. Blair, G. Nicholson, J. Belleruche, J.-M. Gallo, C. C. Miller, C. E. Shaw, 2009, "Mutations in FUS, an RNA Processing Protein, Cause Familial Amyotrophic Lateral Sclerosis Type 6", *Science*, Vol. 323, pp. 1208-1211.
- Veldink, J. H., P. R. Bär, E. A. J. Joosten, M. Otten, J. H. J. Wokke, L. H. van den Berg, 2003, "Sexual Differences in Onset of Disease and Response to Exercise in a Transgenic Model of ALS", *Neuromuscular Disorders*, Vol. 13, pp. 737-743.
- Wang D. G., J. B. Fan, C. J. Siao, A. Berno, P. Young, R. Sapolsky, G. Ghandour, N. Perkins, E. Winchester, J. Spencer, L. Kruglyak, L. Stein, L. Hsie, T. Topaloglou, E. Hubbell, E. Robinson, M. Mittmann, M. S. Morris, N. Shen, D. Kilburn, J. Rioux, C.

- Nusbaum, S. Rozen, T. J. Hudson, R. Lipshutz, M. Chee and E. S. Lander, 1998, "Large-scale Identification, Mapping, and Genotyping of Single-nucleotide Polymorphisms in the Human Genome", *Science*, Vol. 280, pp. 1077-1082.
- Wang, H. Y., I. F. Wang, J. Bose and C. K. Shen, 2004, "Structural Diversity and Functional Implications of The Eukaryotic TDP Gene Family", *Genomics*, Vol. 83, pp. 130-139.
- Wang, T. H. and H. S. Wang, 2009, "A Genome-wide Association Study Primer for Clinicians", *Taiwanese Journal of Obstetrics & Gynecology*, Vol. 48, pp. 89-95.
- Williamson, T.L., L. B. Corson, L. Huang, A. Burlingame, J. Liu, L. I. Bruijn, D. and W. Cleveland, 2000, "Toxicity of ALS-Linked SOD1 Mutants", *Science*, Vol. 288, pp. 399.
- Wu, D., W. Yu, H. Kishikawa, R. D. Folkerth, A. J. Iafrate, Y. Shen, W. Xin, K. Sims and G. F. Hu, 2007, "Angiogenin Loss-of-function Mutations in Amyotrophic Lateral Sclerosis", *Annals of Neurology*, Vol. 62, pp. 609-617.
- Xu Z., L. C. Cork, J. W. Griffin and D. W. Cleveland, 1993, "Increased Expression of Neurofilament Subunit NF-L Produces Morphological Alterations that Resemble the Pathology of Human Motor Neuron Disease." *Cell*, Vol.73, pp.23-33.
- Xu, Z., C. Jung, C. Higgins, J. Levine and J. Kong, 2004, "Mitochondrial Degeneration in Amyotrophic Lateral Sclerosis.", *Journal of Bioenergetics and Biomembrans*, Vol. 36, pp. 395-399.
- Yamazaki, H., T. Nakata, T., Y. Okada and N. Hirokawa, 1996, "Cloning and Characterization of KAP3: a Novel Kinesin Superfamily-associated Protein of KIF3A/3B", *Proceedings of the National Academy of Sciences of the United States of America*, Vol. 93, pp. 8443-8448.

- Yau, C. and C. Holmes, 2008, "CNV Discovery Using SNP Genotyping Arrays", *Cytogenetic and Genome Research*, Vol. 123, pp. 307-312.
- Yim, M. B., J. H. Kang, H. S. Yim, H. S. Kwak, P. B. Chock and E. R. Stadtman, 1996, "A Gain-of-Function of an Amyotrophic Lateral Sclerosis-Associated Cu,Zn-Superoxide Dismutase Mutant: An Enhancement of Free Radical Formation due to a Decrease in K_m for Hydrogen Peroxide", *Proceedings of the National Academy of Science of The United States of America*, Vol. 93, pp. 5709-5714.
- Yoshihara, T., S. Ishigaki, M. Yamamoto, Y. Liang, J. Niwa, H. Takeuchi, M. Doyu and G. Sobue, 2002, "Differential Expression of Inflammation- and Apoptosis-related Genes in Spinal Cords of a Mutant SOD1 Transgenic Mouse Model of Familial Amyotrophic Lateral Sclerosis", *Journal of Neurochemistry*, Vol. 80, pp. 158-167.
- Zelko, I. N., T. J. Mariani, R. J. Folz, 2002, "Superoxide Dismutase Multigene Family: A Comparison of the CuZn-SOD (SOD1), Mn-SOD (SOD2), and EC-SOD (SOD3) Gene Structures, Evolution, and Expression", *Free Radical Biology & Medicine*, Vol. 33, pp.337-349.
- Zetterstrom, P., H. G. Stewart, D. Bergemalm, P. A. Jonsson, K. S. Graffmo, P. M. Andersen, T. Brannstrom, M. Oliveberg and S. L. Marklund, 2007, "Soluble Misfolded Subfractions of Mutant Superoxide Dismutase-1 are Enriched in Spinal Cords Throughout Life in Murine ALS Models", *Proceedings of the National Academy of Sciences of the United States of America*, Vol. 104, pp. 14157-14162.